Networks with mixed-delay constraints

Homa Nikbakht

INSTITUT POLYTECHNIQUE DE PARIS

NNT : 2020IPPAT046

Thèse de doctorat

Networks with Mixed-Delay Constraints

Thèse de doctorat de l'Institut Polytechnique de Paris
préparée à Télécom Paris

École doctorale n^{0}626 Institut Polytechnique de Paris (ED IP Paris)
Spécialité de doctorat: Réseaux, Information et Communications

Thèse présentée et soutenue à Palaiseau, le 15 December 2020, par

Homa NIKBAKHT

Composition du Jury :

M. Walid Hachem Chargé de recherche, CNRS / LIGM	Président
M. Osvaldo Simeone Professeur, Kings College London	Rapporteur
M. Jean-Marie Gorce Professeur, INSA-INRIA	Rapporteur
M. Shlomo Shamai Professeur, Technion	Examinateur
Mme Mari Kobayashi Professeur, Supelec-TUM	Examinateur
M. Malcolm Egan Chargé de recherche, INSA-INRIA	Examinateur
Mme Michèle Wigger Professeur,Télécom Paris	Directeur de thèse
Mme Sarah Kamel Chargé de recherche, Télécom Paris	Co-directeur de thèse

To

My mother Maliheh

And

My best friend Faezeh

Acknowledgements

I wish to thank those who made my Ph.D. studies so memorable. First of all, I would like to express my sincere gratitude to my supervisor Prof. Michèle Wigger. Her immense knowledge, patience and motivation have deeply inspired me. It was a great privilege and honor to work and study under her guidance.

I would like to thank Prof. Shlomo Shamai for providing me with a golden opportunity to collaborate with him. I could not have done this thesis without his thoughtful comments, dedicated support and guidance. I am also very thankful to my coauthors Prof. Aylin Yener, Dr. Walid Hachem and Dr. Sarah Kamel whose contributions enriched my thesis.

I am grateful to Prof. Osvaldo Simeone and Prof.Jean-Marie Gorce for serving as my thesis reviewers. They provided a critical analysis, valuable suggestions and insightful comments that have been very important for the improvement of my work. I would also like to thank Prof. Mari Kobayashi and Dr. Malcolm Egan for serving on my orals committee and participating in my defense.

I am very thankful to my friends in Iran, Amoon, Bakhsh, Tachi and Tayare, and my friends at Telecom Paris, Mehrasa, Akram, Mustapha, Aymen as well as many others for all the fun that we have had in the past three years.

My deepest thanks go to my family, for all their love and devotion, and especially to my mother, Maliheh, for encouraging me to persevere. Last but not the least, I am thankful to my partner Raphael. My life would not have been the same without him. He has been a constant source of support and encouragement throughout these years.

Résumé

Les réseaux de communication sans fil modernes doivent s'adapter à différents types de trafic de données avec des contraintes de latence différentes. Les applications vidéo sensibles à la latence, en particulier, représentent une part croissante du trafic de données. En outre, les réseaux modernes doivent accepter des débits de données élevés, ce qu'ils peuvent faire par exemple avec des terminaux coopératifs ou avec l'assistance de relais tels que les drones. Cependant, la coopération introduit généralement des retards de communication supplémentaires et n'est donc pas applicable au trafic de données sensibles à la latence. Cette thèse porte sur les réseaux d'interférence avec des contraintes de latence mixtes et sur les architectures de systèmes où des émetteurs et/ou des récepteurs voisins peuvent coopérer. Dans de tels systèmes, les messages sensibles à la latence doivent être encodés et décodés sans délai et ainsi ne peuvent pas bénéficier des liens de coopération disponibles.

Nous proposons différents schémas de codage pour permettre la transmission simultanée de messages sensibles et insensibles à la latence. Pour les schémas proposés, nous analysons les gains de multiplexage (MG) qu'ils réalisent sur le réseau de transfert intercellulaire souple de Wyner, le réseau symétrique de Wyner, le réseau hexagonal et le réseau hexagonal sectorisé. Pour le réseau de transfert souple de Wyner et le réseau symétrique de Wyner, nous identifions aussi des résultats étroits s'agissant de leurs limites en théorie de l'information et nous définissons ainsi l'ensemble exact de paires MG qui peuvent être obtenus simultanément pour les données sensibles et insensibles à la latence. Ces résultats montrent que lorsque les émetteurs et les récepteurs peuvent coopérer et que les taux de coopération sont suffisamment élevés, il est possible d'obtenir le plus grand MG possible pour les messages sensibles à la latence sans pénaliser la somme maximale des MG pour l'ensemble des messages sensibles et insensibles à la latence. Cependant, la somme des MG des systèmes que nous proposons pour le modèle hexagonal est diminuée en présence de données sensibles à la latence. Cette pénalité disparaît dans le cas du réseau hexagonal sectorisé quand chaque cellule est divisée en trois secteurs non interférents en équipant les stations de base d'antennes

directionnelles.

Nous proposons, de surcroît, des schémas de codage similaires en fonction de différents types d'activité aléatoire de la part des usagers du réseau. Nous considérons plus particulièrement deux configurations. Dans la première configuration, chaque émetteur envoie toujours des données insensibles à la latence et reçoit aléatoirement des données sensibles à la latence. Dans la seconde configuration, les arrivées de données sensibles et insensibles à la latence sont aléatoires, et chaque transmetteur n'envoie ou ne reçoit qu'un seul type de données à un instant donné. Pour ces deux configurations, nous proposons des schémas de codage généraux et caractérisons leurs régions de MG réalisables pour différents réseaux. Dans les deux cas, les régions de MG obtenues montrent que le MG moyen des données insensibles à la latence diminue lorsque davantage d'utilisateurs sont actifs. Les régions MG obtenues montrent également que dans la première configuration, l'augmentation du taux de MG correspondant aux données sensibles à la latence diminue toujours la somme des MG. En revanche, dans la seconde configuration, pour certains paramètres, la plus grande somme des MG est obtenue au maximum du taux de MG correspondant aux données sensibles à la latence et donc l'augmentation des MG sensibles à la latence améliore la somme des MG.

Nous étudions aussi un réseau d'accès radio "cloud" avec des contraintes de latence mixtes, c'est-à-dire où chaque utilisateur mobile peut simultanément envoyer un flux sensible à la latence et un flux qui la tolère et où seules les données sensibles sont décodées conjointement au sein du cloud. Pour ce réseau, nous dérivons les limites intérieures et extérieures de la région de capacité sous des contraintes de latence mixtes, et nous caractérisons précisément la région MG optimale. Lorsque le rapport signal / bruit (SNR) est élevé, nos résultats démontrent que, pour des capacités frontales modérées, le MG maximal pour les messages sensibles à la latence reste inchangé sur une large gamme de petits et moyens MG de messages sensibles à la latence. La somme des MG est donc améliorée si certains messages peuvent être décodés directement aux stations de base. Pour un SNR modéré, les résultats montrent que lorsque le débit de messages sensibles à la latence est faible ou modéré, nous obtenons une somme de débit de données constante.

Abstract

Modern wireless communication networks have to accommodate different types of data traffic with different latency constraints. In particular, delay-sensitive video-applications represent an increasing portion of data traffic. Modern networks also have to accommodate high total data rates, which they can accomplish for example with cooperating terminals or with helper relays such as drones. However, cooperation typically introduces additional communication delays, and is thus not applicable to delay-sensitive data traffic. This thesis focuses on interference networks with mixed-delay constraints and on system architectures where neighbouring transmitters and/or neighbouring receivers can cooperate. In such systems, delay-sensitive messages have to be encoded and decoded without further delay and thus cannot benefit from available cooperation links.

We propose various coding schemes that can simultaneously accommodate the transmission of both delay-sensitive and delay-tolerant messages. For the proposed schemes we analyze the multiplexing gains (MG) they achieve over Wyner's soft hand-off network, Wyner's symmetric network, the hexagonal network and the sectorized hexagonal network. For Wyner's soft hand-off network and Wyner's symmetric network, we also provide tight information-theoretic converse results and thus establish the exact set of MG pairs that can simultaneously be achieved for delay-sensitive and delay-tolerant data. These results demonstrate that when both transmitters and receivers cooperate and the cooperation rates are sufficiently large, it is possible to achieve the largest MG for delay-sensitive messages without penalizing the maximum sum MG of both delay-sensitive and delay-tolerant messages. In contrast, under our proposed schemes, the sending of delay-sensitive data in hexagonal models decreases the maximum sum MG. This penalty vanishes when we consider the sectorized hexagonal network where each cell is divided into three non-interfering sectors by employing directional antennas at the base stations.

We further propose similar coding schemes for scenarios with different types of random user activity. We specifically consider two setups. In the first setup, each active transmitter always has delay-tolerant data to

send and delay-sensitive data arrival is random. In the second setup, both delay-tolerant and delay-sensitive data arrivals are random, and only one of them is present at any given transmitter. For both setups, we propose general coding schemes and characterize their achievable MG regions for different networks. In both cases, the obtained MG regions show that the average MG for delay-tolerant data decreases when more users are active. The obtained MG regions also show that in the first setup, increasing the delay-sensitive MG always decreases the sum MG. In contrast, in the second setup, for certain parameters, the highest sum MG is achieved at maximum delay-sensitive MG and thus increasing the delay-sensitive MG provides a gain in sum MG. Additionally, we also study a cloud radio access network with mixed delay constraints, i.e., where each mobile user can simultaneously send a delay-sensitive and a delay-tolerant stream and only the delay-tolerant data is jointly decoded at the cloud unit. For this network, we derive inner and outer bounds on the capacity region under mixed delay constraints, and we exactly characterize the optimal MG region. At high signal-to-noise ratio (SNR), our results show that for moderate fronthaul capacities, the maximum MG for delay-sensitive messages remains unchanged over a large regime of small and moderate MGs of delay-sensitive messages. The sum MG is thus improved if some of the messages can directly be decoded at the base stations. At moderate SNR, the results show that when the data rate of delay-sensitive messages is small or moderate, the achievable sum rate is constant.

Contents

List of Figures

List of Abbreviations

BS Base Station

CoMP Coordinated Multi Point

CRAN Cloud Radio Access Network

CSI Channel State Information

CU Cloud Unit

DoF Degree of Freedom

MG Multiplexing Gain

MIMO Multiple-Input Multiple-output

MU Mobile User

Rx Receiver

Tx Transmitter

UE User Equipment

Chapter 1

Introduction

1.1 Background and Motivation

One of the main challenges for the new generation of wireless communication systems is to accommodate different types of data traffic with different delay constraints. Delay-tolerant traffic, such as enhanced mobile broadband (eMBB) data, allows for higher transmission rates by exploiting techniques such as advanced coding, joint decoding or cooperation between terminals. Delay-sensitive traffic, such as video-applications or ultra-reliable low-latency communication (URLLC) data, is subject to stringent delay constraints and is not compatible with techniques that delay encoding and decoding processes. The following techniques are examples that cannot be applied to delay-sensitive traffic.

- In wireless fading channels where transmissions experience multiple fading realizations, ergodic capacity is only achievable using long codewords and thus only on delay-tolerant traffic. The achievable rate of delay-sensitive traffic degrades because codewords have to be short.
- In cloud radio access networks (C-RAN) where base stations (BSs) are connected to a cloud unit (CU) via fronthaul links, delay-tolerant traffic is typically decoded jointly at the CU to achieve higher transmission rates. Meanwhile, delay-sensitive traffic has to be decoded immediately at the BSs, and consequently cannot profit from joint processing.
- In interference networks where neighbouring transmitters (Txs) and/or neighbouring receivers (Rxs) can cooperate over dedicated *cooperation links* to alleviate the effect of interference, delay-sensitive traffic has to be encoded and decoded without further delay and thus cannot profit from cooperation.

The design of coding schemes for transmission of such mixed-delay traffic is the focus of recent works,

notably [1–7]. In particular, wireless fading channels with mixed delay traffic are studied in [1–4]. Reference [1] studies the fundamental limits of dynamic resource allocation over fading broadcast channels where some users have delay-sensitive data and the others have delay-tolerant data. They solve a convex optimization problem that minimizes the average transmission power at the BS. The optimization problem is constrained by the *average* transmit rate over fading states for users with delay-tolerant data, and the *constant* transmit rate at any fading state for users with delay-sensitive data. The key to solve this problem is a two-layer Lagrange duality method. The work in [1] also proposes a scheduling algorithm that prioritizes delay-sensitive messages over delay-tolerant messages. In particular, in their model delay-sensitive messages can be stored in the buffer for only one scheduling period.

The work in [2] proposes a broadcasting approach over a single-antenna fading channel to communicate a stream of delay-sensitive messages and a stream of delay-tolerant messages. In this approach, delay-sensitive messages have to be sent over a single coherence block, while delay-tolerant messages can be sent over multiple blocks. During the decoding of each delay-sensitive block, the decoder treats the delay-tolerant parts as noise. The decoded delay-sensitive parts are fed to the Rxs before decoding the delay-tolerant blocks. To manage the interference more effectively, the work in [3] proposes to combine such a broadcasting approach with decoder-cooperation. Another similar approach is taken in [4] for a broadcast scenario with K users. Instead of superposing delay-tolerant messages on delay-sensitive messages, this work proposes a scheduling approach to give preference to the communication of delay-sensitive messages.

Cooperative interference networks under mixed-delay traffic have not been well-addressed in the literature. This thesis thus focuses on interference networks under mixed-delay constraints where certain Txs and/or certain Rxs can cooperate. We propose various coding schemes to accommodate the transmission of both delay-sensitive and delay-tolerant messages [8–11]. In the proposed schemes, delay-sensitive messages have to be encoded and decoded without further delay and thus cannot profit from cooperation. We also propose similar coding scheme for scenarios with different kinds of random users activities [12]. The impact of random user activity on cellular networks has been previously studied in [13–15]. Reference [13] uses the rate of a two-tap input erasure channel to characterize the throughput of Wyner's soft-handoff network [16] with random user activity. The work in [14] uses the same tool to derive the outage probability of this network. Reference [15] extends the results in [13] to more than one user per cell.

We also study a C-RAN with mixed delay constraints, i.e., where each mobile user can simultaneously send a delay-sensitive and a delay-tolerant stream and only the delay-tolerant data is jointly decoded at the CU. Mixed delay constraints in C-RANs have also been studied in [5] and [6]. In particular, [5] proposes a

scheme where users close to the BSs send only delay-sensitive messages (URLLC data) and it is assumed that these communications do not interfere. Users located further away send delay-tolerant messages (eMBB data) and their interference pattern is modeled by Wyner's symmetric network [16–18] with static channel coefficients. In our work, communications between users and BSs are modeled by Wyner's soft-handoff network with random time-varying channel coefficients [19].

1.2 Contributions

Throughout this thesis, delay-sensitive messages are called "fast" messages and delay-tolerant messages "slow" messages. The followings are the main contributions of this thesis:

- For Wyner's soft-handoff network with *only* Tx or *only* Rx cooperation:
  - We determine the set of all achievable "fast" and "slow" multiplexing gain (MG) pairs, that is, the *optimal MG region*, in function of the prelogs of the cooperation links and the total number of cooperation rounds allowed for "slow" messages. We also propose inner and outer bounds on the capacity region under mixed delay constraints with only Rx cooperation.
  - Our results indicate that the sum rate of "fast" and "slow" messages is approximately constant when "fast" messages are sent at small rates. In this regime, the stringent decoding delay of "fast" messages does not cause a loss in overall performance. When "fast" messages have large rates, this is not the case. In this regime, increasing the rate of "fast" messages by Δ requires that the rate of "slow" messages be reduced by approximately $2 \cdot \Delta$. Our results also show a duality between only Tx-and only Rx -cooperation in the high signal-to-noise ratio (SNR) regime.
- For Wyner's soft-handoff network with *both* Tx and Rx cooperation:
  - We determine the *optimal MG region*, in function of the prelogs of the cooperation links and the total number of cooperation rounds allowed for "slow" messages.
  - The obtained results show that it is possible to accommodate the largest possible MG for "fast" messages without decreasing the maximum sum MG, when the cooperation rates are sufficiently large and both Txs and Rxs can cooperate. The stringent delay constraints thus do not harm the overall performance in this scenario.
- For a general interference network with both Rx-and Tx-cooperation:

  - We propose a general coding scheme that accommodates the transmissions of "slow" and "fast" messages simultaneously. We apply this coding scheme to three cellular network models: a Wyner's symmetric model, a hexagonal model, and a sectorized hexagonal model.
  - The results for Wyner's symmetric model show that it is possible to accommodate the largest possible MG for "fast" messages, without penalizing the maximum sum MG of both "fast" and "slow" messages. The results for the hexagonal model show that there is always a penalty in sum-MG at any "fast" MG. In contrast, for the sectorized hexagonal model where each cell is divided into three non-interfering sectors by employing directional antennas at the BSs, it is possible to eliminate this penalty and accommodate the largest possible MG for "fast" messages without penalizing the maximum sum MG.

- For a general interference network with random users activity and Rx-cooperation:
  - We consider two setups under mixed delay constraints. In both setups, each Tx is active with probability $\rho \in [0, 1]$, and the goal is to maximize the average expected "slow" rate of the network, while the rate of each "fast" message is fixed to a target value. In the first setup, each active Tx transmits a "slow" message, and with probability $\rho_f \in [0, 1]$ also transmits an *additional* "fast" message. In the second setup, each active Tx sends either a "fast" message with probability ρ_f or a "slow" message with probability $1 - \rho_f$.
  - For both setups, we propose general coding schemes and characterize their achievable MG regions for three networks: Wyner's soft-handoff network, Wyner's symmetric network and the hexagonal network. The achievable MG region is shown to be optimal for Wyner's soft-handoff network. In both setups, the obtained MG regions show that the average "slow" MG decreases i) with increasing number of interfering links, and ii) with increasing user activity parameter ρ.
  - The obtained MG regions also show that in the first setup, the maximum sum MG is always attained at 0 "fast" MG, and increasing the "fast" MG decreases the sum MG by a penalty that tends to increase with the number of interference links in the network and with the user activity parameter ρ. In contrast, in the second setup, for certain parameters the sum MG is achieved at maximum "fast" MG and thus increasing the "fast" MG provides a gain in sum MG, where we observe that the gain decreases with the number of interferers and the activity parameter ρ.

- For the uplink of a fading C-RAN where "slow" messages are jointly decoded in the CU, whereas

"fast" messages have to be decoded immediately at the BSs:

- We derive inner and outer bounds on the capacity region under mixed delay constraints. Furthermore, we characterize the exact MG region.

- At high SNR, the results show that for moderate fronthaul capacities, the maximum "slow" MG remains unchanged over a large regime of small and moderate "fast" MG. The sum MG is thus improved if some of the messages can be decoded directly at the BSs. In contrast, for large fronthaul capacities or large "fast" MGs, this sum-MG deteriorates by Δ if one further increases the "fast" MG by Δ.

- At moderate SNR, the results show that when the "fast" rate is small or moderate, the achievable sum rate is constant. When the "fast" rate is large, the achievable sum rate decreases by a factor γ times Δ when the rate of "fast" messages increases by Δ. The penalty factor γ is approximately 1 for static channel coefficients and typically higher for random coefficients. The stringent delay constraint on "fast" messages thus seems to be more harmful at moderate SNR and for time-varying channel conditions than at high SNR or for static channels.

1.3 Organization of the Thesis

In Chapter 2 we describe the channel model of interference networks and introduce tools used in the literature to manage interference with and without cooperation. Chapter 3 proposes a coding scheme that accommodates the transmission of "fast" and "slow" messages simultaneously. Chapter 4 presents our results for Wyner's soft-handoff model under mixed-delay constraints and when only Txs or only Rxs can cooperate and the results when Txs *and* Rxs can cooperate. In Chapter 5, we propose a general coding scheme for any interference network with both Tx- and Rx-cooperation. We specialize the results to Wyner's symmetric model, to the hexagonal model and to the sectorized hexagonal model. In Chapter 6, we combine random user activity with mixed-delay traffic. We then propose general coding schemes and characterize the achievable MG regions for three networks: Wyner's soft-handoff network, Wyner's symmetric network and the hexagonal network. Chapter 7 presents the results for the uplink of a fading C-RAN under mixed delay constraints.

1.4 Notation

We use the shorthand notations “Rx" for “Receiver" and “Tx" for “Transmitter". The set of all integers is denoted by $\mathbb{Z}$, the set of positive integers by $\mathbb{Z}^+$ and the set of real numbers by $\mathbb{R}$. For other sets we use calligraphic letters, e.g., $\mathcal{X}$. Random variables are denoted by uppercase letters, e.g., X, and their realizations by lowercase letters, e.g., x. For vectors we use boldface notation, i.e., upper case boldface letters such as $\mathbf{X}$ for random vectors and lower case boldface letters such as $\mathbf{x}$ for deterministic vectors.) Matrices are depicted with sans serif font, e.g., H. We write X^n for the tuple of random variables $(X_1, \ldots, X_n)$ and $\mathbf{X}^n$ for the tuple of random vectors $(\mathbf{X}_1, \ldots, \mathbf{X}_n)$. We denote the entropy function by $H(\cdot)$, and the mutual information function by $I(\cdot)$.

Chapter 2

Multiplexing Gains of Interference Networks

2.1 Interference Networks Without Cooperation

2.1.1 Problem Setup

Consider a Gaussian interference network with K Tx-Rx pairs and define $\mathcal{K} \triangleq \{1, \ldots, K\}$. Each Tx is equipped with L_t antennas and each Rx with L_r antennas. To describe the interference network, let $\boldsymbol{X}_k \in \mathbb{R}^{\mathsf{L}_t \times 1}$ denote Tx k's input signal and $\boldsymbol{Y}_k \in \mathbb{R}^{\mathsf{L}_r}$ Rx k's output signal and define the interference sets

$$\mathcal{I}_{\mathrm{Rx},k} \triangleq \{\tilde{k} \in \mathcal{K}\backslash\{k\} \colon \boldsymbol{X}_k^n \text{ interferes } \boldsymbol{Y}_{\tilde{k}}^n\}, \tag{2.1}$$

$$\mathcal{I}_{\mathrm{Tx},k} \triangleq \{\tilde{k} \in \mathcal{K}\backslash\{k\} \colon \boldsymbol{X}_{\tilde{k}}^n \text{ interferes } \boldsymbol{Y}_k^n\}. \tag{2.2}$$

The input-output relation of the network is then described as

$$\boldsymbol{Y}_k = \mathsf{H}_{k,k}\boldsymbol{X}_k + \sum_{\tilde{k} \in \mathcal{I}_{\mathrm{Tx},k}} \mathsf{H}_{\tilde{k},k}\boldsymbol{X}_{\tilde{k}} + \boldsymbol{Z}_k, \quad \forall k \in \mathcal{K} \tag{2.3}$$

where $\boldsymbol{Z}_k \in \mathcal{N}(0, \mathsf{I}_{\mathsf{L}_r})$ is the additive white Gaussian noise at Rx k, and $\mathsf{H}_{\tilde{k},k} \in \mathbb{R}^{\mathsf{L}_r \times \mathsf{L}_t}$ is the channel transfer matrix from Tx $\tilde{k}$ to Rx k. The Txs are assumed to operate under an average power constraint P, i.e., the power consumed by Tx k is not allowed to exceed P on average.

Each Tx k attempts to transmit the message M_k to Rx k over the interference channel (2.3). A communication scheme consists of an encoder-decoder pair for each message. The scheme is reliable if all the messages can be reconstructed at their respective Rxs with a high probability of success. For a single-user channel, Shannon [20] established that coding over multiple symbols is the key to reliable communication

through noisy channels. To this end, we consider block coding frameworks where communication schemes operate over $n \geq 1$ channel uses at a time. Thus for a fixed rate tuple $(R_1, R_2, \ldots, R_K)$, the message M_k is assumed to be a uniform random variable whose values belong to a finite set $\mathcal{M}_k = \{1, 2, \ldots, \lfloor 2^{nR_k} \rfloor\}$.

In block coding, each Tx k computes its channel inputs $\boldsymbol{X}_k^n$ as a function of its message:

$$\boldsymbol{X}_k^n = f_k^{(n)}(M_k), \tag{2.4}$$

where $f_k^{(n)}$ denotes an encoding function on appropriate domains. Each Rx k decodes its desired message as

$$\hat{M}_k = g_k^{(n)}(\boldsymbol{Y}_k^n), \tag{2.5}$$

where $g_k^{(n)}$ denotes a decoding function on appropriate domains.

The rate tuple $(R_1, R_2, \ldots, R_K)$ is achievable if, and only if, there exists a sequence of block codes satisfying the average block power constraints

$$\mathbb{E}\left[\frac{1}{n}\sum_{t=1}^{n} ||\boldsymbol{X}_k(t)||^2\right] \leq \mathsf{P}_k, \quad \forall k \in \mathcal{K}, \tag{2.6}$$

and the probability of decoding error tends to zero as $n \to \infty$. The capacity region $\mathcal{C}$ is defined as the closure of the set of achievable rate tuple, and the sum capacity is defined as:

$$\mathcal{C}_{\text{sum}} = \max_{(R_1, R_2, \ldots, R_K) \in \mathcal{C}} R_1 + R_2 + \ldots + R_K. \tag{2.7}$$

Except in some special cases, determining the exact capacity region of Gaussian interference networks remains an open problem [21]. In the regime of high signal to noise ratios (SNR) (i.e., high powers P_k in (2.6)), the capacity region of an interference channel is approximately characterized by the *multiplexing gain* (MG)[1] region. Roughly speaking, the capacity region at high SNR is equal to the MG region scaled by $\frac{1}{2}\log \text{SNR}$. The sum MG captures the number of interference-free sessions that can be scheduled simultaneously over an interference channel. In other words, we say that the MG tuple $(\mathsf{S}_1, \mathsf{S}_2, \ldots, \mathsf{S}_K)$ is achievable if there exists an achievable rate tuple $(R_1(\mathsf{P}), R_2(\mathsf{P}), \ldots, R_K(\mathsf{P}))$ satisfying

$$\mathsf{S}_k = \limsup_{\mathsf{P}\to\infty} \frac{R_k(\mathsf{P})}{\frac{1}{2}\log \mathsf{P}}, \quad \forall k \in \mathcal{K}. \tag{2.8}$$

[1] Also known as degree of freedom or capacity prelog.

The MG region $\mathcal{S}$ is defined as the closure of the set of all achievable MG tuples. The sum MG is defined as

$$\mathcal{S}_{\text{sum}} = \max_{(\mathsf{S}_1,\mathsf{S}_2,\ldots,\mathsf{S}_K)\in\mathcal{S}} \mathsf{S}_1 + \mathsf{S}_2 + \ldots + \mathsf{S}_K. \tag{2.9}$$

2.1.2 Non-Cooperative Interference Management Tools

Managing interference among users sharing the same frequency band is central to wireless communications. The following are some of the well-known tools to manage interference without cooperation:

- **Treating interference as noise:** when the interference is weak, the interfering signal can be simply treated as noise. Many practical schemes operate in this mode and results for more than two users are available [22–24].

- **Orthogonal access:** When the strength of interference is comparable to the strength of desired signal, one often wishes to orthogonalize channel access for the various users. This approach corresponds to sharing the available resources between the K users. In particular, the single MG achievable for a given Tx-Rx pair will be shared between the K users resulting in a per user achievable MG of $\frac{1}{K}$.

- **Decoding interference** When the interference is strong, decoding the interference may improve the rate for the desired signal [25].

- **Han-Kobayashi** The main idea of this technique is to split each Tx's signal into common and private parts. The common part then can be decoded by all Rxs which reduces the overall interference level.

- **Interference Alignment (IA):** The main insight of this technique is to use beamforming over infinite symbol extensions and restrict all interference at every Rx to approximately half of the received signal space. This renders the other half-space interference-free [26,27] and allows each Tx to send with MG equal to $\frac{1}{2}$. To illustrate the main concept of this technique, we present a toy example for which we allow the channel gains and inputs to be complex numbers and the noise samples circular complex Gaussian. Such a channel is easily simulated from (2.3) by fixing all the direct channel coefficients at 1 and all the cross channnel coefficients at $j = \sqrt{-1}$. Each Tx only sends a real Gaussian signal with power P. Each Rx k thus observes the channel output:

$$Y_k = X_k + j \sum_{\tilde{k}\in\mathcal{I}_{\text{Tx},k}} \mathsf{X}_{\tilde{k}} + Z_k, \quad \forall k \in \mathcal{K}, \tag{2.10}$$

where here Z_k is a complex circularly symmetric Gaussian. Each Rx can now simply ignore all imaginary parts of its received signal and decode its desired message based on the interference-free real part of the signal. The scheme achieves one MG for every two real channel uses, and thus an effective MG of $\frac{1}{2}$ per dimension and per user.

2.2 Interference Networks with Cooperation

2.2.1 Problem Setup

Consider a Gaussian interference network with K Tx/Rx pairs where neighbouring Txs and neighbouring Rxs can communicate with each other over dedicated orthogonal links, as first introduced in Willems seminal work [28] and subsequently used in the relevant literature such as [29, 30]. In particular, each Tx k computes its channel inputs $\mathbf{X}_k^n = (\boldsymbol{X}_{k,1}, \ldots, \boldsymbol{X}_{k,n}) \in \mathbb{R}^{\mathsf{L} \times n}$ as a function of the message M_k and of all the conferencing information that it obtained from its neighbouring Txs during the preceding communication phase. The channel inputs again have to satisfy the average block-power constraint in (2.6).

At the Rx side, Rxs first communicate with their neighbours over dedicated noise-free but rate-limited links, and then they decode their intended messages based on their outputs and based on the conferencing information obtained from their neighbours.

2.2.2 Cooperative Interference Management Tools

The following are some of the well-known tools to manage interference when cooperation links are available.

- **Dirty Paper Coding (DPC):** If interference is known at a Tx before communication starts, e.g., through cooperative communication as explained above, the Tx can mitigate this interference through *Dirty Paper Coding* [31]. To illustrate the key concept of this technique, we present a toy example. Consider the Gaussian interference channel

$$Y_k^n = X_k^n + W_k^n + Z_k^n, \tag{2.11}$$

where $Z_k \sim \mathcal{N}(0,1)$ and we assume that also $W_k \sim \mathcal{N}(0, \mathsf{P})$, e.g., because it comes from a Gaussian codebook. If W_k^n is unknown to both the Tx and the Rx, the capacity of above channel is equal to $\frac{1}{2}\log(1 + \frac{\mathsf{P}}{1+\mathsf{P}})$. Costa [31] shows that with W_k known only to the Tx (i.e., in advance before the communication starts), we can achieve a capacity of $\frac{1}{2}\log(1+\mathsf{P})$ if we use the DPC technique. We

summarize the dirty paper encoding and decoding process as follows.

- Define $U_k^n = X_k^n + \alpha W_k^n$ with $\alpha = \frac{\mathsf{P}}{1+\mathsf{P}}$. Fix $\epsilon > 0$ arbitrary small.
- Generate $2^{n(I(U_k;Y_k)-\epsilon)}$ sequences U_k^n with components drawn according to $\mathcal{N}\left(0, \mathsf{P}(1+\alpha^2)\right)$. Place these sequences into $2^{n(\frac{1}{2}\log(1+\mathsf{P})-2\epsilon)}$ bins with $2^{n(I(U_k;W_k)+\epsilon)}$ sequences each. Reveal the codebooks and the bins to the Rx and the Tx.
- Given $W_k^n = \tilde{W}^n$ and a message $M_k \in \{1, \ldots, \lfloor 2^{nR_k} \rfloor\}$, the Tx k looks for a jointly typical pair $(U_k^n, \tilde{W}^n)$ in bin M_k. Call $\tilde{U}^n$ the suitable sequence. Tx k then calculates $\tilde{X}^n = \tilde{U}^n - \alpha\tilde{W}^n$ and sends it over the channel. Note that Tx k declares an error if it cannot find an appropriate sequence $\tilde{U}^n$.
- Rx k observes $Y_k^n = \tilde{Y}^n$ and looks for a sequence U_k^n such that $(U_k^n, \tilde{Y}^n)$ are jointly typical. Rx k declares an error if it finds more than one or no such sequence. With high probability, Rx k finds only one such sequence and it is equal to $\tilde{U}^n$. Rx k then sets $\hat{M}_k$ as the index of the bin containing this sequence.

- **Successive Interference Cancellation (SIC):** The key concept of this technique is that Rxs send their decoded messages to their neighbours so that the interference from already decoded messages can be cancelled [32]. As an example, assume that all Rxs in $\mathcal{I}_{\mathrm{Tx},k}$ can decode their desired messages and send them to Rx k over the cooperation link. Rx k then uses these cooperation messages to delete the interference term $\sum_{\tilde{k}\in\mathcal{I}_{\mathrm{Tx},k}} \mathsf{H}_{\tilde{k},k}\boldsymbol{X}_{\tilde{k}}^n(\hat{M}_{\tilde{k}})$ from its output sequence Y_k^n, i.e., it forms

$$\hat{\boldsymbol{Y}}_k^n = \boldsymbol{Y}_k^n - \sum_{\tilde{k}\in\mathcal{I}_{\mathrm{Tx},k}} \mathsf{H}_{\tilde{k},k}\boldsymbol{X}_{\tilde{k}}^n(\hat{M}_{\tilde{k}}), \tag{2.12}$$

  and decodes its desired message M_k based on $\hat{\boldsymbol{Y}}_k^n$.

- **Multiple access channel (MAC):** In the ideal case of infinite backhaul capacity at the Rx side, all Rxs can learn all their signals observed at the other Rxs. The setup then specializes to a single-receiver multiple-access channel (MAC). The capacity of a MAC is achieved by superposition coding and SIC decoding [33–35]. When interference is weak, then the simpler beamforming technique, or equivalently a network-wide zero-forcing strategy, suffices to approximately achieve capacity.

- **Broadcast channel (BC):** Transmit beamformer is used to send each user's codeword across all the BSs to succesfuly encode each user's codeword while treating the already encoded messages as

known interference [36]. In practice, lattice precoding strategies [37] are used to implement DPC approximately. Similar to the uplink case, when the interfering links are much weaker than the direct links the zero forcing strategy is again near optimal.

- **Coordinated Multi Point (CoMP) Reception:** Rxs quantize and share their received signals over the cooperation links to a dedicated Rx that jointly decodes all the signals based on the obtained quantization outputs [38–41]. This technique can be viewed as a practical implementation of the MAC setup introduced above.

- **CoMP Transmission:** Txs exchange parts of their messages and then jointly encode their transmit signals based on this set of messages [42–44]. This technique can be viewed as a practical implementation of the BC setup introduced above.

- **Clustered Cooperation:** The (quantized version of) received signals of each Rx is shared within a local cluster of Rxs. Similarly, the messages of each Tx is shared within a local cluster of Txs [45–49].

- **Process and Share:** Rxs process their channel output signals and the signals they receive from the other Rxs. They then share their messages with the other Rxs. Similarly, Txs jointly process their own messages and the cooperative messages they receive from the other Txs. They then share their messages with the other Txs [50–52].

2.3 Related Works

Various forms of interference management techniques have been the focus of recent research. Notably, recent theoretical results [27, 53–55] show that transmission schemes based on IA are able to provide a MG of $\frac{1}{2}$ for every user in the network. In particular, [27] establishes that in a K user fully-connected time-varying interference channel, IA enables each user to achieve reliable communication at rates approaching half of the achievable capacity in the absence of all interference. Equivalently, at high SNR, a sum-MG of $\frac{K}{2}$ is achievable in a fully-connected K user interference channel.

IA-based schemes achieve a significant theoretical gain compared to the conventional interference mitigation techniques. Practical scenarios, however, do not find this gain achievable [56] due to the exponentially-large delay or exponentially accurate channel estimation required in such schemes. To implement IA without asymptotic symbol expansion, hybrid scenarios where IA is combined with cooperative techniques are of more practical use [56, 57]. In particular, [56] studies a non-linear *process and share* cooperation approach

for the uplink of a large sectorized hexagonal network. In this approach, a successive decoding scheme is used where each Rx decodes its desired message by processing its own channel outputs and the decoded messages received from a set of neighbouring Rxs. This Rx then transmits its decoded message to a set of Rxs that have not yet decoded their messages. This backhaul cooperation changes the interference graph of the network in such a way that practical one-shot IA without symbol extensions is possible and $\frac{1}{2}$ MG per user is achievable. Reference [57] proposes to combine IA with CoMP transmission and reception techniques where each message is jointly transmitted by M_t successive Txs, and is jointly decoded by M_r Rxs. The results in [57] show that a sum MG of K is achievable for a K user fully-connected interference channel only if $M_t + M_r \geq K + 1$. In the general case, i.e., for arbitrary values of M_t and M_r, the MG is bounded by $\lceil \frac{K+M_t+M_r-2}{2} \rceil$. This implies that, when K is very large compared to M_t and M_r, CoMP transmission and reception do not significantly improve the sum MG compared to the pure IA based schemes.

Towards the different levels of pure cooperative techniques, [58] studies a scheme known as *interference-coordination* where BSs share the channel state information (CSI) of both the direct and interfering channels (obtained from the users via feedback channels) to coordinate their signaling strategies. Signaling strategies can include scheduling, power control and beamforming. A simple example of joint power control and scheduling across the multiple BSs is the *interference pricing* approach [59]. In this approach the impact of each Tx's interference level on its neighbouring transmissions is measured, then Txs are coordinated in such a way that Txs causing excessive interference to neighbouring Tx/Rx pairs reduce their transmit power. This basic level of cooperation requires a low amount of backhaul communication and can improve the performance of current cellular interference networks when many users co-exist in the system.

When high-capacity delay-free backhaul links are available among BSs, a further significant improvement in data rate is possible if, in addition to CSI, each BS shares the full data signals of its users with other BSs. Under this cooperative technique, known as *MIMO cooperation* [60] technique, all propagation links (including interfering ones) are exploited to carry useful data. As a result, the uplink channel is equivalent to a multiple access channel (MAC) with multiple Txs and a single multi-antenna Rx, and the downlink channel is equivalent to a broadcast channel (BC) with a single multi-antenna Tx and multiple Rxs.

In case BSs are connected via limited-capacity backhaul links, a partial interference cancellation or an increase in the transmission rate is still possible if BSs first share CSI then a quantized version of their antenna signal [61]. An example of the rate increase can be seen in the uplink of a two-user interference channel with Han-Kobayashi [62] common-private information splitting style. In this network, the common message rate is increased if each Rx sends a bin index of the decoded part over the rate-limited cooperation

links to the neighbouring Rxs after decoding its common message. Similarly in the downlink of such networks, if the Txs are equipped with rate-limited cooperation rates, a rate increase of common messages is possible if Txs cooperatively send these messages. Furthermore, a partial interference cancellation is possible if they share part of their private messages as well.

The main drawbacks of the MIMO Network approach are i) they require high backhaul loads, ii) increase delay in communications, and iii) make interference to propagate across the network. To reduce the backhaul load requirements of the Network MIMO technique, [45, 46, 48] propose a cluster cooperation technique. In this technique, the network is divided into smaller subnets and the interference management approaches are employed for each subnet individually. This clustered cooperation technique also reduces communication delay and avoids interference to propagate across the entire network.

The work in [46] employs clustered cooperation technique in a Wyner's soft-handoff network where neighbouring Txs and neighbouring Rxs can cooperate over *rate-limited and noise-free* links that do not interfere with the main communication channels and where this cooperative communication is limited to a couple of rounds. Due to this cooperation constraint, the network is divided into interference-free subnets by switching off a set of Txs. The results in [46] show that for small cooperation prelogs, a single cooperation round at the Txs or at the Rxs achieves the same MG as when the number of cooperation rounds is unlimited. On the other hand, for large cooperation prelogs, the maximum per user MG increases with every additional cooperation round that is permitted either at the Txs or at the Rxs.

To sum up, cooperative and non-cooperative interference networks have been well-studied in the literature. Now, the question is how interference networks should deal with heterogeneous traffic where parts of messages cannot benefit from cooperation because they are subject to stringent delay constraints. In the next chapter, we propose a coding scheme that accommodates the transmission of such heterogeneous traffic over an interference network.

Chapter 3

Interference Networks Under Mixed Delay Constraints

In this chapter, we propose a model for interference networks with mixed delay constraints when neighbouring Txs and Rxs cooperate. Specifically, our model accommodates not only "slow" messages that can tolerate the delays introduced by cooperation, but also "fast" messages that have to be encoded and decoded without further delay and thus cannot profit from cooperation. The standard approach to combine the transmissions of "slow" and "fast" messages is to apply a smart scheduling algorithm and thus to time-share a scheme for only "slow" messages with a scheme for only "fast" messages. In our model, each Tx can simultaneously convey "fast" and "slow" messages to its corresponding Rx.

3.1 Problem Setup

We consider cellular interference networks with K cells each consisting of one Tx and Rx pair. Txs and Rxs are equipped with $\mathsf{L}_t = \mathsf{L}_r = \mathsf{L}$ antennas and in the networks we consider regular interference patterns except at the edges. As an example, Fig. 3.1 shows Wyner's symmetric network, where each cell corresponds to a Tx/Rx pair and the interference pattern is depicted with black dashed lines. Each Tx $k \in \mathcal{K}$ wishes to send a pair of independent messages $M_k^{(F)}$ and $M_k^{(S)}$ to a specific Rx $k \in \mathcal{K}$. The "fast" message $M_k^{(F)}$ is uniformly distributed over the set $\mathcal{M}_k^{(F)} \triangleq \{1, \ldots, \lfloor 2^{nR_k^{(F)}} \rfloor\}$ and needs to be decoded subject to a stringent delay constraint, as we explain shortly. The "slow" message $M_k^{(S)}$ is uniformly distributed over $\mathcal{M}_k^{(S)} \triangleq \{1, \ldots, \lfloor 2^{nR_k^{(S)}} \rfloor\}$ and is subject to a less stringent decoding delay constraint. Here, n denotes the blocklength of transmission and $R_k^{(F)}$ and $R_k^{(S)}$ the rates of transmissions of the "fast" and "slow" messages.

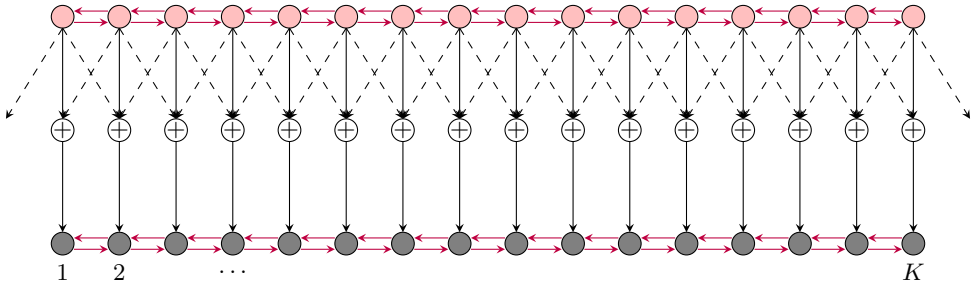

Figure 3.1: Illustration of the symmetric Wyner network. Pink circles indicate Txs and gray circles indicate Rxs, purple arrows indicate the available cooperation links at Txs and at Rxs side, and black dashed lines indicate that the communication in neighbouring cells interfere.

We consider three different cooperation scenarios:

- Neighbouring Txs cooperate by communicating during $\mathrm{D_{Tx}} > 0$ rounds over dedicated cooperation links. Rxs cannot cooperate, and so the number of Rx-cooperation rounds is $\mathrm{D_{Rx}} = 0$. (This scenario is termed “Tx-cooperation Only")
- Neighbouring Rxs cooperate by communicating during $\mathrm{D_{Rx}} > 0$ rounds over dedicated cooperation links. Txs cannot cooperate, and so the number of Tx-cooperation rounds is $\mathrm{D_{Tx}} = 0$. (Termed “Rx-cooperation Only")
- Neighbouring Txs cooperate during $\mathrm{D_{Tx}} > 0$ rounds over dedicated cooperation links and neighbouring Rxs cooperate during $\mathrm{D_{Rx}} > 0$ rounds. (Termed “Tx- and Rx-cooperation").

The cooperative communication is subject to a total delay constraint

$$\mathrm{D_{Tx}} + \mathrm{D_{Rx}} \leq \mathrm{D}, \tag{3.1}$$

where $\mathrm{D} \geq 0$ is a given parameter of the system and the values of $\mathrm{D_{Tx}}$ and $\mathrm{D_{Rx}}$ are design parameters and can be chosen arbitrary such that (3.1) is satisfied. As we will see, in our setup the cooperative communication only concerns “slow" messages, because “fast" messages are subject to a stringent delay constraint and thus have to be transmitted and decoded without further delay. In the following we explain the encoding and the decoding procedure of “Tx- and Rx-cooperation" scenario. The procedure can be easily adjusted for “Tx-cooperation Only" and “Rx-cooperation Only" scenarios.

We describe the encoding at the Txs. Neighbouring Txs first communicate to each other over dedicated noise-free, but rate-limited, links. Communication takes place over $\mathrm{D_{Tx}} > 0$ rounds and can depend only on the “slow" messages but not on the “fast" messages. To describe this cooperative communication more

formally, define for each $k \in \mathcal{K}$ the *Tx-neighbouring set* $\mathcal{N}_{\mathrm{Tx}}(k)$ as the set of all Txs that can directly exchange cooperation messages with Tx k. In each cooperation round $j \in \{1, \ldots, \mathrm{D_{Tx}}\}$, Tx k sends a cooperation message $T_{k\to\ell}^{(j)}\Big(M_k^{(S)}, \{T_{\ell'\to k}^{(1)}, \ldots, T_{\ell'\to k}^{(j-1)}\}_{\ell'\in\mathcal{N}_{\mathrm{Tx}}(k)}\Big)$ to Tx ℓ if $\ell \in \mathcal{N}_{\mathrm{Tx}}(k)$. The rate-limitation on the cooperation link imposes

$$\sum_{j=1}^{\mathrm{D_{Tx}}} H(T_{k\to\ell}^{(j)}) \leq \pi_{\mathrm{Tx}}, \qquad k \in \mathcal{K},\ \ell \in \mathcal{N}_{\mathrm{Tx}}(k), \tag{3.2}$$

where $\pi_{\mathrm{Tx}} \triangleq \mu_{\mathrm{Tx}} \cdot \frac{n}{2}\log(\mathsf{P})$ for a given *Tx-cooperation prelog* $\mu_{\mathrm{Tx}} > 0$.

Tx k finally computes its channel inputs $\mathbf{X}_k^n = (\boldsymbol{X}_{k,1}, \ldots, \boldsymbol{X}_{k,n}) \in \mathbb{R}^{\mathsf{L}\times n}$ as a function of its "fast" and "slow" messages and of all the $\mathrm{D_{Tx}}|\mathcal{N}_{\mathrm{Tx}}(k)|$ cooperation messages that it obtained from its neighbouring transmitters:

$$\mathbf{X}_k^n = f_k^{(n)}\Big(M_k^{(F)}, M_k^{(S)}, \{T_{\ell'\to k}^{(1)}, \ldots, T_{\ell'\to k}^{(\mathrm{D_{Tx}})}\}_{\ell'\in\mathcal{N}_{\mathrm{Tx}}(k)}\Big). \tag{3.3}$$

The channel inputs have to satisfy the average block-power constraint

$$\frac{1}{n}\sum_{t=1}^{n} ||\mathbf{X}_{k,t}||^2 \leq \mathsf{P}, \quad \forall\ k \in \mathcal{K}, \tag{3.4}$$

almost surely.

We now describe the decoding. For each $k \in \mathcal{K}$, define the *Rx-neighbouring set* $\mathcal{N}_{\mathrm{Rx}}(k)$ as the set of all receivers that can directly exchange cooperation messages with Rx k, and recall the *interference set* $\mathcal{I}_{\mathrm{Tx},k}$ as the the set of all Txs whose signals interfere at Rx k.

Decoding takes place in two phases. During the first *fast-decoding phase*, each Rx k decodes its intended "fast" message $M_k^{(F)}$ based on its own channel outputs $\mathbf{Y}_k^n = (\boldsymbol{Y}_{k,1}, \ldots, \boldsymbol{Y}_{k,n}) \in \mathbb{R}^{\mathsf{L}\times n}$ where

$$\mathbf{Y}_k^n = \mathsf{H}_{k,k}\boldsymbol{X}_k^n + \sum_{\hat{k}\in\mathcal{I}_{\mathrm{Tx},k}} \mathsf{H}_{\hat{k},k}\boldsymbol{X}_{\hat{k}}^n + \boldsymbol{Z}_{k,k}^n, \tag{3.5}$$

and $\boldsymbol{Z}_{k,k}^n$ is i.i.d. standard Gaussian noise, the interference set $\mathcal{I}_{\mathrm{Tx},k}$ is defined in (2.2), and the fixed L-by-L full-rank matrix $\mathsf{H}_{\hat{k},k}$ models the channel from Tx $\hat{k}$ to the receiving antennas in Cell k.

So, Rx k produces:

$$\hat{M}_k^{(F)} = g_k^{(n)}(\mathbf{Y}_k^n), \tag{3.6}$$

where $g_k^{(n)}$ denotes a decoding function on appropriate domains.

In the subsequent *slow-decoding phase*, Rxs first communicate with their neighbours during $\mathrm{D_{Rx}} \geq 0$ rounds over dedicated noise-free but rate-limited links, and then they decode their intended "slow" messages based on their outputs and based on this exchanged information. Specifically, in each cooperation round $j \in \{1, \ldots, \mathrm{D_{Rx}}\}$, each Rx k, for $k \in \{1, \ldots, K\}$, sends a cooperation message $Q_{k\to\ell}^{(j)}\Big(\mathbf{Y}_k^n, \{Q_{\ell'\to k}^{(1)}, \ldots, Q_{\ell'\to k}^{(j-1)}\}_{\ell'\in\mathcal{N}_{\mathrm{Rx}}(k)}\}\Big)$ to Rx ℓ if $\ell \in \mathcal{N}_{\mathrm{Rx}}(k)$. The rate-limitation on the cooperation link imposes

$$\sum_{j=1}^{\mathrm{D_{Rx}}} H(Q_{k\to\ell}^{(j)}) \leq \pi_{\mathrm{Rx}}, \qquad k \in \{1, \ldots, K\},\ \ell \in \mathcal{N}_{\mathrm{Rx}}(k), \tag{3.7}$$

where $\pi_{\mathrm{Rx}} \triangleq \mu_{\mathrm{Rx}} \cdot \frac{n}{2}\log(\mathsf{P})$ for some given *Rx-conferencing prelog* $\mu_{\mathrm{Rx}} > 0$.

After the last conferencing round, each Rx k decodes its desired "slow" messages as

$$\hat{M}_k^{(S)} = b_k^{(n)}\Big(\mathbf{Y}_k^n, \Big\{Q_{\ell'\to k}^{(1)}, \ldots, Q_{\ell'\to k}^{(\mathrm{D_{Rx}})}\Big\}_{\ell'\in\mathcal{N}_{\mathrm{Rx}}(k)}\Big), \tag{3.8}$$

where $b_k^{(n)}$ denotes a decoding function on appropriate domains.

We assume that interference is short range, and thus only from neighbouring Txs and Rxs. More precisely, we assume that the interference set $\mathcal{I}_{\mathrm{Tx},k}$ of Rx k is a subset of both the k-th Tx-neighbouring set $\mathcal{N}_{\mathrm{Tx}}(k)$ and the k-th Rx-neighbouring set:

$$\mathcal{I}_{\mathrm{Tx},k} \subseteq \{\mathcal{N}_{\mathrm{Rx}}(k) \cap \mathcal{N}_{\mathrm{Tx}}(k)\}. \tag{3.9}$$

Given power $\mathsf{P} > 0$, maximum delay $\mathrm{D} \geq 0$, and cooperation rates $\pi_{\mathrm{Rx}}, \pi_{\mathrm{Tx}} \geq 0$, average rates $(\bar{R}_K^{(S)}(\mathsf{P}), \bar{R}_K^{(F)}(\mathsf{P}))$ are called achievable, if there exist rates $\{(R_k^{(F)}, R_k^{(S)})\}_{k=1}^K$ satisfying

$$R^{(F)} \triangleq \frac{1}{K}\sum_{k=1}^{K} R_k^{(F)}, \quad \text{and} \quad R^{(S)} \triangleq \frac{1}{K}\sum_{k=1}^{K} R_k^{(S)}, \tag{3.10}$$

and encoding, cooperation, and decoding functions for these rates satisfying constraints (3.1), (3.2), (3.4), and (3.7) and so that the probability of error vanishes:

$$p(\text{error}) \triangleq \mathbb{P}\Big[\bigcup_{k\in\mathcal{K}}\Big(\big(\hat{M}_k^{(F)} \neq M_k^{(F)}\big) \cup \big(\hat{M}_k^{(S)} \neq M_k^{(S)}\big)\Big)\Big] \to 0 \quad \text{as} \quad n \to \infty. \tag{3.11}$$

Definition 1. *Given power constraint* $\mathsf{P} > 0$*, maximum delay D, and maximum cooperation rates* π_{Tx} *and*

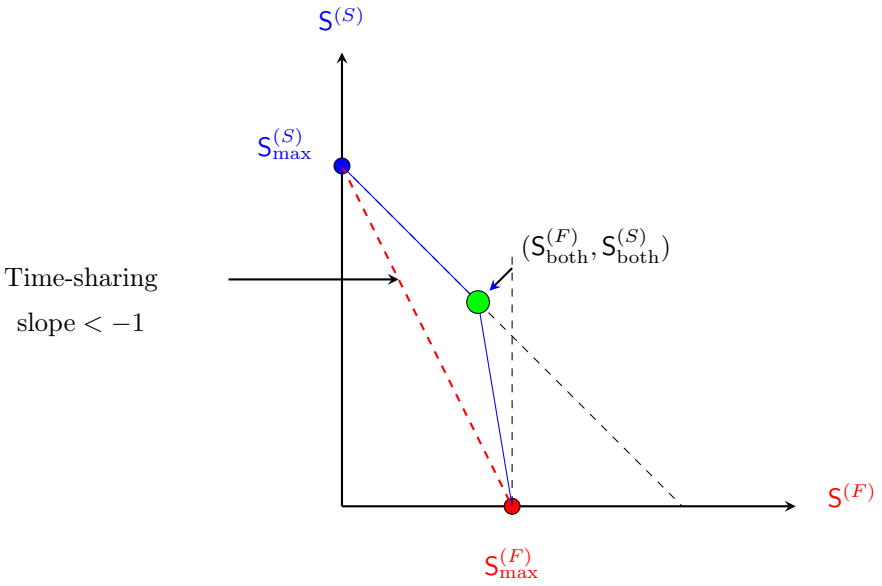

Figure 3.2: Schematic representation of a typical optimal MG region

π_{Rx}, *the* capacity region $\mathsf{C}(\mathsf{P}, \pi_{\text{Tx}}, \pi_{\text{Rx}}, D)$ *is the closure of the set of all rate pairs* $(\bar{R}^{(F)}, \bar{R}^{(S)})$ *that are achievable.*

An MG pair $(\mathsf{S}^{(F)}, \mathsf{S}^{(S)})$ is called *achievable*, if for every positive integer K and power $\mathsf{P} > 0$ there exist achievable average rates $\{R^{(F)}(\mathsf{P}), R^{(S)}(\mathsf{P})\}_{\mathsf{P}>0}$ satisfying

$$\mathsf{S}^{(F)} \triangleq \varlimsup_{K\to\infty} \varlimsup_{\mathsf{P}\to\infty} \frac{R^{(F)}(\mathsf{P})}{\frac{1}{2}\log(\mathsf{P})}, \quad \text{and} \quad \mathsf{S}^{(S)} \triangleq \varlimsup_{K\to\infty} \varlimsup_{\mathsf{P}\to\infty} \frac{R^{(S)}(\mathsf{P})}{\frac{1}{2}\log(\mathsf{P})}. \tag{3.12}$$

Definition 2. *The closure of the set of all achievable MG pairs* $(\mathsf{S}^{(F)}, \mathsf{S}^{(S)})$ *is called* optimal MG region *and denoted* $\mathcal{S}^\star(\mu_{\text{Tx}}, \mu_{\text{Rx}}, D)$.

As we will see, in some cases, the maximum sum MG $\mathsf{S}^{(F)} + \mathsf{S}^{(S)}$ can also be achieved at positive "fast" MGs (or even for all "fast" MGs) implying that the more stringent constraints on transmission of "fast" messages do not harm the overall performance of the system. This is for example the case for all MG pairs $(\mathsf{S}^{(F)}, \mathsf{S}^{(S)})$ that in Fig. 3.2 lie on the straight line connecting the blue point $\mathsf{S}^{(S)}_{\max}$ and the green point $(\mathsf{S}^{(F)}_{\text{both}}, \mathsf{S}^{(S)}_{\text{both}})$. In comparison, scheduling schemes that alternate between transmissions of "fast" and "slow" messages can achieve only the straight line (see the dashed red line in Fig. 3.2)) connecting the largest MG of "fast" and the largest MG of "slow" messages. For scheduling schemes, the sum MG thus decreases

linearly with the “fast” MG whenever the maximum “fast” MG is smaller than the maximum “slow” MG.

Chapter 4

Wyner's Soft-Handoff Model Under Mixed Delay Constraints

In this chapter, we consider Wyner's soft-handoff network and derive inner and outer bounds on the set of MG pairs that are simultaneously achievable for "fast" and "slow" messages. Scenarios with Tx-cooperation, Rx-cooperation or both are considered. We also propose inner and outer bounds on the capacity region of this network when only Rxs can cooperate.

The MG bounds are tight in special cases and allow us to obtain the following conclusions. For large cooperation rates, and when both Txs and Rxs can cooperate, it is possible to simultaneously attain maximum MG for "fast" messages and maximum sum MG for all messages. When only Txs or only Rxs can cooperate (but not both), the largest achievable sum MG decreases linearly with the MG of "fast" messages if "fast" messages have moderate or large MG. In contrast, if the MG of "fast" messages is small, the maximum sum MG can be achieved even with only Tx or only Rx cooperation. A similar conclusion holds in the finite SNR regime when only Rxs can cooperate.

4.1 System Model Description

Consider Wyner's soft-handoff network with K Txs and K Rxs that are aligned on two parallel lines so that each Tx k has two neighbours, Tx $k-1$and Tx $k+1$, and each Rx k has two neighbours, Rx $k-1$ and Rx $k+1$. Interference is short-range in the sense that the signal sent by Tx k is observed only by Rx k and by the neighbouring Rx $k+1$ (see Figure 4.1). Let Txs and Rxs be equipped with $\mathsf{L} > 0$ antennas each.

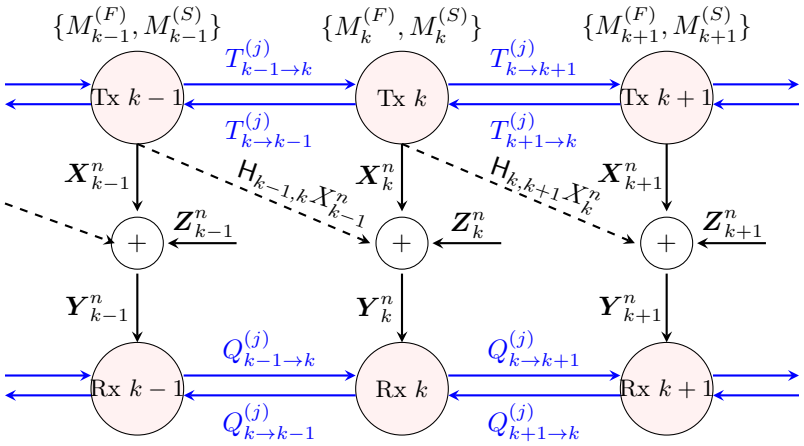

Figure 4.1: System model with Tx- and Rx-cooperation.

The time-t channel output at Rx k is then described as

$$\boldsymbol{Y}_{k,t} = \mathsf{H}_{k,k}\boldsymbol{X}_{k,t} + \mathsf{H}_{k-1,k}\boldsymbol{X}_{k-1,t} + \boldsymbol{Z}_{k,t}, \tag{4.1}$$

where $\boldsymbol{X}_{k,t}$and $\boldsymbol{X}_{k-1,t}$ are the real L-dimensional vectors sent by Tx k and Tx $k-1$ at time t; $\{\boldsymbol{Z}_{k,t}\}$ is a noise sequence consisting of i.i.d. standard Gaussian vectors; $\mathsf{H}_{k,k}$ and $\mathsf{H}_{k-1,k}$ are fixed full rank channel matrices; and $\boldsymbol{X}_{0,t} = \mathbf{0}$ for all t.

In the following sections, we consider the Rx-cooperation only scenario and the Tx-cooperation only scenario. For each scenario we present coding schemes and the optimal MG region. We also present an inner bound on the capacity region with only Rx-cooperation. The scenario with both Tx-and Rx-cooperation is treated in Section 4.5.

4.2 Optimal MG Region and Coding Schemes for Rx-cooperation Only

In this section, we consider only Rx-cooperation but no Tx-cooperation. So,

$$\mu_{\text{Rx}} > 0 \quad \text{and} \quad \mu_{\text{Tx}} = 0. \tag{4.2}$$

Theorem 1 (Optimal Multiplexing Gain Region: Rx-cooperation Only)**.** *For any given $\mu_{\text{Rx}} > 0$, the MG*

region $\mathcal{S}^\star(\mu_{\mathrm{Rx}}, D)$ *is the set of all nonnegative pairs* $(\mathsf{S}^{(F)}, \mathsf{S}^{(S)})$ *satisfying*

$$2\mathsf{S}^{(F)} + \mathsf{S}^{(S)} \leq \mathsf{L} \tag{4.3}$$

$$\mathsf{S}^{(F)} + \mathsf{S}^{(S)} \leq \min\left\{\frac{\mathsf{L}}{2} + \mu_{Rx},\ \ \mathsf{L}\cdot\frac{2D+1}{2D+2}\right\}. \tag{4.4}$$

Proof. The converse to (4.3) is proved in Appendix A.1.1.The converse to (4.4) is proved in Appendix A.1.2. For the achievability, define the following five MG pairs:

$$\left(\mathsf{S}^{(F)} = \frac{\mathsf{L}}{2},\ \mathsf{S}^{(S)} = 0\right), \tag{4.5a}$$

$$\left(\mathsf{S}^{(F)} = 0,\ \mathsf{S}^{(S)} = \mathsf{L}\cdot\frac{2\mathrm{D}+1}{2\mathrm{D}+2}\right), \tag{4.5b}$$

$$\left(\mathsf{S}^{(F)} = 0,\ \mathsf{S}^{(S)} = \frac{\mathsf{L}}{2} + \mu_{\mathrm{Rx}}\right), \tag{4.5c}$$

$$\left(\mathsf{S}^{(F)} = \frac{\mathsf{L}}{2\mathrm{D}+2},\ \mathsf{S}^{(S)} = \mathsf{L}\cdot\frac{2\mathrm{D}}{2\mathrm{D}+2}\right), \tag{4.5d}$$

$$\left(\mathsf{S}^{(F)} = \frac{\mathsf{L}}{2} - \mu_{\mathrm{Rx}},\ \mathsf{S}^{(S)} = 2\mu_{\mathrm{Rx}}\right). \tag{4.5e}$$

In the following Subsection 4.2.1 we show that when $\mu_{\mathrm{Rx}} \geq \mu_{\max}$, where

$$\mu_{\max} \triangleq \mathsf{L}\cdot\frac{\mathrm{D}}{2\mathrm{D}+2}, \tag{4.6}$$

the MG pairs (4.5a), (4.5b), and (4.5d) are achievable. When $\mu_{\mathrm{Rx}} < \mu_{\max}$ the MG pairs (4.5a), (4.5c), and (4.5e) are achievable. The proof of achievability of Theorem 1 then follows from simple time-sharing arguments. □

Figure 4.2 depicts the MG region in Theorem 1 for different values of μ_{Rx}. When there are only "slow" messages, the maximum MG is $\min\{\frac{\mathsf{L}}{2} + \mu_{\mathrm{Rx}}, \mathsf{L}\cdot\frac{2\mathrm{D}+1}{2\mathrm{D}+2}\}$ which by a rate-transfer argument is equal to the maximum sum MG. Interestingly, this sum MG remains unchanged whenever the "fast" MG $\mathsf{S}^{(F)}$ is below a certain threshold. Mathematically, this is described by the slope of the maximum $\mathsf{S}^{(S)}$ in function of $\mathsf{S}^{(F)}$ boundary being equal to -1 when

$$\mathsf{S}^{(F)} \leq \max\left\{\frac{\mathsf{L}}{2} - \mu_{\mathrm{Rx}}, \frac{\mathsf{L}}{2\mathrm{D}+2}\right\}. \tag{4.7}$$

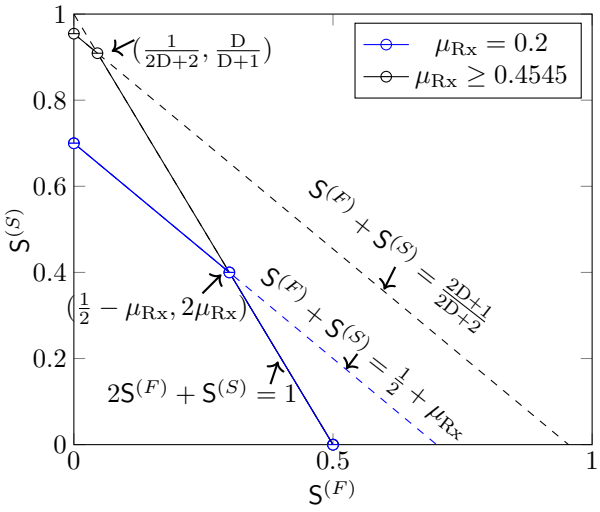

Figure 4.2: The optimal MG region $\mathcal{S}^{\star}(\mu_{\mathrm{Rx}}, \mathrm{D})$ for Rx-cooperation only, for different values of μ_{Rx} and $\mathrm{D} = 10$ and $\mathsf{L} = 1$.

For

$$\mathsf{S}^{(F)} > \max\left\{\frac{\mathsf{L}}{2} - \mu_{\mathrm{Rx}}, \frac{\mathsf{L}}{2\mathrm{D}+2}\right\}, \tag{4.8}$$

the slope is -2. In this latter regime, increasing the MG of "fast" messages by Δ requires decreasing the MG of "slow" messages by 2Δ. There is thus a penalty in sum MG caused by the more stringent delay constraints on "fast" messages.

4.2.1 Schemes Proving Achievability of Theorem 1

We prove achievability of the MG pairs in (4.5).

1. MG pair in (4.5a): Periodically silence every second Tx. This splits the network into $\lceil K/2 \rceil$ non-interfering point-to-point links. Send a "fast" message over each of these links (see Figure 4.3), but no "slow" message at all. The described scheme achieves the MG pair in (4.5a) and requires no cooperation rate.

2. MG pairs in (4.5b) and (4.5c): Let the Txs only send "slow" messages but no "fast" messages. Under this coding assumption, the setup at hand is a multi-antenna version of the setup in Reference [46], but specialized to 0 Tx-cooperation rounds and D Rx-cooperation rounds. The multi-antenna extension of the scheme proposed in Reference [46, Section V] can thus be used to achieve the MG pair in (4.5b) if $\mu_{\mathrm{Rx}} \geq \mu_{\max}$ and the MG pair in (4.5c) if $\mu_{\mathrm{Rx}} < \mu_{\max}$.

For reference in the following subsection, we briefly review the scheme in Reference [46, Section V] when specialized to Rx-cooperation only. For details, see Reference [46]. Consider first the case $\mu_{\mathrm{Rx}} \geq \mu_{\max}$. In

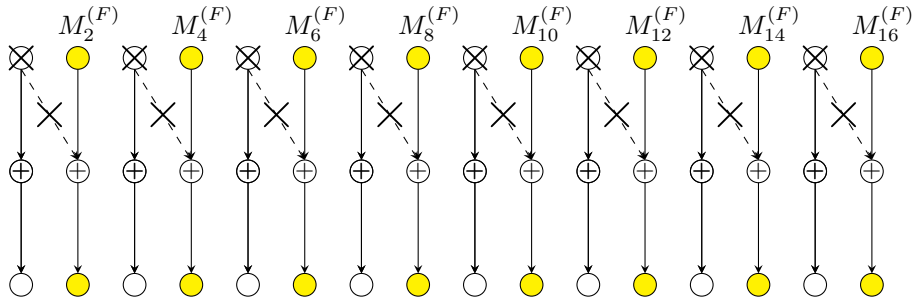

Figure 4.3: Scheme achieving Multiplexing Gain (MG) pair (4.5a) where only "fast" messages are transmitted.

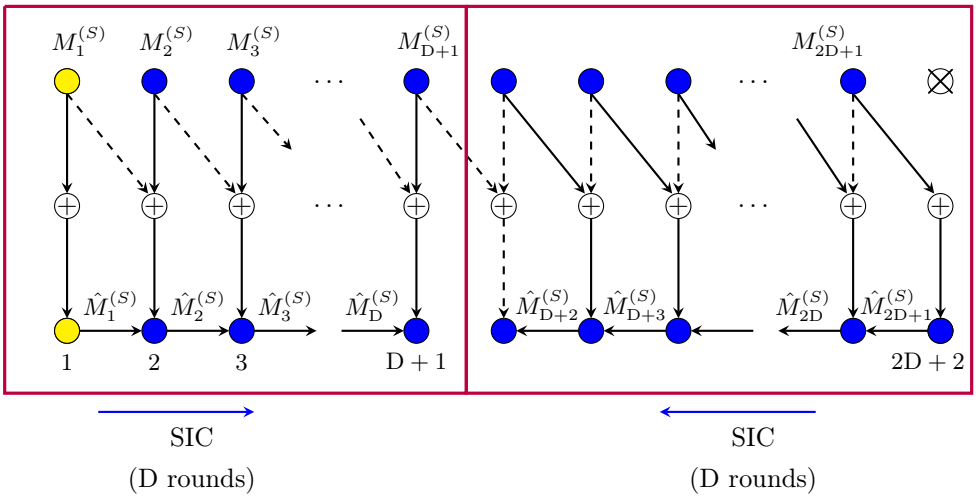

Figure 4.4: Scheme for Rx-cooperation only.

this case, the scheme periodically silences every $2\mathrm{D}+2$nd Tx. This splits the network into smaller subnets, each consisting of $2\mathrm{D}+1$ active Txs and $2\mathrm{D}+2$ active Rxs. We describe the communication in the first subnet, see also Figure 4.4; the others are treated in an analogous way.

Each Tx $k \in \{1, \ldots, 2\mathrm{D}+1\}$ in this first subnet encodes its "slow" message $M_k^{(S)}$ using an L-dimensional Gaussian codebook and then sends the resulting codeword using its L Tx-antennas over the channel. Decoding is performed as follows. Rx 1 decodes its desired message using an optimal point-to-point decoding method based on the interference-free channel outputs $\boldsymbol{Y}_1^n = \mathsf{H}_{1,1}\boldsymbol{X}_1^n + \boldsymbol{Z}_1^n$. Then it sends its decoded message $\hat{M}_1^{(S)}$ over the cooperation link to Rx 2 during the first cooperation round. Rxs 2 to $\mathrm{D}+1$ apply successive interference cancellation (SIC) where they cancel the interference from the preceding Tx with the cooperation message obtained from their left neighbour. After decoding its intended "slow" message, each

Rx $k \in \{2, \ldots, \mathrm{D}\}$ sends its decoded message $\hat{M}_k^{(S)}$ over the cooperation link to Rx $k+1$ during cooperation round k.

We now describe decoding at Rxs $\mathrm{D}+2, \ldots, 2\mathrm{D}+2$. Recall that Tx $2\mathrm{D}+2$ is silenced. Therefore Rx $2\mathrm{D}+2$ observes the interference-free channel outputs $\boldsymbol{Y}_{2\mathrm{D}+2}^n = \mathsf{H}_{2\mathrm{D}+1,2\mathrm{D}+2}\boldsymbol{X}_{2\mathrm{D}+1}^n + \boldsymbol{Z}_{2\mathrm{D}+2}^n$. Based on these outputs, Rx $2\mathrm{D}+2$ decodes the "slow" message $M_{2\mathrm{D}+1}^{(S)}$ intended for Rx $2\mathrm{D}+1$ and transmits the decoded message $\hat{M}_{2\mathrm{D}+1}^{(S)}$ to this Rx over the cooperation link in round 1. Rxs $\mathrm{D}+2$ to $2\mathrm{D}+1$ declare the cooperation message that they receive from their right neighbour as their desired message. They also employ SIC to decode the "slow" message intended for the neighbour to their left. Finally, after this decoding step, each Rx $k \in \{\mathrm{D}+3, \ldots, 2\mathrm{D}+2\}$ sends the decoded message $\hat{M}_{k-1}^{(S)}$ over the cooperation link to its left neighbour during cooperation round $2\mathrm{D}+3-k$. Figure 4.4 illustrates the decodings and conferenced messages.

In the described scheme, $2\mathrm{D}+1$ Txs send a "slow" message using an L-dimensional Gaussian codebook of power P and all these messages can be decoded based on interference-free outputs. An average "slow" MG of $\mathsf{L} \cdot \frac{2\mathrm{D}+1}{2\mathrm{D}+2}$ is thus achieved in each subnet. Moreover, 2D cooperation messages are sent in each subnet, each of prelog equal to the rate of a "slow" message, i.e., L. The *average* cooperation prelog *per link* is thus $\mathsf{L} \cdot \frac{2\mathrm{D}}{2(2\mathrm{D}+2)} = \mu_{\max}$. If one time-shares $2\mathrm{D}+2$ different instances of the described scheme with a different subset of silenced users in each of them, the overall scheme achieves the MG pair $(S^{(F)} = 0, S^{(S)} = \mathsf{L} \cdot \frac{2\mathrm{D}+1}{2\mathrm{D}+2})$ with each cooperation link being loaded at average cooperation prelog $\mu_{\max}$.

When $\mu_{\mathrm{Rx}} < \mu_{\max}$, we can time-share the scheme achieving (4.5b) with a scheme that deactivates every second Tx and sends "slow" messages over the interference-free links. This latter scheme does not require any cooperation. Time-sharing is done according to the available cooperation prelog μ_{Rx}: the first scheme that uses cooperation prelog $\mu_{\max}$ is used over a fraction $\frac{\mu_{\mathrm{Rx}}}{\mu_{\max}}$ of time and the no-cooperation scheme over the remaining fraction $1 - \frac{\mu_{\mathrm{Rx}}}{\mu_{\max}}$ of time. The combined scheme then requires cooperation prelog μ_{Rx} and achieves the MG pair in (4.5c).

3. MG pairs in (4.5d) and (4.5e): Reconsider the coding scheme that achieves MG pair (4.5b) and that is described in the previous subsection and illustrated in Figure 4.4. A close inspection of the scheme reveals that in each subnet, decoding of the message sent by the left-most Tx does not rely on the conferenced information. This first message of each subnet thus satisfies our decoding requirement for "fast" messages.

We propose to apply the above scheme, but to let the first Tx of every subnet (the yellow Tx in Figure 4.4) send a "fast" message and the subsequent 2D Txs of the subnet send "slow" messages. This modified scheme requires the same cooperation prelog $\mu_{\max}$ as before and it achieves the MG pair in (4.5d).

For setups where $\mu_{\text{Rx}} < \mu_{\max}$, we propose to time-share the scheme achieving (4.5d) over a fraction $\frac{\mu_{\text{Rx}}}{\mu_{\max}}$ of time with the scheme achieving (4.5a) over the remaining fraction $1 - \frac{\mu_{\text{Rx}}}{\mu_{\max}}$ of time. This time-sharing scheme has cooperation prelog equal to μ_{Rx}, and thus respects the constraint (3.7). Moreover, it achieves the MG pair in (4.5e).

4.3 Optimal MG Region and Coding Schemes for Tx-Cooperation Only

In this section, we consider only Tx-cooperation but no Rx-cooperation. So,

$$\mu_{\text{Tx}} > 0 \quad \text{and} \quad \mu_{\text{Rx}} = 0. \tag{4.9}$$

Theorem 2 (Optimal MG region: Tx-cooperation Only)**.** *For any given $\mu_{\text{Tx}} > 0$, the MG region $\mathcal{S}^\star(\mu_{\text{Tx}}, D)$ is the set of all nonnegative pairs $(\mathsf{S}^{(F)}, \mathsf{S}^{(S)})$ satisfying*

$$2\mathsf{S}^{(F)} + \mathsf{S}^{(S)} \leq \mathsf{L} \tag{4.10}$$

$$\mathsf{S}^{(F)} + \mathsf{S}^{(S)} \leq \min\left\{\frac{\mathsf{L}}{2} + \mu_{\text{Tx}},\ \ \mathsf{L} \cdot \frac{2D+1}{2D+2}\right\}. \tag{4.11}$$

Proof. The converse to (4.11) is proved in Appendix A.1.1. The converse to (4.10) is proved in Appendix A.1.3. For the achievability, define the following MG pairs:

$$\Big(\mathsf{S}^{(F)} = 0,\ \mathsf{S}^{(S)} = \mathsf{L} \cdot \frac{2\text{D}+1}{2\text{D}+2}\Big), \tag{4.12a}$$

$$\Big(\mathsf{S}^{(F)} = 0,\ \mathsf{S}^{(S)} = \frac{\mathsf{L}}{2} + \mu_{\text{Tx}}\Big), \tag{4.12b}$$

$$\Big(\mathsf{S}^{(F)} = \frac{\mathsf{L}}{2\text{D}+2},\ \mathsf{S}^{(S)} = \mathsf{L} \cdot \frac{2\text{D}}{2\text{D}+2}\Big), \tag{4.12c}$$

$$\Big(\mathsf{S}^{(F)} = \frac{\mathsf{L}}{2} - \mu_{\text{Tx}},\ \mathsf{S}^{(S)} = 2\mu_{\text{Tx}}\Big). \tag{4.12d}$$

In the following Subsection 4.3.1 we show that when $\mu_{\text{Tx}} \geq \mu_{\max}$ the MG pairs (4.5a), (4.12a), and (4.12c) are achievable and when $\mu_{\text{Tx}} < \mu_{\max}$ the MG pairs (4.5a), (4.12b), and (4.12d) are achievable. The achievability proof of the theorem then follows by simple time-sharing arguments. □

Remark 1. *Notice the duality between Theorems 1 and 2, which show that cooperation is equally beneficial for only Tx- or only Rx-cooperation. As we will see in Section 4.5, it is however more beneficial, when Txs* and *Rxs can conference.*

4.3.1 Schemes Proving the Achievability of Theorem 2

We prove achievability of the MG pairs in (4.12). MG pair (4.5a) is achievable as described in the previous section (no cooperation is required at all).

1. MG pairs in (4.12a) and (4.12b): Let the Txs only send "slow" messages but no "fast" messages. Under this coding assumption, the introduced setup corresponds to a multi-antenna version of the setup in Reference [46] but specialized to D Tx-cooperation rounds and 0 Rx-cooperation rounds. Achievability of MG pairs (4.12a) and (4.12b) then follows immediately by specializing [46, Theorem 1] to Tx-cooperation only. In the following we briefly describe the schemes achieving (4.12a) and (4.12b). For details see Reference [46].

We silence every 2D + 2nd Tx. This splits the network into non-interfering subnets, and in a given subnet we apply the scheme depicted in Figure 4.5. Specifically, Tx 1 encodes its message using an L-dimensional power-P Gaussian point-to-point codebook, and sends the resulting codeword $\boldsymbol{X}_1^n$ using its L Tx-antennas over the channel. It also precodes the obtained sequence with the matrix $\mathsf{H}_{2,2}^{-1}\mathsf{H}_{1,2}$, quantises the precoded sequence $\boldsymbol{I}_1^n \triangleq \mathsf{H}_{2,2}^{-1}\mathsf{H}_{1,2}\boldsymbol{X}_1^n$ with a rate-$\frac{\mathsf{L}}{2}\log(1+\mathsf{P})$ quantiser to obtain a quantisation $\hat{\boldsymbol{I}}_1^n$ at noise level, and sends the resulting quantisation message as a first-round cooperation message to Tx 2. For each $k = 2, \ldots, \mathrm{D}+1$, Tx k obtains a round-$(k-1)$ cooperation message from its left neighbour Tx $k-1$ that describes the quantised version $\hat{\boldsymbol{I}}_{k-1}^n$ of $\boldsymbol{I}_{k-1}^n \triangleq \mathsf{H}_{k,k}^{-1}\mathsf{H}_{k-1,k}\boldsymbol{X}_{k-1}^n$. Based on this message, Tx k reconstructs $\hat{\boldsymbol{I}}_{k-1}^n$, encodes its "slow" message $M_k^{(S)}$ using a power P dirty-paper code (DPC) that mitigates the interference $\hat{\boldsymbol{I}}_{k-1}^n$, and sends the resulting DPC sequence $\boldsymbol{X}_k^n$ over the channel. Moreover, it precodes this input sequence with the matrix $\mathsf{H}_{k+1,k+1}^{-1}\mathsf{H}_{k,k+1}$, quantises the precoded sequence $\boldsymbol{I}_k^n \triangleq \mathsf{H}_{k+1,k+1}^{-1}\mathsf{H}_{k,k+1}\boldsymbol{X}_k^n$ with a rate-$\mathsf{L}/2\log(1+\mathsf{P})$ quantiser (for a quantisation at noise level) to obtain $\hat{\boldsymbol{I}}_k^n$, and sends the quantisation message as a round-k cooperation message over the link to its right neighbour. Tx $\mathrm{D}+1$ produces its inputs in a similar way, that is, using DPC, but sends no cooperation message at all.

Rx 1 decodes $M_1^{(S)}$ based on the interference-free outputs

$$\boldsymbol{Y}_1^n = \mathsf{H}_{1,1}\boldsymbol{X}_1^n + \boldsymbol{Z}_1^n, \tag{4.13}$$

using a standard point-to-point decoding rule. Each Rx $k \in \{2, \ldots, \mathrm{D}+1\}$ decodes its desired message

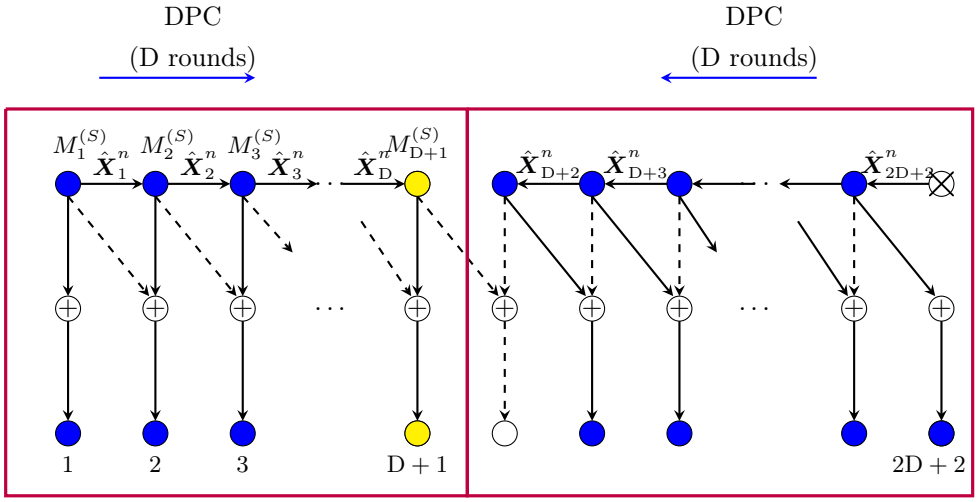

Figure 4.5: Scheme for Tx-cooperation only.

$M_k^{(S)}$ based on the premultiplied outputs

$$\mathsf{H}_{k,k}^{-1}\boldsymbol{Y}_k^n = \mathsf{H}_{k,k}^{-1}\mathsf{H}_{k-1,k}\boldsymbol{X}_{k-1}^n + \boldsymbol{X}_k^n + \mathsf{H}_{k,k}^{-1}\boldsymbol{Z}_k^n, \tag{4.14}$$

using an optimal DPC decoding rule. (Recall that $\boldsymbol{X}_k^n$ was produced as a DPC sequence that mitigates $\hat{\boldsymbol{I}}_{k-1}^n$, a quantised version of $\boldsymbol{I}_{k-1}^n = \mathsf{H}_{k,k}^{-1}\mathsf{H}_{k-1,k}\boldsymbol{X}_{k-1}^n$). Since quantisation was performed at noise level, each message $M_1^{(S)}, \ldots, M_{D+1}^{(S)}$ can be sent reliably with MG L.

Each message M_k, with $k \in \{D+3 \ldots 2D+2\}$, is sent over the path Tx $k \to$Tx $k-1 \to$ Rx k. We describe the transmissions in more detail, starting with the last Tx in the subnet. Tx $2D+2$ does not send any channel inputs, that is, $\boldsymbol{X}_{2D+2}^n = 0^n$. However, it first encodes its "slow" message $M_{2D+2}^{(S)}$ using an L-dimensional Gaussian point-to-point codebook, precodes the codeword $\boldsymbol{U}_{2D+2}^n$ by the matrix $\mathsf{H}_{2D+1,2D+2}^{-1}$, and then quantises this precoded codeword $\boldsymbol{S}_{2D+1}^n \triangleq \mathsf{H}_{2D+1,2D+2}^{-1}\boldsymbol{U}_{2D+2}^n$ with a rate-$\mathsf{L}/2\log(1+\mathsf{P})$ to obtain a quantisation $\hat{\boldsymbol{S}}_{2D+1}^n$ at noise level. It finally sends the quantisation message describing $\hat{\boldsymbol{S}}_{2D+1}^n$ as a first-round cooperation message to Tx $2D+1$. Tx $2D+1$ reconstructs $\hat{\boldsymbol{S}}_{2D+1}^n$ and sends it over the channel, that is, $\boldsymbol{X}_{2D+1}^n = \hat{\boldsymbol{S}}_{2D+1}^n$.

In a similar way, each Tx $k \in \{2D+1, \ldots, D+2\}$ encodes its own "slow" message $M_k^{(S)}$ by means of DPC of power P that mitigates the interference $\mathsf{H}_{k-1,k}^{-1}\mathsf{H}_{k,k}\boldsymbol{X}_k^n$ of the signal sent by Tx k itself; precodes the obtained sequence $\boldsymbol{U}_k^n$ with the matrix $\mathsf{H}_{k-1,k}^{-1}\mathsf{H}_{k,k}$; quantises the precoded sequence $\boldsymbol{S}_{k-1}^n \triangleq \mathsf{H}_{k-1,k}^{-1}\mathsf{H}_{k,k}\boldsymbol{U}_k^n$ to obtain a quantisation $\hat{\boldsymbol{S}}_{k-1}$ at noise level; and sends the corresponding quantisation message as a $(2D+3-k)$-round cooperation message over the link to Tx $k-1$. Tx $k-1$ then reconstructs $\hat{\boldsymbol{S}}_{k-1}^n$ and sends it

over the channel: $\boldsymbol{X}_{k-1}^n = \hat{\boldsymbol{S}}_{k-1}^n$. Rxs $\mathrm{D}+2, \ldots, 2\mathrm{D}+1$ decode their intended messages using an optimal DPC decoding rule based on the premultiplied outputs

$$\mathsf{H}_{k-1,k}^{-1}\boldsymbol{Y}_k^n = \boldsymbol{X}_{k-1}^n + \mathsf{H}_{k-1,k}^{-1}\mathsf{H}_{k,k}\boldsymbol{X}_k^n + \mathsf{H}_{k-1,k}^{-1}\boldsymbol{Z}_k^n. \tag{4.15}$$

Recall that $\boldsymbol{X}_{k-1}^n$ is a quantised version (at noise level) of the precoded signal $\boldsymbol{S}_{k-1}^n \triangleq \mathsf{H}_{k-1,k}^{-1}\mathsf{H}_{k,k}\boldsymbol{U}_k^n$, where $\boldsymbol{U}_k^n$ is a DPC sequence that mitigates the interference $\mathsf{H}_{k-1,k}^{-1}\mathsf{H}_{k,k}\boldsymbol{X}_k^n$. Each of the messages $M_{\mathrm{D}+3}^{(S)}, \ldots, M_{2\mathrm{D}+2}^{(S)}$ can thus be transmitted reliably at full MG L.

In the described scheme, an average "slow" MG of $\mathsf{L} \cdot \frac{2\mathrm{D}+1}{2\mathrm{D}+2}$ is thus achieved in each subnet. Moreover, 2D cooperation messages of prelog L are sent in each subnet, and the *average* cooperation prelog *per link* is $\mathsf{L} \cdot \frac{2\mathrm{D}}{2(2\mathrm{D}+2)} = \mu_{\max}$. If one time-shares $2\mathrm{D}+2$ different instances of the described scheme with a different subset of silenced users in each of them, the overall scheme achieves the MG pair $(S^{(F)} = 0, S^{(S)} = \mathsf{L}\frac{2\mathrm{D}+1}{2\mathrm{D}+2})$ with each cooperation link being loaded at average cooperation prelog $\mu_{\max}$.

When $\mu_{\mathrm{Tx}} < \mu_{\max}$, we propose to time-share above described scheme over a fraction $\frac{\mu_{\mathrm{Tx}}}{\mu_{\max}}$ of time with a scheme that deactivates every second Tx and sends "slow" messages over the interference-free links (which does not require any cooperation) over the remaining fraction $1 - \frac{\mu_{\mathrm{Tx}}}{\mu_{\max}}$ of time. The overall time-sharing scheme achieves the MG pair (4.12b) and loads each Tx-cooperation link at prelog μ_{Tx}.

2. MG pairs in (4.12c) and (4.12d): A close inspection of the coding scheme described above and depicted in Figure 4.5 reveals that in each subnet, the message pertaining to the D+1st Tx does not participate in the cooperation, see Figure 4.5. That means, all conferenced information is independent of this message. The message thus satisfies the constraints imposed on "fast" messages in our scenario. We thus propose to employ above scheme, but where the $\mathrm{D}+1$st Tx in each subnet (the yellow Tx in Figure 4.5) sends a "fast" message and the first and the last D Txs in the subnet send "slow" messages. This scheme requires again cooperation prelog $\mu_{\max}$ and achieves the MG pair in (4.12c).

When $\mu_{\mathrm{Tx}} < \mu_{\max}$, we can time-share this scheme over a fraction $\frac{\mu_{\mathrm{Tx}}}{\mu_{\max}}$ of time with the scheme achieving (4.5a) over the remaining fraction $1 - \frac{\mu_{\mathrm{Tx}}}{\mu_{\max}}$ of time. The time-shared scheme achieves the MG pair (4.12d) and loads each Tx-cooperation link at orelog μ_{Tx}.

Remark 2. *An analogous result can be obtained for the setup where each receiver can send conferencing messages only to its left neighbour or only to its right neighbour. The multiplexing gain region is character-*

ized by (6.25) *and*

$$\mathsf{S}^{(F)} + \mathsf{S}^{(S)} \leq \min\left\{\frac{1}{2} + \frac{\mu}{2},\ \ \frac{D+1}{D+2}\right\}. \tag{4.16}$$

Notice that despite the asymmetry of the network, the result is the same for conferencing to left or right neighbours.

4.4 Results in the Finite SNR Regime with Rx-Cooperation Only

In this section, we propose an inner bound at finite SNR on the capacity region of Wyner's soft-handoff model when only Rxs can cooperate. For simplicity, we assume $\mathsf{L} = 1$ and we fix all the direct channel coefficients at 1 and all the cross channel coefficients at a fixed value $\alpha \in (0, 1)$. This inner bound is based on two schemes. The first scheme assumes $\pi_{\text{Rx}} \leq R^{(F)}$. Each Tx uses a 3-layer superposition code, where it sends its "fast" message in the lowest two layers and its "slow" message in the upper-most layer. Each Rx immediately decodes its intended "fast" message based only on its channel outputs and then sends the part encoded in the lower-most layer to its right neighbour. To decode its intended "slow" message, it first pre-subtracts the interference caused by the lower-most layer of the superposition codeword sent by the Tx to its left. This scheme uses only a single conferencing round.

The second scheme assumes $\pi_{\text{Rx}} > R^{(F)}$ and also exchanges parts of "slow" messages over the conferencing links. Each transmitter employs a $\mathrm{D}+1$-layer superposition code, where the lower-most layer encodes the "fast" message and all higher layers encode parts of the "slow" message. As before, each Rx decodes its intended "fast" message immediately based on its channel outputs. It then sends this decoded message over the conferencing link to its left neighbour during the first conferencing round. Subsequently, after each conferencing round $j = 1, \ldots, \mathrm{D}$, each receiver cancels the interference from the layer-j codeword sent by the transmitter to its left and then decodes the layer-$j+1$ of its intended message. It sends the decoded message part and the conferencing message that it obtained in the previous rounds to its right neighbour.

Theorem 3 (Capacity Inner Bound)**.** *The capacity region* $\mathsf{C}(\mathsf{P}, \pi_{\text{Rx}})$ *includes all rate-pairs* $(R^{(F)}, R^{(S)})$ *that satisfy*

$$R^{(F)} \leq \min\left\{I(U_2;Y),\, I(U_2;Y|U_1) + \pi_{\text{Rx}}\right\} \tag{4.17a}$$

$$R^{(F)} + R^{(S)} \leq \frac{1}{K}\sum_{k=1}^{K}\Big[I(X;Y,U_1'|U_1) + \min\left\{I(U_2;Y),\, I(U_2;Y|U_1) + \pi_{\text{Rx}}\right\}\Big], \tag{4.17b}$$

where triples (U_1, U_2, X) *and* (U_1', U_2', X') *are i.i.d. according to some probability distribution* $P_{U_1U_2X}$ *that*

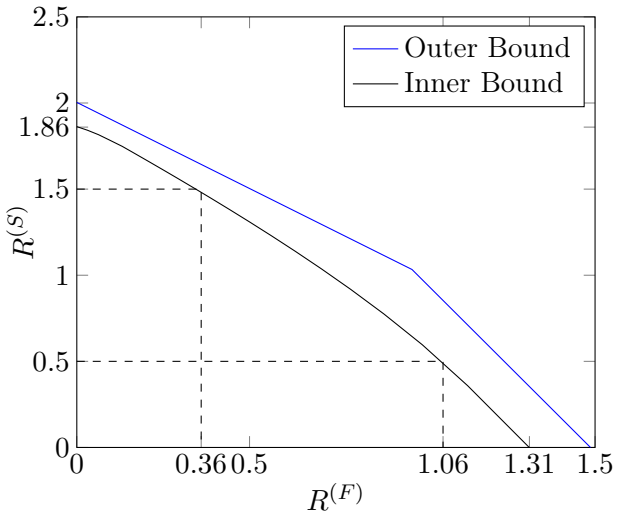

Figure 4.6: The inner bound in Theorem 3 and the outer bound in Theorem 4 on the capacity for $\mathsf{P} = 5$, $\alpha = 0.2$, $\pi_{\mathrm{Rx}} = 0.346$, and $\mathrm{D} = 16$.

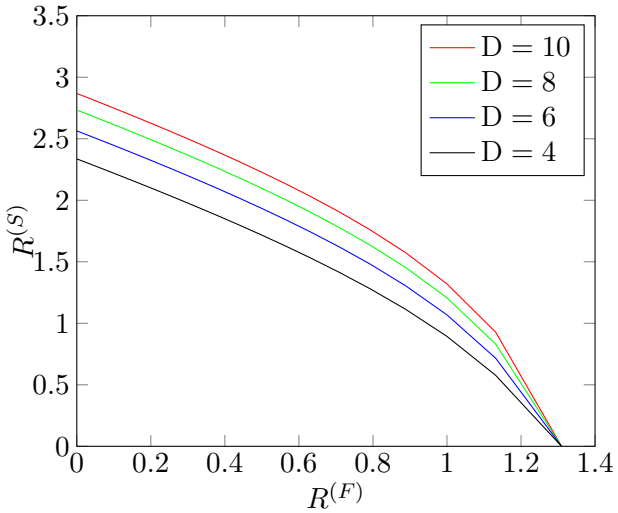

Figure 4.7: Capacity inner bound in Theorem 3 for $\pi_{\mathrm{Rx}} = 2$, $\mathsf{P} = 5$, $\alpha = 0.2$ and different values of D.

satisfies the Markov chain $U_1 \to U_2 \to X$, *and where* $Y = X + \alpha X' + Z$ *with* Z *standard Gaussian independent of* $(U_1, U_2, X, U_1', U_2', X')$.

The capacity region $\mathsf{C}(\mathsf{P}, \pi_{\mathrm{Rx}})$ *also includes all rate-pairs* $(R^{(F)}, R^{(S)})$ *that satisfy*

$$R^{(F)} \le I(U;Y) \tag{4.18a}$$

$$R^{(F)} + R^{(S)} \le I(U;Y) + I(V_1;Y,U'|U) + \sum_{d=2}^{D-1} I(V_d;Y,V_{d-1}'|V_{d-1}) + I(X;Y,X'|V_{D-1}), \tag{4.18b}$$

where the tuples $(U, V_1, \ldots, V_{D-1}, X)$ *and* $(U', V_1', \ldots, V_{D-1}', X')$ *are i.i.d. according to some probability*

distribution $P_{UV_1\ldots V_{D-1}X}$ *satisfying the Markov chain* $U \to V_1 \to V_2 \to \ldots \to V_{D-1} \to X$ *and the rate constraint*

$$I(U;Y) + I(V_1;Y,U'|U) + \sum_{d=2}^{D-1} I(V_d;Y,V'_{d-1}|V_{d-1}) \leq \pi_{\mathrm{Rx}}, \tag{4.19}$$

and where $Y = X + \alpha X' + Z$ *with* Z *independent standard Gaussian.*

Proof: See Appendix A.1.4. ■

Theorem 4 (Capacity Outer Bound)**.** *Any achievable rate pair* $(R^{(F)}, R^{(S)})$ *satisfies the following two conditions:*

$$\begin{aligned} R^{(F)} + R^{(S)} &\leq \frac{\left(\left\lceil \frac{K-1}{2} \right\rceil + 1\right)}{K} \cdot \frac{1}{2}\log\left(1 + (1+\alpha^2)\mathsf{P}\right) \\ &\quad + \frac{\left\lfloor \frac{K-1}{2} \right\rfloor}{K} \cdot \max\{-\log|\alpha|, 0\} + \frac{\left\lfloor \frac{K}{2} \right\rfloor}{K} \cdot \frac{1}{2}\log(1+\alpha^2) + \frac{K-1}{K} \cdot \pi_{\mathrm{Rx}}, \qquad (4.20) \\ 2R^{(F)} + R^{(S)} &\leq \frac{K-1}{K}\left(\frac{1}{2}\log\left((1+(1+\alpha^2)\mathsf{P})(1+\alpha^2)\right) + 2\max\{-\log|\alpha|, 0\}\right) + \frac{1}{K}\log(1+\mathsf{P}). \qquad (4.21) \end{aligned}$$

Proof: Follows by the proof of the bounds (4.3) and (4.4) in Appendices A.1.1 and A.1.2, and by fixing $\mathsf{L} = 1$ and all the direct channel coefficients at 1 and all the cross channel coefficients at $\alpha \in (0,1)$. ■

Fig. 4.6 illustrates the outer bound on the capacity-region in Theorem 4 and the inner bound in Theorem 3 when this latter is evaluated for jointly Gaussian distributions on the inputs and the auxiliaries. For small values of $R^{(F)}$, both the lower and the upper bounds decrease with slope -1. For large values of $R^{(F)}$, they decrease with slope -2. Figure 4.7 illustrates the inner bound on the capacity region for $\mathsf{P} = 5$ and different values of D.

4.5 MG Region for Both Tx-and Rx-Cooperation

In this section we consider both Tx- and Rx-cooperation and we focus again on the high SNR regime, more specifically on the MG region. Recall that the number of Tx- and Rx-cooperation rounds $\mathrm{D_{Tx}}$ and $\mathrm{D_{Rx}}$ is a design parameter over which we can optimize subject to the sum-constraint $\mathrm{D_{Tx}} + \mathrm{D_{Rx}} \leq \mathrm{D}$. For simplicity, in this section we assume that the total number of cooperation rounds D is even.

In the first subsection 4.5.1 we present our inner and outer bounds on the MG region. We also prove that they match in some cases. In the following subsections we then present the coding schemes that allow us to conclude our achievability result.

4.5.1 Results on the MG Region

Let the maximum number of total cooperation rounds D be given. For any pair $\mathrm{D_{Rx}} \in \{1, \ldots, \mathrm{D}-1\}$ and $\mathrm{D_{Tx}} \in \{1, \ldots, \mathrm{D}-1\}$ summing to less than D, define

$$\mu_{\mathrm{Tx,L}}(\mathrm{D_{Tx}}) \triangleq \mathsf{L} \cdot \frac{\mathrm{D_{Tx}}}{2\mathrm{D}+2}, \tag{4.22}$$

$$\mu_{\mathrm{Rx,L}}(\mathrm{D_{Rx}}) \triangleq \mathsf{L} \cdot \frac{\mathrm{D_{Rx}}}{2\mathrm{D}+2}, \tag{4.23}$$

$$\mu_{\mathrm{Tx,H}}(\mathrm{D_{Tx}}) \triangleq \mathsf{L} \cdot \frac{\frac{\mathrm{D}}{2} + \frac{3}{4}\mathrm{D_{Tx}} - \frac{1}{4}}{2\mathrm{D}+2}, \tag{4.24}$$

$$\mu_{\mathrm{Rx,H}}(\mathrm{D_{Rx}}) \triangleq \mathsf{L} \cdot \frac{\frac{\mathrm{D}}{2} + \mathrm{D_{Rx}} - 1}{2\mathrm{D}+2}. \tag{4.25}$$

Notice that $\mu_{\mathrm{Tx,L}}(\mathrm{D_{Tx}}) \leq \mu_{\mathrm{Tx,H}}(\mathrm{D_{Tx}})$ and $\mu_{\mathrm{Rx,L}}(\mathrm{D_{Rx}}) \leq \mu_{\mathrm{Rx,H}}(\mathrm{D_{Rx}})$.

Also, define the five MG pairs:

$$\mathsf{S}^{(F)}_{\mathrm{NoCoop}} \triangleq \Big(\mathsf{S}^{(F)} = \frac{\mathsf{L}}{2},\ \mathsf{S}^{(S)} = 0\Big), \tag{4.26a}$$

$$\mathsf{S}^{(S)}_{\mathrm{NoCoop}} \triangleq \Big(\mathsf{S}^{(F)} = 0,\ \mathsf{S}^{(S)} = \frac{\mathsf{L}}{2}\Big), \tag{4.26b}$$

$$\mathsf{S}_{\mathrm{Coop}} \triangleq \Big(\mathsf{S}^{(F)} = 0,\ \mathsf{S}^{(S)} = \mathsf{L} \cdot \frac{2\mathrm{D}+1}{2\mathrm{D}+2}\Big), \tag{4.26c}$$

$$\mathsf{S}_{\mathrm{Partial}} \triangleq \Big(\mathsf{S}^{(F)} = \mathsf{L} \cdot \frac{2}{2\mathrm{D}+2},\ \mathsf{S}^{(S)} = \mathsf{L} \cdot \frac{2\mathrm{D}-1}{2\mathrm{D}+2}\Big), \tag{4.26d}$$

$$\mathsf{S}_{\mathrm{Interlaced}} \triangleq \Big(\mathsf{S}^{(F)} = \frac{\mathsf{L}}{2},\ \mathsf{S}^{(S)} = \mathsf{L} \cdot \frac{\mathrm{D}}{2\mathrm{D}+2}\Big). \tag{4.26e}$$

Notice that all these MG pairs do not depend on the number of cooperation rounds $\mathrm{D_{Tx}}$ and $\mathrm{D_{Rx}}$. In what follows, we will be interested in convex combinations of these points and therefore define for each $\alpha \in [0,1]$:

$$\mathsf{S}_{\mathrm{Coop}}(\alpha) \triangleq \alpha \cdot \mathsf{S}_{\mathrm{Coop}} + (1-\alpha) \cdot \mathsf{S}^{(S)}_{\mathrm{NoCoop}}, \tag{4.27a}$$

$$\mathsf{S}_{\mathrm{Partial}}(\alpha) \triangleq \alpha \cdot \mathsf{S}_{\mathrm{Partial}} + (1-\alpha) \cdot \mathsf{S}^{(F)}_{\mathrm{NoCoop}}, \tag{4.27b}$$

$$\mathsf{S}_{\mathrm{Interlaced}}(\alpha) \triangleq \alpha \cdot \mathsf{S}_{\mathrm{Interlaced}} + (1-\alpha) \cdot \mathsf{S}^{(F)}_{\mathrm{NoCoop}}, \tag{4.27c}$$

$$\mathsf{S}_{\mathrm{Partial\text{-}Inter}}(\alpha) \triangleq \alpha \cdot \mathsf{S}_{\mathrm{Interlaced}} + (1-\alpha) \cdot \mathsf{S}_{\mathrm{Partial}}. \tag{4.27d}$$

Notice that $\mathsf{S}_{\mathrm{Coop}}(1) = \mathsf{S}_{\mathrm{Coop}}$ and $\mathsf{S}_{\mathrm{Partial}}(1) = \mathsf{S}_{\mathrm{Partial}}$ and $\mathsf{S}_{\mathrm{Interlaced}}(1) = \mathsf{S}_{\mathrm{Interlaced}}$. Moreover, $\mathsf{S}_{\mathrm{Partial\text{-}Inter}}(1) = \mathsf{S}_{\mathrm{Interlaced}}$ and $\mathsf{S}_{\mathrm{Partial\text{-}Inter}}(0) = \mathsf{S}_{\mathrm{Partial}}$.

Theorem 5 (Achievable MG Region: Tx- and Rx-cooperation)**.** *For any choice of odd-valued integers $D_{Tx}, D_{Rx} \in \{1, 3, 5, \ldots, D-1\}$ summing to D, the optimal MG region $\mathcal{S}^\star(\mu_{\text{Tx}}, \mu_{\text{Rx}}, D)$ contains some of the following regions, depending on the available cooperation prelogs μ_{Tx} and μ_{Rx}.*

- *If $\mu_{\text{Tx}} \geq \mu_{Tx,H}(D_{Tx})$ and $\mu_{\text{Rx}} \geq \mu_{Rx,H}(D_{Rx})$, the optimal MG region $\mathcal{S}^\star(\mu_{\text{Tx}}, \mu_{\text{Rx}}, D)$ contains the trapezoidal region*

$$\text{conv hull}\Big((0,0),\ \mathsf{S}^{(F)}_{\text{NoCoop}},\ \mathsf{S}_{\text{Coop}},\ \mathsf{S}_{\text{Interlaced}}\Big). \tag{4.28}$$

- *If $\mu_{\text{Tx}} \geq \mu_{Tx,L}(D_{Tx})$ and $\mu_{\text{Rx}} \geq \mu_{Rx,L}(D_{Rx})$, the optimal MG region $\mathcal{S}^\star(\mu_{\text{Tx}}, \mu_{\text{Rx}}, D)$ contains the pentagon*

$$\text{conv hull}\left((0,0),\ \mathsf{S}^{(F)}_{\text{NoCoop}},\ \mathsf{S}_{\text{Coop}},\ \mathsf{S}_{\text{Partial-Inter}}(\alpha_1^\star),\ \mathsf{S}_{\text{Interlaced}}(\beta_1^\star)\right), \tag{4.29}$$

where

$$\alpha_1^\star \triangleq \min\left\{\frac{\mu_{\text{Tx}} - \mu_{Tx,L}(D_{Tx})}{\mu_{Tx,H}(D_{Tx}) - \mu_{Tx,L}(D_{Tx})}, \frac{\mu_{\text{Rx}} - \mu_{Rx,L}(D_{Rx})}{\mu_{Rx,H}(D_{Rx}) - \mu_{Rx,L}(D_{Rx})}, 1\right\} \tag{4.30}$$

and

$$\beta_1^\star \triangleq \min\left\{\frac{\mu_{\text{Tx}}}{\mu_{Tx,H}(D_{Tx})}, \frac{\mu_{\text{Rx}}}{\mu_{Rx,H}(D_{Rx})}, 1\right\}. \tag{4.31}$$

- *For $\mu_{\text{Tx}} \leq \mu_{Tx,L}(D_{Tx})$ or $\mu_{\text{Rx}} \leq \mu_{Rx,L}(D_{Rx})$, the optimal MG region $\mathcal{S}^\star(\mu_{\text{Tx}}, \mu_{\text{Rx}}, D)$ contains the region*

$$\text{conv hull}\left((0,0),\ \mathsf{S}_{\text{Coop}}(\alpha_2^\star),\ \mathsf{S}_{\text{Partial}}(\alpha_2^\star),\ \mathsf{S}_{\text{Interlaced}}(\beta_2^\star)\right). \tag{4.32}$$

where

$$\alpha_2^\star \triangleq \min\left\{\frac{\mu_{\text{Tx}}}{\mu_{Tx,L}(D_{Tx})}, \frac{\mu_{\text{Rx}}}{\mu_{Rx,L}(D_{Rx})}\right\} \tag{4.33}$$

and

$$\beta_2^\star = \min\left\{\frac{\mu_{\text{Tx}}}{\mu_{Tx,H}(D_{Tx})}, \frac{\mu_{\text{Rx}}}{\mu_{Rx,H}(D_{Rx})}\right\}. \tag{4.34}$$

In Figure 4.8 we schematically illustrate above MG regions (4.28), (4.29) and (4.32). We see that for large cooperation prelogs our MG region is the trapezoid in Figure 4.8a. For smaller cooperation prelogs the MG region turns into a pentagon, see Figure 4.8b, because MG pair $\mathsf{S}_{\text{Interlaced}}$ is not included anymore. Finally, for even smaller cooperation prelogs even the MG pair S_{Coop} is not included anymore, but needs to be replaced by $\mathsf{S}_{\text{Coop}}(0.93)$. Similarly, $\mathsf{S}_{\text{Partial-Inter}}(0.6)$ needs to be replaced by $\mathsf{S}_{\text{Partial}}(0.93)$.

The achievable MG region described in the theorem can also be written as a union over the choice of

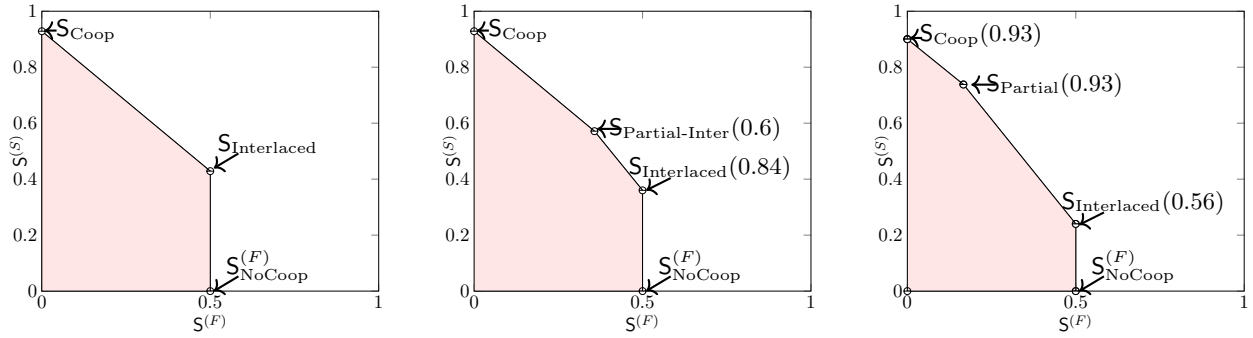

(a) MG region in (4.28) (b) MG region in (4.29) (c) MG region in (4.32)

Figure 4.8: Examples of the three MG regions in (4.28), (4.29) and (4.32). Specifically, we used $\mathrm{D_{Tx}} = 3$, $\mathrm{D_{Rx}} = 3$, and $\mu_{\mathrm{Tx}} \in \{0.4, 0.3, 0.2\}$ and $\mu_{\mathrm{Rx}} \in \{0.4, 0.3, 0.2\}$.

the Tx- and Rx-cooperation rounds $\mathrm{D_{Tx}}$ and $\mathrm{D_{Rx}}$ summing to no more than D. Notice however, that one cannot take the convex hull of this union because of the way we defined the problem setup, the choice of $\mathrm{D_{Tx}}$ and $\mathrm{D_{Rx}}$ needs to be fixed in advance and time-sharing between different choices is not possible.

Proof of Theorem 5. In the following Subsections 4.5.2, 4.5.3 and 4.5.4 we show how to achieve the MG pairs in (4.26c)–(4.26e) with sufficiently large cooperation prelogs μ_{Tx} and μ_{Rx}. In particular, to achieve (4.26c) and (4.26d), cooperation prelogs $\mu_{\mathrm{Tx}} \geq \mu_{\mathrm{Tx,L}}(\mathrm{D_{Tx}})$ and $\mu_{\mathrm{Rx}} \geq \mu_{\mathrm{Rx,L}}(\mathrm{D_{Rx}})$ are required. To achieve (4.26e) cooperation prelogs $\mu_{\mathrm{Tx}} \geq \mu_{\mathrm{Tx,H}}(\mathrm{D_{Tx}})$ and $\mu_{\mathrm{Rx}} \geq \mu_{\mathrm{Rx,H}}(\mathrm{D_{Rx}})$ are required. MG pairs (4.26a) and (4.26b) can be achieved without any Tx- or Rx-cooperation by simply silencing every second transmitter and sending either only “fast" or only "slow" messages over the remaining $K/2$ isolated point-to-point links.

The proof of the theorem follows then by simple time-sharing arguments. In particular, for any $\alpha \in [0, 1]$ the MG pair $\mathsf{S}_{\text{Coop}}(\alpha)$ can be achieved by time-sharing the scheme achieving S_{Coop} over a fraction α of the time with the scheme achieving $\mathsf{S}^{(S)}_{\text{NoCoop}}$ over the remaining fraction of time. Such a time-sharing scheme requires cooperation prelogs of $\mu_{\mathrm{Tx}} \geq \alpha\mu_{\mathrm{Tx,L}}$ and $\mu_{\mathrm{Rx}} \geq \alpha\mu_{\mathrm{Rx,L}}$. The MG pairs $\mathsf{S}_{\text{Partial}}(\alpha)$ and $\mathsf{S}_{\text{Interlaced}}(\alpha)$ are achieved by time-sharing the scheme achieving $\mathsf{S}_{\text{Partial}}$ or the scheme achieving $\mathsf{S}_{\text{Interlaced}}$ over a fraction α of the time with the scheme achieving $\mathsf{S}^{(F)}_{\text{NoCoop}}$ over the remaining fraction of time. The time-sharing scheme leading to $\mathsf{S}_{\text{Partial}}(\alpha)$ requires cooperation prelogs $\mu_{\mathrm{Tx}} \geq \alpha\mu_{\mathrm{Tx,L}}$ and $\mu_{\mathrm{Rx}} \geq \alpha\mu_{\mathrm{Rx,L}}$ and the time-sharing scheme leading to $\mathsf{S}_{\text{Interlaced}}(\alpha)$ requires $\mu_{\mathrm{Tx}} \geq \alpha\mu_{\mathrm{Tx,H}}$ and $\mu_{\mathrm{Rx}} \geq \alpha\mu_{\mathrm{Rx,H}}$. The MG pair $\mathsf{S}_{\text{Partial-Inter}}(\alpha)$ is achieved by time-sharing the scheme achieving $\mathsf{S}_{\text{Interlaced}}$ over a fraction α of the time with the scheme achieving $\mathsf{S}_{\text{Partial}}$ over the remaining fraction of time. This time-sharing scheme requires cooperation prelogs $\mu_{\mathrm{Tx}} \geq \alpha\mu_{\mathrm{Tx,H}} + (1-\alpha)\mu_{\mathrm{Tx,L}}$ and $\mu_{\mathrm{Rx}} \geq \alpha\mu_{\mathrm{Rx,H}} + (1-\alpha)\mu_{\mathrm{Rx,L}}$.

Notice that for all of above time-sharing arguments, it is important that the MG pairs $\mathsf{S}^{(F)}_{\text{NoCoop}}$, $\mathsf{S}^{(S)}_{\text{NoCoop}}$,

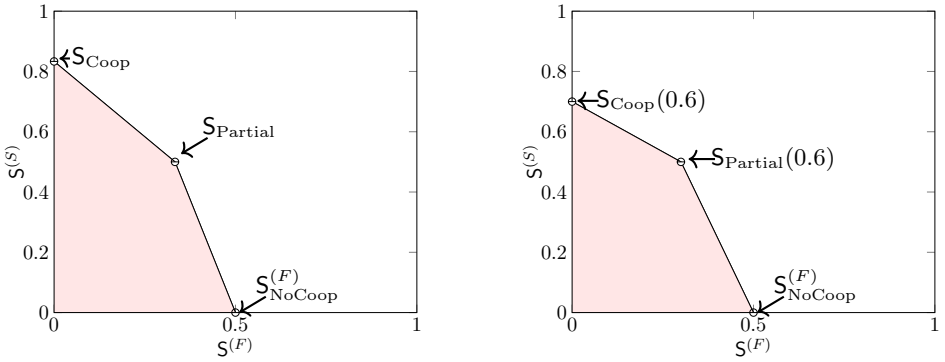

(a) $\mathrm{D_{Tx}} = \mathrm{D_{Rx}} = 2$, $\mu_{\mathrm{Tx}} = \mu_{\mathrm{Rx}} = 0.4$ (b) $\mathrm{D_{Tx}} = \mathrm{D_{Rx}} = 2$, $\mu_{\mathrm{Tx}} = \mu_{\mathrm{Rx}} = 0.2$

Figure 4.9: Examples of the MG regions discussed in Remark 3 for even values of $\mathrm{D_{Tx}}$ and $\mathrm{D_{Rx}}$.

S_{Coop}, $\mathsf{S}_{\text{Partial}}$, and $\mathsf{S}_{\text{Interlaced}}$ can be achieved using the same values of $\mathrm{D_{Tx}}$ and $\mathrm{D_{Rx}}$. As will become clear in the following sections, these MG pairs can be achieved using any values $\mathrm{D_{Tx}}, \mathrm{D_{Rx}} \in \{1, 3, 5, \ldots \mathrm{D}-1\}$ summing to D. The required cooperation prelogs however depend on the specific choices of $\mathrm{D_{Tx}}$ and $\mathrm{D_{Rx}}$. This explains why the allowed time-sharing coefficients α depend on the number of cooperation rounds $\mathrm{D_{Tx}}$ and $\mathrm{D_{Rx}}$. □

Remark 3. *If in Theorem 5 we allow the parameters D_{Tx}, D_{Rx} to take on any values in $\{1, 2, \ldots, D-1\}$ summing to D and we remove the MG points $\mathsf{S}_{\text{Interlaced}}$, $\mathsf{S}_{\text{Interlaced}}(\beta_1^\star)$, $\mathsf{S}_{\text{Interlaced}}(\beta_2^\star)$, and $\mathsf{S}_{\text{Partial-Inter}}(\alpha_1^\star)$, we obtain a different achievable region, which can be larger for certain system parameters.*

To see that this modified region is also achievable, notice that our schemes achieving S_{Coop} and $\mathsf{S}_{\text{Partial}}$ described in Subsections 4.5.2 and 4.5.3 can be run with any number of Tx- and Rx- cooperation rounds D_{Tx} and D_{Rx}, irrespective of whether they are odd or even. Their performance remains unchanged. In contrast, the scheme achieving $\mathsf{S}_{\text{Interlaced}}$ that we present in Subsection 4.5.4 requires that both D_{Tx} and D_{Rx} are both odd.

In Figure 4.9 we schematically illustrate the MG regions that are achieved for D_{Tx} or D_{Rx} even. Specifically, Figure 4.9a shows the MG region for large cooperation prelogs and Figure 4.9b for small cooperation prelogs.

We also have the following converse result.

Proposition 1 (Outer Bound on Optimal MG Region: Both Tx- and Rx-cooperation)**.** *Any MG pair*

$(\mathsf{S}^{(F)}, \mathsf{S}^{(S)})$ *in* $\mathcal{S}^\star(\mu_{\mathrm{Tx}}, \mu_{\mathrm{Rx}}, D)$ *satisfies*

$$\mathsf{S}^{(F)} \leq \frac{\mathsf{L}}{2}, \tag{4.35a}$$

$$\mathsf{S}^{(F)} + \mathsf{S}^{(S)} \leq \min\left\{\frac{\mathsf{L}}{2} + \mu_{\mathrm{Tx}} + \mu_{\mathrm{Rx}},\ \mathsf{L}\cdot\frac{2D+1}{2D+2}\right\}. \tag{4.35b}$$

Proof. Follows from the converse result in Reference [46] and by a rate-transfer argument from "fast" to "slow" messages. □

Figure 4.10 depicts our inner and outer bounds (Theorem 5, Remark 3, and Proposition 1) on the optimal MG region with $\mu_{\mathrm{Tx}} = \mu_{\mathrm{Rx}} = 0.45$ and $\mathrm{D} = 10$ for different values of $\mathrm{D_{Tx}}$ and $\mathrm{D_{Rx}}$. For $\mathrm{D_{Rx}} = \mathrm{D}/2 = 5$ and $\mathrm{D_{Tx}} = \mathrm{D}/2 = 5$,

$$\mu_{\mathrm{Tx}} \geq \mu_{\mathrm{Tx,H}} \qquad \text{and} \qquad \mu_{\mathrm{Rx}} \geq \mu_{\mathrm{Rx,H}}, \tag{4.36}$$

and the inner bound is given by the trapezoidal region defined in (4.28). It coincides with the outer bound, and thus establishes the exact MG region. Notice that in this case, the MG region is solely constrained by the fact that the MG of "fast" messages cannot exceed $\frac{\mathsf{L}}{2}$ and that the sum MG of all messages cannot exceed $\mathsf{L}\cdot\frac{2\mathrm{D_{Rx}}+2\mathrm{D_{Tx}}+1}{2\mathrm{D_{Rx}}+2\mathrm{D_{Tx}}+2}$. Imposing a stringent constraint on the decoding delay of the "fast" messages in this case never penalises the sum-MG of the system. Our inner bounds obtained for odd-valued cooperation-rounds $(\mathrm{D_{Tx}}, \mathrm{D_{Rx}}) \in \{(1,9),(3,7),(7,3),(9,1)\}$ coincide with the outer bound only if $\mathsf{S}^{(F)} \leq \mathsf{L}\cdot\frac{2(1-\alpha_1^\star)+\alpha_1^\star\cdot(\mathrm{D}+1)}{2\mathrm{D}+2}$, where $\alpha_1^\star$ depends on the choice of $(\mathrm{D_{Tx}}, \mathrm{D_{Rx}})$ and is defined in (4.30). The inner bounds for even-valued cooperation-rounds $(\mathrm{D_{Tx}}, \mathrm{D_{Rx}}) \in \{(2,8),(4,6),(6,4),(8,2)\}$ all coincide and attain the outer bound only if $\mathsf{S}^{(F)} \leq \mathsf{L}\cdot\frac{2}{2\mathrm{D}+2}$.

Figure 4.11 depicts our inner and outer bounds on the optimal MG region for the same $\mathrm{D} = 10$ but smaller values of $\mu_{\mathrm{Tx}} = \mu_{\mathrm{Rx}} = 0.3$. In Figure 4.11, we see that by decreasing μ_{Tx} and μ_{Rx} from 0.45 to 0.3, our inner and outer bounds do not coincide for all values of $\mathsf{S}^{(F)}$. Our inner bound for $\mathrm{D_{Rx}} = 5$ and $\mathrm{D_{Tx}} = 5$ contains all other inner bounds and it matches the outer bound in the regime $\mathsf{S}^{(F)} \leq \mathsf{L}\cdot\frac{2(1-\alpha_1^\star)+\alpha_1^\star\cdot(\mathrm{D}+1)}{2\mathrm{D}+2}$, where for the definition of $\alpha_1^\star$ in (4.30) one should set $\mathrm{D_{Tx}} = \mathrm{D_{Rx}} = 5$.

Figure 4.12 depicts our inner and outer bounds on the optimal MG region for the same $\mathrm{D} = 10$ but when $\mu_{\mathrm{Tx}} = 0.3$ is smaller than $\mu_{\mathrm{Rx}} = 0.45$. Here, the inner bound obtained for $(\mathrm{D_{Tx}} = 3, \mathrm{D_{Rx}} = 7)$ includes all other inner bounds and it matches the outer bound in the regime $\mathsf{S}^{(F)} \leq \mathsf{L}\cdot\frac{2(1-\alpha_1^\star)+\alpha_1^\star\cdot(\mathrm{D}+1)}{2\mathrm{D}+2}$, where $\alpha_1^\star$ is defined in (4.30) with $\mathrm{D_{Tx}} = 3$ and $\mathrm{D_{Rx}} = 7$.

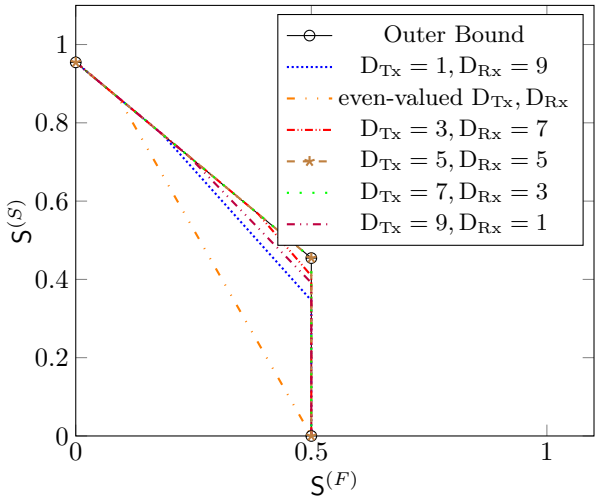

Figure 4.10: Bounds on $\mathcal{S}^\star(\mu_{\mathrm{Tx}}, \mu_{\mathrm{Rx}}, \mathrm{D})$ for $\mu_{\mathrm{Tx}} = 0.45$, $\mu_{\mathrm{Rx}} = 0.45$, $\mathrm{D} = 10$ and $\mathsf{L} = 1$ with both Tx- and Rx-cooperation.

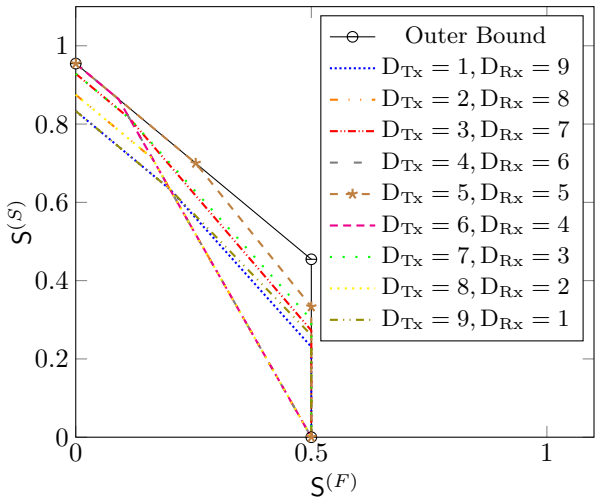

Figure 4.11: Bounds on $\mathcal{S}^\star(\mu_{\mathrm{Tx}}, \mu_{\mathrm{Rx}}, \mathrm{D})$ for $\mu_{\mathrm{Tx}} = 0.3$, $\mu_{\mathrm{Rx}} = 0.3$, $\mathrm{D} = 10$ and $\mathsf{L} = 1$ with both Tx- and Rx-cooperation.

The following corollaries generalise these observations.

Corollary 1. *If there exist integers $D_{Tx}, D_{Rx} \in \{1, 3, 5, \ldots, D-1\}$ summing to D such that the two constraints*

$$\mu_{\mathrm{Tx}} \geq \mu_{\mathrm{Tx,H}}(D_{Tx}) \tag{4.37a}$$

$$\mu_{\mathrm{Rx}} \geq \mu_{\mathrm{Rx,H}}(D_{Rx}) \tag{4.37b}$$

are simultaneously satisfied, then the optimal MG region $\mathcal{S}^\star(\mu_{\mathrm{Tx}}, \mu_{\mathrm{Rx}}, D)$ coincides with the trapezoidal

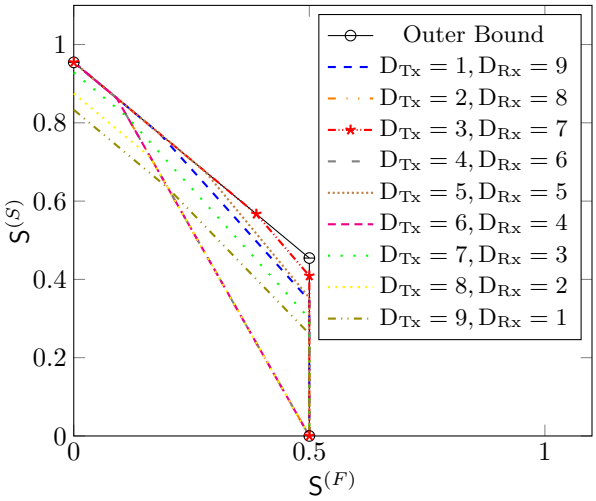

Figure 4.12: Bounds on $\mathcal{S}^\star(\mu_{\mathrm{Tx}}, \mu_{\mathrm{Rx}}, \mathrm{D})$ for $\mu_{\mathrm{Tx}} = 0.3$, $\mu_{\mathrm{Rx}} = 0.45$, $\mathrm{D} = 10$ and $\mathsf{L} = 1$ with both Tx- and Rx-cooperation.

region in (4.28). *That means,* $\mathcal{S}^\star(\mu_{\mathrm{Tx}}, \mu_{\mathrm{Rx}}, D)$ *is the set of all nonnegative pairs* $(\mathsf{S}^{(F)}, \mathsf{S}^{(S)})$ *satisfying*

$$\mathsf{S}^{(F)} \leq \frac{\mathsf{L}}{2}, \tag{4.38}$$

$$\mathsf{S}^{(F)} + \mathsf{S}^{(S)} \leq \mathsf{L} \cdot \frac{2D+1}{2D+2}. \tag{4.39}$$

Proof. Follows directly from the achievability result in Theorem 5, see (4.28), and the converse result in Proposition 1. For the converse result notice in particular that under constraints (4.37) the sum $\mu_{\mathrm{Tx}} + \mu_{\mathrm{Rx}}$ exceeds $\mathsf{L} \cdot \frac{\mathrm{D}}{2\mathrm{D}+2}$. □

Remark 4. *Under conditions* (4.37) *there is no penalty in sum-MG due to the stringent decoding constraint on "fast" messages. These "fast" messages can be submitted at maximum MG without decreasing the overall performance of the system.*

The following corollaries present partial characterizations of the optimal MG region $\mathcal{S}^\star(\mu_{\mathrm{Tx}}, \mu_{\mathrm{Rx}}, \mathrm{D})$ for $\mathsf{S}^{(F)}$ below a certain threshold.

Corollary 2. *If a pair of integers* $D_{Tx}, D_{Rx} \in \{1, 3, \ldots, D-1\}$ *summing to* D *satisfies*

$$\mu_{\mathrm{Tx}} \geq \mu_{\mathrm{Tx,L}}(D_{Tx}), \tag{4.40a}$$

$$\mu_{\mathrm{Rx}} \geq \mu_{\mathrm{Rx,L}}(D_{Rx}), \tag{4.40b}$$

then the optimal MG region $\mathcal{S}^\star(\mu_{\mathrm{Tx}}, \mu_{\mathrm{Rx}}, D)$ *contains the MG pair* $(\mathsf{S}^{(F)}, \mathsf{S}^{(S)})$ *with*

$$\mathsf{S}^{(F)} \leq \frac{\mathsf{L}}{2}\left(1 - \frac{D-1}{D+1}(1-\alpha_1^\star)\right) \tag{4.41}$$

(where $\alpha_1^\star$ *is defined in* (4.30) *and depends on the choice of* D_{Tx}, D_{Rx} *and on* μ_{Tx}, μ_{Rx}*) if, and only if,*

$$\mathsf{S}^{(F)} + \mathsf{S}^{(S)} \leq \mathsf{L} \cdot \frac{2D+1}{2D+2}. \tag{4.42}$$

Similarly, if a pair of integers $D_{Tx}, D_{Rx} \in \{2, 4, \ldots, D-2\}$ *summing to* D *satisfies* (4.40)*, then the optimal MG region* $\mathcal{S}^\star(\mu_{\mathrm{Tx}}, \mu_{\mathrm{Rx}}, D)$ *contains the MG pair* $(\mathsf{S}^{(F)}, \mathsf{S}^{(S)})$ *with*

$$\mathsf{S}^{(F)} \leq \frac{\mathsf{L}}{2} \cdot \frac{2}{D+1} \tag{4.43}$$

if, and only if,

$$\mathsf{S}^{(F)} + \mathsf{S}^{(S)} \leq \mathsf{L} \cdot \frac{2D+1}{2D+2}. \tag{4.44}$$

Noting the fundamental bound $S^{(F)} \leq \frac{\mathsf{L}}{2}$, one observes that when there is a odd-valued pair $\mathrm{D_{Tx}}, \mathrm{D_{Rx}} \in \{1, 3, \ldots, \mathrm{D}-1\}$ such that (4.40) holds and $\alpha_1^\star = 1$, then the first part of Corollary 2 recovers Corollary 1 and determines the entire optimal MG region $\mathcal{S}^\star(\mu_{\mathrm{Tx}}, \mu_{\mathrm{Rx}}, \mathrm{D})$.

Proof. Achievability of (4.42) follows from Theorem 5, see (4.29), because the two components of $\mathsf{S}_{\text{Inter-Partial}}(\alpha_1^\star) = (\mathsf{S}^{(S)}, \mathsf{S}^{(F)})$ satisfy:

$$\mathsf{S}^{(F)} = \alpha_1^\star \frac{\mathsf{L}}{2} + (1-\alpha_1^\star)\frac{\mathsf{L}}{2}\frac{2}{\mathrm{D}+1} = \frac{\mathsf{L}}{2}\left(1 - \frac{\mathrm{D}-1}{\mathrm{D}+1}(1-\alpha_1^\star)\right) \tag{4.45}$$

and

$$\mathsf{S}^{(S)} + \mathsf{S}^{(F)} = \mathsf{L} \cdot \frac{2\mathrm{D}+1}{2\mathrm{D}+2}. \tag{4.46}$$

Achievability of (4.44) can be proved in a similar way from Remark 3. The converse to both results follows from Proposition 1 because constraint (4.42) implies that the sum $\mu_{\mathrm{Tx}} + \mu_{\mathrm{Rx}}$ exceeds $\mathsf{L} \cdot \frac{\mathrm{D}}{2\mathrm{D}+2}$. □

Corollary 3. *If*

$$\mu_{\mathrm{Rx}} + \mu_{\mathrm{Tx}} \quad < \quad \mathsf{L} \cdot \frac{D}{2D+2} \tag{4.47}$$

and if a pair $D_{Tx}, D_{Rx} \in \{1, 2, 3, \ldots, D-1\}$ *(both odd and even values are allowed) summing to* D *satisfies*

$$\frac{\mu_{\mathrm{Tx}}}{D_{Tx}} \quad = \quad \frac{\mu_{\mathrm{Rx}}}{D_{Rx}}, \tag{4.48}$$

then the optimal MG region $\mathcal{S}^{\star}(\mu_{\mathrm{Tx}}, \mu_{\mathrm{Rx}}, D)$ *contains the MG pair* $(\mathsf{S}^{(F)}, \mathsf{S}^{(S)})$ *with*

$$\mathsf{S}^{(F)} \leq \frac{\mathsf{L}}{2}\left(1 - \mu_{Tx}\frac{2(D-1)}{\mathsf{L} \cdot D_{Tx}}\right) \tag{4.49}$$

if, and only if,

$$\mathsf{S}^{(F)} + \mathsf{S}^{(S)} \leq \frac{\mathsf{L}}{2} + \mu_{\mathrm{Tx}} + \mu_{\mathrm{Rx}}. \tag{4.50}$$

Proof. The result (4.50) follows from the converse result in Proposition 1 and the achievability results in Theorem 5, see (4.32), and Remark 3. More specifically, to prove achievability let D_{Tx} and D_{Rx} be such that Condition (4.48) is satisfied. Then,

$$\frac{\mu_{\mathrm{Tx,L}}(\mathrm{D}_{\mathrm{Tx}})}{\mu_{\mathrm{Tx}}} = \frac{\mu_{\mathrm{Rx,L}}(\mathrm{D}_{\mathrm{Rx}})}{\mu_{\mathrm{Rx}}} \tag{4.51}$$

and Condition (4.47) implies that both inequalities

$$\mu_{\mathrm{Tx}} < \mu_{\mathrm{Tx,L}} \qquad \text{and} \qquad \mu_{\mathrm{Rx}} < \mu_{\mathrm{Rx,L}} \tag{4.52}$$

are satisfied. Moreover, $\alpha_2^{\star}$ as defined in (4.33) satisfies

$$\alpha_2^{\star} = \frac{\mu_{\mathrm{Tx}}}{\mu_{\mathrm{Tx,L}}} = \mu_{\mathrm{Tx}}\frac{2\mathrm{D}+2}{\mathsf{L} \cdot \mathrm{D}_{\mathrm{Tx}}} = \frac{\mu_{\mathrm{Rx}}}{\mu_{\mathrm{Rx,L}}} = \mu_{\mathrm{Rx}}\frac{2\mathrm{D}+2}{\mathsf{L} \cdot \mathrm{D}_{\mathrm{Rx}}}. \tag{4.53}$$

Notice next that for the two MG pairs $\mathsf{S}_{\mathrm{Coop}}(\alpha_2^{\star})$ and $\mathsf{S}_{\mathrm{Partial}}(\alpha_2^{\star})$, which are achievable by either Theorem 5 or Remark 3, the sum of the two components satisfies

$$\mathsf{S}^{(F)} + \mathsf{S}^{(S)} = \alpha_2^{\star} \cdot \frac{\mathsf{L}}{2} \cdot \frac{2\mathrm{D}+1}{\mathrm{D}+1} + (1-\alpha_2^{\star})\frac{\mathsf{L}}{2} = \frac{\mathsf{L}}{2} + \frac{\mu_{\mathrm{Tx}}}{\mathrm{D}_{\mathrm{Tx}}}\mathrm{D} = \frac{\mathsf{L}}{2} + \mu_{\mathrm{Tx}} + \mu_{\mathrm{Rx}}, \tag{4.54}$$

where in the last equation we used (4.48). Moreover, the "fast" MG $\mathsf{S}^{(F)}$ in $\mathsf{S}_{\text{Coop}}(\alpha_2^\star)$ equals 0, whereas in $\mathsf{S}_{\text{Partial}}(\alpha_2^\star)$ it equals

$$\mathsf{S}^{(F)} = \alpha_2^\star \cdot \frac{\mathsf{L}}{2} \cdot \frac{2}{\mathrm{D}+1} + (1-\alpha_2^\star)\frac{\mathsf{L}}{2} = \frac{\mathsf{L}}{2}\left(1 - \mu_{\text{Tx}}\frac{2(\mathrm{D}-1)}{\mathsf{L}\cdot \mathrm{D}_{\text{Tx}}}\right) = \frac{\mathsf{L}}{2}\left(1 - \mu_{\text{Rx}}\frac{2(\mathrm{D}-1)}{\mathsf{L}\cdot \mathrm{D}_{\text{Rx}}}\right). \tag{4.55}$$

Since one can always choose to transmit at smaller MGs and because the convex hull of all achievable MG pairs is also achievable, this concludes the proof of achievability. □

Remark 5. *For both corollaries, in the regimes where we could characterize the optimal MG region, i.e., for "fast" MGs below a certain threshold, the sum-MG is at its maximum. We can thus conclude that for sufficiently small $\mathsf{S}^{(F)}$ the sum-MG is not decreased due to the stringent constraint on the "fast" messages.*

In the following subsections we present the coding schemes achieving the MG regions in Theorem 5 and Remark 3.

4.5.2 Scheme Achieving MG Pair (4.26c)

Let each Tx only send "slow" messages but no "fast" messages. Under this coding assumption, our setup is a multi-antenna version of the setup in [46]. Achievability of (4.26c) then follows immediately by the multi-antenna version of [46, Theorem 1]. We redescribe the coding schemes achieving (4.26c) for completeness and reference in the next subsection.

We silence every 2D+2nd Tx, which splits the network into smaller subnets. In each subnet, we combine the SIC idea explained for the setup with only Rx-cooperation (see Subsection 4.2.1) with the DPC coding idea that was explained for the setup with only Tx-cooperation (see Subsection 4.3.1). The scheme for the first subnet is illustrated in Figure 4.13 and will be explained in the following. Communication in the other subnets is similar.

The Tx/Rx pairs of the first subnet are assigned to four groups, depending on their mode of operation. Notice that the Tx/Rx pair $\mathrm{D}_{\text{Rx}} + 2\mathrm{D}_{\text{Tx}} + 2$ is assigned to both groups $\mathcal{G}_3$ and $\mathcal{G}_4$, whereas all other Tx/Rx pairs are assigned to only one group. The reason is that message $M^{(S)}_{\mathrm{D}_{\text{Rx}}+2\mathrm{D}_{\text{Tx}}+2}$ is split into two parts $(M^{(S,3)}_{\mathrm{D}_{\text{Rx}}+2\mathrm{D}_{\text{Tx}}+2}, M^{(S,4)}_{\mathrm{D}_{\text{Rx}}+2\mathrm{D}_{\text{Tx}}+2})$ of equal rates, and part $M^{(S,3)}_{\mathrm{D}_{\text{Rx}}+2\mathrm{D}_{\text{Tx}}+2}$ is communicated in the same way as the messages for Tx/Rx pairs in group $\mathcal{G}_3$, whereas $M^{(S,4)}_{\mathrm{D}_{\text{Rx}}+2\mathrm{D}_{\text{Tx}}+2}$ is communicated in the same way as the messages for Tx/Rx pairs in group $\mathcal{G}_4$.

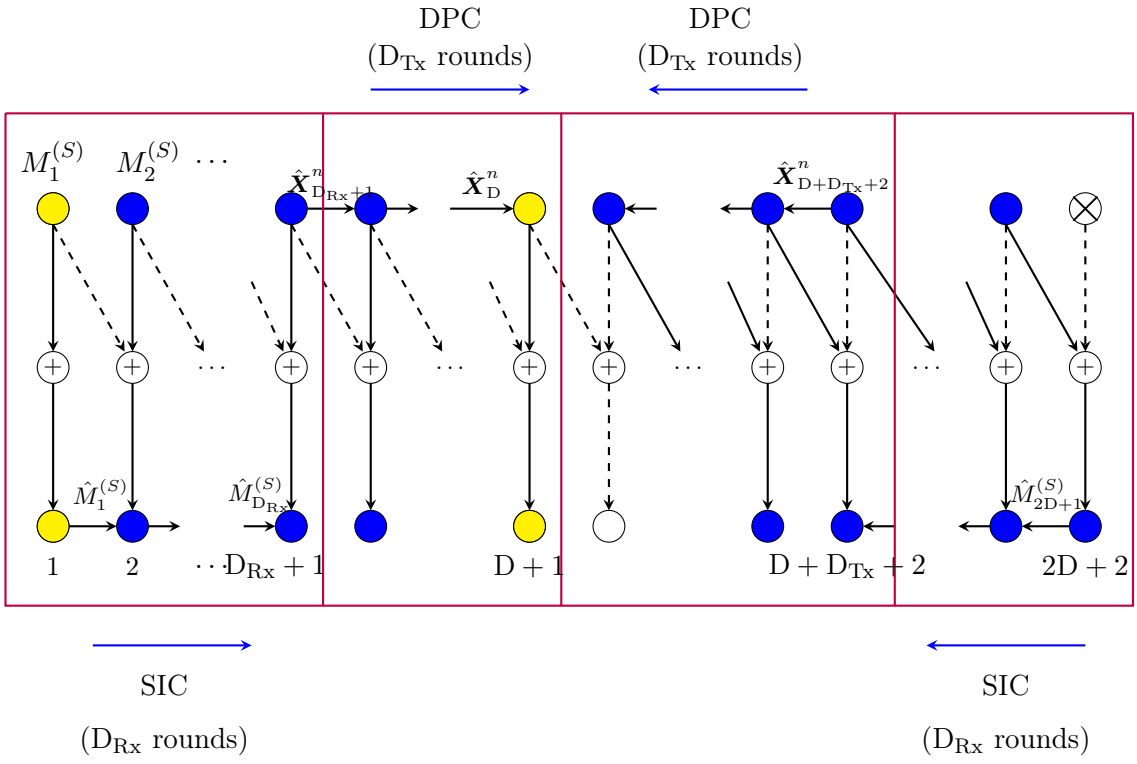

Figure 4.13: Scheme with Rx- and Tx-cooperation.

Group $\mathcal{G}_1 \triangleq \{1, \ldots, D_{Rx}+1\}$*:* Each Tx $k \in \mathcal{G}_1$ encodes its "slow" message $M_k^{(S)}$ using a codeword $\boldsymbol{X}_k^n(M_k^{(S)})$ from a Gaussian point-to-point code of power P, and transmits this codeword over the channel: $\boldsymbol{X}_k^n = \boldsymbol{X}_k^n(M_k^{(S)})$. Each Rx $k \in \mathcal{G}_1$ uses the cooperation message received from its left neighbour Rx $k-1$ for SIC, i.e., to delete the interference term $\mathsf{H}_{k-1,k}\boldsymbol{X}_{k-1}^n(\hat{M}_{k-1}^{(S)})$ from its output sequence $\boldsymbol{Y}_k^n$:

$$\hat{\boldsymbol{Y}}_k^n = \boldsymbol{Y}_k^n - \mathsf{H}_{k-1,k}\boldsymbol{X}_{k-1}^n(\hat{M}_{k-1}^{(S)}), \tag{4.56}$$

and to decode its desired message $M_k^{(S)}$ based on $\hat{\boldsymbol{Y}}_k^n$. Rx k also describes its decoded message $\hat{M}_k$ over the cooperation link to Rx $k+1$, so as to facilitate SIC at this next Rx.

To facilitate the transmissions in the next group, the last Tx of group $\mathcal{G}_1$, Tx $\mathrm{D_{Rx}}+1$, precodes its channel inputs $\boldsymbol{X}_{\mathrm{D_{Rx}}+1}^n$ with the matrix $\mathsf{H}_{\mathrm{D_{Rx}}+2,\mathrm{D_{Rx}}+2}^{-1}\mathsf{H}_{\mathrm{D_{Rx}}+1,\mathrm{D_{Rx}}+2}$, quantises the produced sequence $\boldsymbol{I}_{\mathrm{D_{Rx}}+1}^n \triangleq \mathsf{H}_{\mathrm{D_{Rx}}+2,\mathrm{D_{Rx}}+2}^{-1}\mathsf{H}_{\mathrm{D_{Rx}}+1,\mathrm{D_{Rx}}+2}\boldsymbol{X}_{\mathrm{D_{Rx}}+1}^n$ with a rate-$\mathsf{L}/2\log(1+\mathsf{P})$ quantiser to obtain the quantisation $\hat{\boldsymbol{I}}_{\mathrm{D_{Rx}}+1}^n$ at noise level and sends the resulting quantisation index as a first-round cooperation message to the first Tx in group $\mathcal{G}_2$, i.e. to Tx $\mathrm{D_{Rx}}+2$.

Group $\mathcal{G}_2 \triangleq \{D_{Rx}+2,\ldots,D_{Rx}+D_{Tx}+1\}$*:* Each Tx $k \in \mathcal{G}_2$ obtains a cooperation message from its left neighbour Tx $k-1$ that describes the quantised version $\hat{\boldsymbol{I}}_{k-1}^n$ of $\boldsymbol{I}_{k-1}^n \triangleq \mathsf{H}_{k,k}^{-1}\mathsf{H}_{k-1,k}\boldsymbol{X}_{k-1}^n$. Based on this message, Tx k reconstructs $\hat{\boldsymbol{I}}_{k-1}^n$, encodes its "slow" message $M_k^{(S)}$ using a power P DPC that mitigates the interference $\hat{\boldsymbol{I}}_{k-1}^n$, and sends the resulting DPC sequence $\boldsymbol{X}_k^n$ over the channel. Moreover, it precodes this input sequence with the matrix $\mathsf{H}_{k+1,k+1}^{-1}\mathsf{H}_{k,k+1}$, quantises the precoded sequence $\boldsymbol{I}_k^n \triangleq \mathsf{H}_{k+1,k+1}^{-1}\mathsf{H}_{k,k+1}\boldsymbol{X}_k^n$ with a rate-$\mathsf{L}/2\log(1+\mathsf{P})$ quantiser (for a quantisation at noise level) to obtain $\hat{\boldsymbol{I}}_k^n$, and sends the quantisation message as a round-k cooperation message over the link to its right neighbour. Tx $\mathrm{D_{Tx}}+\mathrm{D_{Rx}}+1$ produces its inputs in a similar way, i.e., using DPC, but sends no cooperation message at all. Rxs in $\mathcal{G}_2$ use a standard DPC decoding rule based on the premultiplied outputs

$$\mathsf{H}_{k,k}^{-1}\boldsymbol{Y}_k^n = \mathsf{H}_{k,k}^{-1}\mathsf{H}_{k-1,k}\boldsymbol{X}_{k-1}^n + \boldsymbol{X}_k^n + \mathsf{H}_{k,k}^{-1}\boldsymbol{Z}_k^n, \tag{4.57}$$

to decode their intended "slow" messages. (Recall that $\boldsymbol{X}_k^n$ was produced as a DPC sequence that mitigates $\hat{\boldsymbol{I}}_{k-1}^n$, a quantised version of $\mathsf{H}_{k,k}^{-1}\mathsf{H}_{k-1,k}\hat{\boldsymbol{X}}_{k-1}^n$). Since quantisation was performed at noise level, each message $M_{\mathrm{D_{Rx}}+2}^{(S)},\ldots,M_{\mathrm{D}+1}^{(S)}$ can be sent reliably with MG L.

Group $\mathcal{G}_3 \triangleq \{D_{Rx}+D_{Tx}+2,\ldots,D_{Rx}+2D_{Tx}+2\}$*:* This group of Tx/Rx pairs participates in the transmission of the "slow" messages

$$M_{\mathrm{D_{Rx}}+\mathrm{D_{Tx}}+3}^{(S)},\ldots,M_{\mathrm{D_{Rx}}+2\mathrm{D_{Tx}}+1}^{(S)},M_{\mathrm{D_{Rx}}+2\mathrm{D_{Tx}}+2}^{(S,3)}. \tag{4.58}$$

In particular, Tx $\mathrm{D_{Rx}}+2\mathrm{D_{Tx}}+2$ does not send an own message to its corresponding Rx.

Each of the messages in (4.58) is transmitted over the communication path Tx $k \to$ Tx $k-1 \to$ Rx k for some $k \in \{\mathrm{D_{Rx}}+\mathrm{D_{Tx}}+3,\ldots,\mathrm{D_{Rx}}+2\mathrm{D_{Tx}}+2\}$.

For each $k \in \{\mathrm{D_{Rx}}+\mathrm{D_{Tx}}+3,\ldots,\mathrm{D_{Rx}}+2\mathrm{D_{Tx}}+2\}$, Tx k encodes its own "slow" message $M_k^{(S)}$ by means of DPC of power P that mitigates the interference $\mathsf{H}_{k-1,k}^{-1}\mathsf{H}_{k,k}\boldsymbol{X}_k^n$ of the signal sent by Tx k itself; precodes the obtained sequence $\boldsymbol{U}_k^n$ with the matrix $\mathsf{H}_{k-1,k}^{-1}\mathsf{H}_{k,k}$; quantises the precoded sequence $\boldsymbol{S}_{k-1}^n \triangleq \mathsf{H}_{k-1,k}^{-1}\mathsf{H}_{k,k}\boldsymbol{U}_k^n$ to obtain a quantisation $\hat{\boldsymbol{S}}_{k-1}$ at noise level; and sends the corresponding quantisation message as a $(2\mathrm{D}+3-k)$-round cooperation message over the link to Tx $k-1$. Tx $k-1$ then reconstructs $\hat{\boldsymbol{S}}_{k-1}^n$ and sends it over the channel: $\boldsymbol{X}_{k-1}^n = \hat{\boldsymbol{S}}_{k-1}^n$. The construction of the transmit signal $X_{\mathrm{D_{Rx}}+2\mathrm{D_{Tx}}+2}^n$ mentioned above, is explained in the following paragraph. RXs $\mathrm{D_{Rx}}+\mathrm{D_{Tx}}+3,\ldots,\mathrm{D_{Rx}}+2\mathrm{D_{Tx}}+2$ decode

their intended "slow" messages using an optimal DPC decoding rule based on the premultiplied outputs

$$\mathsf{H}_{k-1,k}^{-1}\boldsymbol{Y}_k^n = \boldsymbol{X}_{k-1}^n + \mathsf{H}_{k-1,k}^{-1}\mathsf{H}_{k,k}\boldsymbol{X}_k^n + \mathsf{H}_{k-1,k}^{-1}\boldsymbol{Z}_k^n. \tag{4.59}$$

Recall that $\boldsymbol{X}_{k-1}^n$ is a quantised version (at noise level) of the precoded signal $\boldsymbol{S}_{k-1}^n \triangleq \mathsf{H}_{k-1,k}^{-1}\mathsf{H}_{k,k}\boldsymbol{U}_k^n$ for $\boldsymbol{U}_k^n$ a DPC sequence that mitigates the interference $\mathsf{H}_{k-1,k}^{-1}\mathsf{H}_{k,k}\boldsymbol{X}_k^n$. Each of the messages $M_{\mathrm{D}+3}^{(S)}, \ldots, M_{2\mathrm{D}+2}^{(S)}$ can thus be transmitted reliably at full MG L.

Group $\mathcal{G}_4 \triangleq \{D_{Rx} + 2D_{Tx} + 2, \ldots, 2D_{Rx} + 2D_{Tx} + 2\}$*:* This group of Tx/Rx pairs participates in the transmission of the "slow" messages

$$M_{\mathrm{D_{Rx}}+2\mathrm{D_{Tx}}+2}^{(S,4)}, M_{\mathrm{D_{Rx}}+2\mathrm{D_{Tx}}+3}^{(S)}, \ldots, M_{2\mathrm{D_{Rx}}+2\mathrm{D_{Tx}}+1}^{(S)}. \tag{4.60}$$

Tx $2\mathrm{D_{Rx}}+2\mathrm{D_{Tx}}+2$ thus is not sending an own message to its corresponding Rx. The messages in (4.60) are transmitted over the path Tx $k \to$ Rx $k+1 \to$ Rx k, for some $k \in \{\mathrm{D_{Rx}} + 2\mathrm{D_{Tx}} + 2, \ldots, 2\mathrm{D_{Rx}} + 2\mathrm{D_{Tx}} + 2\}$.

Each Tx $k \in \{\mathrm{D_{Rx}} + 2\mathrm{D_{Tx}} + 2, \ldots, 2\mathrm{D_{Rx}} + 2\mathrm{D_{Tx}} + 1\}$ encodes its "slow" message $M_k^{(S)}$ (or $M_k^{(S,4)}$ if $k = \mathrm{D_{Rx}} + 2\mathrm{D_{Tx}} + 2$) using a codeword from a Gaussian codebook of power P, and sends this codeword over the channel $\boldsymbol{X}_k^n = \boldsymbol{X}_k^n(M_k^{(S)})$ (or $\boldsymbol{X}_k^n = \boldsymbol{X}_k^n(M_k^{(S,4)})$ if $k = \mathrm{D_{Rx}} + 2\mathrm{D_{Tx}} + 1$).

Rx $2\mathrm{D_{Rx}} + 2\mathrm{D_{Tx}} + 2$ decodes $M_{2\mathrm{D_{Rx}}+2\mathrm{D_{Tx}}+1}^{(S)}$ based on an interference-free output $\boldsymbol{Y}_{2\mathrm{D_{Rx}}+2\mathrm{D_{Tx}}+2}^n = \mathsf{H}_{2\mathrm{D_{Rx}}+2\mathrm{D_{Tx}}+1,2\mathrm{D_{Rx}}+2\mathrm{D_{Tx}}+2}\boldsymbol{X}_{2\mathrm{D_{Rx}}+2\mathrm{D_{Tx}}+1}^n + \boldsymbol{Z}_{2\mathrm{D_{Rx}}+2\mathrm{D_{Tx}}+2}^n$, and sends the decoded message $\hat{M}_{2\mathrm{D_{Rx}}+2\mathrm{D_{Tx}}+1}^{(S)}$ over the cooperation link to the intended Rx $2\mathrm{D_{Rx}} + 2\mathrm{D_{Tx}} + 1$. For $k = 2\mathrm{D_{Rx}}+2\mathrm{D_{Tx}}+1, \ldots, \mathrm{D_{Rx}}+2\mathrm{D_{Tx}}+3$, Rx k uses the cooperation message received from its right neighbour Rx $k+1$ to decode $M_{k-1}^{(S)}$ (or $M_{k-1}^{(S,4)}$ if $k = \mathrm{D_{Rx}} + 2\mathrm{D_{Tx}} + 2$) using SIC, i.e., to first delete the interference $\mathsf{H}_{k,k}\boldsymbol{X}_k^n$ from $\boldsymbol{Y}_k^n$ and then decode message $M_{k-1}^{(S)}$ (or $M_{k-1}^{(S,4)}$ if $k = \mathrm{D_{Rx}} + 2\mathrm{D_{Tx}} + 2$) from an interference-free signal. Rx k then sends the decoded message $\hat{M}_{k-1}^{(S)}$ (or $\hat{M}_{k-1}^{(S,4)}$ if $k = \mathrm{D_{Rx}} + 2\mathrm{D_{Tx}} + 2$) over the cooperation link to its left neighbour Rx $k-1$, which is the intended Rx for this message.

In the described scheme, each transmitted message is either decoded based on interference-free outputs or using DPC. Since precoding matrices do not depend on the power and quantizations are performed at noise levels, all messages can be transmitted reliably at MG L. Tx $\mathrm{D_{Rx}}+2\mathrm{D_{Tx}}+2$ sends two "slow" messages and $2\mathrm{D_{Rx}} + 2\mathrm{D_{Tx}} - 1$ other Txs send one "slow" message. An average "slow" MG of $\mathsf{L} \cdot \frac{2\mathrm{D_{Rx}}+2\mathrm{D_{Tx}}+1}{2\mathrm{D_{Rx}}+2\mathrm{D_{Tx}}+2}$ is thus achieved in each subnet. Moreover, $2\mathrm{D_{Rx}} + 2\mathrm{D_{Tx}}$ cooperation messages of prelog L are sent in each subnet:

- Rxs in $\mathcal{G}_1$ send $\mathrm{D_{Rx}}$ Rx-cooperation messages with prelog L;

- Txs in $\mathcal{G}_2$ send $\mathrm{D_{Tx}}$ Tx-cooperation messages with prelog L;

- Txs in $\mathcal{G}_3$ send $\mathrm{D_{Tx}}$ Tx-cooperation messages with prelog L;

- Rxs in $\mathcal{G}_4$ send $\mathrm{D_{Rx}}$ Rx-cooperation messages with prelog L.

The *average* cooperation prelog *per link* at the Tx-side is $\mu_{\mathrm{Tx,L}}$ and at the Rx-side it is $\mu_{\mathrm{Rx,L}}$. If one time-shares $2\mathrm{D}+2$ different instances of the described scheme with a different subset of silenced users in each of them, the overall scheme still achieves the MG pair $(S^{(F)}=0, S^{(S)}=\mathsf{L}\frac{2\mathrm{D}+1}{2\mathrm{D}+2})$ in (4.26d), each Tx-cooperation link is loaded at exactly this average cooperation prelog $\mu_{\mathrm{Tx,L}}$, and each Rx-cooperation link is loaded at the average cooperation prelog $\mu_{\mathrm{Rx,L}}$.

4.5.3 Scheme Achieving MG Pair (4.26d)

Consider the scheme described in the previous Subsection 4.5.2 and depicted in Figure 4.13. Notice that the first Tx in each subnet does not at all participate in the cooperation, and decoding of its message also does not rely on cooperation messages. The same observation applies also to the $\mathrm{D_{Rx}}+\mathrm{D_{Tx}}+1$st Tx of each subnet and its message. The first and the $\mathrm{D_{Rx}}+\mathrm{D_{Tx}}+1$st message of each subnet (the yellow Txs in Figure 4.13) thus satisfy the requirements on "fast" messages. We propose to use this scheme but let the first and the $(\mathrm{D_{Rx}}+\mathrm{D_{Tx}}+1)$st messages in each subnet be "fast" messages and all other messages be "slow" messages. This achieves the MG pair (4.26d).

The required cooperation rates equal $\mu_{\mathrm{Tx,L}}$ and $\mu_{\mathrm{Rx,L}}$, as explained in the previous Subsection 4.5.2.

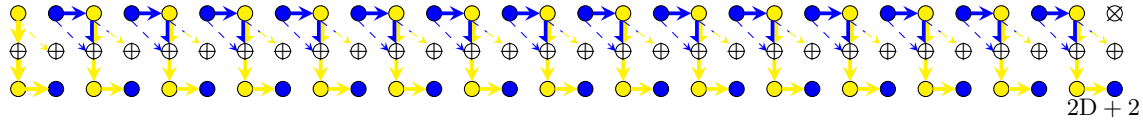

(a) Communicating "fast" messages

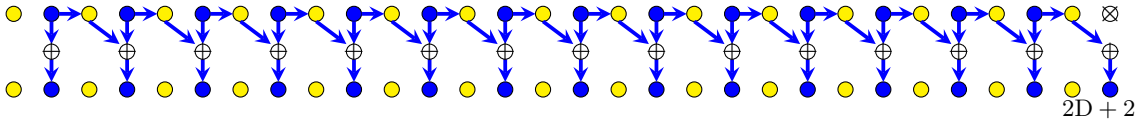

(b) Interference graph of "slow" messages transmissions

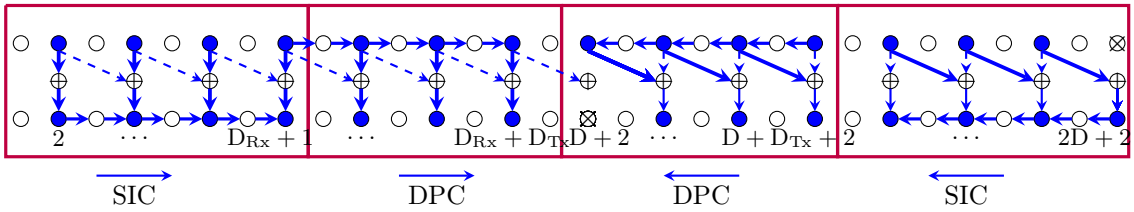

(c) Communicating "slow" messages

Figure 4.14: An illustration of the scheme achieving MG pair (4.26e). Notice that since D is even, the last Tx of $\mathcal{G}_2$ sends a "fast" message. And since D_{Rx} is odd, also the first Tx in $\mathcal{G}_4$ sends a "fast" message.

4.5.4 Schemes Achieving MG Pair (4.26e)

We periodically silence every $2D+2$-nd Tx to split the network into smaller subnets. Then we send a "fast" message on all odd Txs and a "slow" message on all even Txs, except for the previously silenced Txs (which are all even). See Fig. 4.14.

In what follows, we describe and analyze transmissions over the first subnet. Other subnets are treated analogously.

Odd Txs $1, 3, 5, \ldots, 2D+1$*:* Each odd Tx encodes its "fast" message $M_k^{(F)}$ using a codeword $\boldsymbol{U}_k^n(M_k^{(F)})$ from a Gaussian codebook of power P that depends on the Tx and the channel realizations and is explained later. Tx 1 simply sends this Gaussian codeword $\boldsymbol{X}_1^n = \boldsymbol{U}_1^n(M_1^{(F)})$. Any other odd Tx k first considers the cooperation message it received from its left neighbour Tx $k-1$ and reconstructs $\hat{\boldsymbol{X}}_{k-1}^n$, a quantised version of Tx $k-1$th input $\boldsymbol{X}_{k-1}^n$. Tx k then sends the input signal

$$\boldsymbol{X}_k^n = \boldsymbol{U}_k^n(M_k^{(F)}) - \mathsf{H}_{k,k}^{-1}\mathsf{H}_{k-1,k}\hat{\boldsymbol{X}}_{k-1}^n. \tag{4.61}$$

Odd Txs relay some of the cooperation messages they obtain from their neighbours, as will become clear in the following, but they do not create new cooperation messages.

Odd Rxs $1, 3, 5, \ldots, 2D+1$*:* Given the precanceling at odd Txs described above, each odd Rx k observes an almost interference-free signal:

$$\boldsymbol{Y}_k^n = \mathsf{H}_{k,k}\boldsymbol{U}_k^n + \mathsf{H}_{k-1,k}(\boldsymbol{X}_{k-1}^n - \hat{\boldsymbol{X}}_{k-1}^n) + \boldsymbol{Z}_{k,k}, \tag{4.62}$$

where notice that $\hat{\boldsymbol{X}}_{k-1}^n$ is a quantised version of $\boldsymbol{X}_{k-1}^n$ at noise level. Each odd Rx k therefore decodes its desired fast message $M_k^{(F)}$ using standard point-to-point decoding. It also sends the decoded message $\hat{M}_k^{(F)}$ over the cooperation link to its right neighbour Rx $k+1$ as a first round cooperation message.

Odd Rxs also relay some of the cooperation messages they obtain from their neighbours, as will become clear in the following.

Before describing the operations at the even Tx/Rx pairs, we make the following observations based on the operations at the odd Tx/Rx pairs. Irrespective of the operations performed at the even Txs, each even Rx k observes the sum of a signal depending only on "slow" messages and a signal depending only on its left-neighbour's "fast" message (the signal $\mathsf{H}_{k-1,k}\boldsymbol{U}_{k-1}^n$). Since odd Rxs convey their decoded "fast" messages to their right-neighbour, even Rxs can cancel the signals depending on "fast" messages whenever they have been decoded correctly. There is thus no loss in reliable communication rate caused by the transmission of "fast" messages. And transmission of "slow" messages at even Txs can be designed as if no "fast" messages were present. However, if "slow" Rxs wish to send cooperation messages that do not depend on the "fast" transmissions, they have to wait for the second round.

Even Txs $2, 4, 6, \ldots, 2D$*:* Each even Tx k, for $k = 2, \ldots, 2\mathrm{D}$, performs the same steps as Tx k in the scheme described in Section 4.5.2, but where the scheme needs to be adapted to include only even Txs. In particular, if an even Tx k previously sent a quantisation message to its direct left- or right-neighbour Tx $k-1$ or $k+1$, now it will send it to the previous or following *even* Tx $k-2$ or Tx $k+2$. (This simply means that the odd Tx lying between them has to relay the cooperation message as we already mentioned previously.) Similarly, when using DPC, if Tx k previously mitigated the quantised sequence $\hat{\boldsymbol{I}}_{k-1}^n$ or $\hat{\boldsymbol{S}}_{k+1}^n$, now it mitigates the quantised sequence $\hat{\boldsymbol{I}}_{k-2}^n$ or $\hat{\boldsymbol{S}}_{k+2}^n$. Notice that since D is even, Tx D is the last even Tx in $\mathcal{G}_2$ (so the last Tx in $\mathcal{G}_2$ sending a "slow" message). Tx-cooperation in group $\mathcal{G}_2$ thus takes place only during the first $\mathrm{D_{Tx}} - 1$ rounds. The only Tx-cooperation message in round $\mathrm{D_{Tx}}$ is the message sent from

Tx $\mathrm{D}+3$ to Tx $\mathrm{D}+2$ in group $\mathcal{G}_3$.

In addition, if this is not already done as part of the scheme in Section 4.5.2, any even Tx k also quantizes its channel inputs $\boldsymbol{X}_k^n$ at rate $\mathsf{L}\cdot 1/2\log(1+\mathsf{P})$ to generate the quantised sequence $\hat{\boldsymbol{I}}_k^n$. The quantisation message describing $\hat{\boldsymbol{I}}_k^n$ is then sent as a $\mathrm{D_{Tx}}$-round cooperation message over the link to Tx $k+1$ to allow this Tx to precancel this interference in the way that was described previously. Even Tx $\mathrm{D}+2$ (the first Tx in group $\mathcal{G}_3$) does not need to send this round-$\mathrm{D_{Tx}}$ cooperation message because its right neighbour Tx $\mathrm{D}+3$ already learns the Tx signal $\boldsymbol{X}_{\mathrm{D}+2}^n$ as part of the proposed scheme in Section 4.5.2. Since all even Txs (except for Tx $\mathrm{D}+2$) receive their last cooperation message in round $\mathrm{D_{Tx}}-1$, they can indeed compute their input perior to the last round $\mathrm{D_{Tx}}$ and thus perform the proposed round-$\mathrm{D_{Tx}}$ cooperation.

Even Rxs $2,4,6,\ldots,2D+2$*:* Using the round-1 Rx-cooperation messages from its left neighbour, each even Rx k, for $k=2,\ldots,2\mathrm{D}+2$, first subtracts the interference caused by the transmission of the "fast" message $M_{k-1}^{(F)}$ at its left neighbour. That means, it forms

$$\tilde{\boldsymbol{Y}}_k^n=\boldsymbol{Y}_k^n-\mathsf{H}_{k-1,k}\boldsymbol{U}_{k-1}^n. \tag{4.63}$$

It then proceeds with this modified output sequence $\tilde{\boldsymbol{Y}}_k^n$ and performs all the steps as Rx k did in the scheme in Section 4.5.2, but where the scheme again needs to be adapted to include only even Rxs and it also needs to be adapted to start only at cooperation round 2. This allows even Rxs to calculate (4.63) before performing the other steps. Notice that since the first Txs of $\mathcal{G}_1$ and $\mathcal{G}_4$ only send "fast" messages (the latter holds because $\mathrm{D_{Rx}}$ is odd), there is no harm in waiting for this second round. To adapt the scheme in Section 4.5.2 only to even Rxs, any even Rx k that previously sent its decoded message to its direct left- or right-neighbour Rx $k-1$ or Rx $k+1$, now sends it to the previous or following *even* Rx $k-2$ or Rx $k+2$. Similarly, any Rx k that previously applied the SIC step to cancel the interference from Tx $k-1$ or Tx $k+1$, now cancels the interference from Tx $k-2$ or Tx $k+2$.

In the described scheme, all odd Txs of a subnet can send reliably a "fast" message of MG L and the even Txs $\{2,4,\ldots,2\mathrm{D}\}$ each can send reliably a "slow" message of MG L. The scheme thus achieves the MG pair in (4.26e): $(\mathsf{S}^{(F)}=\frac{\mathsf{L}}{2},\mathsf{S}^{(S)}=\mathsf{L}\cdot\frac{\mathrm{D}}{2\mathrm{D}+2})$.

We now analyze the cooperation prelog of the described scheme. Recall that in this scheme each even Tx sends a quantised version of its inputs to its right neighbour and each odd Rx sends its decoded message to its right neighbour. Since each of these cooperation messages is of prelog L the described messages consume a Tx-cooperation prelog of $\mathsf{L}\cdot\mathrm{D}$ and a Rx-cooperation prelog of $\mathsf{L}\cdot\mathrm{D}$.

In addition, for encoding and decoding of "slow" messages:

- Rxs in $\mathcal{G}_1$ send $\mathrm{D_{Rx}}-1$ Rx-cooperation messages with prelog L. (The cooperation message from Rx 1 to Rx 2 has already been counted in the previous paragraph.)
- Txs in $\mathcal{G}_2$ send $(\mathrm{D_{Tx}}-1)/2$ Tx-cooperation messages with prelog L. (The cooperation message from even to odd Txs in $\mathcal{G}_2$ have already been counted in the previous paragraph.)
- Txs in $\mathcal{G}_3$ send $\mathrm{D_{Tx}}$ Tx-cooperation messages with prelog L.
- Rxs in $\mathcal{G}_4$ send $\mathrm{D_{Rx}}-1$ Rx-cooperation messages with prelog L. (The first Rx in $\mathcal{G}_4$ does not obtain a cooperation message because it is a "fast" Tx.)

To summarize, the described scheme requires an *average prelog per Tx-cooperation link* of $\mu_{\mathrm{Tx,H}} = \mathsf{L}\cdot\frac{\frac{\mathrm{D}}{2}+\frac{3}{4}\mathrm{D_{Tx}}-\frac{1}{4}}{2\mathrm{D}+2}$ and an *average prelog per Rx-cooperation link* of $\mu_{\mathrm{Rx,H}} = \mathsf{L}\cdot\frac{\frac{\mathrm{D}}{2}+\mathrm{D_{Rx}}-1}{2\mathrm{D}+2}$. (Notice that this is larger than in the scheme in Subsection 4.5.2.) If one time-shares $2\mathrm{D}+2$ different instances of the described scheme with a different subset of silenced users in each of them, the required prelog on each Tx-cooperation link is exactly $\mu_{\mathrm{Tx,H}}$ and the required prelog on each Rx-cooperation link is exactly $\mu_{\mathrm{Rx,H}}$. This concludes the proof.

Chapter 5

Mixed Delay Coding Scheme with CoMP Transmission and Reception

In this chapter, we propose a general coding scheme for arbitrary networks that accommodates the transmissions of "slow" and "fast" messages simultaneously. We apply this coding scheme to three cellular network models: Wyner's symmetric model, the hexagonal model, and the sectorized hexagonal model. The results for Wyner's symmetric model show that it is possible to accommodate the largest possible MG for "fast" messages, without penalizing the maximum sum MG of both "fast" and "slow" messages. The results for the hexagonal model show that there is always a penalty in sum-MG at any "fast" MG. In contrast, for the sectorized hexagonal model where each cell is divided into three non-interfering sectors by employing directional antennas at the BSs, it is possible to eliminate this penalty and accommodate the largest possible MG for "fast" messages without penalizing the maximum sum MG.

5.1 Coding Schemes and Achievable Multiplexing Gains

An important building block in our coding schemes is coordinated multi point (CoMP) transmission or CoMP reception. Depending on which of the two is used, the scheme requires more Tx- or Rx-cooperation rates. So, depending on the application, any of the two can be advantageous. In some applications, cooperation rates might however be too low to employ either of the two. In this case, the proposed schemes can be time-shared with alternative schemes that require less or no cooperation rates at all. Alternatively, the proposed schemes can be employed with a smaller number of cooperation rounds $D' < D$, which also reduces the required cooperation prelog in all our schemes.

The rest of the section is organized as follows. We first describe our coding schemes that simultaneously send "fast" and "slow" messages; they either employ CoMP reception (Subsections 5.1.1) or CoMP transmission (Subsection 5.1.2). Next, we describe schemes that send only "slow" messages (Subsection 5.1.3) or do not use any kind of cooperation (Subsection 5.1.4).

5.1.1 Coding Scheme to Transmit Both "Fast" and "Slow" Messages with CoMP Reception

This scheme splits the total number of cooperation rounds between Tx- and Rx-cooperation as:

$$\mathrm{D_{Tx}} = 1 \quad \text{and} \quad \mathrm{D_{Rx}} = \mathrm{D} - 1. \tag{5.1}$$

1) Creation of subnets and message assignment:

Each network is decomposed into three subsets of Tx/Rx pairs, $\mathcal{T}_{\text{silent}}$, $\mathcal{T}_{\text{fast}}$ and $\mathcal{T}_{\text{slow}}$, where

- Txs in $\mathcal{T}_{\text{silent}}$ are silenced and Rxs in $\mathcal{T}_{\text{silent}}$ do not take any action.
- Txs in $\mathcal{T}_{\text{fast}}$ send only "fast" messages. The corresponding Tx/Rx pairs are henceforth called "fast" Txs/Rxs.
- Txs in $\mathcal{T}_{\text{slow}}$ send only "slow" messages. The corresponding Tx/Rx pairs are henceforth called "slow" Txs/Rxs.

We choose the sets $\mathcal{T}_{\text{silent}}$, $\mathcal{T}_{\text{fast}}$ and $\mathcal{T}_{\text{slow}}$ in a way that:

- the signals sent by the "fast" Txs do not interfere; and
- silencing the Txs in $\mathcal{T}_{\text{silent}}$ decomposes the network into non-interfering subnets such that in each subnet there is a dedicated Rx, called *master Rx*, that can send a cooperation message to any other "slow" Rx in the same subnet in at most $\left\lfloor \frac{\mathrm{D_{Rx}}-1}{2} \right\rfloor$ cooperation rounds.

For example, consider Wyner's symmetric model (described in details in Section 5.2) where Txs and Rxs are aligned on a grid and cooperation is possible only between neighbouring Txs or Rxs. Interference at a given Rx is only from adjacent Txs. The network is illustrated in Figure 5.1a. This figure also shows a possible decomposition of the Tx/Rx pairs into the sets $\mathcal{T}_{\text{silent}}$ (in white), $\mathcal{T}_{\text{fast}}$ (in yellow) and $\mathcal{T}_{\text{slow}}$ (in blue) when $\mathrm{D} = 6$. The proposed decomposition creates subnets with 7 active Tx/Rx pairs where the Rx

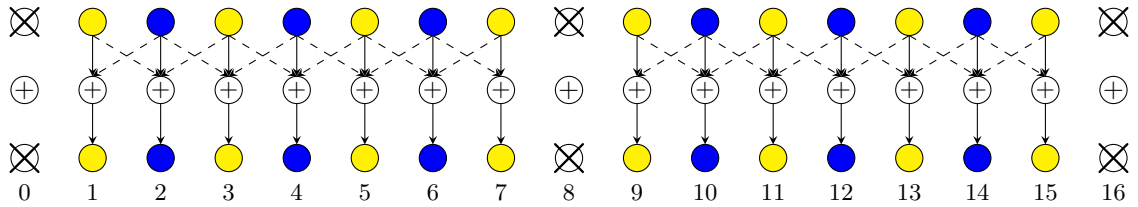

(a) Silencing every D + 2nd Tx creates interference-free subnets. Txs in yellow send "fast" messages and Txs in blue send "slow" messages.

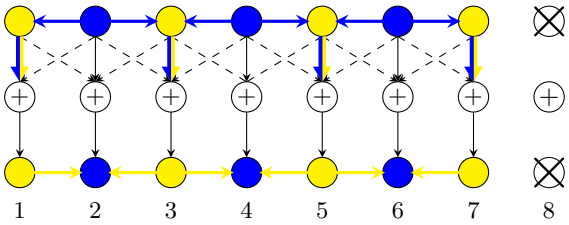

(b) Blue arrows illustrate the quantized "slow" signals transmitted to the "fast" Txs during the single Tx-cooperation round. Yellow arrows indicate the decoded "fast" messages transmitted to the "slow" Rxs during the first Rx-cooperation round.

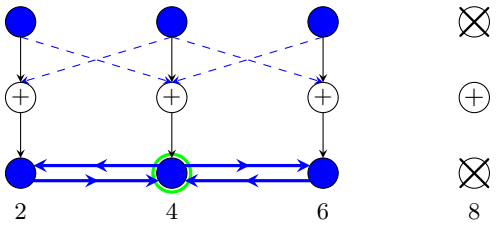

(c) Canceling the interference of "slow" signals on other "slow" signals using CoMP reception. The green Rx is the master Rx. The blue arrows indicate the flows of the Rx-cooperation messages in rounds 3–6, which enable CoMP reception.

Figure 5.1: Flow of cooperation communication in Wyner's symmetric model for D = 6 and for the scheme transmitting both "fast" and "slow" messages with CoMP reception.

in the center of any subnet (e.g. Rx 4 in the first subnet) can serve as a master Rx as it reaches any slow (blue) Rx in the same subnet in at most $\lfloor \mathrm{D_{Rx}} - 1/2 \rfloor = \lfloor (\mathrm{D}-2)/2 \rfloor = 2$ cooperation rounds. As required, transmissions from fast (yellow) Txs are only interfered by transmissions from slow (blue) Txs.

2) Precanceling of "slow" interference at "fast" Txs:

Any "slow" Tx k' quantizes its pre-computed input signal $\boldsymbol{X}_{k'}^n$ (how this signal is generated will be described under item 5)) and describes the quantised signal $\hat{\boldsymbol{X}}_{k'}^n$ during the last Tx-cooperation round to all its neighbouring "fast" Txs. (Here, there is only a single Tx-cooperation round, but this item will be reused in later subsections where $\mathrm{D_{Tx}} > 1$.) Fig. 5.1b illustrates the sharing of the described quantization information with neighbouring "fast" Txs for Wyner's symmetric model.

"Fast" Txs precancel the interference from their neighboring "slow" Txs. To describe this formally, recall the set $\mathcal{I}_{\text{Tx},k}$ from (2.2), for each $k \in \{1,\ldots,K\}$, then we define the *"slow" interfering set*

$$\mathcal{I}_k^{(S)} \triangleq \mathcal{I}_{\text{Tx},k} \cap \mathcal{T}_{\text{slow}}, \tag{5.2}$$

as the set of "slow" Txs whose signals interfere at a given Rx k. Also, we denote by $\boldsymbol{U}_k^n(M_k^{(F)})$ the non-precoded input signal precomputed at a given "fast" Tx k. (The following item 3) explains how to obtain $\boldsymbol{U}_k^n(M_k^{(F)})$.) Tx k sends the inputs

$$\boldsymbol{X}_k^n = \boldsymbol{U}_k^n(M_k^{(F)}) - \sum_{k' \in \mathcal{I}_k^{(S)}} \mathsf{H}_{k,k}^{-1}\mathsf{H}_{k',k}\hat{\boldsymbol{X}}_{k'}^n, \tag{5.3}$$

over the channel. Since each "fast" Rx k is not interfered by the signal sent at any other "fast" Tx, the precoding in (5.3) makes that a "fast" Rx k observes the almost interference-free signal

$$\boldsymbol{Y}_k^n = \mathsf{H}_{k,k}\boldsymbol{U}_k^n + \underbrace{\sum_{k' \in \mathcal{I}_k^{(S)}} \mathsf{H}_{k',k}(\boldsymbol{X}_{k'}^n - \hat{\boldsymbol{X}}_{k'}^n) + \boldsymbol{Z}_k^n}_{\text{disturbance}}, \tag{5.4}$$

where the variance of above disturbance is around noise level and does not grow with P.

3) Transmission of "fast" messages:

Each "fast" Tx k encodes its desired message $M_k^{(F)}$ using a codeword $\mathbf{U}_k^{(n)}(M_k^{(F)})$ from a Gaussian point-to-point code of power P. The corresponding Rx k applies a standard point-to-point decoding rule to directly decode this "fast" codeword without Rx-cooperation from its "almost" interference-free outputs $\mathbf{Y}_k$, see (5.4).

4) Canceling "fast" interference at "slow" Rxs:

According to the previous item 3), all "fast" messages are decoded directly from the outputs without any Rx-cooperation. During the first Rx-cooperation round, all "fast" Rxs can thus share their decoded messages with all their neighbouring "slow" Rxs, which can cancel the corresponding interference from their receive signals. More formally, we then define the *fast interference set*

$$\mathcal{I}_k^{(F)} \triangleq \mathcal{I}_{\text{Tx},k} \cap \mathcal{T}_{\text{fast}} \tag{5.5}$$

as the set of "fast" Txs whose signals interfere at Rx k. Each "slow" Rx k forms the new signal

$$\hat{\boldsymbol{Y}}_k^n := \boldsymbol{Y}_k^n - \sum_{\hat{k}\in\mathcal{I}_k^{(F)}} \mathsf{H}_{\hat{k},k}\boldsymbol{X}_{\hat{k}}^n(\hat{M}_{\hat{k}}^{(F)}), \tag{5.6}$$

and decodes its desired "slow" message based on this new signal following the steps described in the following item 5). Fig. 5.1b illustrates with yellow arrows the sharing of decoded "fast" messages with neighbouring "slow" Rxs in Wyner's symmetric model.

5) Transmission and reception of "slow" messages using CoMP reception:

Each "slow" Tx k encodes its message $M_k^{(S)}$ using a codeword $\boldsymbol{X}_k^n(M_k^{(S)})$ from a Gaussian point-to-point code of power P. "Slow" messages are decoded based on the new outputs $\hat{\boldsymbol{Y}}_k^n$ in (5.6). CoMP reception is employed to decode all "slow" messages in a given subnet. By item 4) the CoMP reception can ignore interference from "fast" Txs, but has to account for the modified interference graph and the modified channel matrix from "slow" Txs caused by the precanceling in item 2). For example, in Fig. 5.1c we depict with blue dashed lines the modified interference graph for Wyner's symmetric model.

CoMP reception involves that each "slow" Rx k applies a rate-$\frac{\mathsf{L}}{2}\log(1+\mathsf{P})$ quantizer to the new output signal $\hat{\boldsymbol{Y}}_k^n$, and relays the quantization information over the cooperation links to the master Rx in its subnet. By definition of master Rxs (see item 1)) this can be performed in Rx-cooperation rounds $2,\dots,\lfloor\frac{\mathrm{D_{Rx}}-1}{2}\rfloor+1$. (Fig. 5.1c illustrates with blue arrows the exchanged quantization information for Wyner's symmetric model.) Each master Rx reconstructs all the quantized signals received from "slow" Txs and jointly decodes these "slow" messages. During Rx-cooperation rounds $\lfloor\frac{\mathrm{D_{Rx}}-1}{2}\rfloor+2,\dots,2\lfloor\frac{\mathrm{D_{Rx}}-1}{2}\rfloor+1$, it shares each of the decoded messages over the conferencing links with its intended Rx. (Fig. 5.1c illustrates with blue arrows the sharing of decoded "slow" messages with the corresponding Rxs.)

6) MG Analysis:

In the described scheme, all transmitted "fast" and "slow" messages can be sent reliably at MG L because all interference is canceled (up to noise level) either at the Tx or the Rx side, and because Txs and Rxs are equipped with L antennas each.

The presented coding scheme thus achieves the MG pair

$$\left(\mathsf{S}^{(F)}=\mathsf{S}_{\mathrm{both}}^{(F)},\ \ \mathsf{S}^{(S)}=\mathsf{S}_{\mathrm{both}}^{(S)}\right), \tag{5.7}$$

where

$$\mathsf{S}_{\text{both}}^{(F)} \triangleq \mathsf{L} \cdot \overline{\lim_{K\to\infty}} \frac{|\mathcal{T}_{\text{fast}}|}{K} \quad \text{and} \quad \mathsf{S}_{\text{both}}^{(S)} \triangleq \mathsf{L} \cdot \overline{\lim_{K\to\infty}} \frac{|\mathcal{T}_{\text{slow}}|}{K}. \tag{5.8}$$

The scheme we described so far requires different cooperation rates on the various Tx- or Rx-cooperation links. To evenly balance the load on the Tx-cooperation links and on the Rx-cooperation links, different versions of the scheme with different choices of the sets $\mathcal{T}_{\text{silent}}$, $\mathcal{T}_{\text{fast}}$ and $\mathcal{T}_{\text{slow}}$ and different cooperation routes can be time-shared. The main quantity of interest is then the *average cooperation load*, which for the scheme above is characterized as follows. During the single Tx-cooperation round, each "fast" Tx k receives a quantised version of the transmit signal of each of its "slow" interferers $\hat{k} \in \mathcal{I}_k^{(S)}$. Since each quantisation message is of prelog L, the average required Tx-cooperation prelog equals

$$\mu_{\text{Tx,both}}^{(\text{r})} \triangleq \mathsf{L} \cdot \overline{\lim_{K\to\infty}} \frac{\sum_{k\in\mathcal{T}_{\text{fast}}} |\mathcal{I}_k^{(S)}|}{\mathcal{Q}_{K,\text{Tx}}}, \tag{5.9}$$

where $\mathcal{Q}_{K,\text{Tx}}$ denotes the total number of Tx-cooperation links in the network.

There are three types of Rx-cooperation messages. In the first Rx-cooperation round, each "slow" Rx k obtains a decoded message from each of its "fast" interferers $\hat{k} \in \mathcal{I}_k^{(F)}$. The total number of messages sent in this first round is thus $\sum_{k\in\mathcal{T}_{\text{slow}}} |\mathcal{I}_k^{(F)}|$ and each is of prelog L. In Rx-cooperation rounds $2, \ldots, \lfloor \frac{\text{D}_{\text{Rx}}-1}{2} \rfloor + 1$, "slow" Rxs send quantized versions of their output signals to the master Rx in the same network. Each of these messages is of prelog L and the total number of such messages equals $\sum_{k\in\mathcal{T}_{\text{slow}}} \gamma_{\text{Rx},k}$, where $\gamma_{\text{Rx},k}$ denotes the number of cooperation rounds required for "slow" Rx k to reach the master Rx in its subnet. In rounds $\lfloor \frac{\text{D}_{\text{Rx}}-1}{2} \rfloor + 2, \ldots, \text{D}_{\text{Rx}}$, the master Rx sends the decoded messages to all the "slow" Rxs in the subnet. Each of these messages is again of prelog L and the total number of such messages is again $\sum_{k\in\mathcal{T}_{\text{slow}}} \gamma_{\text{Rx},k}$. To summarize, each of the transmitted messages is of prelog L and thus the average cooperation prelog required per Rx-cooperation link is:

$$\mu_{\text{Rx,both}}^{(\text{r})} \triangleq \mathsf{L} \cdot \overline{\lim_{K\to\infty}} \frac{\sum_{k\in\mathcal{T}_{\text{slow}}} \left(|\mathcal{I}_k^{(F)}| + 2\gamma_{\text{Rx},k} \right)}{\mathcal{Q}_{K,\text{Rx}}}, \tag{5.10}$$

where $\mathcal{Q}_{K,\text{Rx}}$ denotes the total number of Rx-cooperation links in the network.

Remark 6. *If the master Rx of a subnet is a "fast" Rx, it does not have to send its decoded message to its "slow" neighbours, because it decodes all "slow" messages jointly. In this case, less Rx-cooperation prelog is required.*

5.1.2 Coding Scheme to Transmit Both "Fast" and "Slow" Messages with CoMP Transmission

This second scheme splits the total number of cooperation rounds between Tx- and Rx-cooperation as:

$$\mathrm{D_{Tx}} = \mathrm{D} - 1 \quad \text{and} \quad \mathrm{D_{Rx}} = 1. \tag{5.11}$$

Similarly to the previous Subsection 5.1.1, the scheme is described by 5 items:

1) Creation of subnets and message assignment:

This item is similar to item 1) of Subsection 5.1.1, but the sets $\mathcal{T}_{\text{silent}}$, $\mathcal{T}_{\text{fast}}$ and $\mathcal{T}_{\text{slow}}$ are chosen in a way that:

- as before, the signals sent by the "fast" Txs do not interfere; and
- silencing the Txs in $\mathcal{T}_{\text{silent}}$ decomposes the network into non-interfering subnets so that in each subnet there is a dedicated *master Tx* that can send a cooperation message to any other "slow" Tx in the same subnet in at most $\left\lfloor \frac{\mathrm{D_{Tx}}-1}{2} \right\rfloor$ cooperation rounds.

Items 2)-4) remain as described in Subsection 5.1.1. Item 5) is replaced by the following item.

5) Transmission and reception of "slow" messages using CoMP transmission:

"Slow" messages are transmitted using standard CoMP transmission techniques that can ignore interference from "fast" Txs (due to the post-processing in item 4)) but has to account for the modified interference graph and the modified channel matrix between slow messages caused by the precanceling performed under item 2). The receivers decode based on the newly constructed outputs $\hat{\boldsymbol{Y}}_k^n$ defined in (5.6).

We describe CoMP transmission in this context more formally. During the first $\lfloor \frac{\mathrm{D_{Tx}}-1}{2} \rfloor$ Tx-cooperation rounds, each "slow" Tx of a subnet, sends its message to the master Tx of the subnet. This latter encodes all received "slow" messages using individual Gaussian codebooks and precodes them so as to cancel all the interference from other "slow" messages at the corresponding Rxs. I.e., it produces signals so that when they are transmitted over the active antennas in the cell, the signal observed at each "slow" Rx only depends on the "slow" message sent by the corresponding Tx but not on the other "slow" messages. The master Tx applies a Gaussian vector quantizer on these precoded signals and sends the quantization information over the cooperation links to the corresponding Txs during the Tx-cooperation rounds $\lfloor \frac{\mathrm{D_{Tx}}-1}{2} \rfloor + 1$ to $\mathrm{D_{Tx}} - 1$.

This is possible by the way we defined the master Txs. All "slow" Txs reconstruct the quantized signals $\hat{\boldsymbol{X}}_k^n$ intended for them and send them over the network: $\boldsymbol{X}_k^n \triangleq \hat{\boldsymbol{X}}_k^n$.

Each "slow" Rx k decodes its desired message from the modified output sequence $\hat{\boldsymbol{Y}}_k^n$ defined in (5.6) using a standard point-to-point decoder.

6) MG Analysis

Similarly to Subsection 5.1.1, each transmitted message can be sent reliably at MG L, and thus the scheme achieves the MG pair in (5.7).

The load on the different cooperation links is again unevenly distributed across links, and thus, by time-sharing and symmetry arguments, the average Rx- and Tx-cooperation rates are the limiting quantities. The required average Rx-cooperation rate is easily characterized as:

$$\mu_{\text{Rx,both}}^{(\text{t})} \triangleq \mathsf{L} \cdot \overline{\lim_{K\to\infty}} \frac{\sum_{k\in\mathcal{T}_{\text{slow}}} |\mathcal{I}_k^{(F)}|}{\mathcal{Q}_{K,\text{Rx}}}, \tag{5.12}$$

because Rx-cooperation takes place in a single round, during which each "slow" Rx k learns all decoded "fast" messages that interfere their receive signals and these messages are of MG L. To calculate the required average Tx-cooperation rate, define for each $k \in \mathcal{T}_{\text{slow}}$ the positive parameter $\gamma_{\text{Tx},k}$ to be the number of cooperation hops required from Tx k to reach the master Tx in its subnet. During the first $\lfloor \frac{\text{D}_{\text{Tx}}-1}{2} \rfloor$ Tx-cooperation rounds, a total of $\sum_{k\in\mathcal{T}_{\text{slow}}} \gamma_{\text{Tx},k}$ cooperation messages of MG L are transmitted from the "slow" Txs to the master Txs in their subnet. The same number of Tx-cooperation messages, all of MG L, is also conveyed during rounds $\lfloor \frac{\text{D}_{\text{Tx}}-1}{2} \rfloor + 1, \ldots, 2\lfloor \frac{\text{D}_{\text{Tx}}-1}{2} \rfloor$, now from the master Tx to the "slow" Txs in the subnet. During the last round, "slow" Txs convey their messages to the adjacent "fast" Txs that are interfered by their signals. Some of these signals, however have already been shared during Tx-cooperation rounds $\lfloor \frac{\text{D}_{\text{Tx}}-1}{2} \rfloor + 1, \ldots, 2\lfloor \frac{\text{D}_{\text{Tx}}-1}{2} \rfloor$, and thus do not have to be sent again. The total number of cooperation messages during the last Tx-cooperation rounds is thus only equal to $\sum_{k\in\mathcal{T}_{\text{fast}}} |\mathcal{I}_k^{(S)}| - q$, where q denotes the number of the messages that have already been sent in previous rounds. We will chracterize the value of q when we analyze specific networks. To summarize, the average required Tx-cooperation rate of our scheme is:

$$\mu_{\text{Tx,both}}^{(\text{t})} \triangleq \mathsf{L} \cdot \overline{\lim_{K\to\infty}} \frac{\sum_{k\in\mathcal{T}_{\text{slow}}} 2\gamma_{\text{Tx},k} + \sum_{k\in\mathcal{T}_{\text{fast}}} |\mathcal{I}_k^{(S)}| - q}{\mathcal{Q}_{K,\text{Tx}}}. \tag{5.13}$$

5.1.3 Coding Scheme to Transmit Only "Slow" Messages with CoMP Reception and Transmission

In principle, since any "fast" message satisfies the constraints on "slow" messages, we can use the schemes provided in Subsections 5.1.1 and 5.1.2 to send only "slow" messages. In some cases, it is however possible to design a purely CoMP-based scheme that requires less Tx- and Rx-cooperation rates than our previously described schemes. Specifically (and similarly to items 1) of Subsection 5.1.1 and Subsection 5.1.2), each network is decomposed into two subsets of Tx/Rx pairs, $\mathcal{T}_{\text{silent}}$ and $\mathcal{T}_{\text{slow}}$, where Txs in $\mathcal{T}_{\text{silent}}$ are silenced and Txs in $\mathcal{T}_{\text{slow}}$ send a "slow" message. Specifically, we choose the set $\mathcal{T}_{\text{silent}}$ so that silencing its Txs decomposes the remaining Tx/Rx pairs into non-interfering subnets and in each subnet there is a dedicated Rx, called *master Rx*, that in at most $\lfloor \frac{\mathrm{D}}{2} \rfloor$ cooperation rounds can reach any other Rx in the same subnet. CoMP reception as described in item 5) of Subsections 5.1.1 is then used for transmission of the "slow" messages in each subnet. This scheme requires positive Rx-cooperation rate but no Tx-cooperation. Alternatively, the set $\mathcal{T}_{\text{silent}}$ can be chosen so that each created subnet contains a dedicated Tx, called *master Tx*, that in at most $\lfloor \frac{\mathrm{D}}{2} \rfloor$ cooperation rounds can reach any other Tx in the same subnet and messages are sent by means of CoMP transmission as described in item 5) of Subsection 5.1.2. This scheme requires positive Tx-cooperation rate but no Rx-cooperation.

The MG pair achieved by both schemes is characterized as

$$\left(\mathsf{S}^{(F)} = 0,\ \ \mathsf{S}^{(S)} = \mathsf{S}^{(S)}_{\max}\right), \tag{5.14}$$

where

$$\mathsf{S}^{(S)}_{\max} \triangleq \mathsf{L} \cdot \overline{\lim_{K\to\infty}} \frac{|\mathcal{T}_{\text{slow}}|}{K}. \tag{5.15}$$

The CoMP-reception scheme requires an average Rx-cooperation rate of

$$\mu^{(\mathrm{r})}_{\mathrm{Rx},\mathsf{S}} \triangleq \mathsf{L} \cdot \overline{\lim_{K\to\infty}} \frac{\sum_{k\in\mathcal{T}_{\text{slow}}} 2\gamma_{\mathrm{Rx},k}}{\mathcal{Q}_{K,\mathrm{Rx}}}, \tag{5.16}$$

and the CoMP-transmission scheme an average Tx-cooperation rate of

$$\mu^{(\mathrm{t})}_{\mathrm{Tx},\mathsf{S}} \triangleq \mathsf{L} \cdot \overline{\lim_{K\to\infty}} \frac{\sum_{k\in\mathcal{T}_{\text{slow}}} 2\gamma_{\mathrm{Tx},k}}{\mathcal{Q}_{K,\mathrm{Tx}}}, \tag{5.17}$$

where recall that $\gamma_{\mathrm{Rx},k}, \gamma_{\mathrm{Tx},k} \in \{1, \ldots, \lfloor \frac{\mathrm{D}}{2} \rfloor\}$ denote the number of cooperation hops required from a Rx k

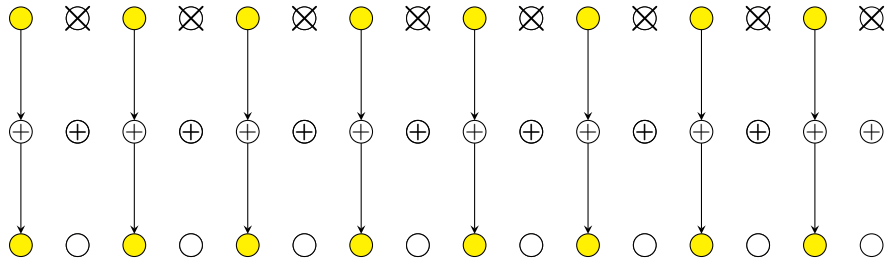

Figure 5.2: Illustration of the scheme without cooperation in Wyner's symmetric model.

or a Tx k to reach the master Rx or the master Tx in its subnet.

5.1.4 Coding Scheme without Cooperation

In this scheme, we silence a set of Txs, denoted by $\mathcal{T}_{\text{silent}}$, in a way that the transmissions of non-silenced Txs do not interfere, and the network is thus decomposed into non-interfering point-to-point links. See Fig. 5.2 where even Txs are silenced. Independent Gaussian codes are used to communicate over the individual links without any Tx- or Rx-cooperation. Each non-silenced Tx can choose to send either a "slow" or a "fast" message. If $\beta \in [0,1]$ fraction of the non-silenced Txs send a "fast" message and the other send "slow" messages, this scheme achieves MG pair

$$\left(\mathsf{S}^{(F)} = \beta \mathsf{S}_{\text{no-coop}},\ \ \mathsf{S}^{(S)} = (1-\beta)\mathsf{S}_{\text{no-coop}}\right), \tag{5.18}$$

where

$$\mathsf{S}_{\text{no-coop}} \triangleq \mathsf{L} \cdot \varlimsup_{K\to\infty} \left(1 - \frac{|\mathcal{T}_{\text{silent}}|}{K}\right). \tag{5.19}$$

The cases $\beta = 0$ and $\beta = 1$ will be of special interest.

In the following sections we specialize the results obtained in this section to three different networks. Notice that it suffices to describe for each of the schemes the choice of the Tx/Rx sets $\mathcal{T}_{\text{silent}}$, $\mathcal{T}_{\text{slow}}$, $\mathcal{T}_{\text{fast}}$.

5.2 Wyner's Symmetric Model

5.2.1 Network and Cooperation Model

Consider Wyner's symmetric linear cellular model where cells are aligned in a single dimension and signals of users that lie in a given cell interfere only with signals sent in the two adjacent cells. Since the focus of this chapter is on the MG, for simplicity, we assume only a single mobile user in each cell, each wishing to

communicate with the corresponding BS of the cell. We shall further assume that the number of cells K and the maximum delay D are even.

The input-output relation of the network is

$$\boldsymbol{Y}_{k,t} = \mathsf{H}_{k,k}\boldsymbol{X}_{k,t} + \mathsf{H}_{k-1,k}\boldsymbol{X}_{k-1,t} + \mathsf{H}_{k+1,k}\boldsymbol{X}_{k+1,t} + \boldsymbol{Z}_{k,t}, \tag{5.20}$$

where $\boldsymbol{X}_{0,t} = \mathbf{0}$ for all t, and the interference set at a given user k is

$$\mathcal{I}_{\mathrm{Tx},k} = \{k-1, k+1\}, \tag{5.21}$$

where indices out of the range $\{1, \ldots, K\}$ should be ignored. In this model, Rxs and Txs can cooperate with the two Rxs and Txs in the adjacent cells, so

$$\mathcal{N}_{\mathrm{Tx}}(k) = \{k-1, k+1\} \quad \text{and} \quad \mathcal{N}_{\mathrm{Rx}}(k) = \{k-1, k+1\}. \tag{5.22}$$

Fig. 3.1 illustrates the interference pattern of the network and the available cooperation links. As can be seen from this figure, Txs 1 and K and Rxs 1 and K have a single outgoing cooperation link and all other Txs and Rxs in this network have two outgoing cooperation links. Thus, the total numbers of Tx- and of Rx-cooperation links both are

$$\mathcal{Q}_{K,\mathrm{Tx}} = \mathcal{Q}_{K,\mathrm{Rx}} = 2K - 2. \tag{5.23}$$

5.2.2 Tx/Rx Set Associations

We specialize the coding schemes proposed in Section 5.1 to Wyner's symmetric model.

Transmitting both "fast" and "slow" messages with CoMP reception

Consider the scheme in Subsection 5.1.1, where we set $\mathrm{D}_{\mathrm{Tx}} = 1$ and $\mathrm{D}_{\mathrm{Rx}} = \mathrm{D}-1$. Choose the cell association in Fig. 5.1a, where "fast" Tx/Rx pairs are in yellow, "slow" Tx/Rx pairs in blue, and silenced Tx/Rx pairs in white. More formally, choose

$$\mathcal{T}_{\mathrm{silent}} = \left\{ \ell\,(\mathrm{D}+2) : \ell = 1, \ldots, \left\lfloor \frac{K}{\mathrm{D}+2} \right\rfloor \right\}, \tag{5.24a}$$

$$\mathcal{T}_{\mathrm{fast}} = \{1, 3, \ldots, K-1\}, \tag{5.24b}$$

$$\mathcal{T}_{\mathrm{slow}} = \{1, \ldots, K\} \backslash \{\mathcal{T}_{\mathrm{silent}}, \mathcal{T}_{\mathrm{fast}}\}. \tag{5.24c}$$

This choice satisfies all the conditions explained under item 1) in Subsection 5.1.1. In particular, transmissions of "fast" messages are interfered only by transmissions of "slow" messages and for any ℓ, the Tx/Rx pairs in

$$\mathcal{T}_\ell \triangleq \{\ell(\mathrm{D}+2)+1,\ldots,(\ell+1)(\mathrm{D}+2)-1\} \tag{5.25}$$

form a subnet for which Rx $\ell(\mathrm{D}+2)+\mathrm{D}/2+1$ can act as the master Rx. Indeed, it can be checked that this Rx can be reached by any *"slow" Rx (i.e., even Rx)* in its subnet in at most $(\mathrm{D}_{\mathrm{Rx}}-1)/2$ cooperation hops.

By (5.8) and (5.24), the scheme achieves the MG pair $(\mathsf{S}^{(F)}=\mathsf{S}^{(F)}_{\mathrm{both}},\mathsf{S}^{(S)}=\mathsf{S}^{(S)}_{\mathrm{both}})$ where

$$\mathsf{S}^{(F)}_{\mathrm{both}} \triangleq \frac{\mathsf{L}}{2} \quad \text{and} \quad \mathsf{S}^{(S)}_{\mathrm{both}} \triangleq \mathsf{L}\cdot\frac{\mathrm{D}}{2(\mathrm{D}+2)}. \tag{5.26}$$

To analyze the required cooperation prelogs of the scheme, $\mu^{(\mathrm{r})}_{\mathrm{Tx,both}}$ and $\mu^{(\mathrm{r})}_{\mathrm{Rx,both}}$, we evaluate the formulas in (5.9) and (5.10). We start with the required Tx-cooperation prelog in this system, which we denote by $\mu^{(\mathrm{r})}_{\mathrm{Tx,both}}$. Notice that in each subnet, the "slow" interfering set $\mathcal{I}^{(S)}_k$, i.e., the set of "slow" Txs interfering at Rx k, is a singleton for the first and the last active Rx in each subnet because we assume D even, and it is of size 2 for the other "fast" Rxs. We then have for each subnet $\ell \in \{1,\ldots,\lfloor K/(\mathrm{D}+2)\rfloor\}$:

$$\sum_{k\in\mathcal{T}_{\mathrm{fast}}\cap\mathcal{T}_\ell} |\mathcal{I}^{(S)}_k| = 2+2(\mathrm{D}/2-1)=\mathrm{D}. \tag{5.27}$$

There can be a last subnet $\ell=\lceil K/(\mathrm{D}+2)\rceil$ with fewer active Tx/Rx pairs and smaller (but positive) Tx-cooperation prelog. Therefore, for fixed K, the required average Tx-cooperation prelog is bounded as

$$\mathsf{L}\cdot\frac{\left\lfloor\frac{K}{\mathrm{D}+2}\right\rfloor\cdot\mathrm{D}}{\mathcal{Q}_{K,\mathrm{Tx}}} \le \mu^{(\mathrm{r})}_{\mathrm{Tx,both}} \le \mathsf{L}\cdot\frac{\left\lceil\frac{K}{\mathrm{D}+2}\right\rceil\cdot\mathrm{D}}{\mathcal{Q}_{K,\mathrm{Tx}}}. \tag{5.28}$$

When $K\to\infty$, the inequalities in (5.28) turn to equalities and by (5.23) we obtain

$$\mu^{(\mathrm{r})}_{\mathrm{Tx,both}} = \mathsf{L}\cdot\frac{\mathrm{D}}{2(\mathrm{D}+2)}. \tag{5.29}$$

To calculate the required Rx-cooperation prelog $\mu^{(\mathrm{r})}_{\mathrm{Rx,both}}$, we start by calculating the cooperation prelog in the first subnet. Notice that each "slow" Rx is interfered by two "fast" Txs and thus $|\mathcal{I}^{(F)}_k|=2$. Since

there are D/2 "slow" Rxs in each subnet $\mathcal{T}_\ell$:

$$\sum_{k\in\mathcal{T}_{\text{slow}}\cap\mathcal{T}_\ell} |\mathcal{I}_k^{(F)}| = 2\cdot\frac{\mathrm{D}}{2} = \mathrm{D}. \tag{5.30}$$

In addition, Rxs also exchange cooperation messages to enable CoMP reception. Thereby, the quantization message produced by a "slow" Rx $k = \ell(\mathrm{D}+2)+i$, for $i\in\{2,4,\ldots,\mathrm{D}-2\}$, has to propagate over $\gamma_{\mathrm{Rx},k} = |\mathrm{D}/2+1-i|$ hops to reach the master Rx in its subnet. If $\mathrm{D}/2+1$ is even,

$$\sum_{k\in\mathcal{T}_{\text{slow}}\cap\mathcal{T}_\ell} \gamma_{\mathrm{Rx},k} = \sum_{i\in\{2,4,\ldots,\mathrm{D}/2-1\}} 2\cdot(\mathrm{D}/2+1-i) = \frac{1}{2}\left(\frac{\mathrm{D}^2}{4}-1\right). \tag{5.31}$$

Then, according to (5.10), (5.23), (5.30), and (5.31), when $\mathrm{D}/2+1$ is even, the average Rx-cooperation prelog is bounded by

$$\mathsf{L}\cdot\frac{\left\lfloor\frac{K}{\mathrm{D}+2}\right\rfloor\left(\mathrm{D}+\frac{\mathrm{D}^2}{4}-1\right)}{2K-2} \le \mu^{(\mathrm{r})}_{\mathrm{Rx,both}} \le \mathsf{L}\cdot\frac{\left\lceil\frac{K}{\mathrm{D}+2}\right\rceil\left(\mathrm{D}+\frac{\mathrm{D}^2}{4}-1\right)}{2K-2}. \tag{5.32}$$

Letting $K\to\infty$ the inequalities in (5.32) turn into equalities, and

$$\mu^{(\mathrm{r})}_{\mathrm{Rx,both}} = \mathsf{L}\cdot\frac{\mathrm{D}+\frac{\mathrm{D}^2}{4}-1}{2(\mathrm{D}+2)}, \quad \text{for } \mathrm{D}/2+1 \text{ even}. \tag{5.33}$$

When $\mathrm{D}/2+1$ is odd, the sum in (5.31) evaluates to $\frac{D^2}{8}$. Moreover, in this case, the master Rx is a "fast" Rx. It does not have to send its decoded message to any neighbour, as it locally decodes all "slow" messages of the subnet. So, (see also Remark 6), the nominator in (5.10) can be reduced by 2. Putting all these together, we obtain $\mu^{(\mathrm{r})}_{\mathrm{Rx,both}} = \mathsf{L}\cdot\frac{\mathrm{D}+\frac{\mathrm{D}^2}{4}-2}{2(\mathrm{D}+2)}$ when $\mathrm{D}/2+1$ is odd.

Transmitting both "fast" and "slow" messages with CoMP transmission

Consider the scheme in Subsection 5.1.2, where we set $\mathrm{D_{Rx}} = 1$ and $\mathrm{D_{Tx}} = \mathrm{D}-1$. Choose the same cell association as for the CoMP reception scheme described in Subsection 5.1.2 and depicted in Fig. 5.1a. Under this cell association, Tx $\mathrm{D}/2+1$ can act as a master Tx because it can be reached by any "slow" (even) Tx in its subnet in at most $(\mathrm{D_{Tx}}-1)/2$ cooperation rounds.

Since the same cell partitioning is used, namely (5.24), this scheme achieves the same MG pair as with CoMP reception, see (5.26). Moreover, by (5.12) and (5.30) and a sandwich argument similar to the one

leading to (5.28), in the limit as $K \to \infty$, the required average Rx-cooperation prelog is

$$\mu^{(\mathrm{t})}_{\mathrm{Rx,both}} = \mathsf{L} \cdot \frac{\mathrm{D}}{2(\mathrm{D}+2)}. \tag{5.34}$$

Similarly, consider (5.13) and (5.27) and notice that for $\mathrm{D}/2+1$ even,

$$\sum_{k \in \mathcal{T}_{\mathrm{slow}} \cap \mathcal{T}_\ell} \gamma_{\mathrm{Tx},k} = \sum_{i \in \{2,4,\ldots,\mathrm{D}/2-1\}} 2(\mathrm{D}/2+1-i) = \frac{1}{2}\left(\frac{\mathrm{D}^2}{4}-1\right), \tag{5.35}$$

whereas for $\mathrm{D}/2+1$ odd, this sum evaluates to $\frac{\mathrm{D}^2}{8}$. We consider the q-term in (5.13), which characterizes the number of quantization messages describing the "slow" signals that are counted twice: once for the CoMP transmission and once for the interference mitigation at "fast" transmitters. In each subnet, $\mathrm{D}/2-1$ such messages are double-counted, when $\mathrm{D}/2+1$ is even, and $\mathrm{D}/2$ messages are double-counted when $\mathrm{D}/2+1$ is odd. Therefore, and according to (5.13), (5.27), (5.35), when $K \to \infty$, the average Tx-cooperation prelog required by the scheme is

$$\mu^{(\mathrm{t})}_{\mathrm{Tx,both}} = \mathsf{L} \cdot \frac{\mathrm{D} + \frac{\mathrm{D}^2}{4} - 1 - \mathrm{D}/2 + 1}{2(\mathrm{D}+2)} = \mathsf{L} \cdot \frac{\mathrm{D}}{8}, \tag{5.36}$$

irrespective of whether $\mathrm{D}/2+1$ is even or odd.

Remark 7. *Despite the symmetry of the network, the sum-cooperation prelog $\mu^{(r)}_{\mathrm{Tx},both}+\mu^{(r)}_{\mathrm{Rx},both}$ in the scheme with CoMP reception, see* (5.29) *and* (5.33)*, exceeds the sum-cooperation prelog $\mu^{(t)}_{\mathrm{Tx},both}+\mu^{(t)}_{\mathrm{Rx},both}$ in the scheme with CoMP transmission, see* (5.34) *and* (5.36)*. This can be explained as follows. In both schemes the transmissions of "fast" and "slow" messages are disentangled through one round of Tx-cooperation and one round of Rx-cooperation. The Tx-cooperation messages relay information about "slow" transmit signals and this cooperation information can be reused in the context of CoMP transmission. In contrast, the Rx-cooperation messages only relay information about "fast" signals and are not useful to enable CoMP reception. As a result, the additional cooperation rate required to enable CoMP reception is larger than for CoMP transmission.*

Transmitting only "slow" messages with CoMP reception and transmission

Consider the scheme in Subsection 5.1.3 that transmits only "slow" messages, either using CoMP transmission or CoMP reception. For both schemes we regularly silence every $\mathrm{D}+2$nd Tx, i.e., as in the two

previous subsections, $\mathcal{T}_{\text{silent}} \triangleq \{\ell(D+2)\colon \ell = 1, \ldots, \lfloor \frac{K}{\mathrm{D}+2} \rfloor\}$. Also, we set $\mathcal{T}_{\text{slow}} = \{1, \ldots, K\} \backslash \mathcal{T}_{\text{silent}}$. These choices are permissible, because all Txs (or Rxs) in a subnet $\mathcal{T}_\ell = \{(\ell-1)(\mathrm{D}+2)+1, \ldots, \ell(\mathrm{D}+2)-1\}$ can reach the subnet's central Tx $(\ell-1)(\mathrm{D}+2)+\mathrm{D}+1$ (or Rx $(\ell-1)(\mathrm{D}+2)+\mathrm{D}+1$) in at most D/2 cooperation hops.

By (5.15), the scheme in Subsection 5.1.3 achieves the MG pair $(\mathsf{S}^{(F)} = 0,\ \mathsf{S}^{(S)} = \mathsf{S}^{(S)}_{\max})$ where

$$\mathsf{S}^{(S)}_{\max} \triangleq \mathsf{L} \cdot \frac{\mathrm{D}+1}{\mathrm{D}+2}. \tag{5.37}$$

With CoMP reception, this scheme does not use any Tx-cooperation. To calculate the Rx-cooperation prelog, we use the fact that Rx $k = \ell(\mathrm{D}+2)+i$, for positive integers ℓ and $i \leq \mathrm{D}+1$, reaches the master Rx in its subnet in $\gamma_{\mathrm{Rx},k} = |\mathrm{D}/2+1-i|$ hops. Since:

$$2\sum_{k\in\mathcal{T}_\ell} \gamma_{\mathrm{Rx},k} = 4\sum_{i=1}^{\mathrm{D}/2} i = \frac{\mathrm{D}(\mathrm{D}+2)}{2}, \tag{5.38}$$

by (5.16), in the limit as $K \to \infty$, the average Rx-cooperation prelog tends to

$$\mu^{(\mathrm{r})}_{\mathrm{Rx},\mathsf{S}} = \mathsf{L} \cdot \frac{\mathrm{D}}{4}. \tag{5.39}$$

Similar conclusions show that when CoMP transmission is used instead of CoMP reception, the scheme requires zero Rx-cooperation prelog and a Tx-cooperation prelog of $\mu^{(\mathrm{t})}_{\mathrm{Tx},\mathsf{S}} = \mu^{(\mathrm{r})}_{\mathrm{Rx},\mathsf{S}}$.

No-cooperation scheme

Consider the no-cooperation scheme in Subsection 5.1.4. For Wyner's symmetric network we create non-interfering point-to-point links by silencing all even Txs in the network, i.e., by choosing $\mathcal{T}_{\text{silent}} \triangleq \{2, 4, \ldots 2\lfloor \frac{K}{2} \rfloor\}$. Since all odd receivers remain active, the sum-prelog in (5.19) for this network evaluates to

$$\mathsf{S}^{(F)}_{\max} \triangleq \frac{\mathsf{L}}{2}. \tag{5.40}$$

If active Txs send only "fast" messages, (set $\beta = 1$ in (5.18)), this scheme achieves the MG pair $(\mathsf{S}^{(F)} = \mathsf{S}^{(F)}_{\max},\ \mathsf{S}^{(S)} = 0)$ and if the active Txs send only "slow" messages (set $\beta = 0$ in (5.18)), this scheme achieves the MG pair $(\mathsf{S}^{(F)} = 0,\ \mathsf{S}^{(S)} = \mathsf{S}^{(F)}_{\max})$.

Time-Sharing and Operating with a Reduced Number of Rounds

Each of the proposed coding schemes requires certain Tx- and Rx-cooperation prelogs. If these prelogs exceed the available cooperation prelogs μ_{Tx} and μ_{Rx}, the corresponding scheme cannot be applied directly but instead should be time-shared with any of the other schemes requiring less cooperation rates. Alternatively, it is also possible to reduce the number of cooperation rounds, because the required cooperation prelogs increase with D. Thus, employing above schemes with a reduced parameter $\mathrm{D}' < \mathrm{D}$ allows to meet the cooperation prelog constraints, and in some cases achieves a better MG pair than using time-sharing.

Consider for example the scheme with CoMP-transmission in Subsection 5.1.2 with transmitting both "fast" and "slow" messages but for only D' cooperation rounds where $\mathrm{D}' < \mathrm{D}$. It achieves the MG pair $\left(\mathsf{S}^{(F)} = \mathsf{L}/2, \mathsf{S}^{(S)} = \mathsf{L}\frac{\mathrm{D}'}{2(\mathrm{D}'+2)}\right)$ using cooperation prelogs $\mu_{\text{Rx}} = \mathsf{L} \cdot \frac{\mathrm{D}'}{2(\mathrm{D}'+2)}$ and $\mu_{\text{Rx}} = \mathsf{L} \cdot \frac{\mathrm{D}'}{8}$. We can achieve the same MG pair also by choosing $\beta = \frac{\mathrm{D}'}{\mathrm{D}} < 1$ and time-sharing the same scheme but for parameter D over a β-fraction of time with the no-cooperation scheme in the preceding subsection (which achieves MG pair $(\mathsf{L}/2, 0)$) over the rest of the time. Both approaches require same Tx-cooperation prelog $\mu_{\text{Tx}} = \mathsf{L}\mathrm{D}'/8 = \mathsf{L}\beta\mathrm{D}/8$. However, the former scheme achieves a larger MG pair, namely $\left(\mathsf{S}^{(F)} = \mathsf{L}/2, \mathsf{S}^{(S)} = \mathsf{L}\frac{\mathrm{D}'}{2(\mathrm{D}'+2)}\right)$, than the time-shared scheme, namely $(\mathsf{L}/2, \mathsf{L}\frac{\mathrm{D}'}{2(\mathrm{D}'/\beta+2)})$, at the expense of also requiring a larger Rx-cooperation prelog: $\mu_{\text{Rx}} = \mathsf{L}\frac{\mathrm{D}'}{2(\mathrm{D}'+2)}$ for the former simple scheme and $\mu_{\text{Rx}} = \mathsf{L}\frac{\mathrm{D}'}{2(\mathrm{D}'/\beta+2)}$ for the time-sharing scheme. We conclude that in a setup where the Rx-cooperation prelog is not the stringent resource, the simple scheme with a reduced number of cooperation rounds $\mathrm{D}' < \mathrm{D}$ is advantageous compared to the time-shared scheme. Similar observations also hold for the scheme in Subsection 5.1.1 using CoMP reception and for the schemes in Subsection 5.1.3 sending only "slow" messages.

5.2.3 Achievable MG Regions

Recall the definitions of $\mathsf{S}^{(F)}_{\text{both}}$, $\mathsf{S}^{(S)}_{\text{both}}$, $\mathsf{S}^{(S)}_{\max}$, $\mathsf{S}^{(S)}_{\text{no-coop}}$ in (5.26), (5.37), and (5.40) and the definitions of $\mu^{(\text{r})}_{\text{Tx,both}}, \mu^{(\text{r})}_{\text{Rx,both}}, \mu^{(\text{t})}_{\text{Rx,both}}, \mu^{(\text{t})}_{\text{Tx,both}}$ in(5.29), (5.33), (5.36), and (5.34). Define further

$$\alpha \triangleq \max\left\{\min\left\{\frac{\mu_{\text{Tx}}}{\mu^{(\text{r})}_{\text{Tx,both}}}, \frac{\mu_{\text{Rx}}}{\mu^{(\text{r})}_{\text{Rx,both}}}\right\}, \min\left\{\frac{\mu_{\text{Tx}}}{\mu^{(\text{t})}_{\text{Tx,both}}}, \frac{\mu_{\text{Rx}}}{\mu^{(\text{t})}_{\text{Rx,both}}}\right\}\right\}. \tag{5.41}$$

and

$$\mathsf{S}^{(S)}_{\text{sym},1}(\alpha) \triangleq \alpha\mathsf{S}^{(S)}_{\max} + (1-\alpha)\mathsf{S}^{(S)}_{\text{no-coop}} \tag{5.42}$$

$$\mathsf{S}^{(F)}_{\mathrm{sym},2}(\alpha) \triangleq \alpha \mathsf{S}^{(F)}_{\mathrm{both}} + (1-\alpha)\mathsf{S}^{(F)}_{\mathrm{max}} \qquad \text{and} \qquad \mathsf{S}^{(S)}_{\mathrm{sym},2}(\alpha) \triangleq \alpha \mathsf{S}^{(S)}_{\mathrm{both}} \tag{5.43}$$

$$\mathsf{S}^{(F)}_{\mathrm{sym},3}(\alpha) \triangleq \alpha \mathsf{S}^{(F)}_{\mathrm{both}} \qquad \text{and} \qquad \mathsf{S}^{(S)}_{\mathrm{sym},3}(\alpha) \triangleq \alpha \mathsf{S}^{(S)}_{\mathrm{both}} + (1-\alpha)\mathsf{S}^{(S)}_{\mathrm{max}}. \tag{5.44}$$

According to the arguments in the previous subsection, the following regions of MG pairs are achievable depending on the available cooperation prelogs μ_{Tx} and μ_{Rx}.

Theorem 6 (Achievable MG Region: Wyner's Symmetric Model)**.** *Assume $D \geq 2$.*

When $\mu_{\mathrm{Rx}} \geq \mu^{(r)}_{\mathrm{Rx},both}$ and $\mu_{\mathrm{Tx}} \geq \mu^{(r)}_{\mathrm{Tx},both}$; or when $\mu_{\mathrm{Rx}} \geq \mu^{(t)}_{\mathrm{Rx},both}$ and $\mu_{\mathrm{Tx}} \geq \mu^{(t)}_{\mathrm{Tx},both}$:

$$\text{convex hull}\Big((0,0),\ (0,\mathsf{S}^{(S)}_{max}),\ (\mathsf{S}^{(F)}_{both},\mathsf{S}^{(S)}_{both}),\ (\mathsf{S}^{(F)}_{max},0) \Big) \subseteq \mathcal{S}^{\star}(\mu_{\mathrm{Tx}},\mu_{\mathrm{Rx}},D). \tag{5.45}$$

When $\mu_{\mathrm{Rx}} \geq \mu^{(r)}_{\mathrm{Rx},\mathsf{S}}$ and $\mu_{\mathrm{Tx}} < \mu^{(r)}_{\mathrm{Tx},both}$; or when $\mu_{\mathrm{Tx}} \geq \mu^{(t)}_{\mathrm{Tx},\mathsf{S}}$ and $\mu_{\mathrm{Rx}} < \mu^{(t)}_{\mathrm{Rx},both}$:

$$\text{convex hull}\Big((0,0),\ (0,\mathsf{S}^{(S)}_{max}),\ (\mathsf{S}^{(F)}_{sym,3}(\alpha),\mathsf{S}^{(S)}_{sym,3}(\alpha)),\ (\mathsf{S}^{(F)}_{sym,2}(\alpha),\mathsf{S}^{(S)}_{sym,2}(\alpha)),\ (\mathsf{S}^{(F)}_{max},0) \Big) \subseteq \mathcal{S}^{\star}(\mu_{\mathrm{Tx}},\mu_{\mathrm{Rx}},D). \tag{5.46}$$

When $\mu_{\mathrm{Rx}} < \mu^{(r)}_{\mathrm{Rx},both}$ or when $\mu_{\mathrm{Tx}} < \mu^{(t)}_{\mathrm{Tx},both}$:

$$\text{convex hull}\Big((0,0),\ (0,\mathsf{S}^{(S)}_{sym,1}(\alpha)),\ (\mathsf{S}^{(F)}_{sym,2}(\alpha),\mathsf{S}^{(S)}_{sym,2}(\alpha)),\ (\mathsf{S}^{(F)}_{max},0) \Big) \subseteq \mathcal{S}^{\star}(\mu_{\mathrm{Tx}},\mu_{\mathrm{Rx}},D).$$

Proposition 2 (Outer Bound on the MG Region: Wyner's Symmetric Model)**.** *Any MG pair $(\mathsf{S}^{(F)},\mathsf{S}^{(S)})$ in $\mathcal{S}^{\star}(\mu_{\mathrm{Tx}},\mu_{\mathrm{Rx}},D)$ satisfies*

$$\mathsf{S}^{(F)} \leq \frac{\mathsf{L}}{2}, \tag{5.47}$$

$$\mathsf{S}^{(F)} + \mathsf{S}^{(S)} \leq \mathsf{L} \cdot \frac{D+1}{D+2}. \tag{5.48}$$

Proof: Follows by specializing the *MAC-Lemma for interference networks with conferencing* [46, Lemma 1]) to

$$\mathcal{J}_{\mathrm{outputs}} \triangleq \bigcup_{\ell \in \{1,\ldots,\lceil \frac{K}{2(\mathrm{D}+2)} \rceil\}} \{2+(\ell-1)(2\mathrm{D}+4),\ldots,\ell(2\mathrm{D}+4)-1\}, \tag{5.49}$$

$$\mathcal{J}_{\mathrm{inputs}} \triangleq \bigcup_{\ell \in \{1,\ldots,\lceil \frac{K}{2(\mathrm{D}+2)} \rceil\}} \{\mathrm{D}+2+(\ell-1)(2\mathrm{D}+4),\ldots,\mathrm{D}+3+(\ell-1)(2\mathrm{D}+4)\}, \tag{5.50}$$

$$\mathcal{J}_{\mathrm{messages}} \triangleq \bigcup_{\ell \in \{1,\ldots,\lceil \frac{K}{2(\mathrm{D}+2)} \rceil\}} \{\mathrm{D}+2-\mathrm{D}_{\mathrm{Tx}}+(\ell-1)(2\mathrm{D}+4),\ldots,\mathrm{D}+3+\mathrm{D}_{\mathrm{Tx}}+(\ell-1)(2\mathrm{D}+4)\}.$$

(5.51)

■

Corollary 4. *If*

$$\mu_{\mathrm{Rx}} \geq \mu^{(r)}_{\mathrm{Rx},both} \quad and \quad \mu_{\mathrm{Tx}} \geq \mu^{(r)}_{\mathrm{Tx},both}, \tag{5.52}$$

or if

$$\mu_{\mathrm{Rx}} \geq \mu^{(t)}_{\mathrm{Rx},both} \quad and \quad \mu_{\mathrm{Tx}} \geq \mu^{(t)}_{\mathrm{Tx},both}, \tag{5.53}$$

the optimal MG region $\mathcal{S}^{\star}(\mu_{\mathrm{Tx}}, \mu_{\mathrm{Rx}}, D)$ coincides with the trapezoid in (5.45).

Proof: Follows directly by Theorem 6 and Proposition 2. ■

The result of Corollary 4 implies that for large cooperation prelogs μ_{Tx} and μ_{Rx}, imposing a stringent delay constraint on the "fast" messages never penalizes the maximum achievable sum-MG of the system: the same sum-MG can be achieved as if only "slow" messages were sent.

The next corollary characterizes the optimal MG region $\mathcal{S}^{\star}(\mu_{\mathrm{Tx}}, \mu_{\mathrm{Rx}}, \mathrm{D})$ when one of the two cooperation prelogs (μ_{Tx} or μ_{Rx}) is small and the other large, and when $\mathsf{S}^{(F)}$ lies below a certain threshold. The corollary shows that also in this regime the same maximum sum-MG can be achieved as if only "slow" messages were sent. When $\mathsf{S}^{(F)}$ exceeds this threshold, our achievable MG region in (5.46) shows a penalty in sum-MG which increases linearly with the "fast" MG. In this regime we do not have a matching converse result.

Corollary 5. *Assume that*

$$\mu_{\mathrm{Rx}} \geq \mu^{(r)}_{\mathrm{Rx},\mathsf{S}} \quad and \quad \mu_{\mathrm{Tx}} < \mu^{(r)}_{\mathrm{Tx},both} \tag{5.54}$$

hold, or

$$\mu_{\mathrm{Tx}} \geq \mu^{(t)}_{\mathrm{Tx},\mathsf{S}} \quad and \quad \mu_{\mathrm{Rx}} < \mu^{(t)}_{\mathrm{Rx},both} \tag{5.55}$$

hold. For any $\mathsf{S}^{(F)} \in [0, \alpha \cdot \frac{\mathsf{L}}{2}]$, where α is defined in (5.41)*, the pair $(\mathsf{S}^{(F)}, \mathsf{S}^{(S)})$ lies in the optimal MG region $\mathcal{S}^{\star}(\mu_{\mathrm{Tx}}, \mu_{\mathrm{Rx}}, D)$ if, and only if, it is included in the trapezoid region described on the LHS of* (5.46).

Proof: Follows directly by Theorem 6, see (5.46), and by Proposition 2, and because the sum $\mathsf{S}^{(F)}_{\mathrm{sym},3}(\alpha) + \mathsf{S}^{(S)}_{\mathrm{sym},3}(\alpha) = \mathsf{L} \cdot \frac{\mathrm{D}+1}{\mathrm{D}+2}$ coincides with the maximum sum MG. ■

Figure 5.3 illustrates the inner and outer bounds (Theorem 6 and Proposition 2) on the MG region with D = 6 and D = 10, and different values of μ_{Rx} and μ_{Tx}. As can be seen in Figure 5.3a and as also explained in Corollary 4, when $\mu_{\mathrm{Rx}} \geq 2.625$ and $\mu_{\mathrm{Tx}} \geq 1.125$, or when $\mu_{\mathrm{Rx}} \geq 1.125$ and $\mu_{\mathrm{Tx}} \geq 2.25$ the

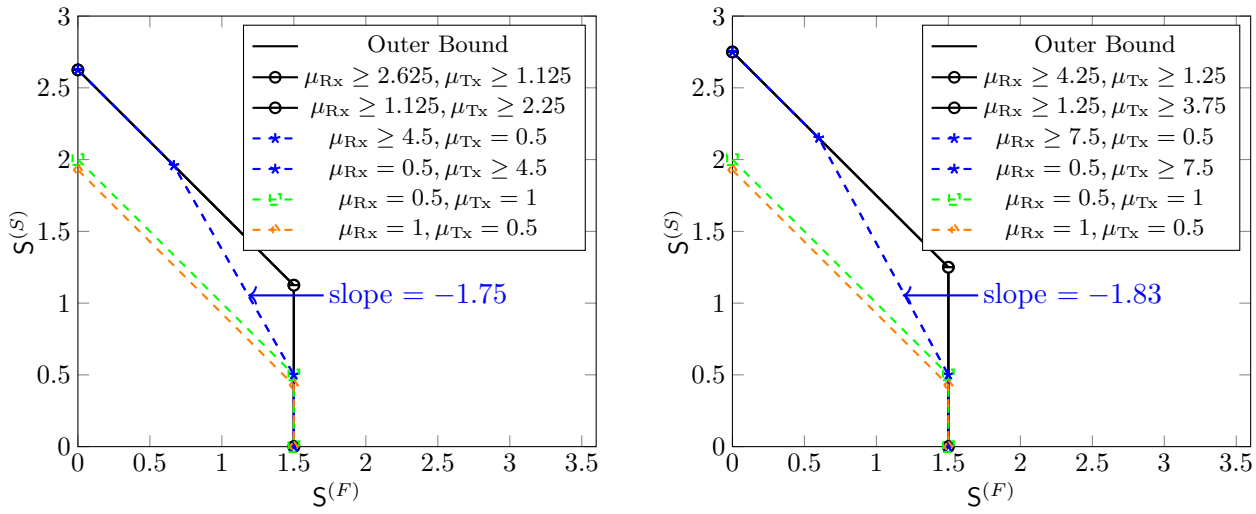

(a) D = 6 (b) D = 10

Figure 5.3: Inner and outer bounds on $\mathcal{S}^{\star}(\mu_{\mathrm{Tx}}, \mu_{\mathrm{Rx}}, \mathrm{D})$ for the symmetric Wyner network for different values of μ_{Rx} and μ_{Tx}, and for $\mathsf{L} = 3$, a) $\mathrm{D} = 6$, and b) $\mathrm{D} = 10$.

inner bound in (5.45) and the outer bound match. In the former case, the inner bound is achievable using the scheme in Subsection 5.2.2 based on CoMP reception, and in the latter case it is achievable using the scheme in Subsection 5.2.2 based on CoMP transmission. As explained in Corollary 5, when only one of the two cooperation prelogs is large and the other small (e.g., $\mu_{\mathrm{Rx}} \geq 4.5$ and $\mu_{\mathrm{Tx}} = 0.5$; or $\mu_{\mathrm{Tx}} \geq 4.5$ and $\mu_{\mathrm{Rx}} = 0.5$) the inner bound in (5.46) matches the outer bound of Proposition 2 only for $\mathsf{S}^{(F)} < \alpha \cdot \frac{\mathsf{L}}{2}$, where α is defined in (5.41). For larger values of $\mathsf{S}^{(F)}$, the "slow" MG achieved by our schemes decreases linearly by approximately 1.8Δ when $\mathsf{S}^{(F)}$ increases by Δ, and thus the sum-MG also decreases approximately by 0.8Δ. When both μ_{Rx} and μ_{Tx} are moderate or small, e.g., $\mu_{\mathrm{Rx}} = 0.5$ and $\mu_{\mathrm{Tx}} = 1$ or $\mu_{\mathrm{Rx}} = 1$ and $\mu_{\mathrm{Tx}} = 0.5$, the sum-MG achieved by our inner bound is smaller than for larger cooperation prelogs, but is constant over all regimes of $\mathsf{S}^{(F)}$. We finally notice that these inner bounds are the same for any number of cooperation rounds $\mathrm{D} = 6, 8, 10$. The reason is that for small cooperation prelogs, reducing the number of cooperation rounds to satisfy the cooperation prelogs is more advantageous than time-sharing different schemes with D cooperation rounds, see also the discussion in Subsection 5.2.2.

5.3 Hexagonal Network

5.3.1 Network and Cooperation Model

Consider a cellular network with K hexagonal cells, where each cell consists of one single mobile user (MU) and one basestation (BS). The signals of users that lie in a given cell interfere with the signals sent in the

6 adjacent cells. The interference pattern of our network is depicted by the black dashed lines in Fig. 5.4, i.e., the interference set $\mathcal{I}_{\mathrm{Tx},k}$ contains the indices of the 6 neighbouring cells whose signals interfere with cell k. The input-output relation of the network is as in (3.5).

Each Rx k (BS of a cell) can cooperate with the six Rxs in the adjacent cells, i.e., $|\mathcal{N}_{\mathrm{Rx}}(k)| = 6$. Thus, the number of Rx-cooperation links $\mathcal{Q}_{K,\mathrm{Rx}}$ in this network is approximately equal to $6K$ (up to edge effects). Similarly, each Tx (MU of a cell) can cooperate with the six Txs in the adjacent cells and thus $|\mathcal{N}_{\mathrm{Tx}}(k)| = 6$ and $\mathcal{Q}_{K,\mathrm{Tx}} \approx 6K$.

To describe the setup and our schemes in more detail, we parametrize the locations of the Tx/Rx pair in the k-th cell by a number o_k in the complex plane $\mathbb{C}$. Introducing the coordinate vectors

$$\mathbf{e}_x = \frac{\sqrt{3}}{2} - \frac{1}{2}i \quad \text{and} \quad \mathbf{e}_y = i, \tag{5.56}$$

as in Figure 5.4, the position o_k of Tx/Rx pair k can be associated with an integer pair (a_k, b_k) satisfying

$$o_k \triangleq a_k \cdot \mathbf{e}_x + b_k \cdot \mathbf{e}_y. \tag{5.57}$$

The interference set $\mathcal{I}_{\mathrm{Tx},k}$ and the neighbouring sets can then be expressed as

$$\begin{aligned}\mathcal{N}_{\mathrm{Tx}}(k) = \mathcal{N}_{\mathrm{Rx}}(k) = \mathcal{I}_{\mathrm{Tx},k} = \big\{k' \colon \quad & |a_k - a_{k'}| = 1 \quad \text{and} \quad |b_k - b_{k'}| = 1 \\ & \text{and} \quad |a_k - a_{k'} - b_k + b_{k'}| = 1\big\}.\end{aligned} \tag{5.58}$$

For simplicity we assume an even-valued D satisfying

$$\mathrm{mod}\,\left(\frac{\mathrm{D}}{2} - 1, 3\right) = 0. \tag{5.59}$$

Other cases can be treated in a similar way.

5.3.2 Tx/Rx Set Associations

In this subsection, we propose Tx/Rx set associations for this network that can be used to implement the schemes in section 5.1, and we present the corresponding MG pairs and cooperation prelogs. In Appendix A.2.1, we prove that the proposed associations are indeed permissible and we present details on the evaluations of the achieved MG pairs and the required cooperation prelogs.

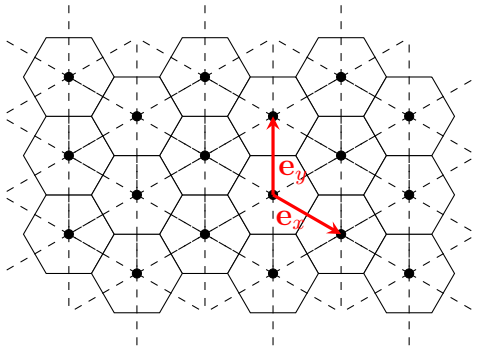

Figure 5.4: Illustration of the hexagonal network. Small circles indicate Txs and Rxs, black solid lines depict the cell borders, and black dashed lines indicate that the communication in two given cells interfere.

We first explain the choice of $\mathcal{T}_{\text{silent}}$ for the no-cooperation scheme in Subsection 5.1.4. Choose

$$\mathcal{T}_{\text{active}} = \{k \in [K]\colon \quad (a_k + b_k) \mod 3 = 0\} \tag{5.60}$$

and $\mathcal{T}_{\text{silent}} = [K] \backslash \mathcal{T}_{\text{active}}$. The corresponding cell association is shown in Figure 5.5a where active cells are depicted in yellow and silenced cells in white. By (5.19), the sum-MG achieved by this scheme is

$$\mathsf{S}_{\text{no-coop}} = \frac{\mathsf{L}}{3}. \tag{5.61}$$

We next explain the choice of the Tx/Rx sets for the schemes sending only "slow" messages described in Subsection 5.1.3. Set $\tau = \frac{\mathrm{D}}{2} + 1$ and choose a Tx k (Rx k) as a master Tx (Rx), if it belongs to the set

$$\mathcal{T}_{\text{master}} = \{k \in [K]\colon (a_k \mod \tau = 0) \text{ and } (b_k \mod \tau = 0) \text{ and } (|a_k + b_k| \mod 3\tau = 0)\}. \tag{5.62}$$

To describe the set of silenced Txs $\mathcal{T}_{\text{silent}}$, we introduce the following notation. For any integers x and $\tau \geq 0$:

$$x_{[-\tau,2\tau]} \triangleq ((x + \tau) \mod 3\tau) - \tau, \tag{5.63}$$

where mod denotes the standard modulo operator. In fact, the operator $x_{[-\tau,2\tau]}$ ressembles the standard mod 3τ operator, but it shifts every number into the interval $[-\tau, 2\tau)$ and not into $[0, 3\tau)$. We then set

$$\mathcal{T}_{\text{silent}} = \left\{k\colon \max\{|a_{k[-\tau,2\tau)}|, |b_{k[-\tau,2\tau)}|, |a_{k[-\tau,2\tau)} - b_{k[-\tau,2\tau)}|\} = \tau\right\} \tag{5.64}$$

and $\mathcal{T}_{\text{slow}} = [K] \backslash \mathcal{T}_{\text{silent}}$. Figure 5.5b shows the proposed cell association for $\mathrm{D} = 6$: blue or yellow are the

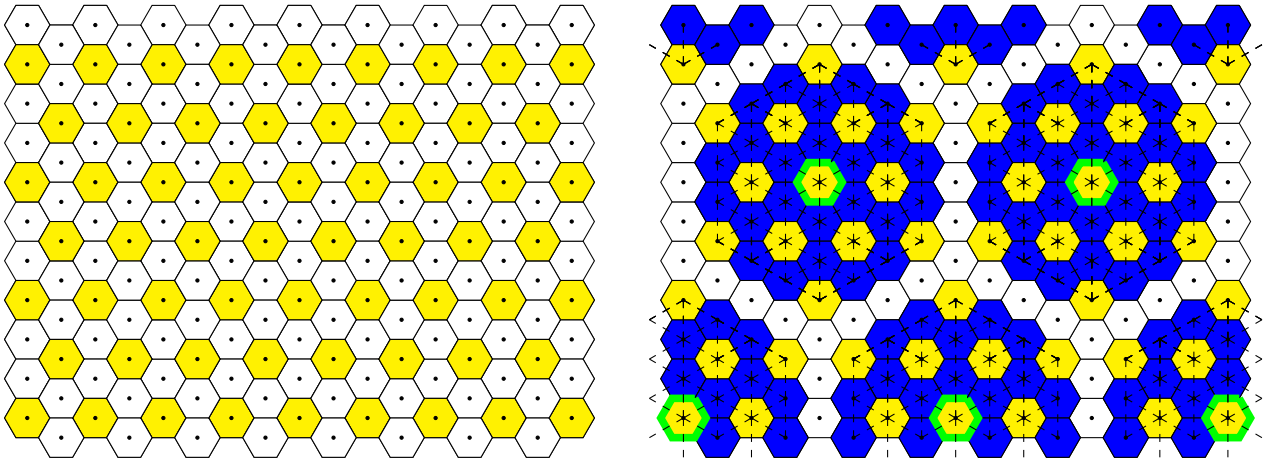

(a) Non-cooperative scheme

(b) Cooperative scheme

Figure 5.5: Illustration of the cell associations for the non-cooperative and the cooperative schemes in the hexagonal network. Txs in white cells are deactivated. In (a), Txs in yellow cells are active. In (b), when transmitting only "slow" messages with $\mathrm{D} = 6$, Txs in blue and yellow cells send "slow" messages. When transmitting both "fast" and "slow" messages with $\mathrm{D} = 8$, Txs in yellow cells send "fast" messages and Txs in blue cells send "slow" messages. Master Txs (Rxs) are depicted with green borders.

active "slow" cells and white the silenced cells. Master Txs (Rxs) are depicted with green borders. We observe that the choice in (5.64) silences all Tx/Rx pairs which lie $\frac{\mathrm{D}}{2}+1$ hops away from a master Tx/Rx pair. As we detail out in Appendix A.2.1, by (5.14) and (5.15), this choice establishes an achievable MG pair of $(\mathsf{S}^{(F)}=0, \mathsf{S}^{(S)}=\mathsf{S}^{(S)}_{\max})$, where

$$\mathsf{S}^{(S)}_{\max} \triangleq \mathsf{L}\cdot\frac{4+3\mathrm{D}(\mathrm{D}+2)}{3(\mathrm{D}+2)^2}. \tag{5.65}$$

Moreover, by (5.16) and (5.17), with CoMP reception or CoMP transmission the scheme requires average Rx- or Tx-cooperation prelogs equal to

$$\mu^{(\mathrm{t})}_{\mathrm{Tx},\mathsf{S}} = \mu^{(\mathrm{r})}_{\mathrm{Rx},\mathsf{S}} = \mathsf{L}\cdot\frac{\mathrm{D}(\mathrm{D}+1)}{9(\mathrm{D}+2)}. \tag{5.66}$$

Finally, we turn to the scheme that sends both "fast" and "slow" messages in Subsections 5.1.1 and 5.1.2. Here, we set $\tau=\frac{\mathrm{D}}{2}$ and choose the set of master Txs (Rxs) as in (5.62), but for this new value of τ. Similarly, we choose the silenced set $\mathcal{T}_{\text{silent}}$ as in (5.64) but again for the new value $\tau=\frac{\mathrm{D}}{2}$. The "fast" transmit set $\mathcal{T}_{\text{fast}}$ is chosen in the same way as $\mathcal{T}_{\text{active}}$ in (5.60), and $\mathcal{T}_{\text{slow}}=\mathcal{T}^{c}_{\text{silent}}\cap\mathcal{T}_{\text{fast}}$. The cell association is depicted in Figure 5.5b for $\mathrm{D}=8$, where "fast" cells are in yellow, "slow" cells in blue, and master cells are designated with green borders. As detailed out in Appendix A.2.1, by (5.8), the proposed

cell association achieves the MG pair $(\mathsf{S}^{(F)} = \mathsf{S}^{(F)}_{\text{both}}, \mathsf{S}^{(S)} = \mathsf{S}^{(S)}_{\text{both}})$ where

$$\mathsf{S}^{(F)}_{\text{both}} \triangleq \frac{\mathsf{L}}{3}\left(1 - \frac{2(\mathrm{D}-2)}{\mathrm{D}^2}\right) \quad \text{and} \quad \mathsf{S}^{(S)}_{\text{both}} \triangleq \frac{2\mathsf{L}}{3}\left(1 - \frac{2}{\mathrm{D}}\right), \tag{5.67}$$

and by (5.9) and (5.10) the required average Tx- and Rx-cooperation prelogs with CoMP reception are

$$\mu^{(\mathrm{r})}_{\text{Tx,both}} \triangleq \mathsf{L} \cdot \frac{(\mathrm{D}-2)(3\mathrm{D}-4)}{9\mathrm{D}^2} \quad \text{and} \quad \mu^{(\mathrm{r})}_{\text{Rx,both}} \triangleq \mathsf{L} \cdot \frac{4\mathrm{D}^3 + 3\mathrm{D}^2 - 42\mathrm{D} + 112}{54\mathrm{D}^2}, \tag{5.68}$$

and with CoMP transmission they are

$$\mu^{(\mathrm{t})}_{\text{Tx,both}} \triangleq \mathsf{L} \cdot \frac{4\mathrm{D}^3 - 3\mathrm{D}^2 - 6\mathrm{D} - 8}{54\mathrm{D}^2} \quad \text{and} \quad \mu^{(\mathrm{t})}_{\text{Rx,both}} \triangleq \mathsf{L} \cdot \frac{(\mathrm{D}-2)(3\mathrm{D}-4)}{9\mathrm{D}^2}. \tag{5.69}$$

5.3.3 Achievable MG Region

Recall the definitions of $\mathsf{S}^{(F)}_{\max}$, $\mathsf{S}^{(S)}_{\max}$, $\mathsf{S}^{(F)}_{\text{both}}$, $\mathsf{S}^{(S)}_{\text{both}}$ in (5.61), (5.65), and (5.67). Define

$$\alpha_1 \triangleq \max\left\{\min\left\{\frac{\mu_{\text{Tx}}}{\mu^{(\mathrm{r})}_{\text{Tx,both}}}, \frac{\mu_{\text{Rx}}}{\mu^{(\mathrm{r})}_{\text{Rx,both}}}\right\}, \min\left\{\frac{\mu_{\text{Tx}}}{\mu^{(\mathrm{t})}_{\text{Tx,both}}}, \frac{\mu_{\text{Rx}}}{\mu^{(\mathrm{t})}_{\text{Rx,both}}}\right\}\right\}, \tag{5.70}$$

$$\alpha_2 \triangleq \max\left\{\frac{\mu_{\text{Tx}}}{\mu^{(\mathrm{t})}_{\text{Tx,S}}}, \frac{\mu_{\text{Rx}}}{\mu^{(\mathrm{r})}_{\text{Rx,S}}}\right\}. \tag{5.71}$$

Also, define

$$\mathsf{S}^{(F)}_{\text{hexa,1}}(\alpha_1) \triangleq \alpha_1 \mathsf{S}^{(F)}_{\text{both}}, \qquad \mathsf{S}^{(S)}_{\text{hexa,1}}(\alpha_1) \triangleq \alpha_1 \mathsf{S}^{(S)}_{\text{both}} + (1-\alpha_1)\mathsf{S}^{(S)}_{\max}, \tag{5.72}$$

$$\mathsf{S}^{(F)}_{\text{hexa,2}}(\alpha_1) \triangleq \alpha_1 \mathsf{S}^{(F)}_{\text{both}} + (1-\alpha_1)\mathsf{S}^{(F)}_{\max}, \qquad \mathsf{S}^{(S)}_{\text{hexa,2}}(\alpha_1) \triangleq \alpha_1 \mathsf{S}^{(S)}_{\text{both}}, \tag{5.73}$$

$$\mathsf{S}^{(S)}_{\text{hexa}}(\alpha_2) \triangleq \alpha_2 \mathsf{S}^{(S)}_{\max} + (1-\alpha_2)\mathsf{S}^{(S)}_{\text{no-coop}}. \tag{5.74}$$

Theorem 7 (Achievable MG Region: Hexagonal Model)**.** *Assume $D \geq 2$.*

- *When $\mu_{\text{Rx}} \geq \max\{\mu^{(r)}_{\text{Rx},both}, \mu^{(r)}_{\text{Rx,S}}\}$ and $\mu_{\text{Tx}} \geq \mu^{(r)}_{\text{Tx},both}$; or when $\mu_{\text{Tx}} \geq \max\{\mu^{(t)}_{\text{Tx},both}, \mu^{(t)}_{\text{Tx,S}}\}$ and $\mu_{\text{Rx}} \geq \mu^{(t)}_{\text{Rx},both}$:*

$$\text{convex hull}\Big((0,0),\ (0,\mathsf{S}^{(S)}_{max}),\ (\mathsf{S}^{(F)}_{both},\mathsf{S}^{(S)}_{both}),\ (\mathsf{S}^{(F)}_{max},0)\Big) \subseteq \mathcal{S}^{\star}(\mu_{\text{Tx}},\mu_{\text{Rx}},D). \tag{5.75}$$

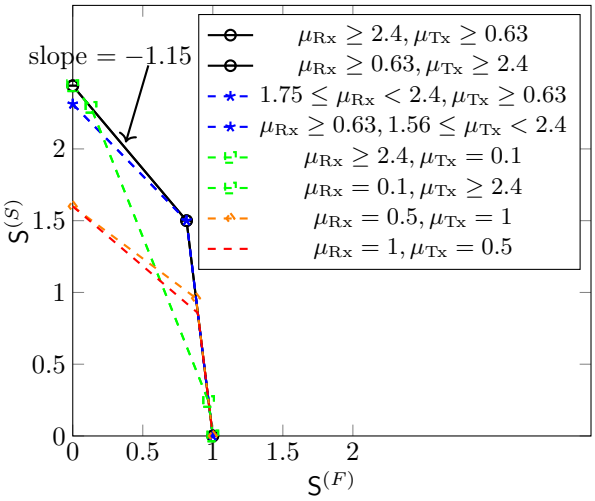

Figure 5.6: Inner bounds on $\mathcal{S}^{\star}(\mu_{\mathrm{Tx}}, \mu_{\mathrm{Rx}}, \mathrm{D})$ for the hexagonal model for $\mathrm{D} = 8$, $\mathsf{L} = 3$ and different values of μ_{Rx} and μ_{Tx}.

- *When* $\mu^{(r)}_{\mathrm{Rx},both} \leq \mu_{\mathrm{Rx}} < \mu^{(r)}_{\mathrm{Rx},\mathsf{S}}$ *and* $\mu_{\mathrm{Tx}} \geq \mu^{(r)}_{\mathrm{Tx},both}$*; or when* $\mu^{(t)}_{\mathrm{Tx},both} \leq \mu_{\mathrm{Tx}} < \mu^{(t)}_{\mathrm{Tx},\mathsf{S}}$ *and* $\mu_{\mathrm{Rx}} \geq \mu^{(t)}_{\mathrm{Rx},both}$*;*

$$\text{convex hull}\Big((0,0),\ (0,\mathsf{S}^{(F)}_{both}+\mathsf{S}^{(S)}_{both}),\ (\mathsf{S}^{(F)}_{both},\mathsf{S}^{(S)}_{both}),\ (\mathsf{S}^{(F)}_{max},0)\Big) \subseteq \mathcal{S}^{\star}(\mu_{\mathrm{Tx}},\mu_{\mathrm{Rx}},D). \tag{5.76}$$

- *When* $\mu_{\mathrm{Rx}} \geq \mu^{(r)}_{\mathrm{Rx},\mathsf{S}}$ *and* $\mu_{\mathrm{Tx}} < \mu^{(r)}_{\mathrm{Tx},both}$*; or when* $\mu_{\mathrm{Tx}} \geq \mu^{(t)}_{\mathrm{Tx},\mathsf{S}}$ *and* $\mu_{\mathrm{Rx}} < \mu^{(t)}_{\mathrm{Rx},both}$*;*

$$\text{convex hull}\Big((0,0),\ (0,\mathsf{S}^{(S)}_{max}),\ (\mathsf{S}^{(F)}_{hexa,1}(\alpha_1),\mathsf{S}^{(S)}_{hexa,1}(\alpha_1)),\ (\mathsf{S}^{(F)}_{hexa,2}(\alpha_1),\ \mathsf{S}^{(S)}_{hexa,2}(\alpha_1)),\ (\mathsf{S}^{(F)}_{max},0)\Big) \subseteq \mathcal{S}^{\star}(\mu_{\mathrm{Tx}},\mu_{\mathrm{Rx}},D). \tag{5.77}$$

- *When* $\mu_{\mathrm{Rx}} < \mu^{(r)}_{\mathrm{Rx},both}$ *or When* $\mu_{\mathrm{Tx}} < \mu^{(t)}_{\mathrm{Tx},both}$*,*

$$\text{convex hull}\Big((0,0),\ (0,\mathsf{S}^{(S)}_{hexa}(\alpha_2)),\ (\mathsf{S}^{(F)}_{hexa,2}(\alpha_1),\mathsf{S}^{(S)}_{hexa,2}(\alpha_1)),\ (\mathsf{S}^{(F)}_{max},0)\Big) \subseteq \mathcal{S}^{\star}(\mu_{\mathrm{Tx}},\mu_{\mathrm{Rx}},D). \tag{5.78}$$

Figure 5.6 illustrates the inner bounds (Theorem 7) on the MG region for $\mathrm{D} = 8$, and different values of μ_{Rx} and μ_{Tx}. This figure shows that unlike the results obtained for Wyner's symmetric model, the sum-MG of this network decreases as $\mathsf{S}^{(F)}$ increases. This can be seen from the slop of the line connecting the $(0, \mathsf{S}^{(S)}_{\mathrm{max}})$ point to the $(\mathsf{S}^{(F)}_{\mathrm{both}}, \mathsf{S}^{(S)}_{\mathrm{both}})$ point which is always smaller than -1. Furthermore, in this network, it is not possible to achieve the maximum $\mathsf{S}^{(F)}$ when transmitting both "fast" and "slow" messages.

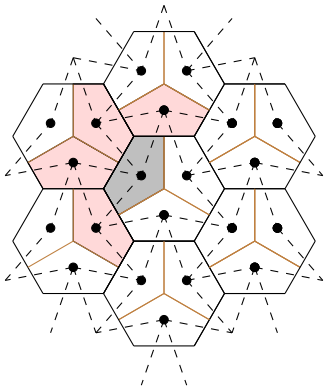

Figure 5.7: Illustration of the sectorized hexagonal network. Small circles indicate Txs (mobile users), black solid lines depict the cell borders, brown lines the sector borders, and dashed lines indicate that the communication in two given sectors interfere.

5.4 Sectorized Hexagonal Model

5.4.1 Network and Cooperation Model

Consider again a cellular network with K hexagonal cells, but where now each cell consists of three sectors. Each Tx is associated with a distinct sector and is equipped with L antennas. Each Rx is associated with a distinct cell and is equipped with $3\mathsf{L}$ directional antenna, where L antennas are pointing to each of the three sectors of the cell. This allows avoiding interference between communications from different sectors in the same cell. Thus, each Rx k observes three channel outputs $\boldsymbol{Y}^n_{k,k_1}$, $\boldsymbol{Y}^n_{k,k_2}$ and $\boldsymbol{Y}^n_{k,k_3}$ where Txs k_1, k_2 and k_3 are the three Txs of the sectors of the cell. More formally, Rx k observes a set of channel outputs $\boldsymbol{Y}(k) = [\boldsymbol{Y}^n_{k,k_1}\boldsymbol{Y}^n_{k,k_2}\boldsymbol{Y}^n_{k,k_3}]$ where the input-output relation $\boldsymbol{Y}^n_{k,\hat{k}}$ for $\hat{k} \in \{k_1, k_2, k_3\}$ is based on (3.5) and the set $\mathcal{I}_{\mathrm{Tx},\hat{k}}$ contain the indices of the 4 neighbouring sectors whose signals interfere with sector $\hat{k}$.

The interference pattern of our network is depicted by the dashed lines in Fig. 5.7, where the three sectors of a cell are separated by brown lines. Notice for example, that transmission in the grey-shaded sector is interfered only by the transmissions in the four adjacent pink-shaded sectors from other cells. In this model, each Rx k (BS of a cell) can cooperate with the six Rxs in the adjacent cells, i.e., $|\mathcal{N}_{\mathrm{Rx}}(k)| = 6$. Thus the number of Rx-cooperation links $\mathcal{Q}_{K,\mathrm{Rx}}$ in this network is approximately $6K$. Each Tx (MU of a cell) can cooperate with the four Txs in the adjacent sectors, i.e. $|\mathcal{N}_{\mathrm{Tx}}(k)| = 4$. Thus the number of Tx-cooperation links $\mathcal{Q}_{K,\mathrm{Tx}}$ is approximately $12K$. Assume that D is even. For simplicity, in this network we only consider the uplink communications with CoMP reception.

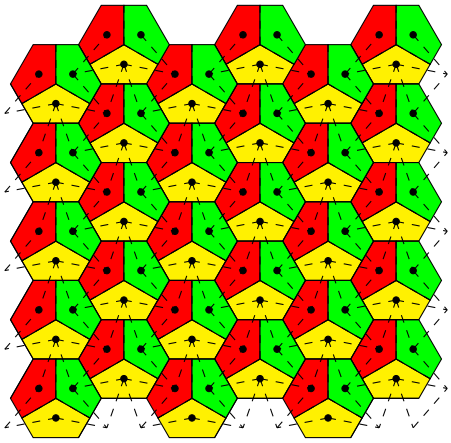

Figure 5.8: Illustration of the sectorized hexagonal network where the sectors labeled by “S" colored in yellow, sectors labeled by“NW” are colored in red, and the sectors labeled by “NE" are colored in green.

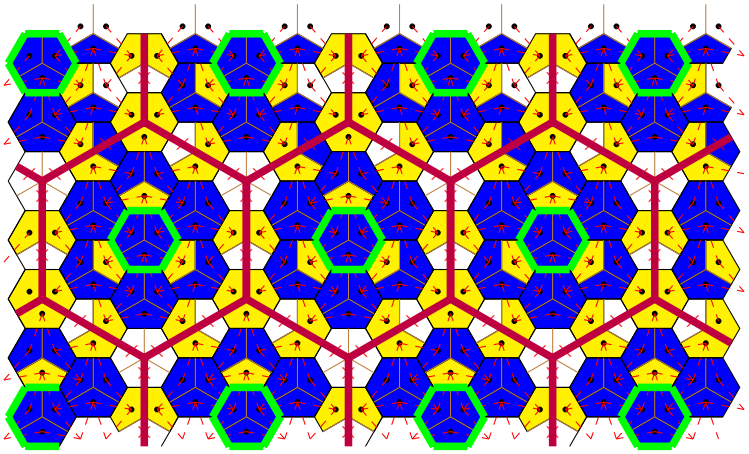

Figure 5.9: Illustration of cell allocation for D = 4 in the sectorized hexagonal network. Txs in white sectors are deactivated, Txs in yellow sectors send “fast” messages and Txs in blue sectors send “slow” messages. Master cells are marked by green.

5.4.2 Tx/Rx Set Associations

We present the sector associations for the schemes in Subsection 5.1.1 for this network. (Recall that in this model each Tx is associated with a given sector and each Rx with a given cell.) Within a cell, we label the three sectors by “S", “NW’, “NE" as colored in yellow, red and green in Figure 5.8.

For the no cooperation scheme, we define the active set $\mathcal{T}_{\text{active}}$ as the set of either the “NW" sectors, the “NE" sectors, or the “S" sectors of all cells as depicted in Figure 5.8. The proposed cell association achieves the sum-MG

$$\mathsf{S}_{\text{no-coop}} \triangleq \frac{\mathsf{L}}{3}. \tag{5.79}$$

For the cooperative schemes, both when we send only “slow" messages or when we send both “fast" and “slow" messages, we pick the set of *master cells* $\mathcal{T}_{\text{master}}$ as in (5.62) for the choice $\tau = \frac{\mathrm{D}}{2}$. Unlike in the

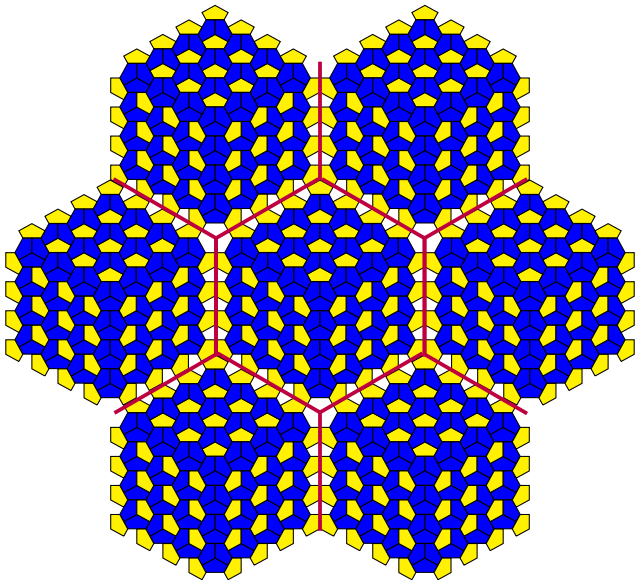

Figure 5.10: Illustration of cell allocation for D = 8 in the sectorized hexagonal network. Txs in white sectors are deactivated, Txs in yellow sectors send "fast" messages and Txs in blue sectors send "slow" messages.

hexagonal model in Section 5.3, we do not need to deactivate the entire τ-th cell layer around each master cell. Instead, for the 6 corner cells that lie exactly τ cell-hops away from 3 different master cells, we silence all users in every second of these corner cells and keep all Txs of the other 3 corner cells active. For the non-corner cells that lie τ cell hops away from only 2 different master cells, we only silence the Txs in the sector that is closest to the next active corner cell, and keep all other Txs active. As for the hexagonal model, all Txs that lie less than τ cell hops from a master cell are kept active. See Figure 5.9 for an illustration of the proposed cell association when D = 4 and Figure 5.10 when D = 8. For the scheme sending only "slow" messages, all Txs in the yellow and blue sectors send "slow" messages. As explained in Appendix A.2.2, for this scheme the proposed sector association achieves the MG pair $(\mathsf{S}^{(F)} = 0, \mathsf{S}^{(S)} = \mathsf{S}^{(S)}_{\max})$ where

$$\mathsf{S}^{(S)}_{\max} \triangleq \mathsf{L} \cdot \frac{3\mathrm{D} - 2}{3\mathrm{D}}, \tag{5.80}$$

and it requires an average Rx-cooperation prelog of

$$\mu^{(\mathrm{r})}_{\mathrm{Rx},\mathsf{S}} = \mathsf{L} \cdot \frac{(\mathrm{D} - 1)}{3}. \tag{5.81}$$

In the scheme sending both "fast" and "slow" messages, the Txs in the "yellow" sectors of Figure 5.9 send "fast" messages and the Txs in the "blue" sectors send "slow" messages. All active Txs that lie τ cell hops away from the next master cells send "fast" messages. Txs that lie $\tau - 1$ cell hops away from the next

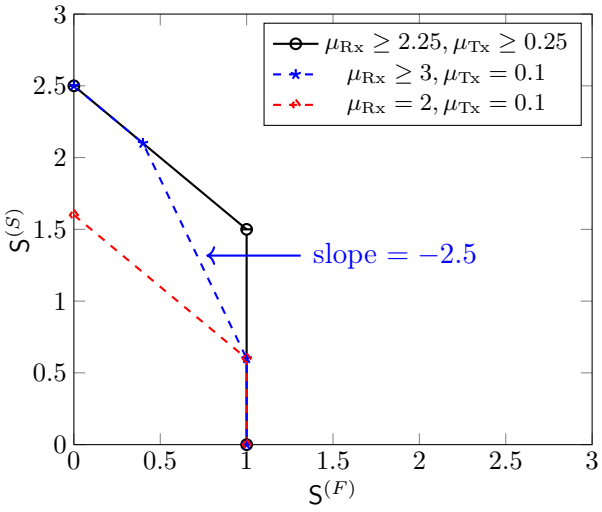

Figure 5.11: Inner bounds on $\mathcal{S}^{\star}(\mu_{\text{Tx}}, \mu_{\text{Rx}}, \mathsf{D})$ for the sectorized hexagonal model for $\mathsf{D} = 4$, $\mathsf{L} = 3$ and different values of μ_{Rx} and μ_{Tx}.

master cell send a "fast" message if their signals do not interfere with an active sector in layer τ; otherwise they send a "slow" message. Similarly, Txs that lie $\tau - i$ cell hops away from the next master cell, for $i = 1, \ldots, \tau$, send a "fast" message if their signals do not interfere with an active sector in the next layer $\tau - i + 1$; otherwise they send "slow" messages. We prove in Appendix A.2.2 that the proposed sector association achieves the MG pair

$$\mathsf{S}^{(F)}_{\text{both}} \triangleq \frac{\mathsf{L}}{3}, \quad \text{and} \quad \mathsf{S}^{(S)}_{\text{both}} \triangleq \mathsf{L} \cdot \frac{2\mathsf{D} - 2}{3\mathsf{D}}, \tag{5.82}$$

and requires average Tx- and Rx-cooperation prelogs

$$\mu^{(\text{r})}_{\text{Tx,both}} \triangleq \mathsf{L} \cdot \frac{(\mathsf{D} - 1)}{9\mathsf{D}} \quad \text{and} \quad \mu^{(\text{r})}_{\text{Rx,both}} \triangleq \mathsf{L} \cdot \frac{2\mathsf{D}^2 - 5}{9\mathsf{D}}. \tag{5.83}$$

5.4.3 Achievable MG Region

Recall the definitions of $\mathsf{S}^{(F)}_{\text{both}}$, $\mathsf{S}^{(S)}_{\text{both}}$, $\mathsf{S}^{(S)}_{\text{max}}$, and $\mathsf{S}_{\text{no-coop}}$ in (5.79), (5.80), and (5.82). Define

$$\alpha_1 \triangleq \frac{\mu_{\text{Tx}}}{\mu^{(\text{r})}_{\text{Tx,both}}} \quad \text{and} \quad \alpha_2 \triangleq \min\left\{ \frac{\mu_{\text{Tx}}}{\mu^{(\text{r})}_{\text{Tx,both}}}, \frac{\mu_{\text{Rx}}}{\mu^{(\text{r})}_{\text{Rx,both}}} \right\}. \tag{5.84}$$

Also, define

$$\mathsf{S}_{\text{sec}}^{(F)}(\alpha_1) \triangleq \alpha_1 \mathsf{S}_{\text{both}}^{(F)}, \quad \mathsf{S}_{\text{sec}}^{(S)}(\alpha_1) \triangleq \alpha_1 \mathsf{S}_{\text{both}}^{(S)} + (1-\alpha_1)\mathsf{S}_{\text{max}}^{(S)}, \tag{5.85}$$

$$\mathsf{S}_{\text{sec}}^{(F)}(\alpha_2) \triangleq \alpha_2 \mathsf{S}_{\text{both}}^{(F)} + (1-\alpha_2)\mathsf{S}_{\text{max}}^{(F)}, \quad \mathsf{S}_{\text{sec}}^{(S)}(\alpha_2) \triangleq \alpha_2 \mathsf{S}_{\text{both}}^{(S)}, \tag{5.86}$$

$$\mathsf{S}_{\text{sec},1}^{(S)}(\alpha_2) \triangleq \alpha_2 \mathsf{S}_{\text{max}}^{(S)} + (1-\alpha_2)\mathsf{S}_{\text{no-coop}}^{(S)}. \tag{5.87}$$

According to the arguments in Appendix A.2.2, the following regions of MG pairs are achievable depending on the available cooperation prelogs μ_{Tx} and μ_{Rx}.

Theorem 8 (Achievable MG Region: Sectorized Hexagonal Model)**.** *Assume $D \geq 2$.*

- *When $\mu_{\text{Rx}} \geq \mu_{\text{Rx},both}^{(r)}$ and $\mu_{\text{Tx}} \geq \mu_{\text{Tx},both}^{(r)}$;*

$$\text{convex hull}\Big((0,0),\ (0,\mathsf{S}_{max}^{(S)}),\ (\mathsf{S}_{both}^{(F)},\mathsf{S}_{both}^{(S)}),\ (\mathsf{S}_{max}^{(F)},0)\Big) \subseteq \mathcal{S}^{\star}(\mu_{\text{Tx}},\mu_{\text{Rx}},D). \tag{5.88}$$

- *When $\mu_{\text{Rx}} \geq \mu_{\text{Rx},\mathsf{S}}^{(r)}$ and $\mu_{\text{Tx}} < \mu_{\text{Tx},both}^{(r)}$;*

$$\text{convex hull}\Big((0,0),\ (0,\mathsf{S}_{max}^{(S)}),\ (\mathsf{S}_{sec}^{(F)}(\alpha_1),\mathsf{S}_{sec}^{(S)}(\alpha_1)),\ (\mathsf{S}_{sec}^{(F)}(\alpha_2),\mathsf{S}_{sec}^{(S)}(\alpha_2)),\ (\mathsf{S}_{max}^{(F)},0)\Big) \subseteq \mathcal{S}^{\star}(\mu_{\text{Tx}},\mu_{\text{Rx}},D). \tag{5.89}$$

- *When $\mu_{\text{Rx}} < \mu_{\text{Rx},both}^{(r)}$ and $\mu_{\text{Tx}} < \mu_{\text{Tx},both}^{(r)}$;*

$$\text{convex hull}\Big((0,0),\ (0,\mathsf{S}_{sec,1}^{(S)}(\alpha_2)),\ (\mathsf{S}_{sec}^{(F)}(\alpha_2),\mathsf{S}_{sec}^{(S)}(\alpha_2)),\ (\mathsf{S}_{max}^{(F)},0)\Big) \subseteq \mathcal{S}^{\star}(\mu_{\text{Tx}},\mu_{\text{Rx}},D). \tag{5.90}$$

Figure 5.11 illustrates the inner bounds (Theorem 8) on the MG region for D = 4, and different values of μ_{Rx} and μ_{Tx}. As can be seen from this figure, when $\mu_{\text{Rx}} \geq 2.25$ and $\mu_{\text{Tx}} \geq 0.25$, there is no penalty in sum Mg even at maximum "fast" MG. This can be seen from the slop of the line connecting the $(0, \mathsf{S}_{\text{max}}^{(S)})$ point to the $(\mathsf{S}_{\text{both}}^{(F)}, \mathsf{S}_{\text{both}}^{(S)})$ point which is equal to -1. Furthermore, in this network, it is possible to achieve the maximum $\mathsf{S}^{(F)}$ when transmitting both "fast" and "slow" messages.

Chapter 6

Random Users Activity with Mixed Delay Traffic

In this chapter, we combine random user activity with mixed delay traffic. Specifically, in each transmission block only a subset of the users has a message to convey to its corresponding Rxs. We specifically consider two setups. In both setups, Rxs can cooperate to decode their desired "slow" messages but not to decode "fast" messages. Each Tx is active with probability $\rho \in [0, 1]$, and the goal is to maximize the average expected "slow" rate of the network, while the rate of each "fast" message is fixed to a target value. In the first setup, each active Tx transmits a "slow" message, and with probability $\rho_f \in [0, 1]$ also transmits an *additional* "fast" message. In the second setup, each active Tx sends either a "fast" message with probability ρ_f or a "slow" message with probability $1 - \rho_f$.

For both setups, we propose general coding schemes and characterize their achievable MG regions for three networks: Wyner's soft-handoff network, Wyner's symmetric network and the hexagonal network. The achievable MG region is shown to be optimal for Wyner's soft-handoff network. In both setups, the obtained MG regions show that the average "slow" MG decreases i) with increasing number of interfering links, and ii) with increasing activity parameter ρ. The obtained MG regions also show that in the first setup, the maximum sum-MG is always attained at 0 "fast" MG, and increasing the "fast" MG decreases the sum-MG by a penalty that roughly speaking increases with the number of interference links in the network and with the activity parameter ρ. In contrast, in the second setup, for certain parameters the sum-MG is achieved at maximum "fast" MG and thus increasing the "fast" MG provides a gain in sum-MG, where we observe that the gain decreases with the number of interferers and the activity parameter ρ.

6.1 Random "Fast" Arrivals Only

6.1.1 Problem Setup

Consider a cellular network with K Tx-Rx pairs $k = 1, \ldots, K$. Each Tx $k \in \mathcal{K} \triangleq \{1, \ldots, K\}$ is *active* with probability $\rho \in [0, 1]$, in which case it sends a "slow" message $M_k^{(S)}$ to its corresponding Rx k. Here, $M_k^{(S)}$ is uniformly distributed over $\mathcal{M}_k^{(S)} \triangleq \{1, \ldots, \lfloor 2^{nR_k^{(S)}} \rfloor\}$, with n denoting the blocklength and $R_k^{(S)}$ the rate of message $M_k^{(S)}$. Given that Tx k is active, with probability $\rho_f \in [0, 1]$, it also sends an additional "fast" message $M_k^{(F)}$ to Rx k. These "fast" messages are subject to stringent delay constraints, and uniformly distributed over the set $\mathcal{M}^{(F)} \triangleq \{1, \ldots, \lfloor 2^{nR^{(F)}} \rfloor\}$. "Fast" messages are thus all of same size and same rate $R^{(F)}$.

We introduce the i.i.d Bernoulli-ρ random variables $A_1, \ldots, A_K$ and the i.i.d Bernoulli-ρ_f random variables $B_1, \ldots, B_K$ and define the active Tx-set as

$$\mathcal{T}_{\text{active}} \triangleq \{k \in \mathcal{K} : A_k = 1\}, \tag{6.1}$$

and the "fast" Tx-set as

$$\mathcal{T}_{\text{fast}} \triangleq \{k \in \mathcal{K} : A_k \cdot B_k = 1\}. \tag{6.2}$$

Then, for each $k \in \mathcal{K}$, Tx k computes its channel inputs $X_k^n \triangleq (X_{k,1}, \ldots, X_{k,n}) \in \mathbb{R}^n$ as

$$X_k^n = \begin{cases} f_k^{(B)}\big(M_k^{(F)}, M_k^{(S)}\big), & \text{if } k \in \mathcal{T}_{\text{fast}} \\ f_k^{(S)}\big(M_k^{(S)}\big), & \text{if } k \in \mathcal{T}_{\text{active}} \backslash \mathcal{T}_{\text{fast}} \\ 0, & \text{if } \mathcal{T}_{\text{active}}^c. \end{cases} \tag{6.3}$$

for some encoding functions $f_k^{(B)}$ and $f_k^{(S)}$ on appropriate domains satisfying the average block-power constraint

$$\frac{1}{n} \sum_{t=1}^{n} X_{k,t}^2 \leq \mathsf{P}, \quad \forall\ k \in \mathcal{K}, \qquad \text{almost surely.} \tag{6.4}$$

The input-output relation of the network is then described as

$$Y_{k,t} = A_k X_{k,t} + \sum_{\tilde{k} \in \mathcal{I}_{\text{Tx},k}} A_{\tilde{k}} h_{\tilde{k},k} X_{\tilde{k},t} + Z_{k,t}, \tag{6.5}$$

where $\{Z_{k,t}\}$ are independent and identically distributed (i.i.d.) standard Gaussians for all k and t and independent of all messages; the interfering set $\mathcal{I}_{\text{Tx},k}$ is defined in (2.2); $h_{\tilde{k},k} > 0$ is the channel coefficient between Tx $\tilde{k}$ and Rx k and is a fixed real number smaller than 1; and $X_{0,t} = 0$ for all t.

Each Rx $k \in \mathcal{T}_{\text{fast}}$ decodes the "fast" message $M_k^{(F)}$ based on its own channel outputs Y_k^n. So, it produces:

$$\hat{M}_k^{(F)} = g_k^{(n)}\big(Y_k^n\big), \tag{6.6}$$

for some decoding function $g_k^{(n)}$ on appropriate domains. It is assumed that receivers can fully cooperate on all receive signals when decoding their "slow" messages. So,

$$\hat{M}_k^{(S)} = b_k^{(n)}\Big(Y_1^n, \ldots, Y_K^n\Big), \tag{6.7}$$

where $b_k^{(n)}$ is a decoding function on appropriate domains.

Given $\mathsf{P} > 0$, a pair $(R^{(F)}(\mathsf{P}), \bar{R}^{(S)}(\mathsf{P}))$ is said achievable, if for each $K > 0$, there exist rates $\{R_k^{(S)}\}_{k=1}^K$ satisfying

$$\bar{R}^{(S)} \leq \varlimsup_{K\to\infty} \frac{1}{K}\mathbb{E}\left[\sum_{k\in\mathcal{T}_{\text{active}}} R_k^{(S)}\right], \tag{6.8}$$

and encoding, cooperation, and decoding functions satisfying constraint (6.4) and so that the probability of error

$$\mathbb{P}\Big[\bigcup_{k\in\mathcal{T}_{\text{fast}}} \big(\hat{M}_k^{(F)} \neq M_k^{(F)}\big) \text{ or } \bigcup_{k\in\mathcal{T}_{\text{active}}} \big(\hat{M}_k^{(S)} \neq M_k^{(S)}\big)\Big] \tag{6.9}$$

goes to 0 as $n \to \infty$.

Given the random arrival of the messages, the definition of the MG region differs from the previous sections. Specifically, an MG pair $(\mathsf{S}^{(F)}, \mathsf{S}^{(S)})$ is called *achievable*, if for all powers $\mathsf{P} > 0$ there exist achievable average rates $\{R^{(F)}(\mathsf{P}), \bar{R}^{(S)}(\mathsf{P})\}_{\mathsf{P}>0}$ satisfying

$$\mathsf{S}^{(F)} \triangleq \varlimsup_{\mathsf{P}\to\infty} \frac{R^{(F)}(\mathsf{P})}{\frac{1}{2}\log(\mathsf{P})} \cdot \rho\rho_f, \tag{6.10}$$

$$\mathsf{S}^{(S)} \triangleq \varlimsup_{\mathsf{P}\to\infty} \mathbb{E}\left[\frac{\bar{R}^{(S)}(\mathsf{P})}{\frac{1}{2}\log(\mathsf{P})}\right]. \tag{6.11}$$

The closure of the set of all achievable MG pairs $(\mathsf{S}^{(F)}, \mathsf{S}^{(S)})$ is called *statistical MG region* and is denoted

$\mathcal{S}^\star(\rho, \rho_f)$.

The MG in (6.11) measures the average expected "slow" MG on the network. Since the "fast" rate is fixed to $R^{(F)}$ at all Txs in $\mathcal{T}_{\text{fast}}$, we multiply the MG in (6.10) by $\rho\rho_f$ to obtain the average expected "fast" MG of the network.

6.1.2 Achievable MG Region and Coding Schemes

In this section, we propose two schemes, one with large "fast" MG and the other with zero "fast" MG.

Transmitting at large $\mathsf{S}^{(F)}$:

Since we wish to transmit at maximum "fast" MG, each "fast" transmission should not be interfered (except for signals up to noise level) by any other ("fast" or "slow") transmission. Therefore, we partition $\mathcal{K}$ into δ subsets $\mathcal{K}_1, \ldots, \mathcal{K}_\delta$, for some positive integer δ, in a way that all the signals sent by Txs in a given subset $\mathcal{K}_i$ do not interfere, i.e., for each $i \in \{1, \ldots, \delta\}$:

$$k' \notin \mathcal{I}_{\text{Rx},k''} \quad \text{and} \quad k'' \notin \mathcal{I}_{\text{Rx},k'}, \quad \forall k', k'' \in \mathcal{K}_i, \tag{6.12}$$

where $\mathcal{I}_{\text{Rx},k}$ is defined in (2.1). We divide the total transmission time into δ equally-sized phases. In the i-th phase,

- each Tx k in $\mathcal{K}_i \cap \mathcal{T}_{\text{fast}}$ sends its entire "fast" message $M_k^{(F)}$ but no part of the "slow" message $M_k^{(S)}$;
- each Tx $k \in \mathcal{K} \backslash (\mathcal{K}_i \cap \mathcal{T}_{\text{fast}})$ sends a part of its "slow" message $M_k^{(S)}$ if

$$\mathcal{I}_{\text{Rx},k} \cap \mathcal{T}_{\text{fast}} \cap \mathcal{K}_i = \emptyset; \tag{6.13}$$

  otherwise it does not send anything.

Condition (6.13) ensures that transmissions of "fast" messages are not interfered at all. By (6.12), the condition is in particular satisfied for all $k \in \mathcal{K}_i \cap (\mathcal{T}_{\text{active}} \backslash \mathcal{T}_{\text{fast}})$.

The described scheme achieves a "fast" rate of $R^{(F)} = \frac{1}{\delta}\frac{1}{2}\log(1+\mathsf{P})$, and thus by (6.10), a "fast" MG of

$$\mathsf{S}_{\max}^{(F)} = \frac{\rho\rho_f}{\delta}. \tag{6.14}$$

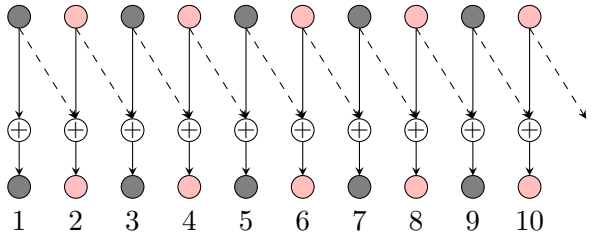

Figure 6.1: An illustration of Wyner's soft-handoff network where the Tx/Rx pairs in $\mathcal{K}_1$ are colored in gray and the Tx/Rx pairs in $\mathcal{K}_2$ in pink. The interference graph is depicted by black dashed lines.

It also achieves an expected "slow" MG of

$$\bar{\mathsf{S}}^{(S)}_{\text{coop}}(K) = \frac{1}{K}\sum_{i=1}^{\delta}\frac{1}{\delta}\Big(\sum_{k\in\mathcal{K}_i}\mathbb{P}\{k\in\mathcal{T}_{\text{active}}\backslash\mathcal{T}_{\text{fast}}\} + \sum_{k\in\mathcal{K}\backslash\mathcal{K}_i}\mathbb{P}\{k\in\mathcal{T}_{\text{active}}\}\mathbb{P}\{\mathcal{I}_{\text{Rx},k}\cap\mathcal{T}_{\text{fast}}\cap\mathcal{K}_i=\emptyset\}\Big) \tag{6.15}$$

$$= \frac{1}{K}\sum_{i=1}^{\delta}\Big(\frac{\rho(1-\rho_f)}{\delta}|\mathcal{K}_i| + \sum_{k\in\mathcal{K}\backslash\mathcal{K}_i}\mathbb{P}\{k\in\mathcal{T}_{\text{active}}\}\prod_{\tilde{k}\in\{\mathcal{I}_{\text{Rx},k}\cap\mathcal{K}_i\}}\mathbb{P}\{\tilde{k}\notin\mathcal{T}_{\text{fast}}\}\Big) \tag{6.16}$$

$$= \frac{\rho}{\delta K}\sum_{i=1}^{\delta}\Big((1-\rho_f)|\mathcal{K}_i| + \sum_{k\in\mathcal{K}\backslash\mathcal{K}_i}(1-\rho\rho_f)^{|\mathcal{I}_{\text{Rx},k}\cap\mathcal{K}_i|}\}\Big). \tag{6.17}$$

Transmitting at $\mathsf{S}^{(F)}=0$:

Each Tx $k\in\mathcal{T}_{\text{active}}$ sends only a "slow" message but no "fast" message. Since perfect cooperation is assumed at the Rxs, each of the "slow" messages can be transmitted with MG 1. The average expected "slow" MG over the network is therefore

$$\bar{\mathsf{S}}^{(S)}_{\text{max}} = \rho, \tag{6.18}$$

while $\mathsf{S}^{(F)}=0$.

Time sharing the two schemes establishes the following:

Proposition 3 (Achievable MG Region)**.** *The inner bound on $\mathcal{S}^{\star}(\rho,\rho_f)$ contains the region:*

$$\text{convex hull}\Big((0,0),\ (0,\bar{\mathsf{S}}^{(S)}_{max}),\ (\mathsf{S}^{(F)}_{max},\bar{\mathsf{S}}^{(S)}_{coop}),\ (\mathsf{S}^{(F)}_{max},0)\Big). \tag{6.19}$$

In the following three sections we specialize this proposition to different interference networks. As we will see, for our first network, we can also prove a corresponding converse result, and thus Proposition 3 exactly characterizes $\mathcal{S}^{\star}(\rho,\rho_f)$.

6.1.3 Wyner's Soft-Handoff Network

Consider Wyner's soft-handoff network shown in Figure 6.1. Interference is short-range in the sense that the signal sent by Tx k is observed only by Rx k and by the neighbouring Rx $k+1$. Thus $\mathcal{I}_{\mathrm{Rx},k} = \{k+1\}$. For this network, we can exactly characterize the statistical MG region $\mathcal{S}^\star(\rho, \rho_f)$:

Theorem 9. *The statistical MG region $\mathcal{S}^\star(\rho, \rho_f)$ of Wyner's soft-handoff network is the set of all nonnegative pairs $(\mathsf{S}^{(F)}, \mathsf{S}^{(S)})$ satisfying*

$$\mathsf{S}^{(F)} \leq \frac{\rho\rho_f}{2}, \tag{6.20}$$

$$(1+\rho)\mathsf{S}^{(F)} + \mathsf{S}^{(S)} \leq \rho. \tag{6.21}$$

Proof: The achievability part follows by specializing Proposition 3 to $\delta = 2$ and to

$$\mathcal{K}_1 = \{1, 3, \ldots, K-1\} \quad \text{and} \quad \mathcal{K}_2 = \{2, 4, \ldots, K\}. \tag{6.22}$$

For this choice $|\mathcal{I}_{\mathrm{Rx},k} \cap \mathcal{K}_i| = 1$. The proof of the converse bound (6.20) is straightforward. The converse bound (6.21) is proved in Appendix A.3.1. ■

By above theorem, the statistical MG region $\mathcal{S}^\star(\rho, \rho_f)$ is a quadrilateral, see also Fig. 6.4, and it is mostly determined by the activity parameter ρ; the "fast" arrival probability ρ_f only determines the vertical *maximum*-$\mathsf{S}^{(F)} = \frac{\rho\rho_f}{2}$ *boundary* of the region. The *maximum*-$\mathsf{S}^{(S)}$ *boundary*, which characterizes the maximum achievable "slow" MG $\mathsf{S}^{(S)}$ in function of the "fast" MG $\mathsf{S}^{(F)}$, is fully characterized by ρ: it's a line segment with slope $-(1+\rho)$. In general, this slope determines the penalty that the maximum "slow" MG $\mathsf{S}^{(S)}$ incurrs when one increases the "fast" MG. This penalty increases with increasing ρ because with more active Txs in the network the probability increases that a given active "fast" Tx is interfered by other active transmitters, which then have to be forced to send at "slow" MG 0 in order not to harm the achievable "fast" MG.

6.1.4 Wyner's Symmetric Network

Consider Wyner's symmetric network in Figure 6.2, where the signal sent by Tx k is observed by Rxs k and $k+1$, and also by Rx $k-1$. Thus $\mathcal{I}_{\mathrm{Rx},k} = \{k-1, k+1\}$ for each $k \in \mathcal{K}$.

Corollary 6. *The statistical MG region $\mathcal{S}^\star(\rho, \rho_f)$ of Wyner's symmetric model includes all nonnegative*

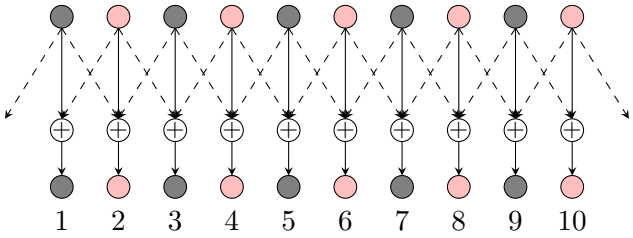

Figure 6.2: An illustration of Wyner's symmetric network where the Tx/Rx pairs in $\mathcal{K}_1$ are colored in gray and the Tx/Rx pairs in $\mathcal{K}_2$ in pink. The interference graph is depicted by black dashed lines.

pairs $(\mathsf{S}^{(F)}, \mathsf{S}^{(S)})$ *satisfying*

$$\mathsf{S}^{(F)} \leq \frac{\rho\rho_f}{2}, \tag{6.23}$$

$$\left(1+\rho(2-\rho\rho_f)\right)\mathsf{S}^{(F)} + \mathsf{S}^{(S)} \leq \rho. \tag{6.24}$$

Proof: Specialize Proposition 3 to $\delta = 2$ and to the sets $\mathcal{K}_1$ and $\mathcal{K}_2$ in (6.22). For this choice $|\mathcal{I}_{\mathrm{Rx},k} \cap \mathcal{K}_i| = 2$. ■

The region in above corollary is again a quadrilateral, but the maximum-$\mathsf{S}^{(S)}$ boundary is now determined by both parameters ρ and ρ_f as its slope is $-\left(1+\rho(2-\rho\rho_f)\right)$. The dependency on ρ_f however vanishes as $\rho \cdot \rho_f \to 0$ in which case the slope approaches $-(1+2\rho)$. Interestingly, this asymptotic slope shows a factor 2 compared to the slope of the maximum-$\mathsf{S}^{(S)}$ boundary in Wyner's soft-handoff network. The reason is that in Wyner's symmetric network $|\mathcal{I}_{\mathrm{Tx},k}| = 2$ whereas in Wyner's soft-handoff network $|\mathcal{I}_{\mathrm{Tx},k}| = 1$. In the next subsection, we will see that in the hexagonal network where $|\mathcal{I}_{\mathrm{Tx},k}| = 6$, this asymptotic slope is $-(1+6\rho)$.

6.1.5 Hexagonal Network

Consider the hexagonal network in Figure 6.3 with K hexagonal cells and each cell including one Tx and one Rx. The signals of Tx/Rx pairs that lie in a given cell interfere with the signals sent in the 6 adjacent cells. The interference pattern is depicted by the dashed black lines in Fig. 6.3.

Corollary 7. *The multiplexing gain region* $\mathcal{S}^\star(\rho, \rho_f)$ *includes all nonnegative pairs* $(\mathsf{S}^{(F)}, \mathsf{S}^{(S)})$ *satisfying*

$$\mathsf{S}^{(F)} \leq \frac{\rho\rho_f}{3}, \tag{6.25}$$

$$\left(1+2\rho(3-3\rho\rho_f+\rho^2\rho_f^2)\right)\mathsf{S}^{(F)} + \mathsf{S}^{(S)} \leq \rho. \tag{6.26}$$

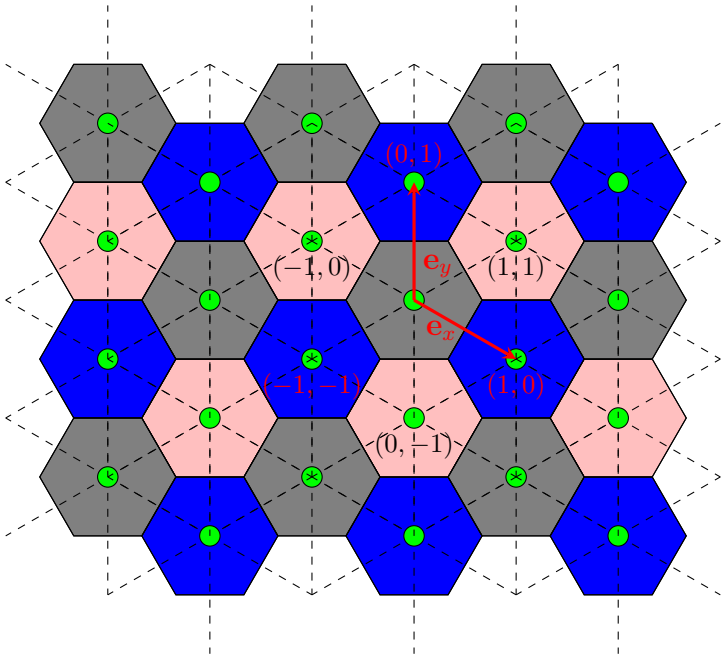

Figure 6.3: An illustration of the hexagonal network where the Tx/Rx pairs in $\mathcal{K}_1$ are colored in gray, the Tx/Rx pairs in $\mathcal{K}_2$ in blue and the Tx/Rxs in $\mathcal{K}_3$ in pink. The interference graph is depicted by black dashed lines.

Proof: Follows by specializing Proposition 3 to $\delta = 3$ and to appropriate sets $\mathcal{K}_1$, $\mathcal{K}_2$ and $\mathcal{K}_3$ shown in Fig. 6.3. To describe these sets, we associate each cell with a different Eisenstein integer similarly to Section 5.3.1. So, we pick a cell in the center of the network and associate it with the origin $(0, 0)$. Using the basis $\mathbf{e}_x \triangleq \frac{-\sqrt{3}}{2} + \frac{1}{2}i$ and $\mathbf{e}_y = i$ in the complex plane, each other cell k is associated to a different pair of integers (a_k, b_k). We choose:

$$\mathcal{K}_1 = \{k \in \mathcal{K}: \quad |a_k + b_k| \mod 3 = 0\}, \tag{6.27a}$$

$$\mathcal{K}_2 = \{k \in \mathcal{K}: \quad |a_k + b_k - 1| \mod 3 = 0\}, \tag{6.27b}$$

$$\mathcal{K}_3 = \{k \in \mathcal{K}: \quad |a_k + b_k - 2| \mod 3 = 0\}. \tag{6.27c}$$

For this choice, $|\mathcal{I}_{\mathrm{Rx},k} \cap \mathcal{K}_i| = 3$. ■

Figure 6.4 evaluates the regions in Theorem 9 and in Corollaries 6 and 7 for $\rho = 0.8$ and ρ_f either 0.3 or 0.6. We observe the quadrilateral shapes of all three regions.

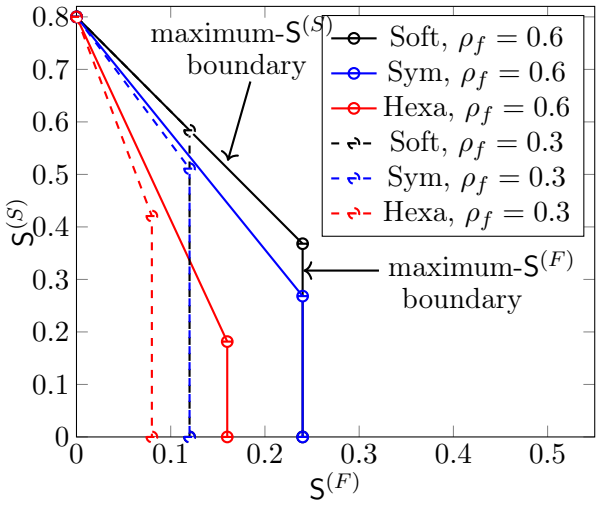

Figure 6.4: MG Region $\mathcal{S}^{\star}(\rho, \rho_f)$ of different networks with $\rho = 0.8$ and different values of ρ_f.

6.2 Random "Fast" and "Slow" Arrivals

6.2.1 Problem setup

The setup considered in this section differs from the previous setup only in that Txs in $\mathcal{T}_{\text{fast}}$ only send a "fast" message but no "slow" message. Thus, defining

$$\mathcal{T}_{\text{slow}} \triangleq \{k \in \mathcal{K} : A_k \cdot (1 - B_k) = 1\}, \tag{6.28}$$

we have

$$X_k^n = \begin{cases} f_k^{(F)}\big(M_k^{(F)}\big), & \text{if } k \in \mathcal{T}_{\text{fast}} \\ f_k^{(S)}\big(M_k^{(S)}\big), & \text{if } k \in \mathcal{T}_{\text{slow}} \\ \mathbf{0} & \text{if } k \in \mathcal{T}_{\text{active}}^c. \end{cases} \tag{6.29}$$

for some function $f_k^{(F)}$ and $f_k^{(S)}$ on appropriate domains that satisfy the average block-power constraint (6.4). All other definitions are as in the previous Section 6.1. We denote the statistical MG region for this setup by $\mathcal{S}_2^*(\rho, \rho_f)$.

6.2.2 Achievable MG Region and Coding Schemes

We again propose two schemes, one for large "fast" MG and the other for zero "fast" MG.

Transmitting at large $\mathsf{S}^{(F)}$:

Similar to the scheme presented in Subsection 6.1.2, we partition $\mathcal{K}$ into sets $\mathcal{K}_1, \ldots, \mathcal{K}_\delta$ and divide the total transmission time into δ equally-sized phases. In the i-th phase, each Tx k in $\mathcal{K}_i \cap \mathcal{T}_{\text{fast}}$ sends its "fast" message and each Tx $k \in \mathcal{T}_{\text{slow}}$ sends its "slow" message if $\mathcal{I}_{\text{Rx},k} \cap \mathcal{T}_{\text{fast}} \cap \mathcal{K}_i = \emptyset$; otherwise it does not send any message. The described scheme achieves a "fast" MG of $\mathsf{S}^{(F)}_{\max} = \frac{\rho\rho_f}{\delta}$, and an expected "slow" MG of

$$\bar{\mathsf{S}}^{(S)}_{\text{coop},2}(K) = \frac{1}{K}\sum_{i=1}^{\delta}\frac{1}{\delta}\Big(\sum_{k\in\mathcal{K}_i}\mathbb{P}\{k\in\mathcal{T}_{\text{slow}}\} + \sum_{k\in\mathcal{K}\setminus\mathcal{K}_i}\mathbb{P}\{k\in\mathcal{T}_{\text{slow}}\}\mathbb{P}\{\mathcal{I}_{\text{Rx},k}\cap\mathcal{T}_{\text{fast}}\cap\mathcal{K}_i=\emptyset\}\Big) \tag{6.30}$$

$$= \frac{1}{K}\sum_{i=1}^{\delta}\Big(\frac{\rho(1-\rho_f)}{\delta}|A_i| + \sum_{k\in\mathcal{K}\setminus A_i}\mathbb{P}\{k\in\mathcal{T}_{\text{active}}\}\prod_{\tilde{k}\in\{\mathcal{I}_{\text{Rx},k}\cap A_i\}}\mathbb{P}\{\tilde{k}\notin\mathcal{T}_{\text{fast}}\}\Big) \tag{6.31}$$

$$= \frac{\rho(1-\rho_f)}{\delta K}\sum_{i=1}^{\delta}\Big(|\mathcal{K}_i| + \sum_{k\in\mathcal{K}\setminus\mathcal{K}_i}(1-\rho\rho_f)^{|\mathcal{I}_{\text{Rx},k}\cap\mathcal{K}_i|}\Big\}\Big). \tag{6.32}$$

Transmitting at $\mathsf{S}^{(F)} = 0$:

Each Tx $k \in \mathcal{T}_{\text{slow}}$ sends a "slow" message with MG 1. The average expected "slow" MG over the network is therefore

$$\bar{\mathsf{S}}^{(S)}_{\max,2} = \rho(1-\rho_f). \tag{6.33}$$

Each Tx $k \in \mathcal{T}_{\text{fast}}$ remains silent and thus $\mathsf{S}^{(F)} = 0$.

Time sharing the two schemes establishes the following:

Proposition 4. *The set $\mathcal{S}^\star_2(\rho,\rho_f)$ contains the region:*

$$\text{convex hull}\Big((0,0),\ (0,\bar{\mathsf{S}}^{(S)}_{max,2}),\ (\mathsf{S}^{(F)}_{max},\bar{\mathsf{S}}^{(S)}_{coop,2}),\ (\mathsf{S}^{(F)}_{max},0)\Big). \tag{6.34}$$

We specialize this result to the interference networks introduced in Sections 6.1.3, 6.1.4 and 6.1.5 using the same choices for δ and the sets $\{\mathcal{K}_i\}_{i=1}^{\delta}$. For Wyner's soft-handoff network this inner bound is again tight.

6.2.3 Wyner's Soft-Handoff Network

Theorem 10. *The statistical MG region $\mathcal{S}^\star_2(\rho,\rho_f)$ is the set of all nonnegative pairs $(\mathsf{S}^{(F)},\mathsf{S}^{(S)})$ satisfying*

$$\mathsf{S}^{(F)} \le \frac{\rho\rho_f}{2}, \tag{6.35}$$

$$\rho(1-\rho_f)\mathsf{S}^{(F)} + \mathsf{S}^{(S)} \leq \rho(1-\rho_f). \tag{6.36}$$

Proof: Achievability follows by specializing Proposition 4 to $\delta = 2$ and to the sets $\mathcal{K}_1$ and $\mathcal{K}_2$ in (6.22). For this choice $|\mathcal{I}_{\mathrm{Rx},k} \cap \mathcal{K}_i| = 1$. The proof of the converse bound (6.35) is straightforward. The converse bound (6.36) is proved in Appendix A.3.2. ■

Like in the previous setup, the statistical MG region $\mathcal{S}_2^\star(\rho, \rho_f)$ is a quadrilateral. Interestingly, now all boundaries depend on both activity parameters ρ and ρ_f, in particular the maximum "slow" MG equals $\rho(1-\rho_f)$. Moreover, the maximum sum-rate is not achieved for this maximum "slow" MG anymore. Formally, this holds because the slope of the maximum-$\mathsf{S}^{(S)}$ boundary is $-\rho(1-\rho_f)$ and thus larger than -1. So, the maximum sum-rate point is obtained for maximum "fast" MG $\mathsf{S}^{(F)} = \frac{\rho\rho_f}{2}$. The underlying intuition is that for $\rho(1-\rho_f) < 1$ it may occur that a "fast" MG can be accommodated without the need to sacrifice a "slow" MG when the single interferer is not active anyways.

6.2.4 Wyner's Symmetric Network

Corollary 8. *The MG region $\mathcal{S}_2^\star(\rho, \rho_f)$ includes all nonnegative pairs $(\mathsf{S}^{(F)}, \mathsf{S}^{(S)})$ satisfying*

$$\mathsf{S}^{(F)} \leq \frac{\rho\rho_f}{2}, \tag{6.37}$$

$$\rho(1-\rho_f)(2-\rho\rho_f)\mathsf{S}^{(F)} + \mathsf{S}^{(S)} \leq \rho(1-\rho_f). \tag{6.38}$$

Proof: Specialize Proposition 4 to $\delta = 2$ and to $\mathcal{K}_1$ and $\mathcal{K}_2$ as in (6.22). For this choice $|\mathcal{I}_{\mathrm{Rx},k} \cap \mathcal{K}_i| = 2$. ■

Here the slope of the maximum-$\mathsf{S}^{(S)}$ boundary is $-\rho(1-\rho_f)(2-\rho\rho_f)$ and can be larger or smaller than -1 depending on the activity parameters. So, depending on these parameters, the maximum sum-MG is either achieved for zero "fast" MG or for maximum "fast" MG. Typically, for large values of ρ_f, i.e., when most of the "active" Txs send "fast" messages, the maximum sum-MG is achieved at maximum "fast" MG. When ρ_f is small and ρ sufficiently large, then most of the users are active and intend to send "slow" messages. In this case, scheduling "fast" messages most likely comes at the expense of silencing active neighbours that wishing to send "slow" messages. It is further interesting to notice that in the limiting regime $\rho\rho_f \to 0$, the slope of the maximum-$\mathsf{S}^{(S)}$ boundary approaches $-2\rho(1-\rho_f)$ and is thus 2 times the slope in Wyner's soft-handoff network. As we will see, the hexagonal model treated next shows a factor 6. For all three networks, the asymptotic slope in the limit $\rho\rho_f \to 0$ is thus given by $-|\mathcal{I}_{\mathrm{Tx},k}|\rho(1-\rho_f)$.

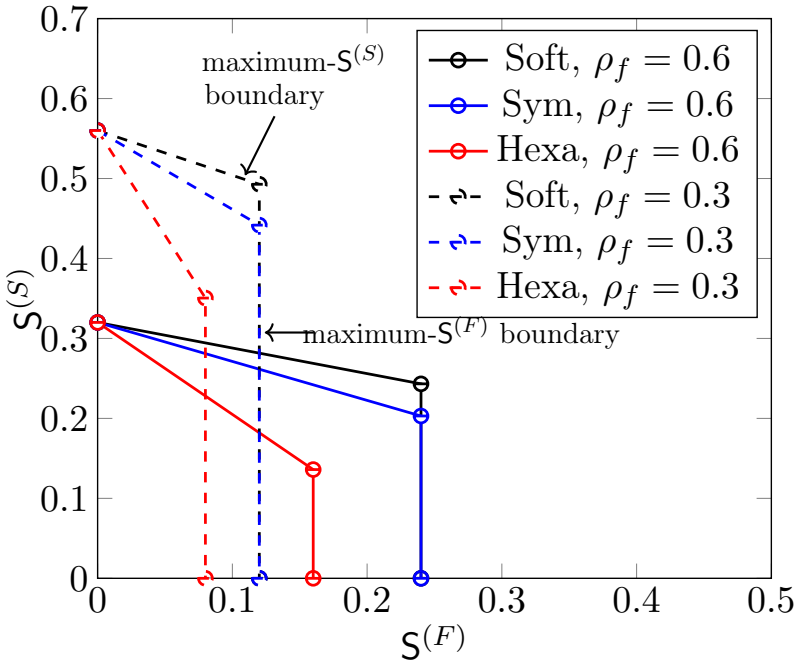

Figure 6.5: statistical MG Region $\mathcal{S}_2^\star(\rho, \rho_f)$ of the three networks with $\rho = 0.8$ and ρ_f equal to 0.3 or 0.6.

6.2.5 Hexagonal Network

Corollary 9. *The MG region $\mathcal{S}_2^\star(\rho, \rho_f)$ includes all nonnegative pairs $(\mathsf{S}^{(F)}, \mathsf{S}^{(S)})$ satisfying*

$$\mathsf{S}^{(F)} \leq \frac{\rho\rho_f}{3}, \tag{6.39}$$

$$2\rho(1-\rho_f)(3-3\rho\rho_f+\rho^2\rho_f^2)\mathsf{S}^{(F)} + \mathsf{S}^{(S)} \leq \rho(1-\rho_f). \tag{6.40}$$

Proof: Specialize Proposition 4 to $\delta = 3$ and to the sets $\mathcal{K}_1$, $\mathcal{K}_2$, and $\mathcal{K}_3$ in (6.27). For this choice $|\mathcal{I}_{\mathrm{Rx},k} \cap \mathcal{K}_i| = 3$. ■

Figure 6.5 illustrates $\mathcal{S}_2^\star(\rho, \rho_f)$ for Wyner's soft-handoff network as well as the inner bounds we obtain for Wyner's symmetric network and the hexagonal network under activity parameters $\rho = 0.8$ and ρ_f is either 0.3 or 0.6.

Chapter 7

Uplink of a Fading C-RAN under Mixed Delay Constraints

In this chapter, a cloud radio access network (C-RAN) is considered where the first hop from the user equipments (UEs) to the basestations (BSs) is modeled by the fading Wyner soft-handoff model. The focus is on mixed-delay constraints where “slow" messages are jointly decoded in the cloud unit (CU), whereas the “fast" messages have to be decoded immediately at the BSs. We present inner and outer bounds on the capacity region for such a setup. Moreover, the MG region is characterized exactly. The results show that for small fronthaul capacity it is beneficial to send both “fast" and “slow" messages. However, when the rate of “fast" messages is already large, then increasing it further, deteriorates the sum rate of the system. In this regime, the stringent decoding delay on the “fast" messages penalizes the overall performance. Our results indicate that this penalty is larger at moderate SNR than at high SNR and it is also larger for random time-varying fading coefficients than for static ones.

7.1 Problem Setup

Consider the uplink communication of a multi-cell C-RAN with K UEs and K BSs. UEs and BSs are indexed by $1, \ldots, K$. Each BS is connected to a CU via a separate fronthaul link of capacity C (see Fig. 7.1). At a given time $t \in \{1, \ldots, n\}$, the signal received at BS k is described as

$$Y_{k,t} = G_{k,t} X_{k,t} + F_{k,t} X_{k-1,t} + Z_{k,t}, \tag{7.1}$$

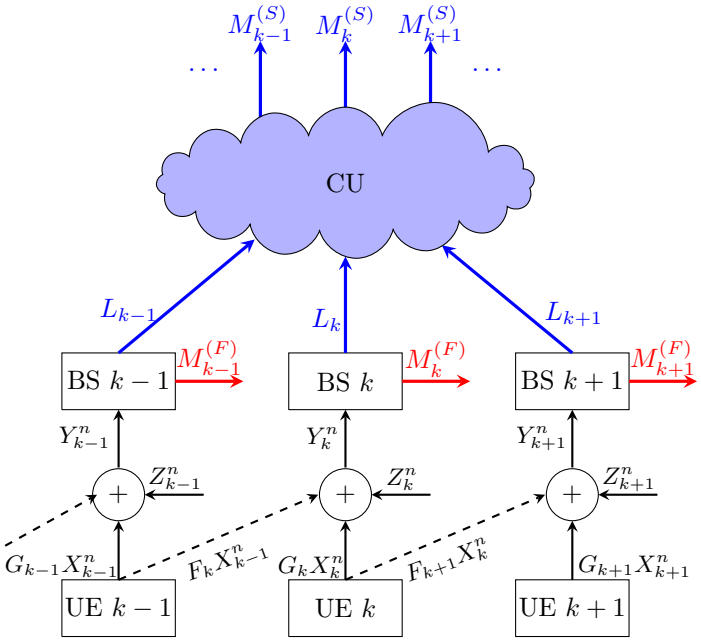

Figure 7.1: System model

where $X_{k,t}$ and $X_{k-1,t}$ are the symbols sent by UE k and UE $k-1$ at time t; $\{Z_{k,t}\}$ are i.i.d circular Gaussian noises of variance 1; and

$$G_{k,t}, F_{k,t} \in \mathbb{C} \tag{7.2}$$

represent the time-t fading coefficients. We assume that the sequence of channel coefficients

$$\left\{(G_{1,t}, G_{2,t}, \ldots, G_{K,t}, F_{1,t}, F_{2,t}, \ldots, F_{K,t})\right\}_{t=1}^{n} \tag{7.3}$$

is i.i.d. over time and distributed according to the K-tuple distribution

$$P_{G_1 \cdots G_K F_1 \cdots F_K} \tag{7.4}$$

of a given stationary and ergodic process $\{(G_i, F_i)\}_{i=-\infty}^{\infty}$ satisfying $\mathbb{E}\left[|G_0|^2\right] < \infty$ and $\mathbb{E}\left[|F_0|^2\right] < \infty$. Each BS k has perfect channel state information (CSI) about its own channel, i.e., it observes the realizations of $\{(G_{k,t}, F_{k,t})\}$ for all $t \in \{1, \ldots, n\}$. The UEs know only the statistics of the random channel coefficients and are said to have no CSI. Figure 7.1 shows an extract of our system model.

Each UE k wishes to convey the pair of independent messages $(M_k^{(F)}, M_k^{(S)})$ to BS k. The "fast" message $M_k^{(F)}$ is uniformly distributed over the set $\mathcal{M}_k^{(F)} := \{1, \ldots, \lfloor 2^{nR_k^{(F)}} \rfloor\}$ and has to be decoded by BS k as we

explain shortly. The "slow" source message $M_k^{(S)}$ is uniformly distributed over $\mathcal{M}_k^{(S)} := \{1, \ldots, \lfloor 2^{nR_k^{(S)}} \rfloor\}$ and is decoded at the CU.

UE k computes its channel inputs $X_k^n := (X_{k,1}, \ldots, X_{k,n})$ as a function of the pair $(M_k^{(F)}, M_k^{(S)})$:

$$X_k^n = \phi_k^{(n)}\big(M_k^{(F)}, M_k^{(S)}\big), \tag{7.5}$$

for some function $\phi_k^{(n)}$ on appropriate domains so that the average block-power constraint (6.4) is satisfied.

Each BS k decodes the "fast" source message $M_k^{(F)}$ based on its own channel outputs $Y_k^n := (Y_{k,1}, \ldots, Y_{k,n})$. So, it produces:

$$\hat{M}_k^{(F)} = \psi_k^{(n)}\big(Y_k^n\big) \tag{7.6}$$

using some decoding function $\psi_k^{(n)}$ on appropriate domains.

It further produces the fronthaul message

$$L_k = q_k^{(n)}(Y_k^n), \tag{7.7}$$

using some encoding function

$$q_k^{(n)} : \mathbb{R}_k^n \to \Big\{1, \ldots, \Big\lfloor 2^{n\mathsf{C}} \Big\rfloor\Big\}. \tag{7.8}$$

The CU then decodes the set of "slow" messages as

$$\big(\hat{M}_1^{(S)}, \ldots, \hat{M}_K^{(S)}\big) := b^{(n)}\Big(L_1, \ldots, L_K\Big) \tag{7.9}$$

by means of a decoding function $b^{(n)}$.

Definition 3 (Capacity Region)**.** *The* capacity region $\mathsf{C}(\mathsf{P}, \mathsf{C})$ *is the closure of the set of all rate pairs* $(R^{(F)}, R^{(S)})$*, defined in* (3.10)*, that are achievable with power* P *and fronthaul link capacity* C*.*

Definition 4 (Multiplexing Gains)**.** *The closure of the set of all achievable MGs* $(\mathsf{S}^{(F)}, \mathsf{S}^{(S)})$*, defined in* (3.12)*, is called* MG region *and denoted* $\mathcal{S}^\star(\mu)$ *where*

$$\mu \triangleq \frac{\mathsf{C}}{\frac{1}{2}\log(1+\mathsf{P})}. \tag{7.10}$$

7.2 Main Results

For each $\beta \in [0,1]$ define $\sigma_\beta^2 \geq 0$ as the unique positive real number satisfying

$$\mathbb{E}\left[\log\left(1+\frac{1+(1-\beta)\mathsf{P}|G_0|^2+|F_0|^2\mathsf{P})}{\sigma_\beta^2}\right)\right]=\mathsf{C} \tag{7.11}$$

and the random process $\{W_i^\beta\}_{i=-\infty}^{\infty}$ as the unique stationary process satisfying:

$$W_i^\beta=\left(1+(1-\beta)\mathsf{P}|G_i|^2\Big(1+\frac{(1-\beta)\mathsf{P}|F_i|^2W_{i-1}^\beta}{1+\sigma_\beta^2+\beta\mathsf{P}|F_i|^2}\Big)^{-1}\right)^{-1}. \tag{7.12}$$

Notice that the joint process $\{(F_i,G_i,W_i^\beta)\}_{i=-\infty}^{\infty}$ is also stationary and ergodic.

For a given $\beta\in[0,1]$, let $\mathcal{R}(\beta)\subseteq\mathbb{R}^2$ be the set of all non-negative pairs $(R^{(F)},R^{(S)})$ that satisfy

$$R^{(F)}\leq\mathbb{E}\left[\log\left(1+\frac{\beta\mathsf{P}|G_0|^2}{(1-\beta)\mathsf{P}|G_0|^2+\mathsf{P}|F_0|^2+1}\right)\right] \tag{7.13a}$$

and

$$R^{(S)}\leq\mathbb{E}\Big[\log\Big(1+\frac{(1-\beta)\mathsf{P}|F_0|^2W_{-1}^\beta}{1+\sigma_\beta^2+\beta\mathsf{P}|F_0|^2}\Big)-\log W_0^\beta\Big]. \tag{7.13b}$$

Theorem 11 (Capacity Inner Bound)**.** *The convex closure of the sets* $\{\mathcal{R}(\beta)\colon\beta\in[0,1]\}$ *is achievable:*

$$\operatorname{conv\,cl}\left(\bigcup_{\beta\in[0,1]}\mathcal{R}(\beta)\right)\subseteq\mathsf{C}(\mathsf{P},\mathsf{C}). \tag{7.14}$$

Proof: See Section 7.3. ∎

Theorem 12 (Capacity Outer Bound)**.** *Assuming* $\log|G_0|$ *and* $\log|F_0|$ *are integrable near 0, any rate pair* $(R^{(F)},R^{(S)})$ *in the capacity region* $\mathsf{C}(\mathsf{P},\mathsf{C})$ *satisfies the following four constraints:*

$$\begin{aligned}2R^{(F)}+R^{(S)}&\leq\mathbb{E}\big[\log(1+(|G_0|^2+|F_0|^2)\mathsf{P})\big]+\mathbb{E}\left[\log\left(1+\frac{|F_0|^2}{|G_0|^2}\right)\right]\\&\quad+\max\left\{\mathbb{E}\left[\log\left(\frac{|G_0|^2}{|F_0|^2}\right)\right],0\right\},\qquad\textit{(7.15a)}\\R^{(F)}+R^{(S)}&\leq\frac{1}{2}\mathbb{E}\big[\log(1+(|G_0|^2+|F_0|^2)\mathsf{P})\big]+\frac{1}{2}\max\left\{\mathbb{E}\left[\log\left(\frac{|G_0|^2}{|F_0|^2}\right)\right],0\right\}\\&\quad+\frac{1}{2}\mathbb{E}\big[\log(1+(|F_0|^2)^{-1})\big]+\frac{\mathsf{C}}{2},\qquad\textit{(7.15b)}\end{aligned}$$

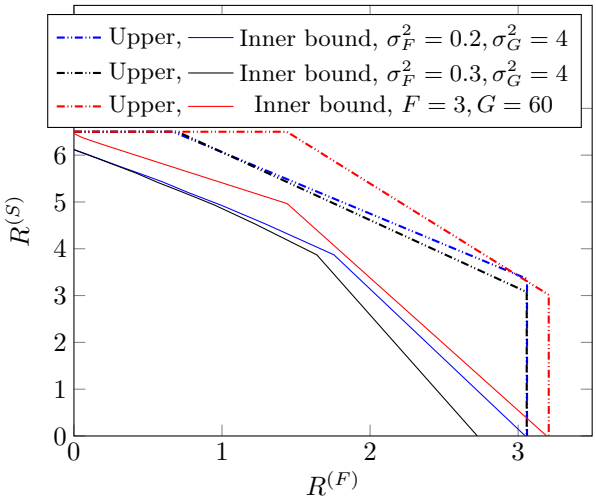

Figure 7.2: Capacity inner bound in Theorem 11 and capacity outer bound in Theorem 12 for $\mathsf{P} = 100$, $\mathsf{C} = 6.5$, and different variances σ_F^2 and σ_G^2 of F and G, and for static G and F.

$$R^{(F)} \leq \frac{1}{2}\mathbb{E}\big[\log(1 + |G_0|^2\mathsf{P})\big], \tag{7.15c}$$

$$R^{(S)} \leq \mathsf{C}. \tag{7.15d}$$

Proof: The proofs to the bounds (7.15a) and (7.15b) follow from the converse bounds in Appendices (A.1.1) and (A.1.2) and by fixing $\mathsf{L} = 1$ and considering the channel coefficient to be time varying. Proofs of the bounds (7.15c) and (7.15d) are straightforward. ■

Corollary 10 (Multiplexing Gain Region)**.** *The multiplexing gain region $\mathcal{S}^\star(\mu)$ is the set of all nonnegative pairs $(\mathsf{S}^{(F)}, \mathsf{S}^{(S)})$ satisfying*

$$2\mathsf{S}^{(F)} + \mathsf{S}^{(S)} \leq 1, \tag{7.16a}$$

$$\mathsf{S}^{(S)} \leq \mu. \tag{7.16b}$$

Proof: The converse holds by Theorem 12 and the achievability by Theorem 11. Specifically, for the achievability part, it suffices to prove that the two pairs

$$\big(\mathsf{S}^{(S)} = 0, \quad \mathsf{S}^{(F)} = 1/2\big), \tag{7.17}$$

$$\big(\mathsf{S}^{(S)} = \min\{\mu, 1\}, \quad \mathsf{S}^{(F)} = \max\{0, 1/2 - \mu/2\}\big) \tag{7.18}$$

are achievable. The multiplexing gain pair in (7.17) can be achieved by silencing every second UE, which decomposes the network into $K/2$ non-interfering point-to-point links. If $\mu \geq 1$, the multiplexing gain pair

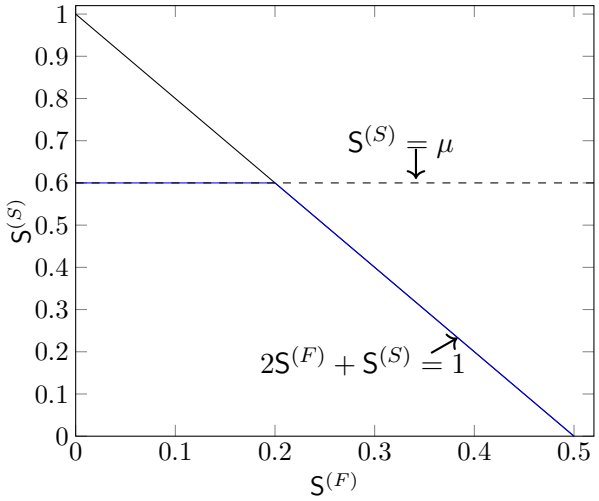

Figure 7.3: Region $\mathcal{S}^\star(\mu)$ for $\mu = 0.6$ in blue and $\mu \geq 1$ in black.

$(\mathsf{S}^{(S)} = 1, \mathsf{S}^{(F)} = 0)$ is achieved by a scheme where each BS quantizes its observed outputs to noise level and the CU decodes all the transmitted "slow" messages based on these quantized outputs. If $\mu < 1$, then the multiplexing gain pair $(\mathsf{S}^{(S)} = \mu, \mathsf{S}^{(F)} = 1/2 - \mu/2)$ in (7.18) is achieved by a scheme that time-shares the schemes above over fractions of $1 - \mu$ and μ of the time. ■

Figure 7.2 illustrates the proposed inner and outer bounds on the capacity region for independent random processes $\{G_i\}$ and $\{F_i\}$, where each F_i is circularly Gaussian of variance σ_F^2 and each G_i is circularly Gaussian of variance σ_G^2. Numerical simulations are performed for different values of σ_F^2. The figure also presents inner and outer bounds on the capacity region assuming static channel coefficients (regions in red). As can be seen from the figure, for small values of $R^{(F)}$, the slope $\frac{\delta R^{(F)}}{\delta R^{(S)}}$ of the inner bound is approximately -1 both for static and random channel coefficients. This means increasing the rate of "fast" messages by Δ, decreases the rate of "slow" messages by Δ and thus the sum-rate remains constant. For large values of $R^{(F)}$ and random time-varying channel coefficients, the slope of the inner bound is around -3.5 for $\sigma_F^2 = 0.2$ and around -4 for $\sigma_F^2 = 0.3$. In contrast, this slope is around -2.7 for static channel coefficients. Increasing an already large "fast" rate $R^{(F)}$ thus penalizes the sum-rate of the system and is more pronounced under random fading. Note that, to reduce the gap between the proposed inner and outer bounds on capacity, one can include more sophisticated multi-user compression techniques [77, 78] at the BSs and the cloud processor.

Figure 7.3 shows the multiplexing gain region for different values of μ. We notice that when $\mu < 1$, for $\mathsf{S}^{(F)} \leq \frac{1}{2} - \frac{\mu}{2}$, the multiplexing gain of "slow" messages is constant and solely limited by the fronthaul capacity. In this regime, the sum-multiplexing gain of the system is increased by decoding parts of the

messages directly at the BSs. When $\mu < 1$ and $\mathsf{S}^{(F)} > \frac{1}{2} - \frac{\mu}{2}$, or when $\mu \geq 1$, the slope of the boundary of the region is -2. In these regimes the maximum sum-multiplexing gain is decreased by Δ when the "fast" multiplexing gain increases by Δ.

7.3 Proof of Theorem 11

Fix $\beta \in [0,1]$. Recall that σ_β^2 was defined so as to verify (see (7.11))

$$\mathbb{E}\left[\log\left(1 + \frac{1 + (1-\beta)\mathsf{P}|G_0|^2 + |F_0|^2\mathsf{P})}{\sigma_\beta^2}\right)\right] = \mathsf{C}. \tag{7.19}$$

For each $k \in \{1, \ldots, K\}$, define

$$X_k = U_k + V_k, \tag{7.20a}$$

$$Y_k = G_k X_k + F_k X_{k-1} + Z_k, \tag{7.20b}$$

$$C_k = G_k V_k + F_k X_{k-1} + Z_k, \tag{7.20c}$$

$$\hat{C}_k = C_k + Q_k, \tag{7.20d}$$

for $\{Q_k\}$, $\{U_k\}$, $\{V_k\}$, and $\{Z_k\}$ independent zero-mean Gaussian random variables with variances σ_β^2, $\beta\mathsf{P}$, $(1-\beta)\mathsf{P}$, and 1.

Random Code Construction: For each $k \in \{1, \ldots, K\}$, generate codebooks $\mathcal{C}_{u,k}$, $\mathcal{C}_{v,k}$, and $\mathcal{C}_{w,k}$ randomly. Codebook

$$\mathcal{C}_{u,k} := \left\{u_k^n(i) \colon \quad i = 1, \ldots, \left\lfloor 2^{nR_k^{(F)}} \right\rfloor\right\} \tag{7.21}$$

is generated by picking all entries i.i.d. circularly Gaussian of variance $\beta\mathsf{P}$. Independently thereof, codebook

$$\mathcal{C}_{v,k} := \left\{v_k^n(j) \colon \quad j = 1, \ldots, \left\lfloor 2^{nR_k^{(S)}} \right\rfloor\right\} \tag{7.22}$$

is generated by picking all entries i.i.d. circularly Gaussian of variance $(1-\beta)\mathsf{P}$. Quantization codebook

$$\mathcal{C}_{c,k} := \left\{\hat{c}_k^n(\ell) \colon \quad \ell = 1, \ldots, \left\lfloor 2^{n\mathcal{C}} \right\rfloor\right\} \tag{7.23}$$

is generated by picking all entries i.i.d. according to $P_{\hat{C}}$.

Reveal all codebooks to all terminals. We explain the encoding and decoding operations assuming that

$$G_k^n = g_k^n \qquad \text{and} \qquad F_k^n = f_k^n. \tag{7.24}$$

(Recall that BS k and the CU know these realizations.)

UE k: Sends

$$x^n = u_k^n\big(M_k^{(F)}\big) + v_k^n\big(M_k^{(S)}\big). \tag{7.25}$$

BS k: Decodes its "fast" message $M_k^{(F)}$ based on its own channel outputs $Y_k^n = y_k^n$. It then looks for a unique $\hat{i}_k$ such that

$$(u_k^n(\hat{i}_k), y_k^n, g_k^n, f_k^n) \in \mathcal{A}_\epsilon^{(n)}(P_{UYG_0F_0}), \tag{7.26}$$

where $\mathcal{A}_\epsilon^{(n)}(\cdot)$ refers to the jointly typical set as defined in [69] and where given $G_0 = g$ and $F_0 = f$ the pair (U, Y) is a centered bivariate Gaussian vector of covariance matrix

$$\mathsf{K}_{UY|g,f} = \begin{pmatrix} \beta\mathsf{P} & g\beta\mathsf{P} \\ g\beta\mathsf{P} & (g^2+f^2)\mathsf{P}+1 \end{pmatrix}. \tag{7.27}$$

If none or more than one such indices $\hat{i}_k$ exist, BS k declares an error. Otherwise it declares

$$\hat{M}_k^{(F)} = \hat{i}_k. \tag{7.28}$$

Subsequently it forms the difference

$$c_k^n := y_k^n - u_k^n(\hat{i}_k), \tag{7.29}$$

and looks for an index ℓ_k such that

$$(\hat{c}_k^n(\ell_k), c_k^n, f_k^n, g_k^n) \in \mathcal{A}_\epsilon^{(n)}(P_{\hat{C}CFG}). \tag{7.30}$$

If none or more than one such indices ℓ_k exist, BS k declares an error. Otherwise it sends $L_k = \ell_k$.

CU: Assume it receives $L_1 = l_1, \ldots, L_K = l_K$. Then, it looks for a unique set of indices $\hat{j}_1, \ldots, \hat{j}_K$ that

satisfy

$$\big(\hat{c}_1^n(\ell_1),\ldots,\hat{c}_K^n(\ell_K),v_1^n(\hat{j}_1),\ldots,v_K^n(\hat{j}_K),g_1^n,\ldots,g_K^n,f_1^n,\ldots,f_K^n\big)\in\mathcal{A}_\epsilon^{(n)}(P_{\hat{C}_1,\ldots,\hat{C}_K,V_1,\ldots,V_K,\mathbb{G},\mathbb{F}}),\tag{7.31}$$

where

$$\mathbb{G}=\{G_{1,t},\ldots,G_{K,t}\}_{t=1}^n,\quad \mathbb{F}=\{F_{1,t},\ldots,F_{K,t}\}_{t=1}^n.\tag{7.32}$$

If none or multiple such indices $\hat{j}_1,\ldots,\hat{j}_K$ exist, the CU declares an error. Otherwise, it declares

$$\hat{M}_k^{(S)}=\hat{j}_k,\qquad k\in\{1,\ldots,K\}.\tag{7.33}$$

Analysis: For any $k\in\{1,\ldots K\}$, decoding in (7.26) is successful with probability tending to 1 as $n\to\infty$, if

$$\begin{aligned}R_k^{(F)}&<I(U_k;Y_k|G_k,F_k)\\&=\mathbb{E}\left[\log\left(1+\frac{\beta\mathsf{P}|G_k|^2}{(1-\beta)\mathsf{P}|G_k|^2+\mathsf{P}|F_k|^2+1}\right)\right].\end{aligned}\tag{7.34}$$

Assuming that this decoding was successful, quantization in (7.30) also succeeds with probability tending to 1 as $n\to\infty$, because by the choice of the quantization noise σ_β^2:

$$\begin{aligned}\mathcal{C}&\geq I(\hat{C}_k;C_k|G_k,F_k)\\&=\mathbb{E}\left[\log\left(1+\frac{1+(1-\beta)\mathsf{P}|G_k|^2+|F_k|^2\mathsf{P})}{\sigma_\beta^2}\right)\right].\end{aligned}\tag{7.35}$$

Now assuming that both the decoding in (7.26) and the quantization in (7.30) were successful, the decoding in (7.31) also succeeds with probability tending to 1 as $n\to\infty$, if

$$\begin{aligned}&\frac{1}{K}\sum_{k=1}^K R_k^{(S)}\\&<\frac{1}{K}I(V_1,\ldots,V_K;\hat{C}_1,\ldots,\hat{C}_K|\mathbb{G},\mathbb{F})\\&=\frac{1}{K}I\Big(\{S_k\}_{k=1}^K\ ;\ \{\tilde{G}_kS_k+\tilde{F}_kS_{k-1}+\Xi_k\}_{k=1}^K\Big|\mathbb{G},\mathbb{F}\Big),\end{aligned}\tag{7.36}$$

where $\{\tilde{Z}_k\}$ and $\{\Xi_k\}$ are sequences of i.i.d. circularly symmetric Gaussian noises of variances $1+\sigma_\beta^2+f_k^2\beta P$

and 1 and

$$S_k := \sqrt{(1-\beta)^{-1/2}P}\cdot V_k, \tag{7.37a}$$

$$\tilde{G}_k := \frac{\sqrt{(1-\beta)P}}{\sqrt{1+\sigma_\beta^2+\beta P|F_k|^2}}\cdot G_k, \tag{7.37b}$$

$$\tilde{F}_k := \frac{\sqrt{(1-\beta)P}}{\sqrt{1+\sigma_\beta^2+\beta P|F_k|^2}}\cdot F_k, \quad k\in\{1,\dots,K\}. \tag{7.37c}$$

By these definitions and assumptions on the channel, the sequences $\{S_k\}$, $\{(\tilde{G}_k,\tilde{F}_k)\}$, $\{\Xi_k\}$ satisfy the conditions in [70, Assumption 1] (where we associate G_k, F_k, and V_k in [70] with $\tilde{G}_k$, $\tilde{F}_k$, and Ξ_k). Therefore in the limit when $K\to\infty$, the mutual information in (7.36) can be evaluated using [70, Theorem1] to obtain:

$$R^{(S)} \le \mathbb{E}\left[\log\left(1+\frac{(1-\beta)\mathsf{P}|F_0|^2W_{-1}^\beta}{1+\sigma_\beta^2+\beta\mathsf{P}|F_0|^2}\right)-\log W_0^\beta\right] \tag{7.38}$$

where $\{W_i\}_{i=-\infty}^{\infty}$ is the unique stationary process satisfying

$$W_i^\beta = \left(1+(1-\beta)\mathsf{P}|G_i|^2\Big(1+\frac{(1-\beta)\mathsf{P}|F_i|^2W_{i-1}^\beta}{1+\sigma_\beta^2+\beta\mathsf{P}|F_i|^2}\Big)^{-1}\right)^{-1}. \tag{7.39}$$

Achievability of the pairs (7.13) follows then from (7.34) and (7.38).

Chapter 8

Summary and Outlook

8.1 Summary

In this thesis we focused on interference networks with mixed-delay constraints and on system architectures where certain transmitters and/or certain receivers can cooperate. In such systems, delay-sensitive messages have to be encoded and decoded without further delay and thus cannot benefit from available cooperation links.

- In Chapter 3, we proposed a cooperative communication model that can accommodate the transmission of both delay-sensitive and delay-tolerant messages.

- In Chapter 4, we considered Wyner's soft-handoff network and characterized the MG region with transmitter and receiver cooperation when delay-sensitive messages are subject to stringent delay constraints. For the setup with *only* transmitter or *only* receiver cooperation, we observed the following. Increasing the MG of delay-sensitive messages by Δ requires decreasing the MG of delay-tolerant messages approximately by 2Δ. This penalty does not occur when both transmitters *and* receivers can cooperate. More precisely, for small cooperation prelogs, when delay-sensitive messages have moderate or small MGs, the *sum* MG is not decreased compared to when only delay-tolerant messages are transmitted. For large cooperation prelogs, this conclusion even holds when delay-sensitive messages have large MGs.

- In Chapter 5, we proposed a coding scheme for general interference networks that accommodates the transmission of both delay-sensitive and delay-tolerant messages. An important building block in this coding scheme used for the transmission of delay-tolerant messages is coordinated multi point

transmission or reception. We characterized the MG region of Wyner's symmetric network and derived inner bounds on the achievable MG region of the hexagonal network and the sectorized hexagonal model. The results for Wyner's symmetric model show that it is possible to accommodate the largest possible MG for "fast" messages, without penalizing the maximum sum MG of both "fast" and "slow" messages. The results for the hexagonal model show that there is always a penalty in sum MG at any "fast" MG. In contrast, for the sectorized hexagonal model where each cell is divided into three non-interfering sectors by employing directional antennas at the BSs, it is possible to eliminate this penalty and accommodate the largest possible MG for "fast" messages without penalizing the maximum sum MG.

- In Chapter 6, we considered two different setups to simultaneously transmit delay-sensitive and delay-tolerant traffic over interference networks with randomly activated users. Under both setups, we characterized the MG region of Wyner's soft-handoff network and derived an inner bound on the MG region of any general interference network. Our results show that in the first setup, where each active Tx always has delay-tolerant data to send, the sum MG is decreased with increasing delay-sensitive MG. The corresponding penalty mostly depends on the activity parameter and the size of the interference set of the network. It increases with both parameters, intuitively because more Txs have to be silent when accommodating delay-sensitive transmissions. In contrast, in the second setup where each active Tx has either a delay-tolerant or a delay-sensitive message to send, depending on the values of the activity parameters, the sum MG is either achieved at maximum delay-sensitive MG or at 0 delay-sensitive MG.

- In Chapter 7, we presented the inner and outer bounds on the capacity region of a C-RAN under mixed delay constraints and characterized the MG region of this network. We learned that when the fronthaul capacities are small, the overall performance of the system can be improved if some of the data streams (the delay sensitive streams) are directly decoded at the BSs. The stringent delay constraint on these streams however becomes harmful when their rate is too large. In this regime the total sum-rate has to be decreased by a penalty factor γ times Δ when the delay-sensitive rate is increased by Δ. The penalty factor $\gamma \approx 1$ for static channel coefficients or in the high-SNR regime, and it can be significantly larger for random channel coefficients and at moderate SNRs.

8.2 Outlook

The following are interesting lines of future works:

- In this thesis, we assumed perfect channel state information (CSI) at the transmitter and the receiver sides. In practice, it seems particularly difficult to obtain such a perfect knowledge at the transmitters side. It is, therefore, of great interest to understand the fundamental limits of transmitter cooperation under finite precision CSIT. This leads us to the next logical step, a generalized degrees of freedom (GDoF) characterization. Readers are encouraged to refer to [71, 72]. The impact of CSI at the transmitter as in Reference [71] but for the considered model with mixed-delay constraints is also of high interest. In particular, a model where CSI is present for en/decoding delay-tolerant messages but not for en/decoding of delay-sensitive messages is a natural extension of our setup.

- Another outgrowth of our work is the finite-blocklength derivation of achievability and converse bounds. In practice, it is of vital interest to assess the backoff from capacity required to sustain the desired error probability at a given fixed finite blocklength. Readers are encouraged to refer to [73, 74]

- In the schemes that we proposed for the random users activity with mixed delay traffic, users who interfere with delay-sensitive transmissions are deactivated. One can thus consider buffers to store not yet transmitted delay-tolerant messages similar to [75]. It would be interesting to analyze the required size of these buffers, for example.

- In the completely centralized architecture of C-RAN, we introduced a setup where neither BSs nor UEs can cooperate and we only focused on Wyner's soft-handoff model. Our next steps could be to: (i) investigate the influence of the model employed for the network between UEs and BSs, as well as the availability of cooperation links between UEs and/or BSs; and (ii) study mixed delay constraints on transmissions over fog radio access networks (FRAN) where large amount of signal processing and computing is also performed in BSs and UEs. Readers are encouraged to refer to [76].

  In the scheme proposed for C-RAN, we used simple point-to-point compression techniques. One can reduce the gap between the proposed inner and outer capacity bounds by including more sophisticated multi-user compression techniques such as successive Wyner-Ziv compression and noisy network coding [77, 78] at the BSs and the cloud processor.

Appendix A

Proofs

A.1 Proofs of Chapter 4

A.1.1 Proof of the Converse to (4.3)

We start by proving bound (4.3). For convenience of notation, define for any $k \in \mathcal{K}$:

$$M_k \triangleq (M_k^{(F)}, M_k^{(S)}). \tag{A.1}$$

For each power $\mathsf{P} > 0$, fix a sequence (in the blocklength n) of encoding and decoding functions respecting the power constraints and the Rx-cooperation rate-limitations (recall that we consider a setup with only Rx-cooperation but no Tx-cooperation) such that the error probability $p(\text{error}) \to 0$ as the blocklength $n \to \infty$.

By Fano's Inequality there exists a sequence ϵ_n satisfying $\frac{\epsilon_n}{n} \to 0$ as $n \to \infty$ such that for any $k \in [1 : K-1]$ and each blocklength n:

$$\begin{aligned}
R_k^{(F)} \quad + \quad & R_k^{(S)} + R_{k+1}^{(F)} = \frac{1}{n}\Big[H(M_k^{(F)}) + H(M_k^{(S)}) + H(M_{k+1}^{(F)})\Big] && \text{(A.2)}\\
= \quad & \frac{1}{n}\Big[H(M_k^{(F)}\big|M_{k-1}) \\
& \qquad +H\big(M_k^{(S)}\big|M_1,\ldots,M_{k-1},M_k^{(F)},M_{k+1},\ldots,M_K\big) + H\big(M_{k+1}^{(F)}\big|M_{k-1},M_{k+1}^{(S)}\big)\Big] && \text{(A.3)}\\
\leq \quad & \frac{1}{n}\Big[I(M_k^{(F)};\boldsymbol{Y}_k^n|M_{k-1}) + I(M_k^{(S)};\boldsymbol{Y}_1^n,\ldots,\boldsymbol{Y}_K^n|M_1,\ldots,M_{k-1},M_k^{(F)},M_{k+1},\ldots,M_K) \\
& \qquad +I(M_{k+1}^{(F)};\boldsymbol{Y}_{k+1}^n|M_{k-1},M_{k+1}^{(S)})\Big] + \frac{\epsilon_n}{n} && \text{(A.4)}\\
\overset{(a)}{=} \quad & \frac{1}{n}\Big[I(M_k^{(F)};\boldsymbol{Y}_k^n|M_{k-1}) + I(M_k^{(S)};\boldsymbol{Y}_k^n,\boldsymbol{Y}_{k+1}^n|M_{k-1},M_k^{(F)},M_{k+1})
\end{aligned}$$

$$+I(M_{k+1}^{(F)};\boldsymbol{Y}_{k+1}^{n}|M_{k-1},M_{k+1}^{(S)})\Big]+\frac{\epsilon_n}{n} \tag{A.5}$$

$$\overset{(b)}{=}\ \frac{1}{n}\Big[I(M_k^{(F)},M_k^{(S)};\boldsymbol{Y}_k^n|M_{k-1})+I(M_k^{(S)};\boldsymbol{Y}_{k+1}^n|\boldsymbol{Y}_k^n,M_k^{(F)},M_{k-1},M_{k+1})$$
$$+I(M_{k+1}^{(F)};\boldsymbol{Y}_{k+1}^{n}|M_{k-1},M_{k+1}^{(S)})\Big]+\frac{\epsilon_n}{n} \tag{A.6}$$

$$\leq\ \frac{1}{n}\Big[h(\mathsf{H}_{k,k}\boldsymbol{X}_k^n+\boldsymbol{Z}_k^n)-h(\boldsymbol{Z}_k^n)+h(\mathsf{H}_{k,k+1}\boldsymbol{X}_k^n+\boldsymbol{Z}_{k+1}^n|\mathsf{H}_{k,k}\boldsymbol{X}_k^n+\boldsymbol{Z}_k^n)$$
$$-h(\boldsymbol{Z}_{k+1}^n)+h(\boldsymbol{Y}_{k+1}^n|M_{k+1}^{(S)})-h(\mathsf{H}_{k,k+1}\boldsymbol{X}_k^n+\boldsymbol{Z}_{k+1}^n)\Big]+\frac{\epsilon_n}{n} \tag{A.7}$$

$$\overset{(c)}{\leq}\ \sum_{i=1}^{\mathsf{L}}\frac{1}{2}\log\Big(1+\Big(\sum_{j=1}^{\mathsf{L}}|\mathsf{H}_{k+1,k+1}(i,j)|\Big)^2\mathsf{P}+\Big(\sum_{j=1}^{\mathsf{L}}|\mathsf{H}_{k,k+1}(i,j)|\Big)^2\mathsf{P}\Big)$$
$$+\frac{1}{2}\log\det\big(\mathsf{I}_{\mathsf{L}}+\mathsf{H}_{k,k+1}{\mathsf{H}_{k,k}}^{-1}{\mathsf{H}_{k,k}}^{-\mathsf{T}}\mathsf{H}_{k,k+1}^{\mathsf{T}}\big)$$
$$+\frac{1}{2}\log\det\big(\mathsf{H}_{k,k}^{-1}\mathsf{H}_{k,k}^{-\mathsf{T}}+\mathsf{H}_{k,k+1}^{-1}\mathsf{H}_{k,k+1}^{-\mathsf{T}}\big)+\log\det(\mathsf{H}_{k,k})+\frac{\epsilon_n}{n}, \tag{A.8}$$

where I_{L} denotes the L-by-L identity matrix and $\mathsf{H}_{k+1,k+1}(i,j)$ and $\mathsf{H}_{k,k+1}(i,j)$ denote the elements of matrices $\mathsf{H}_{k+1,k+1}$ and $\mathsf{H}_{k,k+1}$ in row i and column j. Here, (a) follows because given source messages M_{k-1} and M_{k+1}, the triple $(M_k,\boldsymbol{Y}_k^n,\boldsymbol{Y}_{k+1}^n)$ is independent of the rest of the outputs $\boldsymbol{Y}_1^n,\ldots,\boldsymbol{Y}_{k-1}^n,\boldsymbol{Y}_{k+2}^n,\ldots,\boldsymbol{Y}_K^n$ and source messages $M_1,\ldots,M_{k-2},M_{k+2},\ldots,M_K$; (b) follows by the chain rule of mutual information and because M_{k+1} is independent of the tuple $(M_{k-1},M_k,\boldsymbol{Y}_k^n)$; and (c) is obtained by rearranging terms, and the following bounds (A.9), (A.15), and (A.24).

We first bound the term $h(\boldsymbol{Y}_{k+1}^n|M_{k+1}^{(S)})$, and start by noting that because conditioning can only reduce entropy and by the entropy-maximizing property of the Gaussian distribution:

$$h(\boldsymbol{Y}_{k+1}^n|M_{k+1}^{(S)})\ \leq\ \sum_{i=1}^{\mathsf{L}}\sum_{t=1}^{n}h(\mathbf{Y}_{k+1,t}(i))\leq\sum_{i=1}^{\mathsf{L}}\sum_{t=1}^{n}\frac{1}{2}\log((2\pi e)\mathrm{Var}(\mathbf{Y}_{k+1,t}(i))), \tag{A.9}$$

where $\mathbf{Y}_{k+1,t}(i)$ denotes the i-th entry of the vector $\boldsymbol{Y}_{k+1,t}$. Recall that in this setup without Tx-cooperation the input vectors $\boldsymbol{X}_k^n$ and $\boldsymbol{X}_{k+1}^n$ are independent. However the elements of each input vector can be arbitrarily correlated. The variance $\mathrm{Var}(\mathbf{Y}_{k+1,t}(i))$ is maximized if the elements of $\boldsymbol{X}_{k+1,t}$ are fully correlated and thus :

$$\mathrm{Var}(\mathbf{Y}_{k+1,t}(i))\leq 1+\left(\sum_{j=1}^{\mathsf{L}}|\mathsf{H}_{k,k+1}(i,j)|\sqrt{\mathsf{P}_{k,t}(j)}\right)^2+\left(\sum_{j=1}^{\mathsf{L}}|\mathsf{H}_{k+1,k+1}(i,j)|\sqrt{\mathsf{P}_{k+1,t}(j)}\right)^2, \tag{A.10}$$

where $\mathsf{P}_{k,t}(j)$ and $\mathsf{P}_{k+1,t}(j)$ denote the variances of the j-th elements of input vectors $\boldsymbol{X}_{k,t}^n$ and $\boldsymbol{X}_{k+1,t}^n$. In the following we relax the power constraint (3.4) by requiring only that the power of the n channel inputs

produced by any given Tx-antenna cannot exceed $n\mathsf{P}$:

$$\sum_{t=1}^{n} \mathsf{P}_{k,t}(j) \leq n\mathsf{P}, \quad k \in \{1,\ldots,K\} \text{ and } j \in \{1,\ldots,\mathsf{L}\}. \tag{A.11}$$

Since the right-hand side of (A.10) is monotonically increasing and jointly concave in the powers $\{\mathsf{P}_{k,t}(j)\}$ and $\{\mathsf{P}_{k+1,t}(j)\}$, the upper bound on $\mathrm{Var}(\mathbf{Y}_{k+1,t}(i))$ is largest when $\mathsf{P}_{k,t}(j) = \mathsf{P}_{k+1,t}(j) = \mathsf{P}$. Moreover since also the function $x \mapsto \log(1+x)$ is monotonically increasing, we conclude:

$$h(\boldsymbol{Y}_{k+1}^n | M_{k+1}^{(S)}) \;\leq\; n \sum_{i=1}^{\mathsf{L}} \frac{1}{2}\log(2\pi e) \left(1 + \left(\sum_{j=1}^{\mathsf{L}} |\mathsf{H}_{k,k+1}(i,j)|\right)^2 \mathsf{P} + \left(\sum_{j=1}^{\mathsf{L}} |\mathsf{H}_{k+1,k+1}(i,j)|\right)^2 \mathsf{P}\right) \tag{A.12}$$

We next bound the term

$$\begin{aligned}
\frac{1}{n} h(\mathsf{H}_{k,k+1}\boldsymbol{X}_k^n + \boldsymbol{Z}_{k+1}^n | \mathsf{H}_{k,k}\boldsymbol{X}_k^n + \boldsymbol{Z}_k^n) &= \frac{1}{n} h(\boldsymbol{Z}_{k+1}^n - \mathsf{H}_{k,k+1}{\mathsf{H}_{k,k}}^{-1}\boldsymbol{Z}_k^n | \mathsf{H}_{k,k}\boldsymbol{X}_k^n + \boldsymbol{Z}_k^n) && \text{(A.13)}\\
&\leq \frac{1}{n} h(\boldsymbol{Z}_{k+1}^n - \mathsf{H}_{k,k+1}{\mathsf{H}_{k,k}}^{-1}\boldsymbol{Z}_k^n) && \text{(A.14)}\\
&= \frac{1}{2}\log\det(\mathrm{I}_{\mathsf{L}} + \mathsf{H}_{k,k+1}{\mathsf{H}_{k,k}}^{-1}{\mathsf{H}_{k,k}}^{-\mathsf{T}}\mathsf{H}_{k,k+1}^T), && \text{(A.15)}
\end{aligned}$$

where recall that I_{L} denotes the L-by-L identity matrix.

For the last bound, define

$$\boldsymbol{T}_k^n \triangleq \mathsf{H}_{k,k}^{-1}\boldsymbol{Z}_k^n - \mathsf{H}_{k,k+1}^{-1}\boldsymbol{Z}_{k+1}^n. \tag{A.16}$$

Then:

$$\begin{aligned}
&\frac{1}{n} h(\mathsf{H}_{k,k}\boldsymbol{X}_k^n + \boldsymbol{Z}_k^n) - \frac{1}{n} h(\mathsf{H}_{k,k+1}\boldsymbol{X}_k^n + \boldsymbol{Z}_{k+1}^n)\\
&\overset{(e)}{=} \frac{1}{n} h(\boldsymbol{X}_k^n + \mathsf{H}_{k,k+1}^{-1}\boldsymbol{Z}_{k+1}^n + \boldsymbol{T}_k^n) - \frac{1}{n} h(\boldsymbol{X}_k^n + \mathsf{H}_{k,k+1}^{-1}\boldsymbol{Z}_{k+1}^n) + \log\Big(\frac{\det(\mathsf{H}_{k,k})}{\det(\mathsf{H}_{k,k+1})}\Big) && \text{(A.17)}\\
&\overset{(f)}{\leq} \frac{1}{n} h(\boldsymbol{X}_k^n + \mathsf{H}_{k,k+1}^{-1}\boldsymbol{Z}_{k+1}^n + \boldsymbol{T}_k^n) - \frac{1}{n} h(\boldsymbol{X}_k^n + \mathsf{H}_{k,k+1}^{-1}\boldsymbol{Z}_{k+1}^n | \boldsymbol{T}_k^n) + \log\Big(\frac{\det(\mathsf{H}_{k,k})}{\det(\mathsf{H}_{k,k+1})}\Big) && \text{(A.18)}\\
&= \frac{1}{n} I(\boldsymbol{X}_k^n + \mathsf{H}_{k,k+1}^{-1}\boldsymbol{Z}_{k+1}^n + \boldsymbol{T}_k^n; \boldsymbol{T}_k^n) + \log\Big(\frac{\det(\mathsf{H}_{k,k})}{\det(\mathsf{H}_{k,k+1})}\Big) && \text{(A.19)}\\
&\overset{(g)}{\leq} \frac{1}{n} I(\mathsf{H}_{k,k+1}^{-1}\boldsymbol{Z}_{k+1}^n + \boldsymbol{T}_k^n; \boldsymbol{T}_k^n | \boldsymbol{X}_k^n) + \log\Big(\frac{\det(\mathsf{H}_{k,k})}{\det(\mathsf{H}_{k,k+1})}\Big) && \text{(A.20)}\\
&\overset{(g)}{=} \frac{1}{n} I(\mathsf{H}_{k,k+1}^{-1}\boldsymbol{Z}_{k+1}^n + \boldsymbol{T}_k^n; \boldsymbol{T}_k^n) + \log\Big(\frac{\det(\mathsf{H}_{k,k})}{\det(\mathsf{H}_{k,k+1})}\Big) && \text{(A.21)}\\
&\overset{(h)}{=} \frac{1}{n} h(\boldsymbol{T}_k^n) - h(\mathsf{H}_{k,k+1}^{-1}\boldsymbol{Z}_{k+1}^n) + \log\Big(\frac{\det(\mathsf{H}_{k,k})}{\det(\mathsf{H}_{k,k+1})}\Big) && \text{(A.22)}
\end{aligned}$$

$$= \frac{1}{2}\log\frac{\det\left(\mathsf{H}_{k,k}^{-1}\mathsf{H}_{k,k}^{-\mathsf{T}}+\mathsf{H}_{k,k+1}^{-1}\mathsf{H}_{k,k+1}^{-\mathsf{T}}\right)}{\det(\mathsf{H}_{k,k+1}^{-1}\mathsf{H}_{k,k+1}^{-\mathsf{T}})}+\log\left(\frac{\det(\mathsf{H}_{k,k})}{\det(\mathsf{H}_{k,k+1})}\right) \tag{A.23}$$

$$= \frac{1}{2}\log\det\left(\mathsf{H}_{k,k}^{-1}\mathsf{H}_{k,k}^{-\mathsf{T}}+\mathsf{H}_{k,k+1}^{-1}\mathsf{H}_{k,k+1}^{-\mathsf{T}}\right)+\log\det(\mathsf{H}_{k,k}), \tag{A.24}$$

where (e) holds by the definition of $\boldsymbol{T}_k^n$ and because $h(\mathsf{A}\boldsymbol{X}) = \log\det(\mathsf{A}) + h(\boldsymbol{X})$ for any matrix A and vector $\boldsymbol{X}$; (f) holds because conditioning can only reduce entropy; (inequalities) (g) hold again because conditioning can only reduce entropy and by the independence of $\boldsymbol{T}_k^n$ and $\boldsymbol{X}_k^n$; and (h) holds because by the independence of the noise vectors we have $h(\boldsymbol{T}_k^n|\mathsf{H}_{k,k+1}^{-1}\boldsymbol{Z}_{k+1}^n+\boldsymbol{T}_k^n) = h(-\mathsf{H}_{k,k+1}^{-1}\boldsymbol{Z}_k^n|\mathsf{H}_{k,k}^{-1}\boldsymbol{Z}_k^n) = h(\mathsf{H}_{k,k+1}^{-1}\boldsymbol{Z}_k^n)$.

Following similar steps as the ones leading to (A.9), one can also prove that

$$R_1^{(F)} \leq \frac{1}{n}I(M_1^{(F)};\boldsymbol{Y}_1^n|M_1^{(S)})+\frac{\epsilon_n}{n} \tag{A.25}$$

$$\leq \sum_{i=1}^{\mathsf{L}}\frac{1}{2}\log\left(1+\left(\sum_{j=1}^{\mathsf{L}}|\mathsf{H}_{1,1}(i,j)|\right)^2\mathsf{P}\right)+\frac{\epsilon_n}{n}, \tag{A.26}$$

and

$$R_K^{(F)}+R_K^{(S)} \leq \frac{1}{n}I(M_K^{(F)},M_K^{(S)};\boldsymbol{Y}_K^n|M_{K-1})+\frac{\epsilon_n}{n} \tag{A.27}$$

$$\leq \sum_{i=1}^{\mathsf{L}}\frac{1}{2}\log\left(1+\left(\sum_{j=1}^{\mathsf{L}}|\mathsf{H}_{K,K}(i,j)|\right)^2\mathsf{P}\right)+\frac{\epsilon_n}{n}, \tag{A.28}$$

where $\mathsf{H}_{1,1}(i,j)$ and $\mathsf{H}_{K,K}(i,:)$ denote row-i, column-j elements of the matrices $\mathsf{H}_{1,1}$ and $\mathsf{H}_{K,K}$.

We sum up the bound in (A.8) for all values of $k \in \{1,\ldots,K-1\}$, and combine it with (A.26) and (A.28). Taking $n\to\infty$, it follows that because the probability of error $p(\text{error})$ vanishes as $n\to\infty$ (and thus $\frac{\epsilon_n}{n}\to 0$ as $n\to\infty$):

$$\sum_{k=1}^{K}\left(2R_k^{(F)}+R_k^{(S)}\right)$$

$$= R_1^{(F)}+\sum_{k=1}^{K-1}\left(R_k^{(F)}+R_k^{(S)}+R_{k+1}^{(F)}\right)+R_K^{(F)}+R_K^{(S)} \tag{A.29}$$

$$\leq \sum_{k=1}^{K-1}\Bigg[\sum_{i=1}^{\mathsf{L}}\frac{1}{2}\log\Big(1+\Big(\sum_{j=1}^{\mathsf{L}}|\mathsf{H}_{k+1,k+1}(i,j)|\Big)^2\mathsf{P}+\Big(\sum_{j=1}^{\mathsf{L}}|\mathsf{H}_{k,k+1}(i,j)|\Big)^2\mathsf{P}\Big)$$
$$+\frac{1}{2}\log\det\left(\mathrm{I}_{\mathsf{L}}+\mathsf{H}_{k,k+1}\mathsf{H}_{k,k}{}^{-1}\mathsf{H}_{k,k}{}^{-\mathsf{T}}\mathsf{H}_{k,k+1}^T\right)+\frac{1}{2}\log\det\left(\mathsf{H}_{k,k}^{-1}\mathsf{H}_{k,k}^{-\mathsf{T}}+\mathsf{H}_{k,k+1}^{-1}\mathsf{H}_{k,k+1}^{-\mathsf{T}}\right)+\log\det(\mathsf{H}_{k,k})\Bigg]$$

$$+\sum_{i=1}^{\mathsf{L}}\frac{1}{2}\log\left(1+\left(\sum_{j=1}^{\mathsf{L}}|\mathsf{H}_{1,1}(i,j)|\right)^2\mathsf{P}\right)+\sum_{i=1}^{\mathsf{L}}\frac{1}{2}\log\left(1+\left(\sum_{j=1}^{\mathsf{L}}|\mathsf{H}_{K,K}(i,j)|\right)^2\mathsf{P}\right). \tag{A.30}$$

Dividing by K and $\frac{1}{2}\log(\mathsf{P})$ and taking $\mathsf{P}, K \to \infty$, establishes the converse bound (4.3).

A.1.2 Proof of the Converse to (4.4)

We now prove bound (4.4). We assume K is even. For K odd the bound can be proved in a similar way. Divide the set $\mathcal{K}$ into sets $\mathcal{K}_{\text{odd}} \triangleq \{1,3,\ldots,K-1\}$ and $\mathcal{K}_{\text{even}} \triangleq \{2,4,\ldots,K\}$. Recall that $X_0^n = 0$, and define

$$\mathbb{M}_{\text{odd}} := \{M_k\colon \quad k \text{ odd}\}$$
$$\mathbb{M}_{\text{even}} := \{M_k\colon \quad k \text{ even}\}$$
$$\mathbb{X}^n_{\text{odd}} := \{\boldsymbol{X}^n_k\colon k \text{ odd}\}$$
$$\mathbb{X}^n_{\text{even}} := \{\boldsymbol{X}^n_k\colon \quad k \text{ odd}\}$$
$$\mathbb{Y}^n_{\text{odd}} := \{\boldsymbol{Y}^n_k\colon k \text{ odd}\}$$
$$\mathbb{Y}^n_{\text{even}} := \{\boldsymbol{Y}^n_k\colon k \text{ even}\}$$
$$\mathbb{Z}^n_{\text{odd}} := \{\boldsymbol{Z}^n_k\colon k \text{ odd}\}$$
$$\mathbb{Z}^n_{\text{even}} := \{\boldsymbol{Z}^n_k\colon k \text{ even}\}$$

and

$$\mathbb{Q}_{\text{odd}} := \left\{Q^{(1)}_{k\to\tilde{k}},\ldots,Q^{(\text{D})}_{k\to\tilde{k}}\colon \ k \text{ odd },\ \tilde{k}\in\{k-1,k+1\}\right\}$$
$$\mathbb{Q}_{\text{even}} := \left\{Q^{(1)}_{k\to\tilde{k}},\ldots,Q^{(\text{D})}_{k\to\tilde{k}}\colon \ k \text{ even},\ \tilde{k}\in\{k-1,k+1\}\right\}.$$

Also define a genie information $\mathbb{G}$ as

$$\mathbb{G} \triangleq \mathbb{Z}_{\text{odd}} - \mathsf{H}_{\text{odd,odd}}\mathsf{H}^{-1}_{\text{odd,even}}\mathbb{Z}_{\text{even}}, \tag{A.31}$$

where $\mathsf{H}_{\text{odd,odd}}$ denotes the channel matrix from the Txs in $\mathcal{K}_{\text{odd}}$ to the Rxs in $\mathcal{K}_{\text{odd}}$, and $\mathsf{H}_{\text{odd,even}}$ denotes the channel matrix from the Txs in $\mathcal{K}_{\text{odd}}$ to the Rxs in $\mathcal{K}_{\text{even}}$. Because these matrices are square and the channel coefficients are drawn i.i.d according to a continues distribution, they are invertible.

By Fano's inequality, there must exist a sequence $\{\epsilon_n\}_{n=1}^{\infty}$ so that $\frac{\epsilon_n}{n} \to 0$ as $n \to \infty$ and

$$
\begin{aligned}
&\sum_{k=1}^{K} \left(R_k^{(F)} + R_k^{(S)} \right) \\
&= \frac{1}{n} \big[H(\mathbb{M}_{\text{odd}}) + H(\mathbb{M}_{\text{even}}) \big] \\
&\le \frac{1}{n} \big[I(\mathbb{M}_{\text{odd}}; \mathbb{Y}_{\text{odd}}, \mathbb{Q}_{\text{odd}}) + I(\mathbb{M}_{\text{even}}; \mathbb{Y}_{\text{even}}, \mathbb{Q}_{\text{even}} | \mathbb{M}_{\text{odd}}) \big] + \frac{\epsilon_n}{n} \\
&= \frac{1}{n} \big[I(\mathbb{M}_{\text{odd}}; \mathbb{Y}_{\text{odd}}) + I(\mathbb{M}_{\text{even}}; \mathbb{Y}_{\text{even}} | \mathbb{M}_{\text{odd}}) + I(\mathbb{M}_{\text{odd}}; \mathbb{Q}_{\text{odd}} | \mathbb{Y}_{\text{odd}}) + I(\mathbb{M}_{\text{even}}; \mathbb{Q}_{\text{even}} | \mathbb{M}_{\text{odd}}, \mathbb{Y}_{\text{even}}) \big] + \frac{\epsilon_n}{n} \\
&\le \frac{1}{n} \big[h(\mathbb{Y}_{\text{odd}}) - h(\mathbb{Y}_{\text{odd}} | \mathbb{M}_{\text{odd}}) + h(\mathbb{Y}_{\text{even}} | \mathbb{M}_{\text{odd}}) - h(\mathbb{Z}_{\text{even}}) + H(\mathbb{Q}_{\text{odd}}) + I(\mathbb{M}_{\text{even}}; \mathbb{Q}_{\text{even}} | \mathbb{M}_{\text{odd}}, \mathbb{Y}_{\text{even}}) \big] + \frac{\epsilon_n}{n} \\
&\le \frac{1}{n} \big[h(\mathbb{Y}_{\text{odd}}) - h(\mathbb{Y}_{\text{odd}} | \mathbb{M}_{\text{odd}}) + h(\mathbb{Y}_{\text{even}} | \mathbb{M}_{\text{odd}}) - h(\mathbb{Z}_{\text{even}}) + H(\mathbb{Q}_{\text{odd}}) \\
&\qquad + I(\mathbb{M}_{\text{even}}; \mathbb{Q}_{\text{even}} | \mathbb{M}_{\text{odd}}, \mathbb{Y}_{\text{even}}, \mathbb{G}) + I(\mathbb{M}_{\text{even}}; \mathbb{G} | \mathbb{M}_{\text{odd}}, \mathbb{Y}_{\text{even}}) \big] + \frac{\epsilon_n}{n} \\
&\overset{(a)}{\le} \sum_{k \in \mathcal{K}_{\text{odd}}} \sum_{i=1}^{\mathsf{L}} \frac{1}{2} \log(2\pi e) \left(1 + \left(\sum_{j=1}^{\mathsf{L}} |\mathsf{H}_{k-1,k}(i,j)| \right)^2 \mathsf{P} + \left(\sum_{j=1}^{\mathsf{L}} |\mathsf{H}_{k,k}(i,j)| \right)^2 \mathsf{P} \right) \\
&\quad + \sum_{i=1}^{\mathsf{L}} \frac{1}{2} \log(2\pi e) \left(1 + \left(\sum_{j=1}^{\mathsf{L}} |\mathsf{H}_{k,k}(i,j)| \right)^2 \mathsf{P} \right) + \sum_{k \in \mathcal{K}_{\text{even}} \setminus K} \frac{1}{2} \log\det \left(\mathsf{H}_{k,k}^{-1} \mathsf{H}_{k,k}^{-\mathsf{T}} + \mathsf{H}_{k,k+1}^{-1} \mathsf{H}_{k,k+1}^{-\mathsf{T}} \right) + \log\det(\mathsf{H}_{k,k}) \\
&\quad + \pi_{\text{Rx}} K + \frac{1}{2} \sum_{k \in \mathcal{K}_{\text{odd}}} \log\det \left(\mathrm{I}_{\mathsf{L}} + \mathsf{H}_{k,k} \mathsf{H}_{k,k}^{\mathsf{T}} + \mathsf{H}_{k,k+1}^{-1} \mathsf{H}_{k,k+1}^{-\mathsf{T}} \right) + \frac{\epsilon_n}{n}, \qquad \text{(A.32)}
\end{aligned}
$$

where (a) holds because:

- By (A.10) and (A.12):

$$
h(\mathbb{Y}_{\text{odd}}) - h(\mathbb{Z}_{\text{even}}) \le n \sum_{k \in \mathcal{K}_{\text{odd}}} \sum_{i=1}^{\mathsf{L}} \frac{1}{2} \log(2\pi e) \left(1 + \left(\sum_{j=1}^{\mathsf{L}} |\mathsf{H}_{k-1,k}(i,j)| \right)^2 \mathsf{P} + \left(\sum_{j=1}^{\mathsf{L}} |\mathsf{H}_{k,k}(i,j)| \right)^2 \mathsf{P} \right); \qquad \text{(A.33)}
$$

- By (A.15) and (A.24):

$$
\begin{aligned}
&h(\mathbb{Y}_{\text{even}} | \mathbb{M}_{\text{odd}}) - h(\mathbb{Y}_{\text{odd}} | \mathbb{M}_{\text{odd}}) \\
&= h(\boldsymbol{Y}_K^n | M_{K-1}) - h(\boldsymbol{Y}_1^n | M_1) \\
&\quad + \sum_{k \in \mathcal{K}_{\text{even}} \setminus K} \big[h(\mathsf{H}_{k,k} \boldsymbol{X}_k^n + \boldsymbol{Z}_k^n) - h(\mathsf{H}_{k,k+1} \boldsymbol{X}_k^n + Z_{k+1}^n) \big] \\
&\le n \sum_{i=1}^{\mathsf{L}} \frac{1}{2} \log(2\pi e) \left(1 + \left(\sum_{j=1}^{\mathsf{L}} |\mathsf{H}_{k,k}(i,j)| \right)^2 \mathsf{P} \right) \\
&\quad + n \sum_{k \in \mathcal{K}_{\text{even}} \setminus K} \frac{1}{2} \log\det \left(\mathsf{H}_{k,k}^{-1} \mathsf{H}_{k,k}^{-\mathsf{T}} + \mathsf{H}_{k,k+1}^{-1} \mathsf{H}_{k,k+1}^{-\mathsf{T}} \right) + \log\det(\mathsf{H}_{k,k}); \qquad \text{(A.34)}
\end{aligned}
$$

- By the rate-limitation of the cooperation links:

$$H(\mathbb{Q}_{\text{odd}}) \leq n\pi_{\text{Rx}}K; \tag{A.35}$$

- From the tuple $(\mathbb{M}_{\text{odd}}, \mathbb{Y}_{\text{even}}, \mathbb{G})$ it is possible to compute also $\mathbb{Y}_{\text{odd}}$ and thus $\mathbb{Q}_{\text{even}}$:

$$I(\mathbb{M}_{\text{even}}; \mathbb{Q}_{\text{even}}|\mathbb{M}_{\text{odd}}, \mathbb{Y}_{\text{even}}, \mathbb{G}) = 0; \tag{A.36}$$

- By the fact that conditioning reduces entropy:

$$\begin{aligned} &I(\mathbb{M}_{\text{even}}; \mathbb{G}|\mathbb{M}_{\text{odd}}, \mathbb{Y}_{\text{even}}) \\ &\leq h(\mathbb{G}) - h(\mathbb{G}|\mathbb{Z}_{\text{even}}) \\ &= \frac{n}{2} \sum_{k\in\mathcal{K}_{\text{odd}}} \log\det\left(\mathsf{I}_{\mathsf{L}} + \mathsf{H}_{k,k}\mathsf{H}_{k,k}^{\mathsf{T}} + \mathsf{H}_{k,k+1}^{-1}\mathsf{H}_{k,k+1}^{-\mathsf{T}}\right) \end{aligned} \tag{A.37}$$

Taking $n \to \infty$ establishes the proof.

A.1.3 Proof of the Converse to (4.10)

Fix a sequence (in the blocklength n) of encoding and decoding functions respecting the power constraints and the Tx-cooperation rate-limitations (recall that we consider a setup with only Tx-cooperation but no Rx-cooperation) such that the error probability $p(\text{error}) \to 0$ as the blocklength $n \to \infty$.

Let $\mathbf{M}^{(S)} \triangleq (M_1^{(S)}, \ldots, M_K^{(S)})$. By Fano's Inequality there exists a sequence ϵ_n satisfying $\frac{\epsilon_n}{n} \to 0$ as $n \to \infty$ such that for any $k \in \{1, \ldots, K-1\}$ and any blocklength n:

$$\begin{aligned} &R_k^{(F)} + R_{k+1}^{(S)} + R_{k+1}^{(F)} \\ &\quad= \frac{1}{n}\Big[H(M_k^{(F)}|\mathbf{M}^{(S)}, M_{k-1}^{(F)}) + H(M_{k+1}|M_1^{(S)}, \ldots, M_k^{(S)}, M_{k+2}^{(S)}, \ldots, M_K^{(S)})\Big] + \frac{\epsilon_n}{n} \\ &\quad\leq \frac{1}{n}\Big[I(M_k^{(F)}; \boldsymbol{Y}_k^n|\mathbf{M}^{(S)}, M_{k-1}^{(F)}) + I(M_{k+1}; \boldsymbol{Y}_{k+1}^n|M_1^{(S)}, \ldots, M_k^{(S)}, M_{k+2}^{(S)}, \ldots, M_K^{(S)})\Big] + \frac{\epsilon_n}{n} \\ &\quad= \frac{1}{n}\Big[h(\mathsf{H}_{k,k}\boldsymbol{X}_k^n + \boldsymbol{Z}_k^n|\mathbf{M}^{(S)}) - h(\boldsymbol{Z}_k^n) \\ &\qquad\qquad + h(\boldsymbol{Y}_{k+1}^n|M_1^{(S)}, \ldots, M_k^{(S)}, M_{k+2}^{(S)}, \ldots, M_K^{(S)}) - h(\mathsf{H}_{k,k+1}\boldsymbol{X}_k^n + \boldsymbol{Z}_{k+1}^n|\mathbf{M}^{(S)})\Big] + \frac{\epsilon_n}{n} \\ &\quad\overset{(a)}{\leq} \sum_{i=1}^{\mathsf{L}} \frac{1}{2}\log\Big(1 + \Big(\sum_{j=1}^{\mathsf{L}}(|\mathsf{H}_{k+1,k+1}(i,j)| + |\mathsf{H}_{k,k+1}(i,j)|)\Big)^2\mathsf{P}\Big) \end{aligned}$$

$$+\frac{1}{2}\log\det\left(\mathsf{H}_{k,k}^{-1}\mathsf{H}_{k,k}^{-\mathsf{T}}+\mathsf{H}_{k,k+1}^{-1}\mathsf{H}_{k,k+1}^{-\mathsf{T}}\right)+\log\det(\mathsf{H}_{k,k})+\frac{\epsilon_n}{n}, \tag{A.38}$$

where (a) follows by similar steps as lead to (A.15) and (A.24), but where one has to account for the fact that due to the Tx-cooperation, the input vectors $\boldsymbol{X}_k^n$ and $\boldsymbol{X}_{k+1}^n$ can be correlated.

Similarly to (A.24) one can further prove that

$$R_1^{(F)}\leq\sum_{i=1}^{\mathsf{L}}\frac{1}{2}\log\Big(1+\Big(\sum_{j=1}^{\mathsf{L}}|\mathsf{H}_{1,1}(i,j)|\Big)^2\mathsf{P}\Big)+\frac{\epsilon_n}{n}, \tag{A.39}$$

and

$$R_K^{(F)}+R_K^{(S)}\leq\sum_{i=1}^{\mathsf{L}}\frac{1}{2}\log\Big(1+\Big(\sum_{j=1}^{\mathsf{L}}(|\mathsf{H}_{K,K}(i,j)|+|\mathsf{H}_{K-1,K}(i,j)|)\Big)^2\mathsf{P}\Big)+\frac{\epsilon_n}{n}, \tag{A.40}$$

where again one has to consider that because of the Tx-cooperation the various input vectors can be correlated.

We now sum up the bound in (A.38) for all values of $k\in\{1,\ldots,K-1\}$ and combine it with (A.39) and (A.40). Taking $n\to\infty$, it follows that because the probability of error $p(\text{error})$ vanishes as $n\to\infty$ (and thus $\frac{\epsilon_n}{n}\to 0$ as $n\to\infty$):

$$\begin{aligned}
&\sum_{k=1}^{K}\Big(2R_k^{(F)}+R_k^{(S)}\Big)\\
&\quad=\quad R_1^{(F)}+\sum_{k=1}^{K-1}\Big(R_k^{(F)}+R_k^{(S)}+R_{k+1}^{(F)}\Big)+R_K^{(F)}+R_K^{(S)}\Big) \qquad\text{(A.41)}\\
&\quad\leq\quad\sum_{k=1}^{K-1}\Bigg[\sum_{i=1}^{\mathsf{L}}\frac{1}{2}\log\Big(1+\Big(\sum_{j=1}^{\mathsf{L}}(|\mathsf{H}_{k+1,k+1}(i,j)|+|\mathsf{H}_{k,k+1}(i,j)|)\Big)^2\mathsf{P}\Big)\\
&\qquad\qquad+\frac{1}{2}\log\det\left(\mathsf{H}_{k,k}^{-1}\mathsf{H}_{k,k}^{-\mathsf{T}}+\mathsf{H}_{k,k+1}^{-1}\mathsf{H}_{k,k+1}^{-\mathsf{T}}\right)+\log\det(\mathsf{H}_{k,k})\Bigg]\\
&\qquad+\sum_{i=1}^{\mathsf{L}}\frac{1}{2}\log\Big(1+\Big(\sum_{j=1}^{\mathsf{L}}|\mathsf{H}_{1,1}(i,j)|\Big)^2\mathsf{P}\Big)+\sum_{i=1}^{\mathsf{L}}\frac{1}{2}\log\Big(1+\Big(\sum_{j=1}^{\mathsf{L}}(|\mathsf{H}_{K,K}(i,j)|+|\mathsf{H}_{K-1,K}(i,j)|)\Big)^2\mathsf{P}\Big).
\end{aligned}$$

Dividing by K and $\frac{1}{2}\log(\mathsf{P})$ and taking $\mathsf{P},K\to\infty$, establishes the converse bound (4.10).

A.1.4 Proof of Achievability of Theorem 3

Scheme 1: Conferencing only parts of "fast" messages

Fix a small number $\epsilon > 0$ and a joint distribution $P_{U_1U_2X}$ that satisfies the Markov chain $U_1 \to U_2 \to X$. Let (U_1', U_2', X') be an independent copy of (U_1, U_2, X) and define

$$Y = X + \alpha X' + Z, \tag{A.42}$$

where Z is standard Gaussian independent of all other defined random variables.

Split each source message into two parts, $M_k^{(F)} = \big(M_k^{(F_1)}, M_k^{(F_2)}\big)$, of rates $\big(R_k^{(F_1)}, R_k^{(F_2)}\big)$ that sum up to $R_k^{(F)} = R_k^{(F_1)} + R_k^{(F_2)}$ and so that

$$R_k^{(F_1)} < \pi_{\mathrm{Rx}}. \tag{A.43}$$

Codebook construction: For each $k \in \{1, \dots, K\}$, generate codebooks $\mathcal{C}_{1,k}$, $\{\mathcal{C}_{2,k}(i)\}$, and $\{\mathcal{C}_{x,k}(i,j)\}$ randomly. Codebook

$$\mathcal{C}_{1,k} := \Big\{u_{1,k}^n(i) \colon \ \ i = 1, \dots, \Big\lfloor 2^{nR_k^{(F_1)}} \Big\rfloor\Big\} \tag{A.44}$$

is generated by picking all entries i.i.d. according to P_{U_1}. For each $i \in \big\{1, \dots, \big\lfloor 2^{nR_k^{(F_1)}} \big\rfloor\big\}$, codebook

$$\mathcal{C}_{2,k}(i) := \Big\{u_{2,k}^n(j|i) \colon \ \ j = 1, \dots, \Big\lfloor 2^{nR_k^{(F_2)}} \Big\rfloor\Big\} \tag{A.45}$$

is generated by picking the t-th entry of codeword $u_{2,k}^n(j|i)$ independently of all other entries and codewords according to the distribution $P_{U_2|U_1}(\cdot|u_{1,k,t}(i))$. Here, $u_{1,k,t}(i)$ denotes the t-th entry of codeword $u_{1,k}^n(i)$. For each pair (i,j) in $\big\{1, \dots, \big\lfloor 2^{nR_k^{(F_1)}} \big\rfloor\big\} \times \big\{1, \dots, \big\lfloor 2^{nR_k^{(F_2)}} \big\rfloor\big\}$, codebook

$$\mathcal{C}_{x,k}(i,j) := \Big\{x_k^n(\ell|i,j) \colon \ \ \ell = 1, \dots, \Big\lfloor 2^{nR_k^{(S)}} \Big\rfloor\Big\} \tag{A.46}$$

is generated by picking the t-th entry of codeword $x_k^n(\ell|i,j)$ independently of all other entries according to the distribution $P_{X|U_2}(\cdot|u_{2,k,t}(j|i))$. Here, $u_{2,k,t}(j|i)$ denotes the t-th entry of codeword $u_{2,k}^n(j|i)$.

Reveal all codebooks to all terminals.

Encoding: Tx k sends codeword $x_k^n\big(M_k^{(S)} \big| M_k^{(F_1)}, M_k^{(F_2)}\big)$ over the channel.

Decoding: Each Rx k performs the following steps. Given that it observes $Y_k^n = y_k^n$, it first looks for a

unique pair $(\hat{i}, \hat{j})$ such that

$$(u_{1,k}^n(\hat{i}), u_{2,k}^n(\hat{j}|\hat{i}), y_k^n) \in T_\epsilon^{(n)}(P_{U_1U_2Y}). \tag{A.47}$$

If none or more than one such pair $(\hat{i}, \hat{j})$ exists, Rx k declares an error. Otherwise, it declares $\hat{M}_k^{(F)} = (\hat{i}, \hat{j})$, and it sends

$$Q_{k\to k+1}^{(1)} = \hat{i}. \tag{A.48}$$

to its right neighbour, Rx $k+1$.

With the message $Q_{k-1\to k}^{(1)}$, Rx k obtains from its left-neighbour, it decodes also its intended "slow" message. To this end, it looks for an index $\hat{\ell}$ such that

$$\left(u_{1,k}^n(\hat{i}), u_{2,k}^n(\hat{j}|\hat{i}), x_k^n(\hat{\ell}|\hat{i}, \hat{j}), u_{k-1}^n(Q_{k-1\to k}^{(1)}), y_k^n\right) \in T_\epsilon^{(n)}(P_{U_1U_2XU_1'Y}), \tag{A.49}$$

If none or multiple such indices $\hat{\ell}$ exist, an error is declared. Otherwise, Rx k declares $\hat{M}_k^{(S)} = \hat{\ell}$.

Analysis: Decoding in (A.47) is successful with probability tending to 1 as $n \to \infty$, if

$$R_k^{(F_1)} + R_k^{(F_2)} < I(U_2; Y) \tag{A.50}$$

$$R_k^{(F_2)} < I(U_2; Y|U_1). \tag{A.51}$$

Decoding in (A.49) is successful with probability tending to 1 as $n \to \infty$, if

$$R_k^{(S)} < I(X; Y, U_1'|U_1). \tag{A.52}$$

The cooperation constraint is satisfied by (A.43). Apply then Fourier-Motzkin elimination to (A.43), (A.50) and (A.51). Achievability of the pairs (4.17) follows then by a rate-transfer argument that parts of the "slow" messages can also be sent as "fast" messages.

Scheme 2: Conferencing also parts of "slow"-messages

Fix $\epsilon > 0$ and a joint distribution $P_{UV_1\ldots V_{\mathrm{D}-1}X}$ satisfying the Markov chain $U \to V_1 \to V_2 \to \ldots V_{\mathrm{D}-1} \to X$ and the rate constraint

$$R_k^{(F)} < \pi_{\mathrm{Rx}}. \tag{A.53}$$

Let $(U', V_1', V_2', \ldots, V_{\mathrm{D}-1}', X')$ be an independent copy of $(U, V_1, \ldots, V_{\mathrm{D}-1}, X)$ and define

$$Y = X + \alpha X' + Z, \tag{A.54}$$

where Z is independent standard Gaussian.

Split $M_k^{(S)}$ into D parts, $M_k^{(S)} = (M_k^{(S_1)}, \ldots, M_k^{(S_{\mathrm{D}})})$, of rates $(R_k^{(S_1)}, \ldots R_k^{(S_{\mathrm{D}})})$ that sum up to $R_k^{(S)} = \sum_{d=1}^{\mathrm{D}} R_k^{(S_d)}$ and satisfy

$$R_k^{(F)} + \sum_{d=1}^{\mathrm{D}-1} R_k^{(S_d)} < \pi_{\mathrm{Rx}}. \tag{A.55}$$

Codebook construction: For each $k \in \{1, \ldots, K\}$, generate the following codebooks $\mathcal{C}_{1,k}$, $\{\mathcal{C}_{2,k}\}, \ldots, \{\mathcal{C}_{\mathrm{D},k}\}, \{\mathcal{C}_{x,k}\}$ randomly. Codebook

$$\mathcal{C}_{1,k} := \left\{ u_k^n(j) \colon j = 1, \ldots, \left\lfloor 2^{nR_k^{(F)}} \right\rfloor \right\} \tag{A.56}$$

is generated by picking all entries i.i.d. according to P_U. For each $j \in \left\{1, \ldots, \left\lfloor 2^{nR_k^{(F)}} \right\rfloor\right\}$, codebook

$$\mathcal{C}_{2,k}(j) := \left\{ v_{1,k}^n(i_1|j) \colon i_1 = 1, \ldots, \left\lfloor 2^{nR_k^{(S_1)}} \right\rfloor \right\} \tag{A.57}$$

is generated by picking the t-th entry of codeword $v_{1,k}^n(i_1|j)$ independently of all other entries and codewords according to the distribution $P_{V_{1,k}|U}(\cdot|u_{k,t}(i))$. Here, $u_{k,t}(i)$ denotes the t-th entry of codeword $u_k^n(i)$. For each $d \in \{2, \ldots, \mathrm{D}-1\}$, and each tuple $(j, i_1, \ldots, i_{d-1})$ in $\left\{1, \ldots, \left\lfloor 2^{nR_k^{(F)}} \right\rfloor\right\} \times \prod_{\ell=1}^{d-1} \left\{1, \ldots, \left\lfloor 2^{nR_k^{(S_\ell)}} \right\rfloor\right\}$, codebook

$$\mathcal{C}_{d+1,k}(j, i_1, \ldots, i_{d-1}) := \left\{ v_{d,k}^n(i_d|j, i_1, \ldots, i_{d-1}) \colon i_d = 1, \ldots, \left\lfloor 2^{nR_k^{(S_d)}} \right\rfloor \right\} \tag{A.58}$$

is generated by picking the t-th entry of codeword $v_{d,k}^n(i_d|j, i_1, \ldots, i_{d-1})$ independently of all other entries according to the distribution $P_{V_{d,k}|V_{d-1,k}}(\cdot|v_{d-1,k,t}(i_{d-1}|j, i_1, \ldots, i_{d-2}))$. Here, $v_{d-1,k,t}(i_{d-1}|j, i_1, \ldots, i_{d-2})$ denotes the t-th entry of codeword $v_{d-1,k}^n(i_{d-1}|j, i_1, \ldots, i_{d-2})$.

Finally, for each tuple $(j, i_1, \ldots, i_{\mathrm{D}-1})$ in $\left\{1, \ldots, \left\lfloor 2^{nR_k^{(F)}} \right\rfloor\right\} \times \prod_{\ell=1}^{\mathrm{D}-1} \left\{1, \ldots, \left\lfloor 2^{nR_k^{(S_\ell)}} \right\rfloor\right\}$, codebook

$$\mathcal{C}_{x,k}(j, i_1, \ldots, i_{\mathrm{D}-1}) := \left\{ x_k^n(\ell|j, i_1, \ldots, i_{\mathrm{D}-1}) \colon \ \ell = 1, \ldots, \left\lfloor 2^{nR_k^{(S_{\mathrm{D}})}} \right\rfloor \right\} \tag{A.59}$$

is generated by picking the t-th entry of codeword $x_k^n(\ell|j, i_1, \ldots, i_{\mathrm{D}-1})$ independently of all other entries according to the distribution $P_{X_k|V_{\mathrm{D}-1,k}}(\cdot|v_{\mathrm{D}-1,k,t}(i_{\mathrm{D}-1}|j, i_1, \ldots, i_{\mathrm{D}-2}))$. Here, $v_{\mathrm{D}-1,k,t}(i_{\mathrm{D}-1}|j, i_1, \ldots, i_{\mathrm{D}-2})$

denotes the t-th entry of codeword $v^n_{\mathrm{D}-1,k}(i_{\mathrm{D}-1}|j, i_1, \ldots, i_{\mathrm{D}-2})$. Reveal all codebooks to all terminals.

Encoding: Tx k sends codeword

$$x^n_k\big(M^{(S_{\mathrm{D}})}_k | M^{(F)}_k, \ldots, M^{(S_{\mathrm{D}-2})}_k, M^{(S_{\mathrm{D}-1})}_k\big)$$

Decoding: Each Rx k performs the following steps. Given that it observes $Y^n_k = y^n_k$, it first looks for a unique index $\hat{j}$ such that

$$(u^n_k(\hat{j}), y^n_k) \in T^{(n)}_\epsilon(P_{UY}). \tag{A.60}$$

If none or more than one such index $\hat{j}$ exist, Rx k declares an error. Otherwise, it declares $\hat{M}^{(F)}_k = \hat{j}$, and sends

$$Q^{(1)}_{k\to k+1} = \hat{j} \tag{A.61}$$

to its right neighbour, Rx $k+1$.

With the message $Q^{(1)}_{k-1\to k}$, Rx k obtains from its left-neighbour, it looks for an index $\hat{i_1}$ such that

$$\Big(u^n_k(\hat{j}), v^n_{1,k}(\hat{i}_1|\hat{j}), u^n_{k-1}(Q^{(1)}_{k-1\to k}), y^n_k\Big) \in T^{(n)}_\epsilon(P_{UV_1U'Y}). \tag{A.62}$$

If none or multiple such index $\hat{i}_1$ exist, Rx k declares an error. Otherwise, it declares $\hat{M}^{(S_1)}_k = \hat{i_1}$ and sends

$$Q^{(2)}_{k\to k+1} = \hat{i_1} \tag{A.63}$$

to its right neighbour, Rx $k+1$.

In conferencing round d with $d \in \{3, \ldots, \mathrm{D}-1\}$, Rx k obtains $Q^{(d)}_{k-1\to k}$ from its left-neighbour, and looks for an index $\hat{i}_d$

$$\begin{aligned}\Big(u^n_k(\hat{j}), v^n_{1,k}(\hat{i}_1|\hat{j}), \ldots, v^n_{d,k}(\hat{i}_d|\hat{j}, \hat{i}_1, \ldots, \hat{i}_{d-1}), u^n_{k-1}(Q^{(1)}_{k-1\to k}),\\ v^n_{1,k-1}(Q^{(2)}_{k-1\to k}), \ldots, v^n_{d-1,k-1}(Q^{(d)}_{k-1\to k}), y^n_k\Big) \in T^{(n)}_\epsilon(P_{UV_1\ldots V_dU'V'_1\ldots V'_dY}).\end{aligned} \tag{A.64}$$

If none or more than one such index $\hat{i}_d$ exist, an error is declared. Otherwise, Rx k declares $\hat{M}^{(S_\ell)}_k = \hat{i}_d$ and sends

$$Q^{(d)}_{k\to k+1} = \hat{i_d} \tag{A.65}$$

to its right neighbour, Rx $k+1$.

In conferencing round D, Rx k obtains $Q_{k-1\to k}^{(\mathrm{D}-1)}$ from its left-neighbour and looks for an index $\hat{\ell}$

$$\Big(u_k^n(\hat{j}), v_{1,k}^n(\hat{i}_1|\hat{j}), \ldots, v_{\mathrm{D}-1,k}^n(\hat{i}_{\mathrm{D}-1}|\hat{j}, \hat{i}_1, \ldots, \hat{i}_{\mathrm{D}-2}), x_k^n(\hat{i}_{\mathrm{D}}|\hat{j}, \hat{i}_1, \ldots, \hat{i}_{\mathrm{D}-1}), u_{k-1}^n(Q_{k-1\to k}^{(1)}),$$
$$v_{1,k-1}^n(Q_{k-1\to k}^{(2)}), \ldots, v_{\mathrm{D}-1,k-1}^n(Q_{k-1\to k}^{(\mathrm{D}-1)}), y_k^n\Big) \in T_\epsilon^{(n)}(P_{UV_1\ldots V_{\mathrm{D}-1}XU'V_1'\ldots V_{\mathrm{D}-1}'X'Y}). \tag{A.66}$$

If none or multiple such index $\hat{\ell}$ exist, an error is declared. Otherwise, Rx k declares $\hat{M}_k^{(S_\mathrm{D})} = \hat{\ell}$.

Analysis: Decoding in (A.60) is successful with probability tending to 1 as $n \to \infty$, if

$$R_k^{(F)} < I(U;Y) \tag{A.67}$$

Decoding in (A.62) is successful with probability tending to 1 as $n \to \infty$, if

$$R_k^{(S_1)} < I(V_1; Y, U'|U). \tag{A.68}$$

Decoding in (A.64) is successful with probability tending to 1 as $n \to \infty$, if

$$R_k^{(S_d)} < I(V_d; Y, V_{d-1}'|V_{d-1}), \qquad d \in \{2, \ldots, \mathrm{D}-1\}. \tag{A.69}$$

The last decoding step in (A.66) is successful with probability tending to 1 as $n \to \infty$, if

$$R_k^{(S_\mathrm{D})} < I(X; Y, X'|V_{\mathrm{D}-1}). \tag{A.70}$$

The conferencing constraint is satisfied by (A.55). Apply Fourier-Motzkin elimination to (A.55), (A.67), (A.68),(A.69) and (A.70). Achievability of the pairs (4.18) follows then by a rate-transfer argument.

A.2 Proofs of Chapter 5

A.2.1 Coding Scheme and Analysis in the Hexagonal Model

In this appendix we prove that the Tx/Rx set associations proposed in Subsection 5.3.2 are permissible and we provide details on how to compute the corresponding MG pairs and cooperation prelogs.

No Cooperation Scheme

Fig. 5.5a shows the active Txs in yellow and the silenced Txs in white. It is easily seen that transmissions in yellow cells do not interfere, as they pertain to non-neighbouring cells.

More formally, we consider two different Txs k and k' in the active set $\mathcal{T}_{\text{active}}$ defined in (5.60), and we prove by contradiction that Tx k' cannot be in the neighbouring set $\mathcal{I}_{\text{Tx},k}$ of Tx k. Assume that $k' \in \mathcal{I}_{\text{Tx},k}$. Then, by (5.58), either $(a_{k'} = a_k + 1, b_{k'} = b_k + 1)$ or $(a_{k'} = a_k - 1, b_{k'} = b_k - 1)$. Each of these two cases however violates the active set condition (5.60), which implies

$$(a_k + b_k) \mod 3 = 0 \quad \text{and} \quad (a_{k'} + b_{k'}) \mod 3 = 0. \tag{A.71}$$

We thus obtained the desired contradiction.

To see that the scheme achieves a sum-MG of $\mathsf{S}_{\text{no-coop}}$ we notice that in the limit as $K \to \infty$, the active set $\mathcal{T}_{\text{active}}$ defined in (5.60) includes a third of all Txs simply because a third of the integer pairs (a, b) satisfy $(a + b) \mod 3 = 0$ and because for each integer pair (a, b) there corresponds a Tx.

Coding scheme to transmit only "slow" messages with CoMP reception or transmission

As mentioned in the main body, and as is easily seen in Figure 5.5b, the silenced set $\mathcal{T}_{\text{silent}}$ consists of all cells that are exactly $\frac{\mathrm{D}}{2} + 1$ cell hops away from the next master cell. All other cells have a master cell that lies less than $\frac{\mathrm{D}}{2} + 1$ cell hops away. In other words, each master cell is surrounded by $\mathrm{D}/2$ layers of active cells sending "slow" messages, where in total these $\mathrm{D}/2$ layers contain $\sum_{i=1}^{\mathrm{D}/2} 6i = \frac{3}{4}\mathrm{D}(\mathrm{D}+2)$ cells. Such a subnet is then surrounded by a layer of $6 \cdot (\frac{\mathrm{D}}{2} + 1) = 3\mathrm{D} + 6$ silenced cells, each lying $\mathrm{D}/2 + 1$ cell hops away from the master cell. Among these layer-$(\mathrm{D}/2 + 1)$ cells, 6 of them (namely the corner cells) belong to the silenced layer of three different master cells, and the remaining 3D belong to the silenced layer of two master cells.

By these considerations, and because master cells themselves also send "slow" messages,

$$\lim_{K\to\infty} \frac{|\mathcal{T}_{\text{slow}}|}{K} = \frac{1 + \frac{3}{4}\mathrm{D}(\mathrm{D}+2)}{\frac{3}{4}(\mathrm{D}+2)^2} = \frac{4 + 3\mathrm{D}(\mathrm{D}+2)}{3(\mathrm{D}+2)^2}, \tag{A.72}$$

and as a result, by (5.14) and (5.15), the proposed cell association achieves the MG pair $(\mathsf{S}^{(F)} = 0, \mathsf{S}^{(S)} = \mathsf{S}^{(S)}_{\max})$ with $\mathsf{S}^{(S)}_{\max}$ defined in (5.65).

With CoMP reception, the scheme does not send any Tx-cooperation messages but only Rx-cooperation

messages. To calculate the Rx-cooperation prelog, notice that for each Rx k we have $\gamma_{\mathrm{Rx},k} = i \in \{1,\dots,\mathrm{D}/2\}$ if Rx k lies i hops away from the next master cell. Since in a given subnet $\mathcal{T}_{\text{subnet}}$ formed by a master cell and its surrounding $\tau-1$ layers, there are $6i$ Rxs with $\gamma_{\mathrm{Rx},k}=i$, for each $i=1,\dots,\mathrm{D}/2$:

$$2\sum_{k\in\mathcal{T}_{\text{subnet}}}\gamma_{\mathrm{Rx},k} = 2\sum_{i=1}^{\mathrm{D}/2} 6i^2 = \frac{\mathrm{D}(\mathrm{D}+2)(\mathrm{D}+1)}{2}, \tag{A.73}$$

and by similar considerations as leading to (A.72):

$$\lim_{K\to\infty}\frac{2\sum_{k\in\mathcal{T}_{\text{slow}}}\gamma_{\mathrm{Rx},k}}{K} = \frac{\mathrm{D}(\mathrm{D}+2)(\mathrm{D}+1)/2}{\frac{3}{4}(\mathrm{D}+2)^2} = \frac{2\mathrm{D}(\mathrm{D}+1)}{3(\mathrm{D}+2)}. \tag{A.74}$$

Since $\lim_{K\to\infty}\frac{\mathcal{Q}_{K,\mathrm{Rx}}}{K}=6$, according to (5.16) the required Rx-cooperation prelog equals

$$\mu^{(\mathrm{r})}_{\mathrm{Rx},\mathsf{S}} = \mathsf{L}\cdot\frac{\mathrm{D}(\mathrm{D}+1)}{9(\mathrm{D}+2)}. \tag{A.75}$$

With CoMP transmission, this scheme does not require any Rx-cooperation messages and consumes a Tx-cooperation prelog of $\mu^{(\mathrm{t})}_{\mathrm{Tx},\mathsf{S}} = \mu^{(\mathrm{r})}_{\mathrm{Rx},\mathsf{S}}$.

Coding Scheme to transmit both "fast" and "slow" messages with CoMP reception

Notice that the set of silenced cells $\mathcal{T}_{\text{silent}}$ here coincides with the set of silenced cells $\mathcal{T}_{\text{silent}}$ for the scheme sending only "slow" messages when $\mathrm{D}'=\mathrm{D}-2$ cooperation rounds are permitted.

We next determine the fraction of "fast" versus "slow" Txs. To this end, notice that the fraction is the same in each subnet, so we only consider the subnet containing the $\mathrm{D}/2-1$ layers around the master cell situated at the origin. This subnet is characterized by

$$\mathcal{T}_{\text{subnet}\mathbf{0}} = \left\{k\colon \max\{|a_k|,|b_k|,|a_k-b_k|\} < \frac{\mathrm{D}}{2}-1\right\} \tag{A.76}$$

It can be shown that by Assumption (5.59), the number of "fast" Txs in subnet $\mathcal{T}_{\text{subnet}\mathbf{0}}$ equals

$$|\mathcal{T}_{\text{fast}}\cap\mathcal{T}_{\text{subnet}\mathbf{0}}| = \frac{\mathrm{D}^2}{4}-\frac{\mathrm{D}}{2}+1, \tag{A.77}$$

and the number of "slow" Txs in $\mathcal{T}_{\text{subnet}\mathbf{0}}$ equals

$$|\mathcal{T}_{\text{slow}} \cap \mathcal{T}_{\text{subnet}\mathbf{0}}| = \frac{\mathrm{D}^2}{2} - \mathrm{D}. \tag{A.78}$$

By similar considerations as leading to (A.72) (but where D needs to be replaced by $\mathrm{D}-2$), we then obtain that

$$\lim_{K\to\infty} \frac{|\mathcal{T}_{\text{fast}}|}{K} = \frac{\frac{\mathrm{D}^2}{4} - \frac{\mathrm{D}}{2} + 1}{\frac{3\mathrm{D}^2}{4}} = \frac{\mathrm{D}^2 - 2\mathrm{D} + 4}{3\mathrm{D}^2} \tag{A.79}$$

and

$$\lim_{K\to\infty} \frac{|\mathcal{T}_{\text{slow}}|}{K} = \frac{\frac{\mathrm{D}^2}{2} - \mathrm{D}}{\frac{3\mathrm{D}^2}{4}} = \frac{2\mathrm{D}^2 - 4\mathrm{D}}{3\mathrm{D}^2} \tag{A.80}$$

This establishes the achievability of the MG pair (5.67).

We analyze the required cooperation prelog of the described scheme. As in the previous subsection, $\gamma_{\text{Tx},k} = \gamma_{\text{Rx},k} = i$ for every Tx/Rx k that lies i cell hops away from its next master cell, for $i = 1, \ldots, \mathrm{D}/2-1$. Moreover, for each "fast" Tx k with $\gamma_{\text{Tx},k} \in \{1, \ldots, \mathrm{D}/2 - 2\}$ the size of the "slow" interfering set $\mathcal{I}_k^{(S)}$ is equal to 6, and when $\gamma_{\text{Tx},k} = \mathrm{D}/2 - 1$ the size of this set is equal to 3 for the corner "fast"-Txs and is equal to 4 for the other "fast"-Txs of this layer. To calculate the average cooperation prelog, it is required to calculate the number of "fast"-Txs each with $\gamma_{\text{Tx},k} = i$. We can prove that for each $i \in \{1, \ldots, \frac{\mathrm{D}}{2} - 1\}$:

$$|\{k \in \mathcal{T}_{\text{fast}} \cap \mathcal{T}_{\text{subnet}\mathbf{0}} : \gamma_{\text{Tx},k} = i\}| = 6\left(\frac{(2i-1) - \mod(2i-1,3)}{3} - \frac{i + \mod(3 - \mod(i,3),3)}{3} + 1\right). \tag{A.81}$$

By the above argument and Assumption (5.59), thus the number of "fast"-Txs each with $\gamma_{\text{Tx},k} = \frac{\mathrm{D}}{2} - 1$ is

$$\left|\left\{k \in \mathcal{T}_{\text{fast}} \cap \mathcal{T}_{\text{subnet}\mathbf{0}} : \gamma_{\text{Tx},k} = \frac{\mathrm{D}}{2} - 1\right\}\right| = \mathrm{D} - 2. \tag{A.82}$$

By (A.77) and (A.82), we have

$$\left|\left\{k \in \mathcal{T}_{\text{fast}} \cap \mathcal{T}_{\text{subnet}\mathbf{0}} : \gamma_{\text{Tx},k} \neq \frac{\mathrm{D}}{2} - 1\right\}\right| = \frac{\mathrm{D}^2}{4} - \frac{\mathrm{D}}{2} + 1 - (\mathrm{D} - 2) = \frac{\mathrm{D}^2 - 6\mathrm{D} + 12}{4} \tag{A.83}$$

We can then conclude that

$$\sum_{k\in\mathcal{T}_{\text{fast}}\cap\mathcal{T}_{\text{subnet}0}} |\mathcal{I}_k^{(S)}| = \sum_{\substack{k\in\mathcal{T}_{\text{fast}}\cap\mathcal{T}_{\text{subnet}0} \\ \gamma_{\text{Tx},k}\neq\frac{\mathrm{D}}{2}-1}} |\mathcal{I}_k^{(S)}| + \sum_{\substack{k\in\mathcal{T}_{\text{fast}}\cap\mathcal{T}_{\text{subnet}0} \\ \gamma_{\text{Tx},k}=\frac{\mathrm{D}}{2}-1}} |\mathcal{I}_k^{(S)}|$$

$$= 6\left(\frac{\mathrm{D}^2-6\mathrm{D}+12}{4}\right)+4(\mathrm{D}-8)+18=\frac{(\mathrm{D}-2)(3\mathrm{D}-4)}{2}. \tag{A.84}$$

According to (5.9), the Tx-cooperation prelog required for the scheme is

$$\mu^{(\mathrm{r})}_{\mathrm{Tx,both}}=\mathsf{L}\cdot\frac{(\mathrm{D}-2)(3\mathrm{D}-4)}{9\mathrm{D}^2}. \tag{A.85}$$

Notice next that for each "slow" Tx k with $\gamma_{\mathrm{Rx},k}\in\{1,\ldots,\mathrm{D}/2-2\}$ the "fast" interfering set $\mathcal{I}_k^{(F)}$ is of size 3, and for each "slow" Tx k with $\gamma_{\mathrm{Rx},k}=\mathrm{D}/2-1$ it is of size 2. Notice that, since the total number of Rxs with $\gamma_{\mathrm{Rx},k}=i$ is equal to $6i$, then by the RHS of (A.81), we can conclude that

$$|\{k\in\mathcal{T}_{\mathrm{slow}}\cap\mathcal{T}_{\mathrm{subnet}\mathbf{0}}:\gamma_{\mathrm{Rx},k}=i\}|=2\left(2i-2+\mod(2i-1,3)+\mod(3-\mod(i,3),3)\right). \tag{A.86}$$

We thus have:

$$\sum_{k\in\mathcal{T}_{\mathrm{slow}}\cap\mathcal{T}_{\mathrm{subnet}\mathbf{0}}}\left(|\mathcal{I}_k^{(F)}|+2\gamma_{\mathrm{Rx},k}\right) \tag{A.87}$$

$$\begin{aligned}&=\sum_{\substack{k\in\mathcal{T}_{\mathrm{slow}}\cap\mathcal{T}_{\mathrm{subnet}0}\\ \gamma_{\mathrm{Rx},k}\neq\frac{\mathrm{D}}{2}-1}}|\mathcal{I}_k^{(S)}|+\sum_{\substack{k\in\mathcal{T}_{\mathrm{slow}}\cap\mathcal{T}_{\mathrm{subnet}0}\\ \gamma_{\mathrm{Rx},k}=\frac{\mathrm{D}}{2}-1}}|\mathcal{I}_k^{(S)}|+2\sum_{i=1}^{\frac{\mathrm{D}}{2}-1}i\times|\{k\in\mathcal{T}_{\mathrm{slow}}\cap\mathcal{T}_{\mathrm{subnet}\mathbf{0}}:\gamma_{\mathrm{Rx},k}=i\}|\\ &=+3\left(\frac{\mathrm{D}^2}{2}-3\mathrm{D}+4\right)+2\times4\left(\frac{\mathrm{D}}{2}-1\right)+6+2\sum_{i=1}^{\frac{\mathrm{D}}{2}-1}i\left(4i-\mod(i,3)\right)\\ &=\frac{4\mathrm{D}^3+3\mathrm{D}^2-42\mathrm{D}+112}{12}.\end{aligned} \tag{A.88}$$

Thus according to (5.10), the average Rx-cooperation prelog required by the scheme is

$$\mu^{(\mathrm{r})}_{\mathrm{Rx,both}}=\mathsf{L}\cdot\frac{4\mathrm{D}^3+3\mathrm{D}^2-42\mathrm{D}+112}{54\mathrm{D}^2}. \tag{A.89}$$

Coding scheme to transmit both "fast" and "slow" messages with CoMP transmission

We choose the same cell association as in the previous subsection.

To analyze the cooperation prelog, notice that because we chose the same cell association as for the scheme with CoMP reception, the parameters $\gamma_{\mathrm{Tx},k}=\gamma_{\mathrm{Rx},k}$ and the single-round Rx-cooperation prelog coincides with the single-round Tx-cooperation prelog in the previous scheme of Subsection A.2.1, i.e., $\mu^{(\mathrm{t})}_{\mathrm{Rx,both}}=\mu^{(\mathrm{r})}_{\mathrm{Tx,both}}$. To calculate the average Tx-cooperation prelog, we first consider the q-term in (5.13),

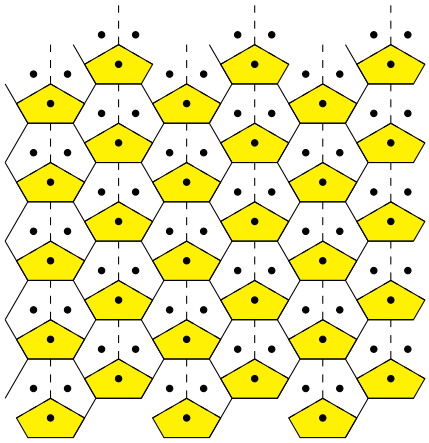

Figure A.1: Illustration of the scheme without cooperation in the sectorized hexagonal network.

which characterizes the number of quantization messages describing the “slow" signals that are counted twice: once for the CoMP transmission and once for the interference mitigation at “fast" Txs. Since the master Tx is a “fast”-Tx, then 6 such messages are counted twice and also for each “fast”-Tx k with $\gamma_{\mathrm{Tx},k} \in \{1, \ldots, \frac{\mathrm{D}}{2} - 2\}$, 2 messages are double-counted. Therefore,

$$q = 6 + 2\left(\frac{\mathrm{D}^2 - 6\mathrm{D} + 12}{4} - 1\right) = \frac{\mathrm{D}^2}{2} - 3\mathrm{D} + 10. \tag{A.90}$$

We then conclude that

$$\sum_{k \in \mathcal{T}_{\mathrm{slow}} \cap \mathcal{T}_{\mathrm{subnet}\mathbf{0}}} 2\gamma_{\mathrm{Tx},k} + \sum_{k \in \mathcal{T}_{\mathrm{fast}} \cap \mathcal{T}_{\mathrm{subnet}\mathbf{0}}} |\mathcal{I}_k^{(S)}| - q = \frac{4\mathrm{D}^3 - 3\mathrm{D}^2 - 6\mathrm{D} - 8}{12}. \tag{A.91}$$

Thus, according to (5.13), the average Tx-cooperation prelog required by the scheme is

$$\mu_{\mathrm{Tx,both}}^{(\mathrm{t})} = \mathsf{L} \cdot \frac{4\mathrm{D}^3 - 3\mathrm{D}^2 - 6\mathrm{D} - 8}{54\mathrm{D}^2}. \tag{A.92}$$

A.2.2 Coding Schemes and Analysis in the Sectorized Hexagonal Model

In this appendix we prove that the Tx/Rx set associations proposed in Subsection 5.4.2 are permissible and we provide details on how to compute the corresponding MG pairs and cooperation prelogs.

No cooperation scheme

Figure A.1 shows the active Txs in yellow and the silenced Txs in white. It is easily seen that transmissions in yellow sectors do not interfere, as they pertain to non-neighbouring sectors. This scheme requires no

cooperation messages and achieves the sum MG in (5.79).

Coding scheme to transmit only "slow" messages with CoMP reception

To transmit only "slow" messages we use the scheme proposed in Subsection 5.1.3. See the cell association of this network in Fig. 5.9 for D = 4 where Txs in white sectors are deactivated, Txs in yellow or blue sectors send "slow" messages. As can be seen from this figure, the master cell of each subnet (the center cell) is surrounded by $\mathrm{D}/2-1$ fully active layers of cells and one semi-active layer of cells. Each semi-active layer consists of 3 fully active corner cells, 3 fully deactivated corner cells and $3\mathrm{D}-6$ non-corner cells of one deactivated sector and 2 active sectors. Notice that corner cells are shared among three master cells and non-corner cells are shared between two master cells. Thus in order to create subnets of $3+3\sum_{i=1}^{\mathrm{D}/2-1} 6i+(3\mathrm{D}-3) = 9\mathrm{D}^2/4-3\mathrm{D}/2$ active sectors, we need to deactivate $(3\mathrm{D}-6)/2+9/3 = 3\mathrm{D}/2$ sectors per subnet.

By these considerations

$$\lim_{K\to\infty}\frac{|\mathcal{T}_{\text{slow}}|}{K} = \frac{9\mathrm{D}^2/4-3\mathrm{D}/2}{9\mathrm{D}^2/4} = \frac{3\mathrm{D}-2}{3\mathrm{D}}, \tag{A.93}$$

and as a result, by (5.14) and (5.15), the proposed cell association achieves the MG pair $(\mathsf{S}^{(F)}=0, \mathsf{S}^{(S)}=\mathsf{S}^{(S)}_{\max})$ with $\mathsf{S}^{(S)}_{\max}$ defined in (5.80).

With CoMP reception, this scheme does not use any Tx-cooperation messages and for each Rx k, $\gamma_{\mathrm{Rx},k}$ takes values over the set $\{1,\ldots,\mathrm{D}/2\}$. Thus in a given subnet $\mathcal{T}_{\text{subnet}}$ formed by a master cell and its surrounding $\frac{\mathrm{D}}{2}$ layers, there are $6i$ Rxs with $\gamma_{\mathrm{Rx},k}=i$, where if $i\in\{1,\ldots\frac{\mathrm{D}}{2}-1\}$ these $6i$ Rxs send in total $18i$ Rx-cooperation messages to the next master Rx, and if $i=\frac{\mathrm{D}}{2}$, they send $3\mathrm{D}-3$ Rx-cooperation messages to the mater Rx. We thus conclude that

$$2\sum_{k\in\mathcal{T}_{\text{subnet}}}\gamma_{\mathrm{Rx},k} = 2\times 3\sum_{i=1}^{\mathrm{D}/2-1} 6i^2+\mathrm{D}(3\mathrm{D}-3) = \frac{3\mathrm{D}^2(\mathrm{D}-1)}{2}. \tag{A.94}$$

and by similar considerations as leading to (A.93):

$$\lim_{K\to\infty}\frac{2\sum_{k\in\mathcal{T}_{\text{slow}}}\gamma_{\mathrm{Rx},k}}{K} = \frac{(3\mathrm{D}^2(\mathrm{D}-1))/2}{\frac{3\mathrm{D}^2}{4}} = 2(\mathrm{D}-1). \tag{A.95}$$

Since $\lim_{K\to\infty}\frac{\mathcal{Q}_{K,\mathrm{Rx}}}{K}=6$, according to (5.16) the required Rx-cooperation prelog equals

$$\mu^{(\mathrm{r})}_{\mathrm{Rx},\mathsf{S}} = \mathsf{L}\cdot\frac{(\mathrm{D}-1)}{3}. \tag{A.96}$$

Coding scheme to transmit both "fast" and "slow" messages with CoMP reception

See the cell association of this network in Fig. 5.9 for D = 4 and in Fig. 5.10 for D = 8 where Txs in white sectors are deactivated, Txs in yellow sectors send "fast" messages and Txs in blue sectors send "slow" messages. We next determine the fraction of "fast" versus "slow" Txs. To this end, notice that the fraction is the same in each subnet. In each layer-i with $i \in \{1, \ldots, \frac{\mathrm{D}}{2}\}$, of a given subnet $\mathcal{T}_{\text{subnet}}$, each non-corner cell has 1 "fast" sector whereas among the 6 corner cells only three of them have 1 "fast" sector each. Thus the number of "fast" Txs in subnet $\mathcal{T}_{\text{subnet}}$ equals

$$|\mathcal{T}_{\text{fast}} \cap \mathcal{T}_{\text{subnet}}| = \sum_{i=1}^{\frac{\mathrm{D}}{2}} (6i - 3) = \frac{3\mathrm{D}^2}{4}, \tag{A.97}$$

and the number of "slow" Txs in this subnet equals

$$|\mathcal{T}_{\text{fast}} \cap \mathcal{T}_{\text{subnet}}| = \frac{6\mathrm{D}^2}{4} - \frac{3\mathrm{D}}{2}. \tag{A.98}$$

By similar considerations as leading to (A.93), we then obtain that

$$\lim_{K \to \infty} \frac{|\mathcal{T}_{\text{fast}}|}{K} = \frac{\frac{3\mathrm{D}^2}{4}}{\frac{9\mathrm{D}^2}{4}} = \frac{1}{3} \tag{A.99}$$

and

$$\lim_{K \to \infty} \frac{|\mathcal{T}_{\text{slow}}|}{K} = \frac{\frac{6\mathrm{D}^2}{4} - \frac{3\mathrm{D}}{2}}{\frac{9\mathrm{D}^2}{4}} = \frac{2\mathrm{D} - 2}{3\mathrm{D}}. \tag{A.100}$$

This establishes the achievability of the MG pair (5.82).

To analyze the cooperation prelog of the described scheme, Figure 5.10 shows that for each "fast" Tx/Rx k with $\gamma_{\text{Rx},k} \in \{1, \ldots, \mathrm{D}/2 - 1\}$ the size of the "slow" interfering set $\mathcal{I}_k^{(S)}$ is equal to 4, and when $\gamma_{\text{Rx},k} = \mathrm{D}/2$ the size of this set is equal to 2 for the three of the corner "fast" Txs and is equal to 3 for the others. Considering the fact that the number of "fast" Txs with $\gamma_{\text{Rx},k} = \frac{\mathrm{D}}{2}$ equals $3\mathrm{D} - 3$, we thus conclude that

$$\sum_{k \in \mathcal{T}_{\text{fast}} \cap \mathcal{T}_{\text{subnet}}} |\mathcal{I}_k^{(S)}| = 4\left(\frac{3\mathrm{D}^2}{4} - (3\mathrm{D} - 3)\right) + 3 \times 2 + 3(3\mathrm{D} - 6) = 3\mathrm{D}(\mathrm{D} - 1). \tag{A.101}$$

According to (5.9), the average Tx-cooperation prelog required for the scheme is

$$\mu^{(\mathrm{r})}_{\mathrm{Tx,both}} = \mathsf{L} \cdot \frac{(\mathrm{D}-1)}{9\mathrm{D}}. \tag{A.102}$$

Fig. 5.10 also shows that the size of the "fast" interference set $\mathcal{I}_k^{(F)}$ is equal to 2 for each "slow" Tx k.We thus conclude that

$$\sum_{k\in\mathcal{T}_{\mathrm{slow}}\cap\mathcal{T}_{\mathrm{subnet}}} |\mathcal{I}_k^{(F)}| + 2\gamma_{\mathrm{Rx},k} = 6\mathrm{D} - 9 + 3\sum_{i=1}^{\frac{\mathrm{D}}{2}-1}(6i-3) + 4\sum_{i=1}^{\frac{\mathrm{D}}{2}-1} i(6i-3) + 6\sum_{i=1}^{\frac{\mathrm{D}}{2}-1} 3i \tag{A.103}$$

$$= \frac{\mathrm{D}(2\mathrm{D}^2-5)}{2}. \tag{A.104}$$

Thus according to (5.10), the average Rx-cooperation prelog required by the scheme is

$$\mu^{(\mathrm{r})}_{\mathrm{Rx,both}} = \mathsf{L} \cdot \frac{2\mathrm{D}^2-5}{9\mathrm{D}}. \tag{A.105}$$

A.3 Proofs of Chapter 6

A.3.1 Proof of the Converse to Theorem 9

Fix K and realizations of the sets $\mathcal{T}_{\mathrm{active}}$ and $\mathcal{T}_{\mathrm{fast}}$. Following the steps in (A.2) in Appendix A.1.1, we prove that for each $k \in \mathcal{T}_{\mathrm{active}}$:

$$\begin{aligned} R_k^{(F)} + R_k^{(S)} + R_{k+1}^{(F)} & \\ &\le \frac{1}{2}\log(1+(1+|h_{k,k+1}|^2)\mathsf{P}) + \frac{1}{2}\log(1+|h_{k,k+1}|^2) \\ &\quad + \max\{-\log|h_{k,k+1}|, 0\} + \frac{\epsilon_n}{n}, \end{aligned} \tag{A.106}$$

where $R_{k+1}^{(F)}$ is the rate of the "fast" message at Rx $k+1$, which is either 0 or equal to $R^{(F)}$. For simplicity, we abbreviate the RHS of (A.106) by Δ, and we sum up this bound for all values of $k \in \mathcal{T}_{\mathrm{active}}$:

$$\sum_{k\in\mathcal{T}_{\mathrm{active}}} \left(R_k^{(F)} + R_k^{(S)} + R_{k+1}^{(F)}\right) \le |\mathcal{T}_{\mathrm{active}}| \cdot \Delta. \tag{A.107}$$

Taking expectation over (A.106) and dividing by K, we obtain:

$$\mathbb{E}[\bar{R}^{(S)}] + R^{(F)}(\rho\rho_f + \rho^2\rho_f) \leq \rho \cdot \Delta, \tag{A.108}$$

because the expected number of indices $k \in \mathcal{T}_{\text{active}}$ for which $R_k^{(F)} = R^{(F)}$ equals $\rho \cdot \rho_f$ and the expected numbers of indices $k \in \mathcal{T}_{\text{active}}$ for which $R_{k+1}^{(F)} = R^{(F)}$ equals $\rho^2 \cdot \rho_f$. Dividing by $\frac{1}{2}\log \mathsf{P}$ and letting $\mathsf{P} \to \infty$ proves (6.21).

A.3.2 Proof of the Converse to Theorem 10

Fix K and realizations of the sets $\mathcal{T}_{\text{slow}}$ and $\mathcal{T}_{\text{fast}}$. Following the steps in (A.2) in Appendix A.1.1, we can prove that for each $k \in \mathcal{T}_{\text{slow}}$:

$$R_k^{(S)} + R_{k+1}^{(F)} \leq \frac{1}{2}\log(1 + (1 + |h|^2)\mathsf{P}) + \frac{1}{2}\log(1 + |h|^2) + \max\{-\log|h|, 0\} + \frac{\epsilon_n}{n}, \tag{A.109}$$

where $R_{k+1}^{(F)}$ is the rate of the "fast" messages at Rx $k+1$, which is either 0 or equal to $R^{(F)}$. For simplicity, we abbreviate the RHS of (A.109) by $\tilde{\Delta}$, and we sum up this bound for all values of $k \in \mathcal{T}_{\text{slow}}$:

$$\sum_{k \in \mathcal{T}_{\text{slow}}} \left(R_k^{(S)} + R_{k+1}^{(F)}\right) \leq |\mathcal{T}_{\text{slow}}| \cdot \tilde{\Delta}. \tag{A.110}$$

Equivalently:

$$K\bar{R}^{(S)} + \sum_{\substack{k \in \mathcal{T}_{\text{slow}} \\ k+1 \in \mathcal{T}_{\text{fast}}}} R^{(F)} \leq |\mathcal{T}_{\text{slow}}| \cdot \tilde{\Delta} \tag{A.111}$$

Taking expectation over (A.111) and dividing by K, we obtain:

$$\mathbb{E}[\bar{R}^{(S)}] + R^{(F)}\left(\rho^2\rho_f(1-\rho_f)\right) \leq \rho(1-\rho_f) \cdot \tilde{\Delta}. \tag{A.112}$$

Dividing by $\frac{1}{2}\log \mathsf{P}$ and letting $\mathsf{P} \to \infty$ proves (6.36).

Bibliography

[1] R. Zhang, "Optimal dynamic resource allocation for multi-antenna broadcasting with heterogeneous delay-constrained traffic," *IEEE J. of Sel. Topics in Signal Proc.*, vol. 2, no. 2, pp. 243–255, Apr. 2008.

[2] K. M. Cohen, A. Steiner, and S. Shamai (Shitz), "The broadcast approach under mixed delay constraints," in *Proc. IEEE ISIT 2012*, Cambridge (MA), USA, July 1–6, pp. 209–213, 2012.

[3] K. M. Cohen, A. Steiner, and S. Shamai (Shitz), "Broadcasting with mixed delay demands", in *Proc.IEEE Conv. Electrical and Electronics Engineers in Israel*, Nov. 2012.

[4] R. Zhang, J. Cioffi, and Y.-C. Liang, "MIMO broadcasting with delay-constrained and no-delay-constrained services," in *Proc. IEEE ICC 2005*, Seoul, South Korea, May 16–20, pp. 783–787, 2005.

[5] R. Kassab, O. Simeone and P. Popovski, "Coexistence of URLLC and eMBB services in the C-RAN uplink: an information-theoretic study," in *Proc. IEEE GLOBECOM*, Abu Dhabi, United Arab Emirates, Dec 9–13, 2018.

[6] A. Matera, R. Kassab, O. Simeone and U. Spagnolini, "Non-orthogonal eMBB-URLLC radio access for cloud radio access networks with analog fronthauling," *Entropy*, vol. 20, no. 9, pp. 661, 2018.

[7] A. Anand, G.d. Veciana and S. Shakkottai, "Joint scheduling of URLLC and eMBB traffic in 5G wireless networks," *IEEE/ACM Trans. on Networking*, vol. 28, no. 2, pp. 477–490, Apr. 2020.

[8] H. Nikbakht, M. Wigger and S. Shamai (Shitz), "Mixed Delay Constraints in Wyner's Soft-Handoff Network", *IEEE International Symposium on Information Theory (ISIT)*, 2018, Vail, CO, USA, 17-22 June, pp. 1171 –1175.

[9] H. Nikbakht, M. Wigger and S. Shamai (Shitz), " Mixed delay constraints at maximum sum-multiplexing gain," in *Proc. IEEE ITW 2018*, Guangzhou, China, Nov 25–29, 2018, pp. 285–289.

[10] H. Nikbakht, M. Wigger and S. Shamai (Shitz), " Multiplexing gain region of sectorized cellular networks with mixed delay constraints," in *Proc. IEEE SPAWC 2019*, Cannes, France, 2–5 July 2019.

[11] H. Nikbakht, M. Wigger and S. Shamai (Shitz), 'Multiplexing gains under mixed-delay constraints on Wyner's soft-handoff model," *Entropy*, vol. 22, no. 2, pp. 182, 2020.

[12] H. Nikbakht, M. Wigger and S. Shamai (Shitz), " Random user activity with mixed delay traffic," submitted in *Proc. IEEE ITW 2020.*

[13] O. Somekh, O. Simeone, H. V. Poor and S. Shamai (Shitz), "The two-tap input-earasure Gaussian channel and its application to cellular communications," in *Proc. Allerton Conference on Communication, Control, and Computing*, IL, USA, Sep 23–26, 2008.

[14] N. Levy and S. Shamai (Shitz), "Information theoretic aspects of users' activity in a Wyner-like cellular model," *IEEE Trans. on Info. Theory*, vol 56, pp. 2241–2248, Apr. 2010.

[15] O. Somekh, O. Simeone, H. V. Poor and S. Shamai (Shitz), "Throughput of cellular uplink with dynamic user activity and cooperative base-stations," in *Proc. IEEE ITW 2019*, Taormina, Italy , Oct 11–16, 2009.

[16] A. D. Wyner, "Shannon-theoretic approach to a Gaussian cellular multiple-access channel," *IEEE Trans. Inf. Theory*, vol. 40, no. 6, pp. 1713–1727, Nov. 1994.

[17] S. V. Hanly and P. A. Whiting, "Information-theoretic capacity of multi-receiver networks," *Telecommunication Systems*, vol. 1, pp. 1–42, 1993.

[18] O. Simeone, N. Levy, A. Sanderovich, O. Somekh, B. M. Zaidel, H. V. Poor and S. Shamai (Shitz), "Cooperative wireless cellular systems: an information-theoretic view," *Found. and Trends in Comm. and Inf. Theory (FnT),* Vol. 8, no. 1–2, 2011, pp. 1–177, Now Publishers, 2012.

[19] H. Nikbakht, M. Wigger, W. Hachem and S. Shamai (Shitz), " Mixed delay constraints on a fading C-RAN uplink," in *Proc. IEEE ITW 2019*, Visby, Sweden, Aug 25–28, 2019.

[20] C. E. Shannon, "A mathematical theory of communication," in *The Bell System Technical Journal*, vol. 27, no. 3, pp. 379–423, July 1948,

[21] V. V. Veeravalli and A. El Gamal, "Interference management in wireless networks: Fundamental bounds and the role of cooperation", *Cambridge University Press*, 2018.

[22] R. Etkin, D. Tse and H. Wang, "Gaussian interference channel capacity to within one bit", *IEEE Trans. Inf. Theory*, vol. 54, no. 12, pp. 5534 –5562, Dec. 2008.

[23] X. Shang, G. Kramer, and B. Chen, "A new outer bound and the noisy-interference sum-rate capacity for Gaussian interference channels," *IEEE Trans. Inf. Theory*, vol. 55, no. 2, pp. 689–699, Feb. 2009.

[24] V. Annapureddy and V. Veeravalli, "Gaussian interference networks: Sum capacity in the low interference regime and new outer bounds on the capacity region," *IEEE Trans. Inf. Theory*, vol. 55, no. 7, pp. 3032–3050, Jul. 2009.

[25] A. B. Carleial, "A case where interference does not reduce capacity," *IEEE Trans. Inf. Theory*, vol. 21, pp. 569–570, 1975.

[26] S. A. Jafar, "Interference alignment a new look at signal dimensions in a communication network," *Found. and Trends in Com. and Inf. Theory*, vol. 7, no. 1, pp. 1–134, 2011.

[27] V. Cadambe and S. A. Jafar, "Interference alignment and degrees of freedom of the K-user interference channel", *IEEE Trans. Inf. Theory*, vol. 54, no. 8, pp. 3425–3441, Aug. 2008.

[28] F. Willems, "The discrete memoryless multiple access channel with partially cooperating encoders (corresp.)," *IEEE Trans. Inf. Theory,* vol. 29, no. 3, pp. 441–445, May 1983.

[29] A. Sendonaris, E. Erkip and B. Aazhang, "User cooperation diversity, part I: System description," *IEEE Trans. on Commun.*, vol. 51, no. 11, pp. 1927–1938, Nov 2003.

[30] A. Sendonaris, E. Erkip and B. Aazhang, "User cooperation diversity, part II: Implementation aspects and performance analysis," *IEEE Trans. on Commun.*, vol. 51, no. 11, pp. 1939–1948, Nov 2003.

[31] M. Costa, "Writing on dirty paper (Corresp.)," in *IEEE Trans. Inf. Theory*, vol. 29, no. 3, pp. 439–441, May 1983.

[32] K. Balachandran, J. H. Kang, K. Karakayali, and K . M. Rege, "NICE: A network interference cancellation engine for opportunistic uplink cooperation in wireless networks," *IEEE Trans. Wireless Commun.*, vol. 10, no. 2, pp. 540–549, Feb. 2011.

[33] S. Verdu, "The capacity region of the symbol-asynchronous Gaussian multiple-access channel," *IEEE Trans. Inf. Theory*, vol. 35, no. 4, pp. 733–751, Jul. 1989.

[34] E. Aktas, J. Evans and S. Hanly, "Distributed decoding in a cellular multiple-access channel," *IEEE Trans. Wireless Commun.*, vol. 7, no. 1, pp. 241–250, Jan 2008.

[35] S. I. Bross, A. Lapidoth and M. A. Wigger, "The gaussian MAC with conferencing encoders," in *Proc. IEEE ISIT 2008*, Toronto, ON, Canada, pp. 2702–2706, July 2008.

[36] H. Weingarten, Y. Steinberg, and S. Shamai, "The capacity region of the Gaussian multiple-input multiple-output broadcast channel," *IEEE Trans. Inf. Theory*, vol. 52, no. 9, pp. 3936–3964, Sept. 2006.

[37] U. Erez, S. Shamai, and R. Zamir, "Capacity and lattice strategies for canceling known interference," *IEEE Trans. Inf. Theory*, vol. 51, no. 1, pp. 3820–3833, Nov. 2005.

[38] L. Zhou and W. Yu, "Uplink multicell processing with limited backhaul via per-base-station successive interference cancellation," *IEEE Journal on Selected Areas in Commun.*, vol. 31, pp. 1981–1993, Oct. 2013.

[39] O. Simeone, O. Somekh, H. V. Poor and S. Shamai (Shitz), "Local base station cooperation via finite-capacity links for the uplink of linear cellular networks," *IEEE Trans. Inf. Theory,* vol. 55, no. 1, pp. 190–204, Jan. 2009.

[40] O. Simeone, N. Levy, A. Sanderovich, O. Somekh, B. M. Zaidel, H. V. Poor and S. Shamai (Shitz), "Cooperative wireless cellular systems: An information-theoretic view," *Foundations and Trends in Commun. and Info. Theory, Now Publishers Inc.*, Hanover MA, vol. 8, no. 1–2, pp. 1–177, 2012.

[41] M. Egan and I. B. Collings, "Low complexity quantization codebooks for CoMP," in *Proc. IEEE Intern. Symp. on Personal, Indoor, and Mobile Radio Commun. (PIMRC)*, pp. 1024–1028, London, 2013.

[42] W. Yu, T. Kwon and C. Shin, "Multicell coordination via joint scheduling, beamforming, and power spectrum adaptation," *IEEE Trans. on Wireless Commun.*, vol. 12, no. 7, pp. 1–14, July 2013.

[43] J. Chen, U. Mitra and D. Gesbert, "Optimal UAV relay placement for single user capacity maximization over terrain with obstacles," in *Proc. IEEE SPAWC 2019*, Cannes, France, pp. 1–5, July 2019.

[44] N. Levy and S. Shamai (Shitz), "Clustered local decoding for Wyner-type cellular models," *IEEE Trans. Inf. Theory*, vol. 55, no. 11, pp. 4976–4985, Nov. 2009.

[45] A. Lapidoth, N. Levy, S. Shamai (Shitz), and M. Wigger, "Cognitive Wyner networks with clustered decoding," *IEEE Trans. Inf. Theory,* vol. 60, no. 10, pp. 6342–6367, Oct. 2014.

[46] M. Wigger, R. Timo, and S. Shamai (Shitz), "Conferencing in Wyner's asymmetric interference network: effect of number of rounds," *IEEE Trans. Inf. Theory*, vol. 63, no. 2, pp. 1199–1226, Feb. 2017.

[47] V. S. Annapureddy, A. El Gamal, and V. V. Veeravalli, "Degrees of freedom of interference channels with CoMP transmission and reception," *IEEE Trans. Inf. Theory*, vol. 58, no. 9, pp. 5740–5760, Sep. 2015.

[48] J. Zhang, R. Chen, J. G. Andrews, A. Ghosh, and R. W. Heath, "Networked MIMO with clustered linear precoding," *IEEE Trans. Wireless Commun.*, vol. 8, no. 4, pp. 1910–1921, Apr. 2009.

[49] S. Shamai (Shitz) and M. A. Wigger, "Rate-limited transmitter cooperation in Wyner's asymmetric interference network," in *Proc. IEEE Int. Symp. Inf. Theory (ISIT)*, Jul. 2011, pp. 425–429.

[50] I. H. Wang and D. N. C. Tse, "Interference mitigation through limited receiver cooperation," *IEEE Trans. Inf. Theory,* vol. 57, no. 5, pp. 2913–2940, May 2011.

[51] I. H. Wang and D. N. C. Tse, "Interference mitigation through limited transmitter cooperation," *IEEE Trans. Inf. Theory*, vol. 57, no. 5, pp. 2941–2965, May 2011.

[52] R. Wu, V. M. Prabhakaran, P. Viswanath, and Y. Wang, "Interference channels with half duplex source cooperation," *IEEE Trans. Inf. Theory,* vol. 60, no. 3, pp. 1753–1781, Mar. 2014.

[53] A. S. Motahari, S. O. Gharan, M. A. Maddah-Ali, and A. K. Khandani, "Real interference alignment: Exploiting the potential of single antenna systems," *IEEE Trans. Inf. Theory*, vol. 60, no. 8, pp. 4799–4810, Aug. 2014.

[54] B. Nazer, M. Gastpar, S. A. Jafar, and S. Vishwanath, "Ergodic interference alignment," *IEEE Trans. Inf. Theory*, vol. 58, no. 10, pp. 6355–6371, Oct. 2012.

[55] M. A. Maddah-Ali, A. S. Motahari, and A. K. Khandani, "Communication over MIMO X channels: Interference alignment, decomposition, and performance analysis," *IEEE Trans. Inf. Theory*, vol. 54, no. 8, pp. 3457–3470, Aug. 2008.

[56] V. Ntranos, M. A. Maddah-Ali, and G. Caire, "Cellular interference alignment," *IEEE Trans. Inf. Theory*, vol. 61, no. 3, pp. 1194–1217, Mar. 2015.

[57] V. S. Annapureddy, A. El Gamal and V. V. Veeravalli, "Degrees of freedom of interference channels With CoMP transmission and reception," *IEEE Trans. Inf. Theory*, vol. 58, no. 9, pp. 5740–5760, Sept. 2012.

[58] D. Gesbert, S. G. Kiani, A. Gjendemsj, and G. E. Oien, "Adaptation, coordination, and distributed resource allocation in interference-limited wireless networks," *Proc. of the IEEE*, vol. 95, no. 5, pp. 2393–2409, Dec. 2007.

[59] C. Shi, R. A. Berry, and M. L. Honig, "Distributed interference pricing for OFDM wireless networks with non-separable utilities," in *Proc.Conf. Info. Science Sys. (CISS)*, pp. 755–760, March 2008.

[60] D. Gesbert, S. Hanly, H. Huang, S. Shamai Shitz, O. Simeone and W. Yu, "Multi-cell MIMO cooperative networks: A new look at interference," in *IEEE Journal on Selec. Areas in Commun.*, vol. 28, no. 9, pp. 1380–1408, Dec. 2010.

[61] M. K. Karakayali, G. J. Foschini, and R. A. Valenzuela, "Network coordination for spectrally efficient communications in cellular systems," *IEEE Wireless Commun.*, vol. 13, no. 4, pp. 56–61, Aug. 2006.

[62] T. Han and K. Kobayashi, "A new achievable rate region for the interference channel," *IEEE Trans. Inf. Theory*, vol. 27, pp. 49–60, Jan. 1981.

[63] W. Huleihel and Y. Steinberg, "Channels with cooperation links that may be absent," *IEEE Trans. Inf. Theory*, vol. 63, no. 9, pp. 5886–5906, Sep. 2017.

[64] G. Sridharan and W. Yu, "Degrees of freedom of mimo cellular networks: Decomposition and linear beamforming design," *IEEE Trans. Inf. Theory*, vol. 61, no. 6, pp. 3339–3364, June 2015.

[65] G. Katz, B. M. Zaidel, and S. Shamai (Shitz), "On layered transmission in clustered cooperative cellular architectures," in *Proc. 2013 IEEE ISIT*, Istanbul, Turkey, Jul. 7–12, pp. 1162–1166, 2013.

[66] A. Khina, T. Philosof and M. Laifenfeld, "Layered uplink transmission in clustered cellular networks," *arXiv:1604.01113*.

[67] S. Gelincik, M. Wigger, and L. Wang, "DoF in sectorized cellular systems with BS cooperation under a complexity constraint," in *Proc. ISWCS 2018*, Lisbon, Portugal, Aug 28–31, 2018.

[68] B. He, N. Yang, X. Zhou, and J. Yuan, "Base station cooperation for confidential broadcasting in multi-cell networks," *IEEE Trans. Wireless Commun.*, vol. 14, no. 10, pp. 5287–5299, Oct. 2015.

[69] T. M. Cover and J. A. Thomas, "Elements of Information Theory" *(Wiley Series in Telecommunications and Signal Processing)*. USA: Wiley-Interscience, 2006.

[70] W. Hachem, A. Hardy, and S. Shamai (Shitz), "Mutual information of wireless channels and block-Jacobi ergodic operators," *arXiv:1811.04734v2*, Mar. 2019.

[71] J. Wang, B. Yuan, L. Huang, and S. A. Jafar, "GDoF of interference channel with limited cooperation under finite precision CSIT", *arXiv:1908.00703 [cs.IT]*, Aug, 2019.

[72] Y. Chan and S. A. Jafar, "Towards an extremal network theory – robust GDoF gain of transmitter cooperation over TIN," *Proc. IEEE Int. Symp. Inf. Theory (ISIT)*, Paris, France, July 2019.

[73] Y. Polyanskiy, H. V. Poor and S. Verdu, "Channel coding rate in the finite blocklength regime," in *IEEE Trans. Inf. Theory*, vol. 56, no. 5, pp. 2307–2359, May 2010.

[74] P. Mary, J. Gorce, A. Unsal and H. V. Poor, "Finite blocklength information theory: What is the practical impact on wireless communications?," *IEEE Globecom Workshops (GC Wkshps)*, Washington, DC, 2016.

[75] A. Steiner and S. Shamai (Shitz), "On queuing and multilayer coding," *IEEE Trans. Inf. Theory*, vol. 56, no 5, pp. 2392–2415, 2010.

[76] R. Karasik, O. Simeone and S. S. Shitz, "Latency limits for content delivery in a Fog-RAN with D2D communication," *Proc. IEEE Int. Symp. Inf. Theory (ISIT)*, Paris, France, July 2019.

[77] I. E. Aguerri, A. Zaidi, G. Caire, and S. Shamai (Shitz), "On the capacity of cloud radio access networks with oblivious relaying," *Proc. IEEE Int. Symp. Inf. Theory (ISIT)*, Aachen, 2017

[78] S. Park, O. Simeone, O. Sahin and S. Shamai (Shitz) , "Robust and Efficient Distributed Compression for Cloud Radio Access Networks," *IEEE Trans. Vehicular. Tech.*, vol. 62, no. 2, pp. 692–703, Feb. 2013.

[79] H. Nikbakht, S. Kamel, M. Wigger and A. Yener, "Stochastic D2D Caching with Energy Harvesting Nodes," *18th International Symposium on Modeling and Optimization in Mobile, Ad Hoc, and Wireless Networks (WiOPT)*, Volos, Greece, 2020, pp. 1-8.

[80] H. Nikbakht, M. Wigger and S. Shamai (Shitz), "Coordinated multi point transmission and reception for mixed delay traffic," *arXiv:2012.07615v1*, Dec. 2020.

ECOLE DOCTORALE

Titre: Réseaux avec contraintes de latence mixtes

Mots clés: Contraintes de latence mixtes, réseaux d'interférence, gain de multiplexage

Résumé: Les réseaux de communication sans fil modernes doivent s'adapter à différents types de trafic de données avec des contraintes de latence différentes. Les applications vidéo sensibles à la latence, en particulier, représentent une part croissante du trafic de données. En outre, les réseaux modernes doivent accepter des débits de données élevés, ce qu'ils peuvent faire par exemple avec des terminaux coopératifs ou avec l'assistance de relais tels que les drones. Cependant, la coopération introduit généralement des retards de communication supplémentaires et n'est donc pas applicable au trafic de données sensibles à la latence. Cette thèse porte sur les réseaux d'interférence avec des contraintes de latence mixtes et sur les architectures de systèmes où des émetteurs et/ou des récepteurs voisins peuvent coopérer.
Nous proposons différents schémas de codage pour permettre la transmission simultanée de messages sensibles et insensibles à la latence. Pour les schémas proposés, nous analysons les gains de multiplexage (MG) qu'ils réalisent sur le réseau de transfert intercellulaire souple de Wyner, le réseau symétrique de Wyner, le réseau hexagonal et le réseau hexagonal sectorisé.
Nous proposons, de surcroît, des schémas de codage similaires en fonction de différents types d'activité aléatoire de la part des usagers du réseau. Nous considérons plus particulièrement deux configurations. Dans la première configuration, chaque émetteur envoie toujours des données insensibles à la latence et reçoit aléatoirement des données sensibles à la latence. Dans la seconde configuration, les arrivées de données sensibles et insensibles à la latence sont aléatoires, et chaque transmetteur n'envoie ou ne reçoit qu'un seul type de données à un instant donné.
Nous étudions aussi un réseau d'accès radio "cloud" avec des contraintes de latence mixtes.Lorsque le rapport signal / bruit (SNR) est élevé, nos résultats démontrent que, pour des capacités frontales modérées, le MG maximal pour les messages sensibles à la latence reste inchangé sur une large gamme de petits et moyens MG de messages sensibles à la latence. La somme des MG est donc améliorée si certains messages peuvent être décodés directement aux stations de base.

Title: Networks with Mixed Delay Constraints

Keywords: Mixed delay constraints, Interference Networks, Multiplexing Gain

Abstract: Modern wireless communication networks have to accommodate different types of data traffic with different latency constraints. In particular, delay-sensitive video-applications represent an increasing portion of data traffic. Modern networks also have to accommodate high total data rates, which they can accomplish for example with cooperating terminals or with helper relays such as drones. However, cooperation typically introduces additional communication delays, and is thus not applicable to delay-sensitive data traffic. This thesis focuses on interference networks with mixed-delay constraints and on system architectures where neighbouring transmitters and/or neighbouring receivers can cooperate.
We propose various coding schemes that can simultaneously accommodate the transmission of both delay-sensitive and delay-tolerant messages. For the proposed schemes we analyze the multiplexing gains (MG) they achieve over Wyner's soft hand-off network, Wyner's symmetric network, the hexagonal network and the sectorized hexagonal network.
We further propose similar coding schemes for scenarios with different types of random user activity. We specifically consider two setups. In the first setup, each active transmitter always has delay-tolerant data to send and delay-sensitive data arrival is random. In the second setup, both delay-tolerant and delay-sensitive data arrivals are random, and only one of them is present at any given transmitter.
Additionally, we also study a cloud radio access network with mixed delay constraints. At high signal-to-noise ratio (SNR), our results show that for moderate fronthaul capacities, the maximum MG for delay-sensitive messages remains unchanged over a large regime of small and moderate MGs of delay-sensitive messages. The sum MG is thus improved if some of the messages can directly be decoded at the base stations.

Institut Polytechnique de Paris
91120 Palaiseau, France